RNA Interference as a Vector Control Mechanism: Reducing *Aedes albopictus* Populations and Disrupting Arbovirus Transmission Cycles

Cumulative Dissertation

to fulfil the

Requirements for the Degree of

"Doctor rerum naturalium" (Dr. rer. nat.)

Submitted to the Council of

the Faculty of Agricultural Sciences, Nutritional Sciences,

and Environmental Management

of the Justus-Liebig University, Giessen

By

Bodunrin Omokungbe, M.Sc.

Giessen, 2025

In memory of Seyifunmi Omokungbe,

whose absence carved strength,

and whose memory lit the way

Prüfungskommission

Vorsitz

Professor Dr. Jan Siemens
Institut für Bodenkunde und Bodenerhaltung
Fachbereich Agrarwissenschaften, Ökotrophologie und Umweltmanagement
Justus-Liebig-Universität Gießen

1. Gutachter

Professor Dr. Andreas Vilcinskas
Institut für Insektenbiotechnologie
Fachbereich Agrarwissenschaften, Ökotrophologie und Umweltmanagement
Justus-Liebig-Universität Gießen

2. Gutachter

Professor Dr. Miklós Bálint
Institut für Insektenbiotechnologie
Fachbereich Agrarwissenschaften, Ökotrophologie und Umweltmanagement
Justus-Liebig-Universität Gießen

1. Prüfer

Professor Dr. Benjamin Lamp
Institut für Virologie
Fachbereich Veterinärmedizin
Justus-Liebig-Universität Gießen.

2. Prüfer

Professor Dr. Thomas Wilke
Institut für Tierökologie und Spezielle Zoologie
Fachbereich Biologie und Chemie
Justus-Liebig-Universität Gießen

Declaration in accordance with the doctoral regulations of Department 09 dated July 7th, 2004, Section 17 (2), amended on May 29, 2019

I declare that the dissertation here submitted is entirely my own work, written without any illegitimate help by any third party and solely with materials as indicated in the dissertation. I have indicated in the text where I have used texts from already published sources, either word for word or in substance, and where I have made statements based on oral information given to me. At all times during the investigations carried out by me and described in the dissertation, I have followed the principles of good scientific practice as defined in the "Statutes of the Justus Liebig University Gießen for the Safeguarding of Good Scientific Practice".

Gießen, 22-10-2025

Place, date

Bodunrin Omokungbe

Summary

Mosquitoes are considered the “most dangerous animals on Earth”. This is not because of the small amount of blood they take from us, but due to the pathogens they can transmit during this process. Key examples are malaria parasites, dengue virus, chikungunya virus, and Zika virus, causing over a million deaths annually. Urbanization, transport, and global trade have led to the spread of invasive species such as the Asian tiger mosquito (*Aedes albopictus*). Originally from Southeast Asia, this species has migrated to other parts of the world. This mosquito can transmit numerous arboviruses, filarial worms, and bacteria. Conventional control relies on chemical insecticides and biological agents, but off-target effects and resistances limit their usefulness. Therefore, targeted approaches like RNA interference (RNAi) are essential. RNAi is a naturally occurring post-transcriptional gene silencing mechanism in most eukaryotes. Silencing essential genes *via* RNAi can induce mortality, distort vital phenotypes, and impair the ability to transmit pathogens.

This thesis evaluated RNAi as a species-specific control strategy against *Ae. albopictus*. Prior successes have demonstrated improving RNAi outcome in other mosquito species using transfection reagents (TRs), so I hypothesized that formulating dsRNA with TRs would enhance uptake and efficacy. However, no TRs are specifically designed for long dsRNA in aedine cell lines, and their undisclosed compositions makes selection difficult. Here, I established an RNAi workflow for aedine cell lines and screened multiple TRs for dsRNA delivery. Their complexing capacity and the cytotoxicity of their complexes were assessed. Most of them formed stable complexes, except HiPerFect, which failed even at a 1:9 (dsRNA:TR) ratio. The complexes were mostly non-cytotoxic, but Lipofectamine 2000 exhibited cytotoxic effects at concentrations above 1 ng/µL. Meanwhile, the five most effective TRs increased cellular uptake of long dsRNA and improved RNAi knockdown efficiency in *Ae. albopictus* U4.4 cells.

Furthermore, candidate genes associated with high mortality in other insects were selected and two dsRNA constructs per gene were designed. Initial evaluation in U4.4 cells was conducted with both unformulated and TR-encapsulated dsRNA. Only one dsRNA against inhibitor of apoptosis (IAP) reduced U4.4 cell viability, yet all selected dsRNA showed significant knockdown of the candidate genes by RT-qPCR. Subsequently, I established RNAi workflow for the *in vivo* assessment in *Ae. albopictus*, but no dsRNA led to significant larval mortality. The knockdown of IAP gene was observed, but only in dissected gut tissue, and not in the whole body. The lack of larval mortality led to further investigations to identify possible barriers limiting RNAi efficacy. Particle sizing indicated optimal dsRNA:TR complex sizes, but only at lower concentrations. Fluorescence imaging confirmed oral uptake, but no spread of the dsRNA beyond the gut. *Ex vivo* assays showed rapid dsRNA degradation by larval gut extract, which were identified in *Ae. albopictus* for the first time and are expressed across larval stages, with the highest expression in gut tissues. The data indicated that the lack of larval mortality was likely due to suboptimal particle size (at higher concentrations), poor systemic spread, and rapid degradation of the selected dsRNA by nucleases.

In addition, a standardized protocol was developed to analyze alphavirus replication in aedine cell lines. Viral inhibition was demonstrated with furin inhibitors using a SFV reporter tagged with mCherry as a model. This workflow thereby provides an *in vitro* platform for evaluating dsRNA against mosquito-borne viruses.

Lastly, the feasibility of RNAi to reduce SFV replication in aedine cell line was assessed using the established protocol. For this, dsRNAs were designed and showed no cytotoxicity. Most of the synthesized dsRNAs inhibited virus spread when encapsulated. The dsRNA against non-structural protein 4 (nsp4) reduced viral replication by up to 80%. A concentration of 0.5 ng/µL of the encapsulated dsRNA was enough to significantly suppress the spread of the reporter virus signal. The antiviral effect of nsp4-dsRNA was validated by RT-qPCR, which confirmed a significant knockdown of the target gene.

The central hypothesis that encapsulation of dsRNA increases efficacy was supported by most of the cell line experiments. However, the *in vitro* successes did not translate to *in vivo* lethality. Therefore, future work should develop optimized formulations to protect dsRNA and promote spread beyond the larval gut. More so, identifying gut-essential genes could enable larval mortality without systemic spread. While suppression of arboviral replication in an aedine cell line was demonstrated here, *in vivo* validation is still required. A potential RNAi bioinsecticide or arboviral transmission inhibitor must be potent, economical, and highly target-specific. Overall, this thesis presented the first comprehensive analysis of TRs for aedine cells, developed an RNAi workflow for evaluating dsRNA in *Ae. albopictus*, established a protocol to measure alphavirus infection in real time, and also showed that RNAi can reduce arboviral replication in mosquito cells.

Zusammenfassung

Stechmücken gelten als die „gefährlichsten Tiere der Welt“. Das liegt nicht an den geringen Blutmengen, die sie uns entnehmen, sondern an den Krankheitserregern, die dabei übertragen werden können. Die bedeutendsten Beispiele sind Malariaerreger, das Dengue-Virus, das Chikungunya-Virus oder das Zika-Virus, die jährlich zu über einer Million Todesfälle führen. Urbanisierung, Transport, und der globale Handel haben zur Ausbreitung invasiver Arten, wie der Asiatischen Tigermücke (*Aedes albopictus*), geführt. Diese ursprünglich aus Südostasien stammende Art hat sich erfolgreich in vielen Teilen der Welt ausgebreitet. Die Stechmücke kann viele Arboviren, Fadenwürmer und Bakterien übertragen und zeichnet sich somit durch ein besonders hohes Vektorpotenzial aus. Die herkömmliche Bekämpfung stützt sich auf chemische Insektizide und biologische Wirkstoffe, deren Nutzen jedoch durch Auswirkungen auf Nichtzielorganismen und Resistenzen eingeschränkt ist. Daher sind spezifische Ansätze wie die RNA-Interferenz (RNAi) von Vorteil. RNAi ist ein natürlich vorkommender posttranskriptioneller Mechanismus zur Regulierung von Gene in meisten Eukaryoten. Das *silencing* essenzieller Gene über RNAi kann je nach Ziel zur Mortalität führen, wichtige Phänotypen beeinträchtigen und die Fähigkeit zur Übertragung von Krankheitserregern reduzieren.

In dieser Arbeit wurde RNAi als artspezifische Bekämpfungsstrategie gegen *Ae. albopictus* untersucht. Frühere Arbeiten haben gezeigt, dass sich die Ergebnisse im Bereich RNAi bei anderen Stechmückenarten durch den Einsatz von Transfektionsreagenzien (TRs) verbessern lassen. Daher stellte ich die Hypothese auf, dass die Formulierung von dsRNA mit TRs die Aufnahme und Wirksamkeit der dsRNA verbessern würde. Jedoch gibt es keine TRs, die speziell für die Transfektion langer dsRNA in aedine Zelllinien entwickelt wurden. Ihre nicht offengelegte Zusammensetzung erschwert die Auswahl. Im Rahmen meines Doktorarbeit, habe ich einen RNAi-Workflow für aedine Zelllinien etabliert und mehrere TRs für die dsRNA-Übertragung untersucht. Ihre Komplexbildungsfähigkeit und die Zytotoxizität ihrer Komplexe wurden untersucht. Die meisten von ihnen bildeten stabile Komplexe, mit Ausnahme von HiPerFect, welches selbst bei einem Verhältnis von 1:9 (dsRNA:TR) keine stabilen Komplexbildung zeigte. Die Komplexe waren größtenteils nicht zytotoxisch, jedoch zeigte Lipofectamine 2000 bei Konzentrationen über 1 ng/µL zytotoxische Effekte. Die fünf wirksamsten TRs erhöhten die zelluläre Aufnahme von langer dsRNA und verbesserten die *knockdown*-Effizienz der dsRNA in U4.4-Zellen.

Darüber hinaus wurden Gene ausgewählt, die bei Applikation zu einer hohen Sterblichkeit bei anderen Insekten führten. Pro Gen wurden zwei dsRNA-Konstrukte designt und synthetisiert. Die erste Evaluierung in U4.4-Zellen wurde sowohl mit unformulierter als auch mit TR-formulierter dsRNA durchgeführt. Nur eine dsRNA gegen den *inhibitor of apoptosis* (IAP, Apoptose-Inhibitor) reduzierte die Viabilität der U4.4-Zellen. Interessanterweise zeigten alle Konstrukte einen signifikanten *knockdown* der mRNA-Expression des jeweiligen Gens in der Analytik mittels RT-qPCR. Anschließend etablierte ich einen RNAi-Workflow für i*n vivo*-Untersuchungen in *Ae. albopictus*, aber keine dsRNA führte zu einer signifikanten Larvensterblichkeit. Ein *knockdown* des IAP-Gens wurde beobachtet, jedoch nur in seziertem Darmgewebe und nicht im gesamten Körper der Stechmücken. Die fehlende Larvensterblichkeit führte zu weiteren Untersuchungen, um mögliche Barrieren zu identifizieren, die die Wirksamkeit der RNAi einschränken. Die Partikelgrößenbestimmung ergab optimale

Komplexgrößen, jedoch nur bei niedrigeren Konzentrationen. Die Fluoreszenzmikroskopie bestätigte die orale Aufnahme, jedoch keine Ausbreitung der dsRNA über den Darm hinaus. *Ex-vivo*-Assays zeigten einen schnellen Abbau der dsRNA. Mittels Homologiesuche konnten zwei bisher unbeschriebene Nukleasen in *Ae. albopictus* identifiziert werden. Durch qPCR-Analytik konnte gezeigt werden, dass die Nukleasen in allen Larvenstadien exprimiert werden und eine besonders hohe Expression im Darmgewebe zu beobachten ist. Die Daten deuteten darauf hin, dass die fehlende Larvensterblichkeit wahrscheinlich auf eine suboptimale Partikelgröße, eine schlechte systemische Ausbreitung und einen raschen Abbau der ausgewählten dsRNA durch Nukleasen zurückzuführen war.

Darüber hinaus wurde ein standardisiertes Protokoll zur Analyse der Alphavirus-Ausbreitung in aedinen Zelllinien entwickelt. Die Virushemmung wurde mit Furin-Inhibitoren unter Verwendung eines mit mCherry markierten SFV-Reporters als Modell nachgewiesen. Dieser Arbeitsablauf bietet somit eine i*n vitro*-Plattform zur Bewertung von dsRNA gegen durch Stechmücken übertragene Viren.

Schließlich wurde der Nutzen von RNAi zur Verringerung der SFV-Ausbreitung in einer aedinen Zelllinien unter Verwendung des etablierten Protokolls bewertet. Dafür wurden dsRNAs entwickelt, die keine Zytotoxizität aufwiesen. Die meisten der synthetisierten dsRNAs hemmten die Replikation, wenn sie mit K4 formuliert wurden. dsRNA gegen das *non-structural protein* 4 (nsp4, Nichtstrukturprotein) reduzierte die Virusreplikation um bis zu 80 %. Eine Konzentration von 0,5 ng/µL der formulierten dsRNA reichte aus, um das Signal des Reportervirus signifikant zu reduzieren. Die antivirale Wirkung von nsp4-dsRNA wurde mittels RT-qPCR validiert, wodurch eine signifikante, niedrigere mRNA-Expression des Zielgens im Vergleich zur Kontrolle bestätigt wurde.

Die zentrale Hypothese, dass die Formulierung von dsRNA deren Wirksamkeit verbessern kann, wurde in den meisten Zelllinienexperimente bestätigt. Die Erfolge *in vitro* ließen sich jedoch nicht auf die Letalität *in vivo* übertragen. Daher sollten in zukünftigen Arbeiten optimierte Formulierungen entwickelt werden, um dsRNA besser zu schützen und die Ausbreitung über den Darm der Larven hinaus zu fördern. Darüber hinaus könnte die Identifizierung von Genen die für den Darm essenziell sind, die Larvensterblichkeit erhöhen, ohne die Notwendigkeit von systemischer Ausbreitung. Obwohl hier die Unterdrückung der Arbovirus-Ausbreitung in einer aedine Zelllinie nachgewiesen wurde, ist noch eine Validierung *in vivo* erforderlich. Ein potenzielles RNAi-Bioinsektizid oder ein Arbovirus-Übertragungshemmer muss wirksam, wirtschaftlich und hochgradig zielspezifisch sein. Insgesamt zeigt diese Arbeit die erste umfassende Analyse von TRs für aedine Zellen. Es wurde ein RNAi-Workflow zur Testung von dsRNA in *Ae. Albopictus* entwickelt und ein Protokoll zur Messung der Alphavirus-Infektion in Echtzeit etabliert. Die Studie zeigt weiterhin, dass RNAi die Arbovirus-Ausbreitung in Stechmückenzellen reduzieren kann.

Table of contents

1 Introduction

Mosquitoes

Mosquitoes are small flies with over 3500 described species, found in almost all habitable regions of the world (Becker et al., 2020). They belong to the order Diptera and are classified under the suborder Nematocera and the family *Culicidae*. They are further divided into two major subfamilies, the *Anophelinae* and the *Culicinae* (Figure 1). An example of the *Anophelinae* is the malaria-transmitting genus *Anopheles* (e.g., *Anopheles gambiae* and *An. funestus*). The subfamily *Culicinae* is further divided into 11 tribes, with the most prominent ones being the *Culicini* (e.g., *Culex pipiens* and *Cx. quinquefasciatus*), and the *Aedini* (e.g., *Aedes aegypti* and *Ae. albopictus*). These two tribes includes the major vectors of arboviral diseases (Foster and Walker, 2019; Harbach, 2007; Wilkerson et al., 2021).

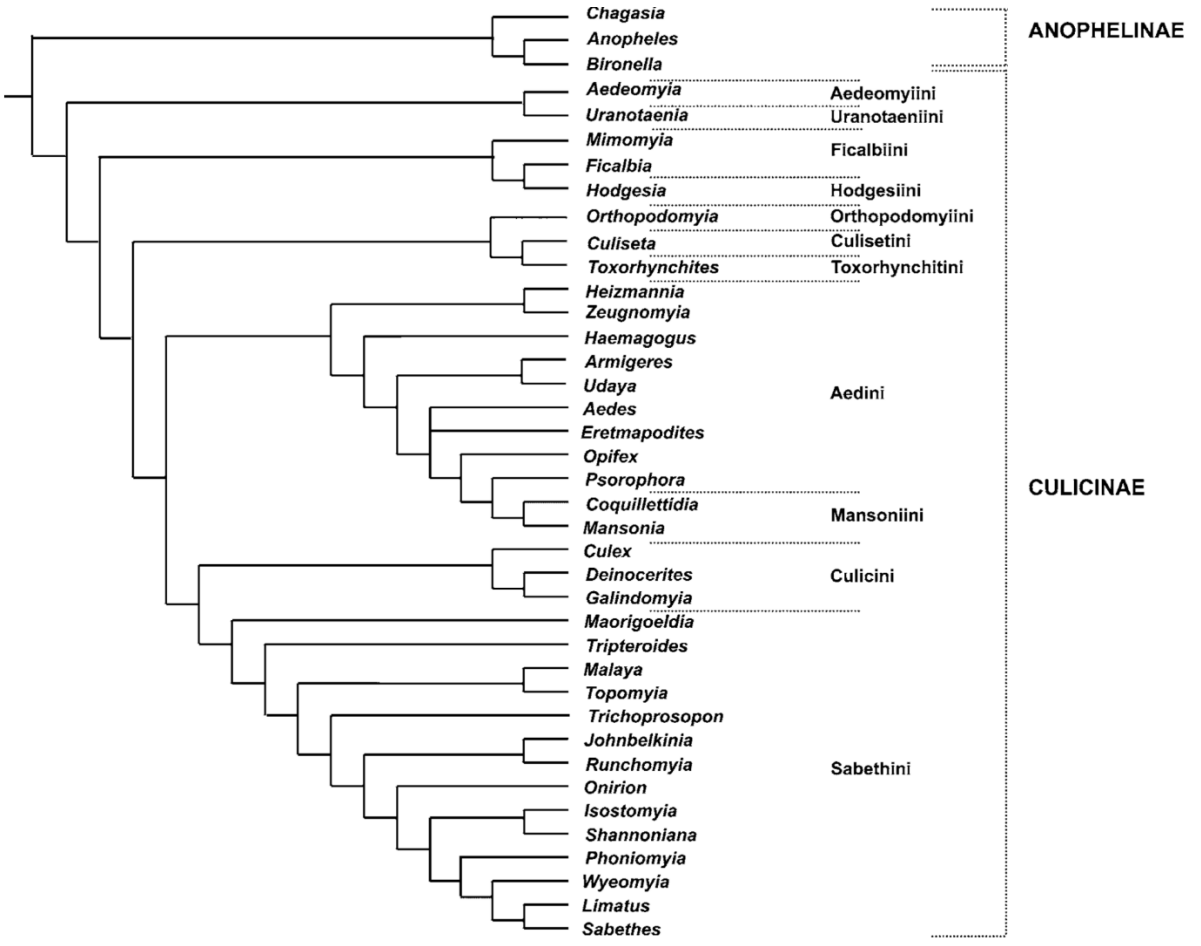

Figure 1. Phylogeny of mosquito genera based on their morphological features, showing the 11 tribes of the subfamily *Culicinae* as well as the 3 genera of the subfamily *Anophelinae*. Modified from Harbach (2007).

Mosquitoes are holometabolous insects, which means they undergo complete metamorphosis. Their life cycle start with eggs that hatch into larvae, which pass through four

instars before molting into pupae, and eventually emerging as adults (Figure 2) (Becker et al., 2020; Hall and Tamïr, 2022). Mosquitoes fall into two groups based on how they lay eggs. The first group includes species (e.g., *Aedes*) whose embryos enter a resting period. This can be an environmentally triggered dormancy or a genetically determined diapause. *Aedes* species lay eggs singly in moist environments, and the eggs do not usually hatch immediately after oviposition. The second group (e.g., *Anopheles* and *Culex*) does not enter a resting period. *Anopheles* also lay their eggs single, while *Culex* species lay them in cluster, forming rafts on the water surface. In these species, hatching typically occurs soon after embryonic maturation and often influenced by environmental conditions, particularly temperature (Becker et al., 2020).

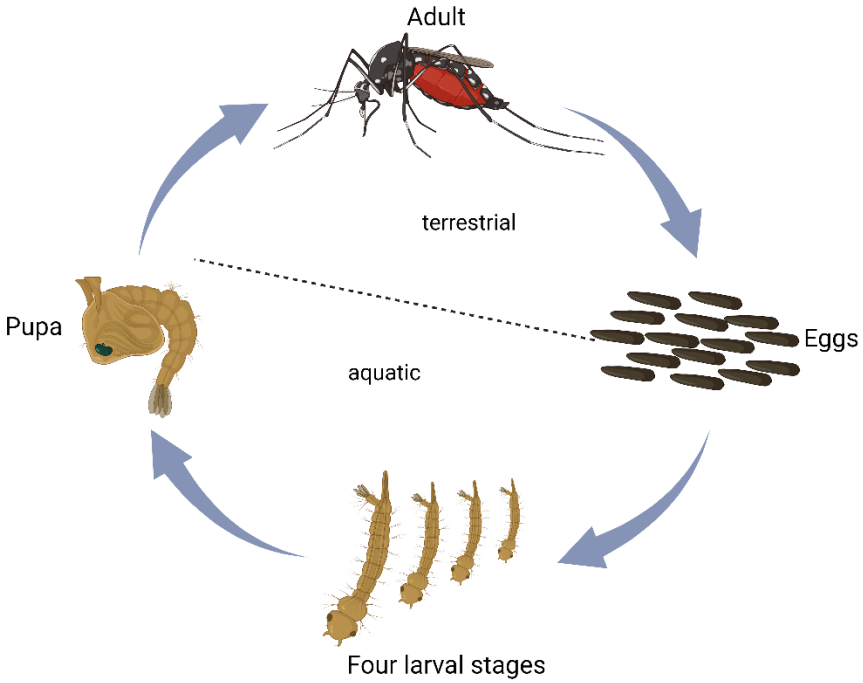

Figure 2. Life cycle of *Aedes albopictus*. The cycle is divided into aquatic life stages (larvae and pupae) and terrestrial life stages (adults and eggs), with eggs deposited singly on substrates in or around water [designed with BioRender].

Mosquito larvae are aquatic and feed primarily on microorganisms, algae, protozoa, invertebrates, and detritus (Chersoni et al., 2021). They molt four times before reaching the pupal stage. With each molt, they transition to the next larval instar, during which the head capsule size increases, while the rest of the body continuously enlarges (Becker et al., 2020). Larval development is influenced by temperature, with some cold-adapted species overwintering as larvae (Becker et al., 2020; Foster and Walker, 2019). In contrast, the larvae of floodwater mosquitoes such as *Aedes* and some *Culex* species do not overwinter (Becker et al., 2020).

The pupal stage lasts about two days, undergoing metamorphosis where some larval organs are histolysed and the body of the adult is formed from the development of imaginal

discs. The head and the thorax are fused, forming the cephalothorax, which is equipped with two respiratory trumpets. Unlike many other insect species, mosquito pupae are mobile and can actively submerge in water when disturbed (Becker et al., 2020; Romoser and Lucas, 1999).

The final stage of the mosquito life cycle is the adult. Upon emergence, mosquitoes begin mating; most females mate only once, storing sufficient sperm for future fertilizations, while males may mate multiple times (Becker et al., 2020; Hall and Tamïr, 2022). Adult mosquitoes feed on plant juices, however, in many species, females also require a vertebrate blood meal to support egg development (Harrison et al., 2021; Hien et al., 2016; Sobhy and Berry, 2024). During blood feeding, females inject saliva containing components such as anticoagulants, vasodilators, immunomodulatory proteins, enzymes, and allergens into the host's skin to facilitate the feeding process. This often triggers an immune response, resulting in inflammation and itching at the bite site (Becker et al., 2020).

A major consequence of blood feeding is the transmission of pathogens, which are introduced into the host's bloodstream along with the mosquito saliva (Becker et al., 2020; Foster and Walker, 2019). The genera *Anopheles*, *Culex*, and *Aedes* are well known for their high vectorial capacity, transmitting a wide range of pathogens, including parasites, bacteria, arboviruses, and filarial worms (Foster and Walker, 2019). Among these, *Plasmodium spp*., the causative agents of malaria, are among the deadliest pathogens. They are transmitted exclusively by female *Anopheles* mosquitoes (e.g., *An. gambiae*). In 2022 alone, malaria was responsible for an estimated 249 million cases and 608,000 deaths worldwide (WHO, 2023). *Culex* species are vector of several important arboviruses, including Japanese encephalitis virus, West Nile virus, and Usutu virus (Madhav et al., 2024). Meanwhile, *Ae. albopictus* alone is known to transmits up to 26 arboviruses, as well as several bacterial pathogens, and filarial worms (Cancrini et al., 2003; Kotsakiozi et al., 2017).

Aedes albopictus and its associated pathogens

The Asian tiger mosquito (*Ae. albopictus*) is a widely recognized invasive species (Cunze et al., 2016). Adults of this mosquito species are usually small and recognizable by the distinctive black and white pattern, which includes a prominent longitudinal white stripe along the center of the scutum and the head (Figure 3) (Becker et al., 2012; Becker et al., 2020). Like many other mosquito species, *Ae. albopictus* is anautogenous, meaning female need a blood meal to develop their eggs. This species shows opportunistic blood feeding behavior. Hosts include birds, reptiles, amphibians, and mammals. This flexibility helps explain its major role in transmitting various zoonotic diseases (Becker et al., 2020; Foster and Walker, 2019).

Figure 3. Adult female of *Aedes albopictus*, showing the distinguishing features of white scale patches on the body, and a white median dorsal stripe on the thorax and head. © Alejandra Centurión (2021)

Originally native to the tropical forests of Southeast Asia, *Ae. albopictus* is now established in various global regions, including Europe (Becker et al., 2020). Its invasiveness is attributed to several factors, including ecological adaptability, strong competitive abilities, inadequate surveillance, and ineffective control measures. Human activities, such as the international transport of used tires and ornamental plants like 'lucky bamboo', have also facilitated its spread (Becker et al., 2012; Becker et al., 2020; Lwande et al., 2020).

In Europe, *Ae. albopictus* was first reported in Albania in 1979, though no further sightings were documented until its reappearance in Italy in 1990. Since then, the species has gradually spread and become established in multiple European countries (Figure 4) (Becker et al., 2012; Muja-Bajraktari et al., 2022). Climate change models predict that *Ae. albopictus* will continue to expand its range as it becomes more tolerance of colder climates (Brady et al., 2014; Kraemer et al., 2019). This adaptation may let it establish in new areas and thereby increase the risk of disease transmission (Marini et al., 2020). This mosquito species is capable of transmitting a wide range of medically and economically significant pathogens. These include dengue virus (DENV), chikungunya virus (CHIKV), Zika virus (ZIKV), Yellow fever virus, and *Dirofilaria immitis* (heartworm) (Cancrini et al., 2003; Kotsakiozi et al., 2017).

The global incidence of dengue fever has surged in recent decades, with an estimated 390 million infections occurring annually (Tayal et al., 2023; WHO, 2009). Dengue vaccines such as Dengvaxia (CYD-TDV) and TAK-003 (Qdenga) are available. Their efficacy ranges between 60% and 80%. However, their use is limited; for example, Dengvaxia is recommended only for individuals with previous dengue exposure because of the risk of antibody dependent

enhancement, which occurs during a subsequent infection with a different dengue serotype (Afzal, 2024; Godói et al., 2017; Tayal et al., 2023).

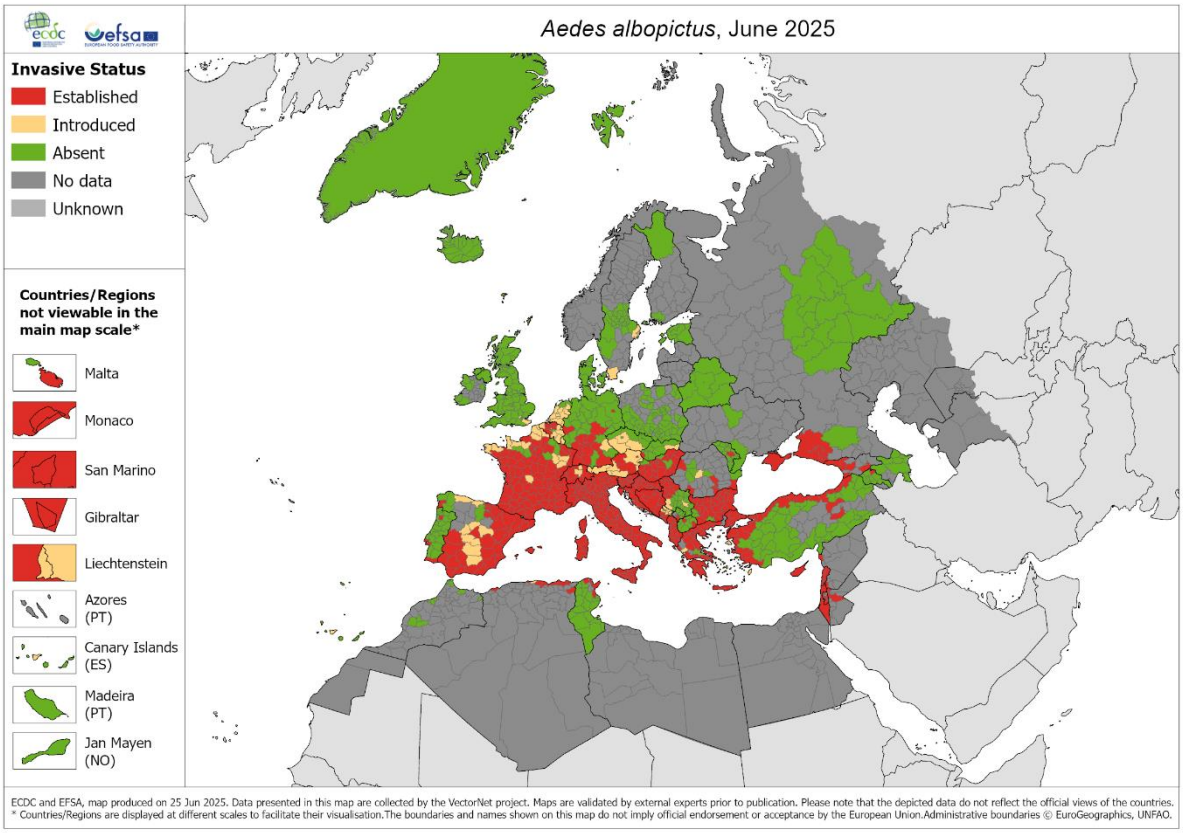

Figure 4. Current distribution of *Aedes albopictus* population in Europe. Data according to the report of the European Centre for Disease Prevention and Control, and the European Food Safety Authority (ECDC-EFSA, 2025).

Chikungunya fever continues to pose a public health threat, with more than 2 million cases reported in Africa, Asia, and the Americas since 2005 (Assis et al., 2023). Outbreaks vary in incidence and severity, depending on location and seasonal factors (Huber et al., 2018). Although, the case fatality rate is generally low, death primarily occurs among older adults, infants, and individuals with pre-existing health conditions. Chikungunya infections usually leads to chronic joint pain in about 40% of infected individuals, which can persist for a very long time (Flandes et al., 2024; Lima Cavalcanti et al., 2022). In Europe, outbreaks such as those in Italy (2007) and France (2017) have been linked to the presence of *Ae. aegypti* and *Ae. albopictus* populations (Calba et al., 2017; Caputo et al., 2020; Petersen and Powers, 2016). In 2025, an outbreak on Réunion Island (France) resulted in imported cases in mainland France. This was followed by the first reports of autochthonous transmission of chikungunya in the Grand Est

region, along with additional locally acquired cases in areas with previous outbreak histories, including Provence-Alpes-Côte d'Azur, Occitanie, and Corse (Fournier et al., 2025).

Major outbreaks of Zika fever occurred in the Americas, Southeast Asia, and the Pacific between 2015 and 2016, with Brazil alone reporting up to 1.3 million suspected cases at the peak of the epidemic in 2016 (Hennessey et al., 2016). Although the number of new cases has since declined significantly, sporadic outbreaks continue to occur, mostly in tropical regions (Seshadri et al., 2023). ZIKV infections are typically mild or asymptomatic, however, the virus is strongly associated with severe congenital abnormalities (e.g., microcephaly), and neurological complications such as Guillain-Barré syndrome (Krauer et al., 2017; Seshadri et al., 2023; Wen et al., 2017).

While most arboviruses pose a significant threat to public health, others such as Semliki Forest virus (SFV) are exceptions. First identified in Uganda in 1942, SFV has remained primarily confined to Africa, where it has been isolated from various mosquito species, including *Ae. albopictus* (Eldridge et al., 2004). Despite posing relatively low risk to humans, SFV shares critical biological features with highly pathogenic alphaviruses such as CHIKV, including mechanisms of cell entry, replication, and immune evasion (Atkins et al., 1999; Contu et al., 2021; Teppor et al., 2021). These similarities make SFV a valuable tool in laboratory research. As a model, it enables researchers to investigate viral behavior, evaluate antiviral compounds, and explore vaccine candidates (Contu et al., 2021; Pohjala et al., 2011).

At present, no vaccines exist for many arboviruses transmitted by *Ae. albopictus*. These include ZIKV, CHIKV, Mayaro virus, La Crosse encephalitis virus, Ross River virus, and Eastern equine encephalitis virus (Flandes et al., 2024; Madewell, 2020). This shows the need for enhanced vector control measures, therapeutic options, and more comprehensive public health strategies to reduce the transmission of arboviruses and prevent future outbreaks (Olliaro et al., 2018; Wilson et al., 2020).

Mosquito control strategies: past, present, and future approaches

Historically, mosquito control has relied heavily on chemical and biological interventions (Huang et al., 2017; Wilson et al., 2020). For instance, larvicides such as copper(II) acetoarsenite, also known as Paris Green, was used in the late 19th and early 20th centuries to target larval breeding sites. Although effective, it required thorough knowledge of the breeding areas and consistent application to be impactful. Paris Green is no longer widely used because its arsenic content makes it highly toxic to humans, animals, and other non-target insects.

Prolonged exposure can cause acute poisoning, organ damage, and even death (Mohammadi et al., 2021; Wilson et al., 2020).

A prominent insecticide used in the 20th century was dichlorodiphenyltrichloroethane (DDT). Its insecticidal properties were discovered in 1939. It gained wide recognition during the Second World War, when it was used to control mosquito and prevent disease transmission. After the war, DDT was applied in large-scale mosquito control programs, and used against agricultural and forestry pests (Jarman and Ballschmiter, 2012; Turusov et al., 2002; van den Berg, 2009). However, DDT has a strong environmental persistence, and it accumulates in the fatty tissues of both wildlife and humans (Tarzwell, 1947; van den Berg, 2009). Its association with increased cancer risk and endocrine disruption raised significant health concerns (Turusov et al., 2002; van den Berg, 2009). Over time, continuous DDT use exerted selective pressure on mosquito populations. Individuals with naturally occurring genetic variations that conferred reduced susceptibility to DDT survived treatment and reproduced, leading to a gradual increase in the frequency of resistance alleles within the population (Kigozi et al., 2012; Ranson and Lissenden, 2016). Additionally, its longevity in soil and water contributed to substantial long term ecological damage. Consequently, these factors prompted many countries to implement bans on DDT starting with Sweden in January 1970, leading to a drastic decline in its usage (Levain et al., 2015; Turusov et al., 2002; van den Berg et al., 2017; Whitney, 2012).

Another widely used insecticide is malathion, an organophosphate compound that has been in use since the 1950s for the control of various insects, including mosquitoes (Newhart, 2006). It inhibits acetylcholinesterase, a critical enzyme for nerve function in insects, resulting in paralysis and subsequent insect death (Jensen and Whatling, 2010). When applied according to safety guidelines, malathion has relatively low acute mammalian toxicity (Newhart, 2006). However, prolonged exposure in humans can lead to neurological effects due to its action on the nervous system and it also poses risks to non-target organisms (Choudhary et al., 2008; Jensen and Whatling, 2010; Newhart, 2006). Although malathion is not banned globally, many countries place strict limits on its use (APVMA, 2024; Tchounwou et al., 2015).

Beyond chemical insecticides, biological control agents have also been used in mosquito control. A prominent example was *Gambusia* fish (*Gambusia affinis*, *G. holbrooki*, and *G. senegalensis*), which were used as natural predators in the 20th century. These fish eat mosquito larvae and thereby reduce the number of emerging adults (Pyke, 2008; Walton et al., 2012). Despite this benefit, maintaining populations across large areas was difficult. Moreover, *Gambusia* fish are very aggressive and outcompete native fish species. For these reasons, their introduction into non-native waters led to losses of aquatic biodiversity and other ecological disruptions (Hurlbert et al., 1972, 1981; Pyke, 2008). In addition, other fish species such as

Aphanius dispar, *Aplocheilus blockii*, *Nothobranchius patrizii*, *Oreochromis zillii*, and *Poecilia reticulata* have also been used for mosquito control (WHO, 2003).

In recent decades, biological control has progressed to incorporate more targeted agents, such as *Bacillus thuringiensis israelensis* (Bti) and *Lysinibacillus sphaericus*. Both are gram-positive bacteria that produce toxins lethal to mosquito larvae. Bti produces Bti toxins (specific combination of Cry and Cyt proteins), while *L. sphaericus* produce binary toxins. Both types of toxins can effectively kill mosquito larvae in water before they can mature into adults (Brühl et al., 2020; Lacey, 2007). Bti is specific to mosquito larvae, but closely related species such as non-biting midges can also be negatively affected due to similarities in larval habitats and physiology (Allgeier et al., 2019; Theissinger et al., 2019). Nevertheless, it is an environmentally safer option than chemical insecticides with a wide range of activity (Belousova et al., 2021; Schweizer et al., 2019). This bioinsecticide does not persist in water for long periods and is most effective in small, contained water bodies. However, it efficacy decreases in large or flowing water bodies, where it can be diluted or dispersed (Schäfer and Lundström, 2014; Singh and Tripathi, 2003).

Currently used insecticides include pyrethroids (e.g., permethrin and deltamethrin), certain organophosphates (e.g., temephos and pirimiphos-methyl), and more recent classes such as insect growth regulators (IGRs). These compounds are usually applied through aerial spraying, larval habitat treatment, and indoor residual spraying (Gajendiran and Abraham, 2018; Tai et al., 2024). Pyrethroids are neurotoxic to insects and usually lead to a rapid death upon contact or ingestion, making them highly effective for quick pest control. They have low level of acute toxicity to humans and other mammals (Ensley, 2018; Gajendiran and Abraham, 2018). In contrast, organophosphate insecticides are primarily exerting their effect by inhibiting acetylcholinesterase (Tai et al., 2024). Recent generations of pyrethroids and organophosphate insecticides degrade quickly, reducing the potential for long-term environmental contamination (Gajendiran and Abraham, 2018; Tai et al., 2024). However, the growing resistances in mosquitoes to these chemicals as well as their negative impact on non-target and beneficial organisms, has led to the exploration of alternative methods (Ensley, 2018; Gajendiran and Abraham, 2018). One such alternative is the use of IGRs, a modern class of insecticides that mimics or inhibits natural hormones involved in several processes like molting, pupation, or reproduction. Commonly used IGRs include juvenile hormone analogs (e.g., pyriproxyfen), chitin synthesis inhibitors (e.g., diflubenzuron), and benzoylphenyl urea compounds (e.g., novaluron) (Fansiri et al., 2022; Herath et al., 2024; Hustedt et al., 2020). For instance, novaluron has been successfully used in many countries to control *Aedes* mosquito larvae by preventing adult emergence. Although effective, novaluron can affect non-target insects such as larvae and pupae of Coleopterans, Dipterans, and Hemipterans (Herath et al., 2024).

Beyond conventional measures, sterile insect technique (SIT) has emerged as a species-specific mosquito control strategy. This technique involves releasing sterile males into wild; these males will mate with wild females, resulting in no offspring. As a result, the population is reduced over time (Benelli, 2015; Gouagna et al., 2020; Oliva et al., 2021). SIT has been evaluated in multiple field trials for mosquito control. For example, the El Salvador SIT Program in 1972 successfully reduced the wild population of *An. albimanus* by 99%, through the release of about 4.3 million chemosterilized males over five months (Breeland et al., 1974; Oliva et al., 2021). Similarly, in 2010, around 3.3 million engineered *Ae. aegypti* males (OX513A strain) were released in the Cayman Islands. This effort reduced the wild population by an estimated 80% (Harris et al., 2012; Oliva et al., 2014). Despite notable successes, several limitations have hindered the broader implementation of SIT programs. These include high operational costs, reduced mating competitiveness of released males, the immigration of fertilized females from untreated areas, and political or regulatory barriers. Consequently, the global adoption of SIT as a mosquito control strategy has advanced slowly (Gouagna et al., 2020; Oliva et al., 2014).

Other innovative strategies also intentionally release modified mosquitoes to suppress populations or to reduce their ability to transmit diseases. A typical example is the use of mosquitoes infected with *Wolbachia*. This bacterium alters mosquito reproduction and can shorten lifespan, which lowers arbovirus transmission (Mains et al., 2019; Yen and Failloux, 2020). For instance, in South Miami, releases of *Wolbachia*-infected WB1 *Ae. aegypti* across approximately 170 acres over six months led to a significant reduction in the local mosquito population (Mains et al., 2019).

In the coming years, mosquito control will likely shift towards selective targeting, smart technologies, and genetics-driven interventions (Karunaratne and Surendran, 2022; Rajak et al., 2024). One promising approach is gene drive, a genetic engineering technique designed to spread specific genes throughout interbreeding populations. Gene drive systems can serve two main purposes for mosquito control: (1) population replacement, which aims to substitute wild mosquitoes with ones that cannot transmit pathogens, or (2) population suppression, which involves reducing overall population by disrupting female fertility or skewing the sex ratio toward males (Hammond and Galizi, 2017; Karunaratne and Surendran, 2022; Wilson et al., 2020). Another genetic tool is CRISPR-Cas9, which enables precise genome editing. This technology can disrupt genes vital for mosquito reproduction or pathogen transmission, offering a powerful method for vector control (Karunaratne and Surendran, 2022; Wickramasinghe et al., 2021). Similarly, paratransgenesis, a genetic modification of symbiotic microorganisms within mosquitoes to block disease transmission, also holds great potential (Ratcliffe et al., 2022). Another important strategy is RNA interference (RNAi), that functions by silencing specific

genes post-transcriptionally to induce mortality, impair reproduction, or reduce pathogen transmission (Airs and Bartholomay, 2017; Wiltshire and Duman-Scheel, 2020). Since RNAi does not alter the genome, it offers a potentially more acceptable GMO-free alternative. Unlike transgenic or gene-drive approaches, which involve permanent modifications that can be inherited across generations, RNAi relies on temporary gene silencing triggered by exogenous RNAi-inducing molecules, which are degraded rapidly in the environment (Müller et al., 2023).

RNA interference as a prospective mosquito control strategy

RNAi is a naturally occurring and evolutionarily conserved mechanism that is found in most eukaryotes, where small RNA molecules trigger post-transcriptional gene silencing. This mechanism plays a crucial role in the innate immune defense system against viral infections, as it enables eukaryotic cells to recognize and degrade the double-stranded RNA (dsRNA), thereby limiting viral replication (Airs and Bartholomay, 2017; Liu et al., 2019; Wiltshire and Duman-Scheel, 2020). Additionally, RNAi also regulates endogenous gene expression for controlling developmental processes, cell differentiation, and immune responses (Kim and Rossi, 2008; Liu et al., 2019).

In 1998, RNAi was discovered in *Caenorhabditis elegans*, where a target specific gene silencing by dsRNA was described (Fire et al., 1998). This discovery later earned Andrew Fire and Craig Mello a Nobel prize in physiology and medicine (Fire, 2007). RNAi research has been extended to other eukaryotic organisms, proving that its mechanism is conserved across multiple species (Almeida et al., 2019; Fang and Qi, 2016; Lax et al., 2020; Olson and Blair, 2015). This mechanism can be artificially triggered by introducing exogenous RNAi-inducing molecules such as dsRNA, small interfering RNA (siRNA), microRNA (miRNA), or short hairpin RNA (shRNA) into cells, thereby modifying gene expression and inducing phenotypical changes. This approach is gaining interest in studying gene function, viral infections, and RNAi-based vector control (Airs and Bartholomay, 2017; Olson and Blair, 2015; Setten et al., 2019).

RNAi for pest control was first demonstrated in beetles and moths (Baum et al., 2007; Mao et al., 2007). Since then, it has been applied to many other pest and vector species (Lopez et al., 2019; Müller et al., 2023; Yadav et al., 2023). For instance, in *Tribolium castaneum*, essential genes such as Ras opposite (ROP), Dre4, nucampholin (NCM), and RNA polymerase II subunit-140 are effective RNAi targets for inducing mortality. Silencing the same genes also produced high mortality in *Diabrotica virgifera virgifera* and *Brassicogethes aeneus* (Knorr et al., 2018).

In mosquitoes, there are three known pathways of RNAi (Figure 5): the miRNA, siRNA, and piwi-interacting RNA (piRNA) (Liu et al., 2019; Lucas et al., 2013). The miRNA-pathway plays

a central role in regulating gene expression during development such as metamorphosis, molting, and reproductive maturation. It also helps to maintain cellular homeostasis by regulating the expression of genes involved in metabolic processes, cell differentiation, and apoptosis. This pathway begins when miRNAs bind to complementary target sites, usually in the 3' untranslated region. This interaction leads to translational repression or mRNA degradation (Lee et al., 2019; Liu et al., 2019). In contrast, the siRNA pathway is triggered when long dsRNA or siRNAs of exogenous origin are detected in the intracellular space. After which the dsRNA has to be processed into siRNAs by the Dicer-2 enzyme. These siRNAs are then loaded into Argonaute-2 within the RNA-induced silencing complex (RISC). After the passenger strand is removed, the guide strand direct cleavage of matching mRNA. This process leads to sequence-specific gene silencing. As a result, this pathway plays a key role in antiviral defense, particularly against RNA viruses such as DENV, ZIKV, and CHIKV. Once the cells are infection, viral dsRNAs are produced, which are then targeted and degraded by this pathway. This process reduces viral load and limits systemic spread (Lee et al., 2019; Liu et al., 2019; Lucas et al., 2013). The last one is the piRNA pathway, which mainly protects the genome from transposable elements (TEs). These elements can disrupt the genome when they insert themselves into new sites. Silencing is stronger in the reproductive organs to preserve genome integrity across generations (Blair, 2011; Liu et al., 2019). Beyond this role, some studies suggest that this pathway can also help control viral replication in certain cases (Lee et al., 2019; Liu et al., 2019).

Delivering RNAi-inducing molecules to mosquitoes is typically achieved using soaking/ingestion, attractive sugar baits, or microinjection, (Munawar et al., 2020; Stewart et al., 2023; Yu et al., 2013). The soaking method involves exposing mosquito larvae to RNAi molecules by placing them directly in a treatment solution or by adding the treatment to their breeding water (Munawar et al., 2020). The attractive sugar bait method combines RNAi molecules with specific attractants in a sugar solution, which adult mosquitoes consume during feeding (Stewart et al., 2023). Soaking for larvae and attractive sugar baits for adults are currently considered the most practical options for potential field applications (Munawar et al., 2020; Stewart et al., 2023). In contrast, microinjection is primarily suited for laboratory experiments (Munawar et al., 2020; Yu et al., 2013). The use of protective carrier systems such as transfection reagents (TRs), chitosan nanoparticles, and polymers to encapsulate RNAi molecules has been shown to significantly enhance RNAi efficacy. The method protects the molecules from degradation and improves their cellular uptake (Dhandapani et al., 2019; Munawar et al., 2020). Other approaches have also been explored, such as using genetically engineered microbes that produce RNAi molecules, which are then ingested by mosquitoes (Hapairai et al., 2017; Munawar et al., 2020).

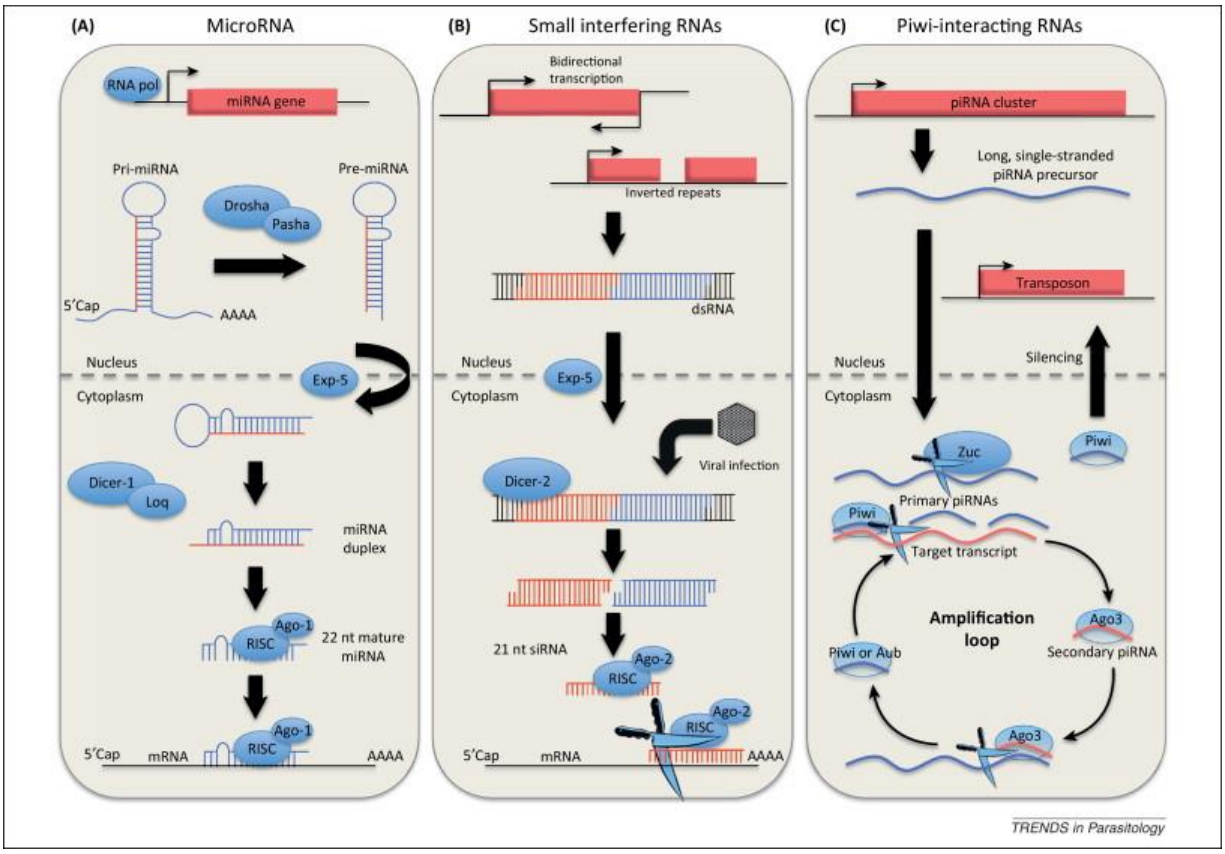

Figure 5. RNAi pathways in mosquitoes. An illustrative depiction of the three known pathways (Lucas et al., 2013).

Silencing essential genes for reproduction, development, or pathogen transmission, can ultimately reduce population size and limit disease transmission (Lopez et al., 2019; Müller et al., 2023). Multiple studies have demonstrated the effectiveness of RNAi in disrupting key physiological processes in mosquitoes. For example, encapsulated dsRNA using chitosan nanoparticles was used to target the dihydroxyphenylacetaldehyde synthase gene in *Ae. aegypti*. Treatment of first-instar larvae resulted in delayed development, abnormal molting, and impaired endo- and exocuticle formation. Injecting the same dsRNA into adult females also led to significant mortality (Chen et al., 2019). Similarly, encapsulated dsRNA in chitosan-sodium tripolyphosphate nanoparticles targeting the inhibitor of apoptosis (IAP), vacuolar-sorting protein, Snakeskin, and offtrack genes, achieved significant knockdown and high larval mortality in *Ae. aegypti* (Dhandapani et al., 2019). Furthermore, RNAi has also been used to disrupt mosquito reproductive capacity. For instance, eggshell organizing factor-1 was identified as essential gene for eggshell formation and melanization in both *Ae. aegypti* and *Ae. albopictus*. Its silencing led to fragile, non-melanized eggshells and non-viable embryos (Isoe et al., 2019). Even though numerous studies have demonstrated the potential of RNAi strategy for mosquito control, research showing significant knockdown and mortality in *Ae. albopictus* are limited, despite the vectorial capacity of this species (Munawar et al., 2020).

Aim of the thesis

Current mosquito control methods, like chemical insecticides, are inadequate due to the development of resistances in mosquito populations, as well as the environmental and health risks (Liu, 2015). Moreover, no specific treatments are available for most of the mosquito-borne arboviral diseases (Flandes et al., 2024; Madewell, 2020). Meanwhile, the few available vaccines are often limited in their efficacy (Afzal, 2024; Tayal et al., 2023). As a result, effective vector control remains one of the most critical strategies for reducing the burden of these diseases. However, more sustainable methods are urgently needed to complement the existing approaches (Jones et al., 2021; Lee et al., 2018). This therefore emphasizes the importance of exploring targeted strategies, such as RNAi for mosquito control (Müller et al., 2023).

The aim of this work was to evaluate RNAi as a species-specific vector control strategy against *Ae. albopictus*. Successful RNAi-induced mortality has been achieved before, but mostly when using genetically engineered yeast to deliver the RNAi molecules (Mysore et al., 2019b). In other mosquito species, protecting dsRNA using carrier systems has improved RNAi efficacy (Cheng et al., 2011). Therefore, this work hypothesized that encapsulating dsRNA in a formulation such as liposome-based TR would enhance delivery and improve RNAi outcomes in *Ae. albopictus*. Specific objectives were defined and addressed experimentally to test this hypothesis, as well as to assess the feasibility of using RNAi in *Ae. albopictus* without genetically modified delivery carriers.

Objective 1 focused on establishing RNAi workflow in *Ae. albopictus* cell lines. For this, dsRNA design and synthesis pipelines were developed, and standardized subculturing procedure were implemented for U4.4 and C6/36 cell lines. Although, cell culture assays provide a valuable platform for RNAi screening, the poor cellular uptake of unformulated (naked) dsRNA often limits their effectiveness (Dhandapani et al., 2019; Ovcharenko et al., 2005). These challenges could be circumvented by encapsulating dsRNA using TRs, as hypothesized. However, there are no TRs which are specifically designed for delivering long dsRNA into aedine cells. Also, the fact that their compositions are usually not disclosed, further complicates TR selection. To address this limitation, TRs were characterized for their ability to enhance dsRNA delivery and improve RNAi efficacy in aedine cell lines U4.4 and C6/36. The assessment was based on criteria such as complexing capacity, cytotoxicity, uptake improvement, as well as transfection efficiency. An mCherry-tagged reporter SFV was used as a model to evaluate the transfection efficiency.

Objective 2 aimed to examine RNAi-mediated silencing of essential genes in *Ae. albopictus* larvae and their impact on survival. Hence, *Ae. albopictus* colony was established, and

essential genes associated with high mortality in various insects were screened. Specific dsRNAs were designed and synthesize for the selected genes. Aedine cell lines were used as an *in vitro* model to assess the lethality of the dsRNAs, using both uncomplexed and complexed dsRNA with TRs. Subsequently, the *in vivo* effects of the dsRNAs were evaluated in the larval stage. Meanwhile, silencing these genes was expected to disrupt critical physiological functions, thereby reducing larval survival. However, dsRNA treatments did not result in significant larval mortality, prompting further investigation. Therefore, complex sizes formed by dsRNA and TR were characterized. Oral uptake of dsRNA in larvae was also evaluated by fluorescence microscopy. To assess whether dsRNA degradation affect efficacy, *in vitro* stability tests were performed with larval gut extracts. Next, the dsRNA-degrading nucleases were identified and characterized, and their gene expression profiles were analyzed. Lastly, an *in vitro* assay was used to test whether TRs could increase dsRNA stability by preventing enzymatic degradation.

Objective 3 was designed solely to establish a protocol to measure alphavirus infection using SFV tagged with mCherry as a model. The protocol was validated using furin inhibitors to show viral suppression. The goal was to provide a reliable platform for screening RNAi molecules and other antiviral compounds**.**

Objective 4 explored the possibility of using RNAi to suppress SFV spread in *Ae. albopictus*. The focus was on designing dsRNAs that target SFV genes and evaluate their effectiveness in reducing the viral spread in mosquito cells. This was done by following the protocol established above. To enhance delivery and silencing efficiency, as hypothesized, the dsRNAs were then encapsulated in TRs.

2 Summary of the publications

Each chapter in the following section summarizes the results from research articles that have been published or are in the process of being published in established peer-reviewed journals. Chapters I to IV correspond to the four objectives outlined in the preceding section.

- **Chapter I** presents the characterization of various TRs and their efficiency in mediating gene silencing in aedine cell lines, using SFV as a model.
- **Chapter II** describes the application of dsRNAs targeting multiple genes to evaluate their lethality in aedine cell lines and *Ae. albopictus* larvae.
- **Chapter III** establishes a standardized protocol for monitoring alphavirus infection dynamics *via* fluorescence microscopy.
- **Chapter IV** assesses the feasibility of using dsRNA as a tool to inhibit arboviral replication within aedine cell lines.

Chapter I

Gene silencing in the aedine cell lines C6/36 and U4.4 using long double-stranded RNA

Bodunrin Omokungbe, Alejandra Centurión, Sabrina Stiehler, Antonia Morr, Andreas Vilcinskas, Antje Steinbrink, Kornelia Hardes

Parasite & Vectors. 2024 June 11;17(1):255. doi: 10.1186/s13071-024-06340-3. PMID: 38863029 PMCID: PMC11167938

Mosquitoes are known not only for being a nuisance but also for transmitting pathogens responsible for several diseases. Human activities and global mobility are contributing to invasive species moving beyond their native habitats. A notable example is the Asian tiger mosquito (*Ae. albopictus*), which can transmit at least 26 arboviruses. Currently, there are limited vaccines and no specific treatments for most of these arboviral diseases. Therefore, vector control still remains a crucial strategy. However, many of the available control measures have led to resistance in mosquito populations and pose risks to non-target organisms, livestock, and humans. Therefore, RNAi offers a promising species-specific approach for mosquito control. Although TR can enhance RNAi efficacy, there are no TRs specifically for aedine cell lines, and standardized protocols for them are missing.

This study evaluated whether commercially available TRs can efficiently support delivery into aedine cell lines. For this, I assessed the complexing capacity of multiple TRs and the cytotoxicity of their complexes. Most TRs formed stable complexes with dsRNA, except

HiPerFect, which failed even at a 1:9 (dsRNA:TR) ratio. Complexes were mostly non-cytotoxic, although Lipofectamine 2000 exhibited cytotoxic effects at concentrations above 1 ng/µL. Subsequently, I tested whether long dsRNA delivered with the best performing TRs is taken up by cells, and evaluated the ability of these formulations to initiate an RNAi response. The five most effective TRs significantly improved long dsRNA uptake in both cell lines. These TRs also enhanced dsRNA efficiency in U4.4 cells using an mCherry-tagged SFV reporter as model. It is noteworthy to state that, dsRNA failed to exert any RNAi effects in C6/36 cells, likely due the lack of a functional RNAi pathway, as previously reported. These findings highlight the importance of selecting appropriate cell lines and establishing standardized protocols for RNAi studies.

Chapter II

RNA interference mediated mortality in *Aedes albopictus*: a challenging journey toward species-specific vector control

---

Bodunrin Omokungbe, Alejandra Centurión, Sabrina Stiehler, Magnus Wolf, Pascal Geisler, Andreas Vilcinskas, Antje Steinbrink, Kornelia Hardes

Parasite & Vectors. 2025 November 14;18(1):463. doi: 10.1186/s13071-025-07113-2. PMID: 41239436 PMCID: PMC12619383

RNAi is regarded as a promising strategy for mosquito vector control due to its species-specific mode of action. Among the mosquito life stages, the larval stage presents the most practical target for control efforts. A simple delivery method is to add dsRNA directly to breeding water because reducing larvae will lowers the number of emerging adults. This approach can be experimentally simulated in the laboratory through soaking or ingestion assays. In this study, several candidate genes were selected based on previous reports demonstrating significant RNAi-induced mortality in other insect species. Two dsRNAs targeting each of these genes were designed and synthesized. Initial evaluations were conducted using U4.4 cells, following the workflow established in chapter I. Both unformulated dsRNA and dsRNA encapsulated in TRs were used. This was followed by an *in vivo* assessment of larval mortality.

Among all the tested dsRNAs, only one of the dsRNA targeting inhibitor of apoptosis (IAP) gene led to a reduced cell viability in U4.4 cell line, especially when delivered using three distinct TRs. Despite this, all selected dsRNA led to a significant knockdown of their corresponding gene in U4.4 cells *via* RT-qPCR analysis. In the larval assay, none of the dsRNAs induced a significant larval mortality. Meanwhile, a knockdown of the IAP gene was observed, but only in dissected

gut tissues and not in the whole-body samples. These results prompted further investigations to identify possible barriers limiting RNAi efficacy. The dsRNA:TR complex size was evaluated, and fluorescence microscopy was used to track their oral uptake in larvae. Particle size analysis revealed optimal sizes were achieved only at lower concentrations, while fluorescent imaging confirmed dsRNA oral uptake but the signal did not spread beyond the gut. *Ex vivo* degradation assays indicated that dsRNA was rapidly degraded by nucleases in the larval gut extract. Therefore, dsRNA-degrading nucleases were identified. The corresponding genes were expressed in all larval stages, with the highest expression in the larval gut tissue. Although, TRs were initially able to protect dsRNA from enzymatic degradation, this protection declined over time. These findings highlight the key challenges limiting RNAi efficacy in *Ae. albopictus* larvae. Overcoming these barriers may require identifying gut-specific essential genes, as well as developing more sophisticated delivery system.

Chapter III

Quantitative fluorescence imaging of alphavirus infection for antiviral screenings

---

Alejandra Centurión*, Bodunrin Omokungbe*, Cross Chambers, Sabrina Stiehler, Andreas Vilcinskas, Kornelia Hardes

* These authors contributed equally as co-first authors

Journal of Visualized Experiments. 2026 March (). doi:10.3791/69384.

Alphaviruses are enveloped, single-stranded RNA viruses primarily transmitted by mosquitoes, causing numerous diseases in humans and animals. Clinically important members include chikungunya virus, Western equine encephalitis virus, as well as Eastern equine encephalitis virus. On the other hand, certain alphaviruses, such as Semliki Forest virus, exhibit low pathogenicity in humans, making them valuable models for studying viruses with higher pathogenicity. Fluorescently tagged viruses enable real-time visualization of infection to assess the efficacy of dsRNA treatments as well as antiviral compounds.

Here, a standardized protocol for monitoring alphavirus replication was established, using mCherry-tagged SFV as the model system. The protocol includes detailed procedures for preparing compounds, seeding of cells, viral infection, post-infection treatment, fluorescence microscopy for real-time visualization, and quantitative analysis of viral replication. As a demonstration, furin inhibitors were used to illustrate viral inhibition. This workflow provides

a reproducible platform for evaluating antiviral strategies in cell culture and can be adapted for other related viruses.

Chapter IV

Inhibition of Semliki Forest virus replication with long double-stranded RNA in *Aedes albopictus* cells

Alejandra Centurión, Bodunrin Omokungbe, Sabrina Stiehler, Andreas Vilcinskas, Kornelia Hardes

Virus Research. 2025 May 357(2):199584. doi: 10.1016/j.virusres.2025.199584. PMID: 40389163 PMCID: PMC12152901

Eliminating a mosquito species entirely may cause unintended ecological effects. Control strategies could therefore aim to limit viral spread within the mosquito host, rather than eradicate the population. Alphaviruses with low human pathogenicity, such as Semliki Forest virus (SFV), can serve as effective models because they share structural and genetic features.

In this study, RNAi was used to test whether viral spread within mosquitoes can be reduced. Specifically, I contributed to this study by designing dsRNAs that target six regions of the SFV genome. These dsRNAs were then assessed for their antiviral potential in *Ae. albopictus* U4.4 cells. Initial cytotoxicity assays using CellTiter-Glo demonstrated that both uncomplexed and complexed dsRNA were non-toxic to the cells, thereby ruling out any potential effects arising from cell death. Notably, most of the dsRNAs encapsulated with the K4 exhibited antiviral efficacy, reducing viral replication by up to sevenfold compared to uncomplexed dsRNA counterparts. Among the constructs evaluated, the dsRNA designed to target the non-structural protein 4 (nsp4) was the most efficient at suppressing infection. When encapsulated, nsp4-dsRNA reduced viral replication by an 80% at 72 h post-infection. Further concentration-dependent assay showed that 0.5 ng/µL of encapsulated dsRNA was sufficient to achieve significant suppression. Lastly, I also contributed by using RT-qPCR to confirm a significant knockdown of the nsp4 gene, thereby validating the antiviral efficacy of nsp4-dsRNA.

This study successfully showed that encapsulated dsRNA can inhibit arboviral spread within mosquito cell line. However, *in vivo* studies are still needed to confirm the effectiveness and to guide future applications in arbovirus control.

3 Discussion

Mosquitoes, particularly *Ae. albopictus*, are among the deadliest vectors of human diseases, transmitting pathogens responsible for dengue, chikungunya, and Zika virus infections (Becker et al., 2020). These diseases impose a heavy global public health burden, especially in tropical and subtropical regions where vector populations thrive (Becker et al., 2020; Kamerow, 2014). Conventional control measures, such as chemical insecticides, face challenges including resistances, ecological concerns, and broad effects on non-target organisms (Ranson and Lissenden, 2016; Shroff et al., 2020). These necessitate the development of alternative strategies for vector control and pathogen management (Benelli, 2015). RNAi, a conserved and sequence-specific gene silencing mechanism, offers a promising complementary approach. By targeting genes critical to mosquito survival, development, or pathogen transmission, RNAi can provide an environmentally friendly method for mosquito and pathogen management (Lopez et al., 2019; Müller et al., 2023). However, in *Ae. albopictus* the approach faces persistent challenges, including inefficient delivery, degradation of dsRNA by nucleases, and limited systemic spread (Figueiredo Prates *et al.* 2024). For these reasons, this thesis investigated the potential of RNAi as a prospective vector control method against *Ae. albopictus*, and examined practical factors that influence the efficacy.

Improving gene silencing in aedine cell lines using transfection reagents

Chapter I of this thesis focuses on delivering dsRNA into *Ae. albopictus* cell lines by using TRs, since they are known to enhance intracellular delivery of plasmids, dsRNA, siRNA, proteins, and other molecules (Balazs and Godbey, 2011). Despites these advantages, there are no TRs that are specifically designed for delivering long dsRNA into aedine cell lines. Moreover, most reagents does not have their compositions disclosed (Simberg et al., 2000). This lack of transparency makes it difficult to select suitable TRs for aedine cell lines. To address this, I selected several TRs and tested their compatibility in aedine cells. I evaluated four parameters: (1) complexing capacity, (2) cytotoxicity, (3) dsRNA uptake, and (4) transfection efficiency, measured as knockdown of reporter SFV tagged with mCherry.

Evaluating complexing capacity showed clear differences among the tested reagents. The findings indicated that it is necessary to determine optimal dsRNA:TR ratios for each reagent, rather than relying solely on manufacturer's guidelines. Moreover, most recommendations are typically for DNA, mRNA, or sometimes siRNA, but not for long dsRNA. Adjusting the ratios is critical because it balances delivery efficiency and cytotoxicity of the TRs (Kasai et al., 2019). Too much reagent can increase cytotoxicity through non-specific membrane interactions. On the

other hand, too little may leave some dsRNAs unprotected. Both of these scenarios can significantly reduce RNAi efficacy. The gel retardation assay used here offered a simple and reliable way to measure complexing capacity. It helps identify ratios that ensure complete dsRNA binding while limiting excess reagent use. Making this optimization step a routine practice could improve reproducibility across RNAi studies and allow fair comparisons between delivery reagents.

Assessing the cytotoxicity of the TRs and their complexes is necessary to rule out any effect that may arise from the use of the reagents. Cytotoxicity typically depends on the composition of the reagent, the nature of the complexes it forms, residual components, cell line sensitivity, exposure duration, and reagent concentrations (Wang et al., 2018). Meanwhile, only Lipofectamine 2000 reduced cell viability at higher concentrations tested. This was also observed in previous studies in mammalian cells, although the tolerance appears to vary between cell lines (Wang et al., 2018; Yamano et al., 2010). Most commercially available TRs are optimized for mammalian cells and not for insect ones. As such, their charge density, lipid composition, and binding affinities may not be optimal for insect membranes. Therefore, developing reagents specifically for aedine cell lines could lower any potential cytotoxic effects while improving delivery efficiency.

Efficient dsRNA uptake is required to initiate the RNAi pathway (Nikcevic et al., 2003). However, as shown here, uptake alone does not ensure functional gene silencing. While all TRs tested enhanced dsRNA internalization, only in U4.4 cells a significant knockdown of the mCherry viral reporter was observed. Therefore, it is necessary to evaluate both delivery efficiency and functional silencing when selecting reagent for RNAi delivery. The lack of RNAi response in C6/36 cells aligns with previous reports attributing this to the loss of Dicer-2, an essential enzyme for processing dsRNA into siRNAs (Brackney et al., 2010; Scott et al., 2010). This deficiency renders C6/36 cells unsuitable for evaluating RNAi-based strategies, though it has made them a preferred model for virus propagation due to reduced antiviral defense (Miller et al., 2018). In contrast, U4.4 cells, which retain a functional antiviral RNAi pathway, remain a relevant model for studying RNAi efficacy against arboviruses (Attarzadeh-Yazdi et al., 2009). It is noteworthy that U4.4 and C6/36 cells are subclones derived from the same original culture of *Ae. albopictus* neonate larvae. However, the mechanism and timing of the loss of antiviral RNAi functionality in C6/36 cells remain unclear (Weger-Lucarelli et al., 2018). Without confirming the integrity of the RNAi pathway, negative results in certain cell lines may be misinterpreted as inefficient or delivery failure rather than a pathway defect.

Knockdown of the viral reporter gene observed in U4.4 cells supports the central hypothesis of this thesis. To the best of my knowledge, no comprehensive analysis of TRs for

dsRNA delivery into mosquito cells has been reported. This work fills that gap by offering a practical framework to optimize TRs for delivering long dsRNA into aedine cell lines, and potentially other similar insect cell lines. Based on the findings in this chapter, K4, Metafectene Pro, Metafectene SI+, Lipofectamine 2000 (below 1 ng/µL), and CellFectin II are recommended for dsRNA delivery in aedine cell lines.

Potential barriers to RNAi-induced mortality in the larval stage of *Ae. albopictus*

In Chapter II, genes previously associated with high mortality in other insect species were selected, and two dsRNAs were designed and synthesized for each target. Initial evaluation of cytotoxicity, with and without TR encapsulation, showed that only the dsRNA targeting the IAP gene significantly reduced cell viability. Although all selected dsRNAs achieved significant target gene knockdown. *In vivo* larval assays showed IAP knockdown only in gut tissue, with no significant mortality.

To identify potential barriers to efficacy, I evaluated dsRNA:TR complex sizes, oral uptake, degradation by gut nucleases, and TR-mediated protection. Optimal particle sizes were observed only at low concentrations, whereas higher concentrations caused aggregation. This is likely due to the use of sterile water for dilutions (to match larval bioassay conditions), rather than recommended Grace's insect medium. Unknown TR properties could affect particle stability. If there are no stabilizers present, the particles may aggregate through charge neutralization or hydrophobic interactions, which can change the size distribution (Berger *et al.* 2021; Yazdi *et al.* 2025). Fluorescence microscopy showed that dsRNA entered the larval gut. Signal intensity was stronger and more persistent when the dsRNAs were encapsulated in TRs. The signal did not spread beyond the gut, which points to the larval midgut epithelium as a major barrier. The cuticular lining, limited endocytic transport, or restricted RNA movement may prevent dsRNA from reaching other tissues (Figueiredo Prates *et al.* 2024; Müller *et al.* 2023). In *Ae. albopictus*, specially designed formulations may be needed to enhance transcytosis or bypass gut barriers. Alternatively, essential genes that are specific to the gut could be targeted, which may be sufficient to achieve lethal knockdown without the need for systemic spread.

A major barrier to oral RNAi in *Ae. albopictus* is the presence of dsRNases in the gut. The high nuclease activity in the digestive tract quickly degrades ingested dsRNA before it can reach intracellular targets. This problem has been reported in several insects (Chen *et al.* 2021; Fan *et al.* 2021; Prentice *et al.* 2019). This appears particularly pronounced in *Ae. albopictus*, as larval gut extracts rapidly degrade dsRNA. The high dsRNase activity and their elevated gene expression in the gut of *Ae. albopictus* may reflect an evolutionary adaptation to larval habitats

rich in decaying organic matter and environmental RNA. This adaptation enables efficient digestion of dietary nucleic acids as a nutrient source and also serves as a defense against RNA viruses, thereby limiting viral infections (Giesbrecht *et al.* 2020; Hossain *et al.* 2020; Parry *et al.* 2021). Such evolutionary pressures could explain the elevated gut nuclease activity observed in this species. Therefore, any delivery platform for RNAi-based control in *Ae. albopictus* must account for the rapid extracellular degradation in the gut lumen.

One strategy to reduce nuclease activity is to deliver dsRNAs that target the nucleases together with the functional dsRNA. This approach has worked in *Ae. aegypti*, *Leptinotarsa decemlineata*, and *Dalbulus maidis* (Dalaisón-Fuentes et al., 2023; Giesbrecht et al., 2020; Spit et al., 2017). In *Ae. albopictus*, however, it seems less effective. This was likely because both dsRNAs were rapidly degraded before they can act. A previous study showed that co-delivery of shRNA targeting gut RNases did not improve RNAi efficacy in *Ae. albopictus* larvae (Figueiredo Prates et al., 2024). The presence of multiple nucleases in mosquito may also contribute, as functional redundancy could render suppression of a single nuclease insufficient to reduce overall degradation (Giesbrecht et al., 2020). Overcoming this barrier may require simultaneous silencing of multiple nucleases or the development of nuclease-resistant delivery systems. In this chapter, dsRNA encapsulated with various TRs was protected from degradation, although this protection declined over time. This suggest that while TRs are effective in cell culture, they may be suboptimal for *in vivo* larval applications. Moreover, the use of commercially available TRs here was intended for experimental purposes. Their high cost and undisclosed composition make them unsuitable candidates for potential field application.

RNAi has yielded consistent and effective gene knockdown in *Ae. aegypti* using unformulated (naked) dsRNA (Bona et al., 2016; Lopez et al., 2019; Singh et al., 2013), whereas responses in *Ae. albopictus* have been more variable and often less efficient (Figueiredo Prates et al., 2024). This variability may be partly explained by differences in immune gene complexity, as *Ae. albopictus* possesses a larger genome and more gene duplications, including immune-related ones (Chen et al., 2015; Palatini et al., 2020). However, this alone likely does not fully account for the reduced RNAi efficiency. Additional factors may include impaired systemic transport across midgut barriers or differences in the functionality of core RNAi machinery such as Dicer-2, Argonaute-2, and R2D2. While these factors could explain interspecies differences in RNAi responsiveness, direct comparative evidence is lacking. Further research is therefore needed to clarify why *Ae. albopictus* larvae are less responsive to RNAi.

Monitoring alphavirus infection in *Ae. albopictus* cell lines using fluorescence microscopy

Chapter III of this work established a protocol to monitor alphavirus infection in *Ae. albopictus* cell lines. Fluorescence microscopy provides real-time insight into viral dynamics, allowing continuous observation of infection progression without destructive sampling. Unlike endpoint assays such as plaque assay or qPCR analysis, live-cell imaging can reveal early replication events, subtle kinetic delays, and partial inhibitory effects that may be missed by endpoint measurements (Shan et al., 2016; Smither et al., 2013).

In this chapter, I used mCherry-SFV as a fluorescent reporter virus and applied furin inhibitors to demonstrate antiviral inhibition. As in previous chapters, cytotoxicity assessment was a prerequisite for reliable interpretation of antiviral outcomes. Cell line selection was also essential. For example, U4.4 cells can exhibit RNAi response to dsRNA treatment, whereas C6/36 cells, which are suspected to lack functional Dicer-2, are unable to show antiviral RNAi response (Brackney et al., 2010; Scott et al., 2010).

Reporter viruses such as mCherry-SFV can enhance the resolution of infection studies by enabling direct visualization of virus spread, but potential limitations should be acknowledged. For instance, reporter constructs may display altered replication kinetics or genetic instability (Eckert et al., 2014; Jose et al., 2017). Detached dead cells can obscure imaging fields and bias cell counts. Exposing cells to fluorescent dyes like DAPI for long period may also affect cell behavior or viability. Importantly, quantifying "fluorescence intensity per cell" with devices such as the Cytation 5 Cell Imaging Multimode Reader can be unreliable for cells in suspension and is better suited to adherent cell lines. Flow cytometry can provide a more accurate readout for suspended cells. However, it mainly captures cell that have the fluorescence signal, and therefore reflects only intracellular viral signal. As a result, it may underrepresent extracellular viral particles.

The representative result highlights the importance of host factors in viral replication. Consistent with previous studies, furin inhibition reduced viral replication (Hardes et al., 2017). Targeting host factors *via* RNAi therefore represents a promising complementary strategy for limiting arbovirus replication in *Ae. albopictus*. This protocol can be adapted for additional applications, including RNAi-based antiviral screening.

Reducing arboviral infection *via* RNAi within *Ae. albopictus*

RNAi offers a promising tool not only for reducing mosquito populations but also for selectively inhibiting viral replication within the mosquito host, without necessarily killing the

insect. Its specific mode of action enables the design of dsRNAs that targets particular arboviruses, providing an approach for disrupting virus transmission (Caplen et al., 2002). In Chapter IV, SFV was also used as a model to explore RNAi-based inhibition of viral replication. To this end, I designed dsRNAs targeting six distinct regions of the SFV genome.

Cytotoxicity of the synthesized dsRNAs was assessed in aedine U4.4 cells, with no observed cytotoxic effects. This control is essential to ensure that antiviral effects result from sequence-specific RNAi activity rather than non-specific cell death caused by delivery reagents or dsRNA itself. The absence of cytotoxicity supports their use in downstream antiviral assays.

All dsRNAs, except nsp3-dsRNA, significantly reduced SFV replication when delivered using the K4 transfection system. Uncomplexed dsRNA was much less effective. This further supports the central hypothesis that encapsulation improves RNAi efficacy. Among the six regions tested, dsRNAs against nsp1, nsp2, and nsp4 suppress viral spread very strongly. This aligns with previous work showing that RNAi targeting nsp2 and nsp4 suppresses SFV replication (Caplen *et al.* 2002). These proteins are essential for viral replication and transcription. They are critical targets in the replication cycle. Their sensitivity to RNAi likely reflects their indispensability and the limited redundancy in the replication complex (Fazakerley 2002; Kujala *et al.* 2001). Consequently, targeting conserved regions may work against multiple virus strains. It may also reduce the chance of escape mutations (Caplen *et al.* 2002). To confirm the antiviral effects of nsp4-dsRNA, I performed RT-qPCR, which showed a significant knockdown of the gene.

Additionally, dsRNA stability was assessed through fluorescence microscopy and infection assays at several time points. The dsRNA remained stable, indicating that its effect is not limited to a narrow time window. This stability suits delivery scenarios where precise timing is difficult. In future *in vivo* studies, sustained activity over time would allow more flexible application, and may strengthen cumulative antiviral effects. Establishing the minimum effective dose is also essential. It helps to optimize efficacy, minimize costs, and avoid side effects such as cytotoxicity or unintended immune activation. In this work, as little as 0.5 ng/µL dsRNA significantly inhibited viral spread, thereby providing a clear benchmark for future studies.

These findings in aedine cell line are encouraging, but translation to *in vivo* systems is the next critical step. The mosquito midgut epithelium, nucleases, and tissue-specific variability in RNAi pathway can all affect antiviral efficacy. Moreover, environmental conditions, mosquito microbiota, and feeding status could also alter dsRNA uptake and stability (Bachman et al., 2020; Huvenne and Smagghe, 2010). Future research should therefore include *in vivo* validation in adult mosquitoes under conditions that simulate natural infection and transmission cycles. Finally, the RNAi strategy developed here has potential applicability beyond SFV. With careful

target design, it could be adapted to suppress other medically important arboviruses transmitted by *Ae. albopictus*, including CHIKV, ZIKV, and DENV.

Conclusion and future perspectives

This thesis presents the first evaluation of commercially available TRs for delivering long dsRNA into aedine cell lines. It also assessed RNAi-induced mortality, established a real time platform to monitor alphavirus infection, and finally tested dsRNA as an inhibitor of viral spread. All stated objectives were addressed experimentally. Findings from cell line studies support the central hypothesis. Because, encapsulation of dsRNA improved uptake and increased RNAi efficiency. Although, in chapter II only one dsRNA reduced cell viability. *In vivo* assay in larvae led to gene knockdown, but only in the gut tissue with no significant increase in mortality. This was most likely attributed to the rapid degradation of dsRNA by gut nucleases, the suboptimal particle size of dsRNA:TR, and the insufficient systemic spread of the treatment. Therefore, future work should identify gut essential genes as target in *Ae. albopictus* and also develop formulations that protect dsRNA from *in vivo* degradation.

Beyond mosquito population control, chapter IV examined the use of RNAi to inhibit viral spread within mosquitoes. Using SFV as a model, dsRNAs targeting multiple regions of the viral genome significantly reduced replication within an *Ae. albopictus* cell line. These findings point to new avenues that targets mosquito host factors that are critical for viral replication. One such host factor is furin, a proprotein convertase involved in activating viral glycoproteins (Molloy and Thomas, 2002). Synthetic furin inhibitors have shown to reduced viral replication in many cell lines, but their limited specificity raises concerns about effects on other proteases (Hardes et al., 2017; Ivachtchenko et al., 2024; Klein-Szanto and Bassi, 2017). For this reason, future work should test RNAi mediated knockdown of furin genes in *Ae. albopictus* using dsRNA to clarify furin's role in arboviral replication. The use of dsRNA against furin as an antiviral strategy in humans also warrants investigation.

Bridging the gap from laboratory success to practical use will require more advanced delivery strategies. Genetically engineered *Chlorella vulgaris* and *Saccharomyces cerevisiae* that produce shRNA have shown promise in reducing *Ae. albopictus* populations (Deng et al., 2025; Mysore et al., 2019b; Mysore et al., 2019a; Mysore et al., 2021). Public concern on GMOs and added regulatory steps may limit broad adoption (Müller et al., 2023). Alternative delivery platforms that do not use GMOs should be explored further. Examples include chitosan nanoparticles, peptosome-based carrier, cationic polymers, and dendrimers (Chong et al., 2021; Manteghi et al., 2024).

A hypothetical RNAi bioinsecticide should meet key criteria outlined by Müller *et al.* (2023). These include high efficacy, target specificity, suitable formulation, biosafety, product stability, scalability, and cost-effectiveness. Despite current challenges in developing RNAi control for *Ae. albopictus*, this approach could meet most requirements for a bioinsecticide. Future work should also address key gaps, including long term environmental impacts, potential off-target effects, regulatory considerations related to delivery platforms, and integration with other vector management strategies.

4 References

Afzal, M.F., 2024. Systematic review of Dengue Vaccines (CYD-TDV and TAK-003) in children: efficacy, immunogenicity, safety and challenges. J Child Heal Sci 1 (1).

Airs, P.M., Bartholomay, L.C., 2017. RNA Interference for Mosquito and Mosquito-Borne Disease Control. Insects 8 (1).

Allgeier, S., Kästel, A., Brühl, C.A., 2019. Adverse effects of mosquito control using Bacillus thuringiensis var. israelensis: Reduced chironomid abundances in mesocosm, semi-field and field studies. Ecotoxicology and environmental safety 169 (14), 786–796.

Almeida, M.V., Andrade-Navarro, M.A., Ketting, R.F., 2019. Function and Evolution of Nematode RNAi Pathways. Non-coding RNA 5 (1).

APVMA, 2024. Final regulatory decision for malathion reconsideration. Australian Pesticides and Veterinary Medicines Authority. https://www.apvma.gov.au/news-and-publications/news/final-regulatory-decision-malathion-reconsideration. Accessed 20 August 2025.

Assis, T.S.M. de, Lima, A.L.F. de, Carvalho, F.D., 2023. Economic assessments for Chikungunya: a narrative review. Braz. J. Hea. Rev. 6 (4), 14683–14692.

Atkins, G.J., Sheahan, B.J., Liljeström, P., 1999. The molecular pathogenesis of Semliki Forest virus: a model virus made useful? journal of general virology 80 (9), 2287–2297.

Attarzadeh-Yazdi, G., Fragkoudis, R., Chi, Y., Siu, R.W.C., Ulper, L., Barry, G., Rodriguez-Andres, J., Nash, A.A., Bouloy, M., Merits, A., Fazakerley, J.K., Kohl, A., 2009. Cell-to-cell spread of the RNA interference response suppresses Semliki Forest virus (SFV) infection of mosquito cell cultures and cannot be antagonized by SFV. Journal of virology 83 (11), 5735–5748.

Bachman, P., Fischer, J., Song, Z., Urbanczyk-Wochniak, E., Watson, G., 2020. Environmental Fate and Dissipation of Applied dsRNA in Soil, Aquatic Systems, and Plants. Frontiers in plant science 11 (21).

Balazs, D.A., Godbey, W., 2011. Liposomes for use in gene delivery. Journal of drug delivery 2011 (1), 326497.

Baum, J.A., Bogaert, T., Clinton, W., Heck, G.R., Feldmann, P., Ilagan, O., Johnson, S., Plaetinck, G., Munyikwa, T., Pleau, M., Vaughn, T., Roberts, J., 2007. Control of coleopteran insect pests through RNA interference. Nature biotechnology 25 (11), 1322–1326.

Becker, N., Petrić, D., Zgomba, M., Boase, C., Madon, M.B., Dahl, C., Kaiser, A., 2020. Mosquitoes. Springer International Publishing, Cham.

Becker, N., Pluskota, B., Kaiser, A., Schaffner, F., 2012. Exotic Mosquitoes Conquer the World, in: Mehlhorn, H. (Ed.), Arthropods as Vectors of Emerging Diseases, vol. 3. Springer Berlin Heidelberg, Berlin, Heidelberg, pp. 31–60.

Belousova, M.E., Malovichko, Y.V., Shikov, A.E., Nizhnikov, A.A., Antonets, K.S., 2021. Dissecting the Environmental Consequences of Bacillus thuringiensis Application for Natural Ecosystems. Toxins 13 (5).

Benelli, G., 2015. Research in mosquito control: current challenges for a brighter future. Parasitology research 114 (8), 2801–2805.

Blair, C.D., 2011. Mosquito RNAi is the major innate immune pathway controlling arbovirus infection and transmission. Future microbiology 6 (3), 265–277.

Bona, A.C.D., Chitolina, R.F., Fermino, M.L., Castro Poncio, L. de, Weiss, A., Lima, J.B.P., Paldi, N., Bernardes, E.S., Henen, J., Maori, E., 2016. Larval application of sodium channel homologous dsRNA restores pyrethroid insecticide susceptibility in a resistant adult mosquito population. Parasites & vectors 9 (1), 397.

Brackney, D.E., Scott, J.C., Sagawa, F., Woodward, J.E., Miller, N.A., Schilkey, F.D., Mudge, J., Wilusz, J., Olson, K.E., Blair, C.D., Ebel, G.D., 2010. C6/36 Aedes albopictus cells have a dysfunctional antiviral RNA interference response. PLoS neglected tropical diseases 4 (10), e856.

Brady, O.J., Golding, N., Pigott, D.M., Kraemer, M.U.G., Messina, J.P., Reiner Jr, R.C., Scott, T.W., Smith, D.L., Gething, P.W., Hay, S.I., 2014. Global temperature constraints on Aedes aegypti and Ae. albopictus persistence and competence for dengue virus transmission. Parasites & vectors 7 (1), 338.

Breeland, S.G., Jeffery, G.M., Lofgren, C.S., Weidhaas, D.E., 1974. Release of chemosterilized males for the control of Anopheles albimanus in El Salvador. III. Field methods and population control. American Journal of Tropical Medicine and Hygiene 23 (2), 288–297.

Brühl, C.A., Després, L., Frör, O., Patil, C.D., Poulin, B., Tetreau, G., Allgeier, S., 2020. Environmental and socioeconomic effects of mosquito control in Europe using the biocide Bacillus thuringiensis subsp. israelensis (Bti). The Science of the total environment 724 (137800).

Calba, C., Guerbois-Galla, M., Franke, F., Jeannin, C., Auzet-Caillaud, M., Grard, G., Pigaglio, L., Decoppet, A., Weicherding, J., Savaill, M.-C., Munoz-Riviero, M., Chaud, P., Cadiou, B., Ramalli, L., Fournier, P., Noël, H., Lamballerie, X. de, Paty, M.-C., Leparc-Goffart, I., 2017. Preliminary report of an autochthonous chikungunya outbreak in France, July to September 2017. Euro surveillance : bulletin Europeen sur les maladies transmissibles = European communicable disease bulletin 22 (39).

Cancrini, G., Di Frangipane Regalbono, A., Ricci, I., Tessarin, C., Gabrielli, S., Pietrobelli, M., 2003. Aedes albopictus is a natural vector of Dirofilaria immitis in Italy. Veterinary parasitology 118 (3-4), 195–202.

Caplen, N.J., Zheng, Z., Falgout, B., Morgan, R.A., 2002. Inhibition of viral gene expression and replication in mosquito cells by dsRNA-triggered RNA interference. Molecular therapy : the journal of the American Society of Gene Therapy 6 (2), 243–251.

Caputo, B., Russo, G., Manica, M., Vairo, F., Poletti, P., Guzzetta, G., Merler, S., Scagnolari, C., Solimini, A., 2020. A comparative analysis of the 2007 and 2017 Italian chikungunya outbreaks and implication for public health response. PLoS neglected tropical diseases 14 (6), e0008159.

Chen, J., Lu, H.-R., Zhang, L., Liao, C.-H., Han, Q., 2019. RNA interference-mediated knockdown of 3, 4-dihydroxyphenylacetaldehyde synthase affects larval development and adult survival in the mosquito Aedes aegypti. Parasites & vectors 12 (1), 311.

Chen, X.-G., Jiang, X., Gu, J., Xu, M., Wu, Y., Deng, Y., Zhang, C., Bonizzoni, M., Dermauw, W., Vontas, J., Armbruster, P., Huang, X., Yang, Y., Zhang, H., He, W., Peng, H., Liu, Y., Wu, K., Chen, J., Lirakis, M., Topalis, P., van Leeuwen, T., Hall, A.B., Jiang, X., Thorpe, C., Mueller, R.L., Sun, C., Waterhouse, R.M., Yan, G., Tu, Z.J., Fang, X., James, A.A., 2015. Genome sequence of the Asian Tiger mosquito, Aedes albopictus, reveals insights into its biology, genetics, and evolution. Proceedings of the National Academy of Sciences of the United States of America 112 (44), E5907-15.

Cheng, G., Liu, L., Wang, P., Zhang, Y., Zhao, Y.O., Colpitts, T.M., Feitosa, F., Anderson, J.F., Fikrig, E., 2011. An in vivo transfection approach elucidates a role for Aedes aegypti thioester-containing proteins in flaviviral infection. PloS one 6 (7), e22786.

Chersoni, L., Checcucci, A., Malfacini, M., Puggioli, A., Balestrino, F., Carrieri, M., Piunti, I., Dindo, M.L., Mattarelli, P., Bellini, R., 2021. The Possible Role of Microorganisms in Mosquito Mass Rearing. Insects 12 (7).

Chong, Z.X., Yeap, S.K., Ho, W.Y., 2021. Transfection types, methods and strategies: a technical review. PeerJ 9 (e11165).

Choudhary, N., Goyal, R., Joshi, S.C., 2008. Effect of malathion on reproductive system of male rats. Journal of Environmental Biology 29 (2), 259–262.

Contu, L., Balistreri, G., Domanski, M., Uldry, A.-C., Mühlemann, O., 2021. Characterisation of the Semliki Forest Virus-host cell interactome reveals the viral capsid protein as an inhibitor of nonsense-mediated mRNA decay. PLoS pathogens 17 (5), e1009603.

Cunze, S., Koch, L.K., Kochmann, J., Klimpel, S., 2016. Aedes albopictus and Aedes japonicus - two invasive mosquito species with different temperature niches in Europe. Parasites & vectors 9 (1), 573.

Dalaisón-Fuentes, L.I., Pascual, A., Crespo, M., Andrada, N.L., Welchen, E., Catalano, M.I., 2023. Knockdown of double-stranded RNases (dsRNases) enhances oral RNA interference (RNAi) in the corn leafhopper, Dalbulus maidis. Pesticide biochemistry and physiology 196 (105618).

Deng, X., Xue, C., Gao, J., Huang, X., Xu, D., Li, J., Fei, X., 2025. Control of Aedes albopictus populations by silencing of the vesicular GABA transporter (vgat) and the vesicular monoamine transporter (vmat) genes using recombinant Chlorella shRNA. Parasites & vectors 18 (1), 414.

Dhandapani, R.K., Gurusamy, D., Howell, J.L., Palli, S.R., 2019. Development of CS-TPP-dsRNA nanoparticles to enhance RNAi efficiency in the yellow fever mosquito, Aedes aegypti. Scientific reports 9 (1), 8775.

ECDC-EFSA, 2025. European Centre for Disease Prevention and Control and European Food Safety Authority: Mosquito maps [internet]. Stockholm. https://www.ecdc.europa.eu/en/publications-data/aedes-albopictus-current-known-distribution-june-2025. Accessed 3 July 2025.

Eckert, N., Wrensch, F., Gärtner, S., Palanisamy, N., Goedecke, U., Jäger, N., Pöhlmann, S., Winkler, M., 2014. Influenza A virus encoding secreted Gaussia luciferase as useful tool to analyze viral replication and its inhibition by antiviral compounds and cellular proteins. PloS one 9 (5), e97695.
Eldridge, B.F., Scott, T.W., Day, J.F., Tabachnick, W.J., 2004. Arbovirus Diseases, in: Eldridge, B.F., Edman, J.D. (Eds.), Medical Entomology. Springer Netherlands, Dordrecht, pp. 415–460.
Ensley, S.M., 2018. Pyrethrins and Pyrethroids, in: , Veterinary Toxicology, 3rd ed. Academic Press, San Diego, pp. 515–520.
Fang, X., Qi, Y., 2016. RNAi in Plants: An Argonaute-Centered View. The Plant cell 28 (2), 272–285.
Fansiri, T., Pongsiri, A., Khongtak, P., Nitatsukprasert, C., Chittham, W., Jaichapor, B., Pathawong, N., Kijchalao, U., Tiangtrong, S., Singkhaimuk, P., Ponlawat, A., 2022. The impact of insect growth regulators on adult emergence inhibition and the fitness of Aedes aegypti field populations in Thailand. Acta tropica 236 (suppl. 1), 106695.
Figueiredo Prates, L.H., Fiebig, J., Schlosser, H., Liapi, E., Rehling, T., Lutrat, C., Bouyer, J., Sun, Q., Wen, H., Xi, Z., Schetelig, M.F., Häcker, I., 2024. Challenges of Robust RNAi-Mediated Gene Silencing in Aedes Mosquitoes. International journal of molecular sciences 25 (10).
Fire, A., Xu, S., Montgomery, M.K., Kostas, S.A., Driver, S.E., Mello, C.C., 1998. Potent and specific genetic interference by double-stranded RNA in Caenorhabditis elegans. Nature 391 (6669), 806–811.
Fire, A.Z., 2007. Gene silencing by double-stranded RNA (Nobel Lecture). Angewandte Chemie (International ed. in English) 46 (37), 6966–6984.
Flandes, X., Hansen, C.A., Palani, S., Abbas, K., Bennett, C., Caro, W.P., Hutubessy, R., Khazhidinov, K., Lambach, P., Maure, C., Marshall, C., Rojas, D.P., Rosewell, A., Sahastrabuddhe, S., Tufet, M., Wilder-Smith, A., Beasley, D.W.C., Bourne, N., Barrett, A.D.T., 2024. Vaccine value profile for Chikungunya. Vaccine 42 (19S1), S9-S24.
Foster, W.A., Walker, E.D., 2019. Mosquitoes (Culicidae), in: Mullen, Gary R. and Durden, Lance A. (Ed.), Medical and Veterinary Entomology. Elsevier, pp. 261–325.
Fournier, L., Durand, G.A., Cochet, A., Brottet, E., Fiet, C., Mano, Q., Krug, C., Verdurme, L., Blanchot, T., Fournier, R., Paty, M.-C., Grard, G., Franke, F., Calba, C., 2025. Multiple early local transmissions of chikungunya virus, Mainland France, from May 2025. Euro surveillance : bulletin Europeen sur les maladies transmissibles = European communicable disease bulletin 30 (32).
Gajendiran, A., Abraham, J., 2018. An overview of pyrethroid insecticides. Front. Biol. 13 (2), 79–90.
Giesbrecht, D., Heschuk, D., Wiens, I., Boguski, D., LaChance, P., Whyard, S., 2020. RNA Interference Is Enhanced by Knockdown of double-stranded RNases in the Yellow Fever Mosquito Aedes Aegypti. Insects 11 (6).
Godói, I.P., Lemos, L.L.P., Araújo, V.E. de, Bonoto, B.C., Godman, B., Guerra Júnior, A.A., 2017. CYD-TDV dengue vaccine: systematic review and meta-analysis of efficacy, immunogenicity and safety. Journal of comparative effectiveness research 6 (2), 165–180.
Gouagna, L.C., Damiens, D., Oliva, C.F., Boyer, S., Le Goff, G., Brengues, C., Dehecq, J.-S., Raude, J., Simard, F., Fontenille, D., 2020. Strategic Approach, Advances, and Challenges in the Development and Application of the SIT for Area-Wide Control of Aedes albopictus Mosquitoes in Reunion Island. Insects 11 (11).
Hall, M., Tamïr, D. (Eds.), 2022. Mosquitopia: The place of pests in a healthy world. Routledge/Taylor & Francis Group, London Oxon, New York, xxi, 289 pages.
Hammond, A.M., Galizi, R., 2017. Gene drives to fight malaria: current state and future directions. Pathogens and global health 111 (8), 412–423.
Hapairai, L.K., Mysore, K., Chen, Y., Harper, E.I., Scheel, M.P., Lesnik, A.M., Sun, L., Severson, D.W., Wei, N., Duman-Scheel, M., 2017. Lure-and-Kill Yeast Interfering RNA Larvicides Targeting Neural Genes in the Human Disease Vector Mosquito Aedes aegypti. Scientific reports 7 (1), 13223.
Harbach, R., 2007. The Culicidae (Diptera): a review of taxonomy, classification and phylogeny*. Zootaxa 1668 (1).
Hardes, K., Ivanova, T., Thaa, B., McInerney, G.M., Klokk, T.I., Sandvig, K., Künzel, S., Lindberg, I., Steinmetzer, T., 2017. Elongated and Shortened Peptidomimetic Inhibitors of the Proprotein Convertase Furin. ChemMedChem 12 (8), 613–620.
Harris, A., McKemey, A.R., Nimmo, D., Curtis, Z., Black, I., Morgan, S.A., Oviedo, M.N., Lacroix, R., Naish, N., Morrison, N.I., Collado, A., Stevenson, J., Scaife, S., Dafa'alla, T.F.G., Phillips, C., Miles, A., Raduan, N., Kelly, N., Beech, C., Donnelly, C.A., Petrie, W.D., Alphey, L., 2012. Successful

suppression of a field mosquito population by sustained release of engineered male mosquitoes. Nature biotechnology 30 (9), 828–830.
Harrison, R.E., Brown, M.R., Strand, M.R., 2021. Whole blood and blood components from vertebrates differentially affect egg formation in three species of anautogenous mosquitoes. Parasites & vectors 14 (1), 119.
Hennessey, M., Fischer, M., Staples, J.E., 2016. Zika Virus Spreads to New Areas - Region of the Americas, May 2015-January 2016. MMWR. Morbidity and mortality weekly report 65 (3), 55–58.
Herath, J.M.M.K., Silva, W.A.P.P. de, Weeraratne, T.C., Karunaratne, S.H.P.P., 2024. Efficacy of the insect growth regulator novaluron in the control of dengue vector mosquitoes Aedes aegypti and Ae. albopictus. Scientific reports 14 (1), 1988.
Hien, D.F.D.S., Dabiré, K.R., Roche, B., Diabaté, A., Yerbanga, R.S., Cohuet, A., Yameogo, B.K., Gouagna, L.-C., Hopkins, R.J., Ouedraogo, G.A., Simard, F., Ouedraogo, J.-B., Ignell, R., Lefevre, T., 2016. Plant-Mediated Effects on Mosquito Capacity to Transmit Human Malaria. PLoS pathogens 12 (8), e1005773.
Huang, Y.-J.S., Higgs, S., Vanlandingham, D.L., 2017. Biological Control Strategies for Mosquito Vectors of Arboviruses. Insects 8 (1).
Huber, J.H., Childs, M.L., Caldwell, J.M., Mordecai, E.A., 2018. Seasonal temperature variation influences climate suitability for dengue, chikungunya, and Zika transmission. PLoS neglected tropical diseases 12 (5), e0006451.
Hurlbert, S.H., Zedler, J., Fairbanks, D., 1972. Ecosystem Alteration by Mosquitofish (Gambusia affinis) Predation. Science 175 (4022), 639–641.
Hurlbert, S.H., Zedler, J., Fairbanks, D., 1981. Impacts of mosquitofish (Gambusia affinis) predation on plankton communities. Hydrobiologia 83 (1), 125–151.
Hustedt, J.C., Boyce, R., Bradley, J., Hii, J., Alexander, N., 2020. Use of pyriproxyfen in control of Aedes mosquitoes: A systematic review. PLoS neglected tropical diseases 14 (6), e0008205.
Huvenne, H., Smagghe, G., 2010. Mechanisms of dsRNA uptake in insects and potential of RNAi for pest control: a review. Journal of insect physiology 56 (3), 227–235.
Isoe, J., Koch, L.E., Isoe, Y.E., Rascón, A.A., Brown, H.E., Massani, B.B., Miesfeld, R.L., 2019. Identification and characterization of a mosquito-specific eggshell organizing factor in Aedes aegypti mosquitoes. PLoS biology 17 (1), e3000068.
Ivachtchenko, A.V., Khvat, A.V., Shkil, D.O., 2024. Development and Prospects of Furin Inhibitors for Therapeutic Applications. International journal of molecular sciences 25 (17).
Jarman, W.M., Ballschmiter, K., 2012. From coal to DDT: the history of the development of the pesticide DDT from synthetic dyes till Silent Spring. Endeavour 36 (4), 131–142.
Jensen, I.M., Whatling, P., 2010. Chapter 71 - Malathion: A Review of Toxicology, Hayes' Handbook of Pesticide Toxicology (Third Edition) ed. Academic Press, 16 pp.
Jones, R.T., Ant, T.H., Cameron, M.M., Logan, J.G., 2021. Novel control strategies for mosquito-borne diseases. Philosophical transactions of the Royal Society of London. Series B, Biological sciences 376 (1818), 20190802.
Jose, J., Taylor, A.B., Kuhn, R.J., 2017. Spatial and Temporal Analysis of Alphavirus Replication and Assembly in Mammalian and Mosquito Cells. mBio 8 (1).
Kamerow, D., 2014. The world's deadliest animal. BMJ (Clinical research ed.) 348 (g3258).
Karunaratne, S., Surendran, S.N., 2022. Mosquito control: A review on the past, present and future strategies. J. Natn. Sci. Foundation Sri Lanka 50 (0), 277.
Kasai, H., Inoue, K., Imamura, K., Yuvienco, C., Montclare, J.K., Yamano, S., 2019. Efficient siRNA delivery and gene silencing using a lipopolypeptide hybrid vector mediated by a caveolae-mediated and temperature-dependent endocytic pathway. Journal of nanobiotechnology 17 (1), 11.
Kigozi, R., Baxi, S.M., Gasasira, A., Sserwanga, A., Kakeeto, S., Nasr, S., Rubahika, D., Dissanayake, G., Kamya, M.R., Filler, S., Dorsey, G., 2012. Indoor residual spraying of insecticide and malaria morbidity in a high transmission intensity area of Uganda. PloS one 7 (8), e42857.
Kim, D., Rossi, J., 2008. RNAi mechanisms and applications. BioTechniques 44 (5), 613–616.
Klein-Szanto, A.J., Bassi, D.E., 2017. Proprotein convertase inhibition: Paralyzing the cell's master switches. Biochemical pharmacology 140, 8–15.
Knorr, E., Fishilevich, E., Tenbusch, L., Frey, M.L.F., Rangasamy, M., Billion, A., Worden, S.E., Gandra, P., Arora, K., Lo, W., Schulenberg, G., Valverde-Garcia, P., Vilcinskas, A., Narva, K.E., 2018. Gene

silencing in Tribolium castaneum as a tool for the targeted identification of candidate RNAi targets in crop pests. Scientific reports 8 (1), 2061.
Kotsakiozi, P., Richardson, J.B., Pichler, V., Favia, G., Martins, A.J., Urbanelli, S., Armbruster, P.A., Caccone, A., 2017. Population genomics of the Asian tiger mosquito, Aedes albopictus: insights into the recent worldwide invasion. Ecology and evolution 7 (23), 10143–10157.
Kraemer, M., Reiner, R.C., Brady, O.J., 2019. Past and future spread of the arbovirus vectors *Aedes aegypti* and *Aedes albopictus*. Nature microbiology 4, 854–863.
Krauer, F., Riesen, M., Reveiz, L., Oladapo, O.T., Martínez-Vega, R., Porgo, T.V., Haefliger, A., Broutet, N.J., Low, N., 2017. Zika Virus Infection as a Cause of Congenital Brain Abnormalities and Guillain-Barré Syndrome: Systematic Review. PLoS medicine 14 (1), e1002203.
Lacey, L.A., 2007. Bacillus thuringiensis serovariety israelensis and Bacillus sphaericus for mosquito control. Journal of the American Mosquito Control Association 23 (sp2), 133–163.
Lax, C., Tahiri, G., Patiño-Medina, J.A., Cánovas-Márquez, J.T., Pérez-Ruiz, J.A., Osorio-Concepción, M., Navarro, E., Calo, S., 2020. The Evolutionary Significance of RNAi in the Fungal Kingdom. International journal of molecular sciences 21 (24).
Lee, H., Halverson, S., Ezinwa, N., 2018. Mosquito-Borne Diseases. Primary care 45 (3), 393–407.
Lee, W.-S., Webster, J.A., Madzokere, E.T., Stephenson, E.B., Herrero, L.J., 2019. Mosquito antiviral defense mechanisms: a delicate balance between innate immunity and persistent viral infection. Parasites & vectors 12 (1), 165.
Levain, A., Joly, P.B., Barbier, M., Cardon, V., Dedieu, F., Pellissier, F., 2015. Continuous discontinuation – The DDT Ban revisited. 6. International Sustainability Transitions Conference "Sustainability transitions and wider transformative change, historical roots and future pathways", University of Sussex. Brighton, GBR., Aug 2015, Brighton, United Kingdom.
Lima Cavalcanti, T.Y.V. de, Pereira, M.R., Paula, S.O. de, Franca, R.F.d.O., 2022. A Review on Chikungunya Virus Epidemiology, Pathogenesis and Current Vaccine Development. Viruses 14 (5).
Liu, J., Swevers, L., Kolliopoulou, A., Smagghe, G., 2019. Arboviruses and the Challenge to Establish Systemic and Persistent Infections in Competent Mosquito Vectors: The Interaction With the RNAi Mechanism. Frontiers in physiology 10 (890).
Liu, N., 2015. Insecticide resistance in mosquitoes: impact, mechanisms, and research directions. Annual review of entomology 60, 537–559.
Lopez, S.B.G., Guimarães-Ribeiro, V., Rodriguez, J.V.G., Dorand, F.A.P.S., Salles, T.S., Sá-Guimarães, T.E., Alvarenga, E.S.L., Melo, A.C.A., Almeida, R.V., Moreira, M.F., 2019. RNAi-based bioinsecticide for Aedes mosquito control. Scientific reports 9 (1), 4038.
Lucas, K.J., Myles, K.M., Raikhel, A.S., 2013. Small RNAs: a new frontier in mosquito biology. Trends in parasitology 29 (6), 295–303.
Lwande, O.W., Obanda, V., Lindström, A., Ahlm, C., Evander, M., Näslund, J., Bucht, G., 2020. Globe-Trotting Aedes aegypti and Aedes albopictus: Risk Factors for Arbovirus Pandemics. Vector borne and zoonotic diseases (Larchmont, N.Y.) 20 (2), 71–81.
Madewell, Z.J., 2020. Arboviruses and Their Vectors. Southern medical journal 113 (10), 520–523.
Madhav, M., Blasdell, K.R., Trewin, B., Paradkar, P.N., López-Denman, A.J., 2024. Culex-Transmitted Diseases: Mechanisms, Impact, and Future Control Strategies using Wolbachia. Viruses 16 (7).
Mains, J.W., Kelly, P.H., Dobson, K.L., Petrie, W.D., Dobson, S.L., 2019. Localized Control of Aedes aegypti (Diptera: Culicidae) in Miami, FL, via Inundative Releases of Wolbachia-Infected Male Mosquitoes. Journal of medical entomology 56 (5), 1296–1303.
Manteghi, M., Can, O., Kocagoz, T., 2024. Peptosome: A New Efficient Transfection Tool as an Alternative to Liposome. International journal of molecular sciences 25 (13).
Mao, Y.-B., Cai, W.-J., Wang, J.-W., Hong, G.-J., Tao, X.-Y., Wang, L.-J., Huang, Y.-P., Chen, X.-Y., 2007. Silencing a cotton bollworm P450 monooxygenase gene by plant-mediated RNAi impairs larval tolerance of gossypol. Nature biotechnology 25 (11), 1307–1313.
Marini, G., Manica, M., Arnoldi, D., Inama, E., Rosà, R., Rizzoli, A., 2020. Influence of Temperature on the Life-Cycle Dynamics of Aedes albopictus Population Established at Temperate Latitudes: A Laboratory Experiment. Insects 11 (11).
Miller, J.R., Koren, S., Dilley, K.A., Puri, V., Brown, D.M., Harkins, D.M., Thibaud-Nissen, F., Rosen, B., Chen, X.-G., Tu, Z., Sharakhov, I.V., Sharakhova, M.V., Sebra, R., Stockwell, T.B., Bergman, N.H.,

Sutton, G.G., Phillippy, A.M., Piermarini, P.M., Shabman, R.S., 2018. Analysis of the Aedes albopictus C6/36 genome provides insight into cell line utility for viral propagation. GigaScience 7 (3), 1–13.
Mohammadi, L., Pal, K., Bilal, M., Rahdar, A., Fytianos, G., Kyzas, G.Z., 2021. Green nanoparticles to treat patients with Malaria disease: An overview. Journal of Molecular Structure 1229 (19).
Molloy, S.S., Thomas, G., 2002. Furin, in: , Co- and Posttranslational Proteolysis of Proteins, vol. 22. Elsevier, pp. 199–235.
Muja-Bajraktari, N., Kadriaj, P., Zhushi-Etemi, F., Sherifi, K., Alten, B., Petrić, D., Velo, E., Schaffner, F., 2022. The Asian tiger mosquito Aedes albopictus (Skuse) in Kosovo: First record. PloS one 17 (3), e0264300.
Müller, R., Bálint, M., Hardes, K., Hollert, H., Klimpel, S., Knorr, E., Kochmann, J., Lee, K.-Z., Mehring, M., Pauls, S.U., Smets, G., Steinbrink, A., Vilcinskas, A., 2023. RNA interference to combat the Asian tiger mosquito in Europe: A pathway from design of an innovative vector control tool to its application. Biotechnology advances 66 (8), 108167.
Munawar, K., Alahmed, A.M., Khalil, S.M.S., 2020. Delivery Methods for RNAi in Mosquito Larvae. Journal of insect science (Online) 20 (4).
Mysore, K., Li, P., Wang, C.-W., Hapairai, L.K., Scheel, N.D., Realey, J.S., Sun, L., Roethele, J.B., Severson, D.W., Wei, N., Duman-Scheel, M., 2019a. Characterization of a yeast interfering RNA larvicide with a target site conserved in the synaptotagmin gene of multiple disease vector mosquitoes. PLoS neglected tropical diseases 13 (5), e0007422.
Mysore, K., Li, P., Wang, C.-W., Hapairai, L.K., Scheel, N.D., Realey, J.S., Sun, L., Severson, D.W., Wei, N., Duman-Scheel, M., 2019b. Characterization of a broad-based mosquito yeast interfering RNA larvicide with a conserved target site in mosquito semaphorin-1a genes. Parasites & vectors 12 (1), 256.
Mysore, K., Sun, L., Hapairai, L.K., Wang, C.-W., Roethele, J.B., Igiede, J., Scheel, M.P., Scheel, N.D., Li, P., Wei, N., Severson, D.W., Duman-Scheel, M., 2021. A Broad-Based Mosquito Yeast Interfering RNA Pesticide Targeting Rbfox1 Represses Notch Signaling and Kills Both Larvae and Adult Mosquitoes. Pathogens 10 (10).
Newhart, K., 2006. Environmental Fate of Malathion. California Environmental Protection Agency Department of Pesticide Regulation Environmental Monitoring Branch 11, 1–20.
Nikcevic, G., Kovacevic-Grujicic, N., Stevanovic, M., 2003. Improved transfection efficiency of cultured human cells. Cell biology international 27 (9), 735–737.
Oliva, C.F., Benedict, M.Q., Collins, C.M., Baldet, T., Bellini, R., Bossin, H., Bouyer, J., Corbel, V., Facchinelli, L., Fouque, F., Geier, M., Michaelakis, A., Roiz, D., Simard, F., Tur, C., Gouagna, L.-C., 2021. Sterile Insect Technique (SIT) against Aedes Species Mosquitoes: A Roadmap and Good Practice Framework for Designing, Implementing and Evaluating Pilot Field Trials. Insects 12 (3).
Oliva, C.F., Vreysen, M.J.B., Dupé, S., Lees, R.S., Gilles, J.R.L., Gouagna, L.-C., Chhem, R., 2014. Current status and future challenges for controlling malaria with the sterile insect technique: technical and social perspectives. Acta tropica 132 (1), S130-S139.
Olliaro, P., Fouque, F., Kroeger, A., Bowman, L., Velayudhan, R., Santelli, A.C., Garcia, D., Skewes Ramm, R., Sulaiman, L.H., Tejeda, G.S., Morales, F.C., Gozzer, E., Garrido, C.B., Quang, L.C., Gutierrez, G., Yadon, Z.E., Runge-Ranzinger, S., 2018. Improved tools and strategies for the prevention and control of arboviral diseases: A research-to-policy forum. PLoS neglected tropical diseases 12 (2), e0005967.
Olson, K.E., Blair, C.D., 2015. Arbovirus-mosquito interactions: RNAi pathway. Current opinion in virology 15, 119–126.
Ovcharenko, D., Jarvis, R., Hunicke-Smith, S., Kelnar, K., Brown, D., 2005. High-throughput RNAi screening in vitro: from cell lines to primary cells. RNA (New York, N.Y.) 11 (6), 985–993.
Palatini, U., Masri, R.A., Cosme, L.V., Koren, S., Thibaud-Nissen, F., Biedler, J.K., Krsticevic, F., Johnston, J.S., Halbach, R., Crawford, J.E., Antoshechkin, I., Failloux, A.-B., Pischedda, E., Marconcini, M., Ghurye, J., Rhie, A., Sharma, A., Karagodin, D.A., Jenrette, J., Gamez, S., Miesen, P., Masterson, P., Caccone, A., Sharakhova, M.V., Tu, Z., Papathanos, P.A., van Rij, R.P., Akbari, O.S., Powell, J., Phillippy, A.M., Bonizzoni, M., 2020. Improved reference genome of the arboviral vector Aedes albopictus. Genome biology 21 (1), 215.
Petersen, L.R., Powers, A.M., 2016. Chikungunya: epidemiology. F1000Research 5 (82).

Pohjala, L., Utt, A., Varjak, M., Lulla, A., Merits, A., Ahola, T., Tammela, P., 2011. Inhibitors of alphavirus entry and replication identified with a stable Chikungunya replicon cell line and virus-based assays. PloS one 6 (12), e28923.
Pyke, G.H., 2008. Plague Minnow or Mosquito Fish? A Review of the Biology and Impacts of Introduced Gambusia Species. Annu. Rev. Ecol. Evol. Syst. 39 (1), 171–191.
Rajak, P., Ganguly, A., Adhikary, S., Bhattacharya, S., 2024. Smart technology for mosquito control: Recent developments, challenges, and future prospects. Acta tropica 258 (1), 107348.
Ranson, H., Lissenden, N., 2016. Insecticide Resistance in African Anopheles Mosquitoes: A Worsening Situation that Needs Urgent Action to Maintain Malaria Control. Trends in parasitology 32 (3), 187–196.
Ratcliffe, N.A., Furtado Pacheco, J.P., Dyson, P., Castro, H.C., Gonzalez, M.S., Azambuja, P., Mello, C.B., 2022. Overview of paratransgenesis as a strategy to control pathogen transmission by insect vectors. Parasites & vectors 15 (1), 112.
Romoser, W.S., Lucas, E.A., 1999. Buoyancy and diving behavior in mosquito pupae. Journal of the American Mosquito Control Association 15 (2), 194–199.
Schäfer, M.L., Lundström, J.O., 2014. Efficiency of Bti-based floodwater mosquito control in Sweden – four examples. Journal of the European Mosquito Control Association 32, 1–8.
Schweizer, M., Miksch, L., Köhler, H.-R., Triebskorn, R., 2019. Does Bti (Bacillus thuringiensis var. israelensis) affect Rana temporaria tadpoles? Ecotoxicology and environmental safety 181 (1), 121–129.
Scott, J.C., Brackney, D.E., Campbell, C.L., Bondu-Hawkins, V., Hjelle, B., Ebel, G.D., Olson, K.E., Blair, C.D., 2010. Comparison of dengue virus type 2-specific small RNAs from RNA interference-competent and -incompetent mosquito cells. PLoS neglected tropical diseases 4 (10), e848.
Seshadri, H., Jindal, H., Madan, H., Verma, A., Khan, E., Deb, N., Walecha, A., Suresh, V., 2023. Zika Virus Outbreaks: a Narrative Review. Curr Trop Med Rep 10 (4), 332–343.
Setten, R.L., Rossi, J.J., Han, S.-P., 2019. The current state and future directions of RNAi-based therapeutics. Nature reviews. Drug discovery 18 (6), 421–446.
Shan, L., Yang, D., Wang, D., Tian, P., 2016. Comparison of cell-based and PCR-based assays as methods for measuring infectivity of Tulane virus. Journal of virological methods 231 (Suppl. 2), 1–7.
Shroff, S., Mir, S., Naik, B., Baitharu, I., Behera, A.K., 2020. Chemical Methods for Control of Mosquito Vector, in: Barik, T.K. (Ed.), Molecular Identification of Mosquito Vectors and Their Management. Springer Singapore, Singapore, pp. 35–50.
Simberg, D., Hirsch-Lerner, D., Nissim, R., Barenholz, Y., 2000. Comparison of Different Commercially Available Cationic Lipid-Based Transfection Kits. Journal of Liposome Research 10 (1), 1–13.
Singh, A.D., Wong, S., Ryan, C.P., Whyard, S., 2013. Oral delivery of double-stranded RNA in larvae of the yellow fever mosquito, Aedes aegypti: implications for pest mosquito control. Journal of insect science (Online) 13 (69), 69.
Singh, H., Tripathi, V.N., 2003. Field Trial of Relative Efficacy of Abate and Bacillus thuringiensis Against Simulium himalayense Larvae (Diptera simulidae). Medical journal, Armed Forces India 59 (2), 111–113.
Smither, S.J., Lear-Rooney, C., Biggins, J., Pettitt, J., Lever, M.S., Olinger, G.G., 2013. Comparison of the plaque assay and 50% tissue culture infectious dose assay as methods for measuring filovirus infectivity. Journal of virological methods 193 (2), 565–571.
Sobhy, I.S., Berry, C., 2024. Chemical ecology of nectar-mosquito interactions: recent advances and future directions. Current opinion in insect science 63 (101199).
Spit, J., Philips, A., Wynant, N., Santos, D., Plaetinck, G., Vanden Broeck, J., 2017. Knockdown of nuclease activity in the gut enhances RNAi efficiency in the Colorado potato beetle, Leptinotarsa decemlineata, but not in the desert locust, Schistocerca gregaria. Insect biochemistry and molecular biology 81, 103–116.
Stewart, A.T.M., Mysore, K., Njoroge, T.M., Winter, N., Feng, R.S., Singh, S., James, L.D., Singkhaimuk, P., Sun, L., Mohammed, A., Oxley, J.D., Duckham, C., Ponlawat, A., Severson, D.W., Duman-Scheel, M., 2023. Demonstration of RNAi Yeast Insecticide Activity in Semi-Field Larvicide and Attractive Targeted Sugar Bait Trials Conducted on Aedes and Culex Mosquitoes. Insects 14 (12).
Tai, Z., Connelly, C.R., Kuczynski Lange, S., Foley, N., Leon Rivera, J. de, Lozano, S., Nett, R.J., 2024. A scoping review to determine if adverse human health effects are associated with use of organophosphates for mosquito control. Journal of medical entomology (1), 8–18.

Tarzwell, C.M., 1947. Effects of DDT Mosquito Larviciding on Wildlife: Part I. The Effects on Surface Organisms of the Routine Hand Application of DDT Larvicides for Mosquito Control. Public Health Reports 62 (15), 525–554.
Tayal, A., Kabra, S.K., Lodha, R., 2023. Management of Dengue: An Updated Review. Indian journal of pediatrics 90 (2), 168–177.
Tchounwou, P.B., Patlolla, A.K., Yedjou, C.G., Moore, P.D., 2015. Environmental Exposure and Health Effects Associated with Malathion Toxicity, in: Larramendy, M.L., Soloneski, S. (Eds.), Toxicity and Hazard of Agrochemicals. IntechOpen, Rijeka, Ch.3.
Teppor, M., Žusinaite, E., Karo-Astover, L., Omler, A., Rausalu, K., Lulla, V., Lulla, A., Merits, A., 2021. Semliki Forest Virus Chimeras with Functional Replicase Modules from Related Alphaviruses Survive by Adaptive Mutations in Functionally Important Hot Spots. Journal of virology 95 (20), e0097321.
Theissinger, K., Röder, N., Allgeier, S., Beermann, A.J., Brühl, C.A., Friedrich, A., Michiels, S., Schwenk, K., 2019. Mosquito control actions affect chironomid diversity in temporary wetlands of the Upper Rhine Valley. Molecular ecology 28 (18), 4300–4316.
Turusov, V., Rakirtsky, V., Tomatis, L., 2002. Dichlorodiphenyltrichloroethane (DDT): ubiquity, persistence, and risks. Environmental Health Perspectives 110 (2), 125–128.
van den Berg, H., 2009. Global Status of DDT and Its Alternatives for Use in Vector Control to Prevent Disease. Environmental Health Perspectives 117 (11), 1656–1663.
van den Berg, H., Manuweera, G., Konradsen, F., 2017. Global trends in the production and use of DDT for control of malaria and other vector-borne diseases. Malaria journal 16 (1), 401.
Walton, W.E., Henke, J.A., Why, A.M., 2012. Chapter 22: Gambusia affinis (Baird & Girard) and Gambusia holbrooki Girard (mosquitofish). In: A Handbook of Global Freshwater Invasive Species. Earthscan, New York, 13 pp.
Wang, T., Larcher, L.M., Ma, L., Veedu, R.N., 2018. Systematic Screening of Commonly Used Commercial Transfection Reagents towards Efficient Transfection of Single-Stranded Oligonucleotides. Molecules 23 (10).
Weger-Lucarelli, J., Rückert, C., Grubaugh, N.D., Misencik, M.J., Armstrong, P.M., Stenglein, M.D., Ebel, G.D., Brackney, D.E., 2018. Adventitious viruses persistently infect three commonly used mosquito cell lines. Virology 521, 175–180.
Wen, Z., Song, H., Ming, G., 2017. How does Zika virus cause microcephaly? Genes and develpment 31, 849–861.
Whitney, C., 2012. The silent decade: why it took ten years to ban DDT in the United States. Virginia Tech Undergraduate Historical Review 1 (1).
WHO, 2003. Use of fish for mosquito control. World Health Organization: Regional office for the eastern mediterranean, Cairo, 77 pp.
WHO, 2009. Dengue: Guidelines for Diagnosis, Treatment, Prevention and Control: New Edition. WHO Guidelines Approved by the Guidelines Review Committee. World Health Organization, Geneva.
WHO, 2023. World malaria report 2023. World Health Organization Geneva, 356pp.
Wickramasinghe, S., Silva, G.N., Silva Gunawardene, Y. I. N., Dassanayake, R.S., 2021. Advances in Aedes Mosquito Vector Control Strategies Using CRISPR/Cas9, in: Tyagi, B.K. (Ed.), Genetically Modified and other Innovative Vector Control Technologies: Eco-bio-social Considerations for Safe Application. Springer Singapore, Singapore, pp. 67–87.
Wilkerson, R.C., Linton, Y.M., Strickman, D., 2021. Mosquitoes of the World, Volumes 1 and 2 ed. Johns Hopkins University Press, Baltimore, 1332 pp.
Wilson, A.L., Courtenay, O., Kelly-Hope, L.A., Scott, T.W., Takken, W., Torr, S.J., Lindsay, S.W., 2020. The importance of vector control for the control and elimination of vector-borne diseases. PLoS neglected tropical diseases 14 (1), e0007831.
Wiltshire, R.M., Duman-Scheel, M., 2020. Advances in oral RNAi for disease vector mosquito research and control. Current opinion in insect science 40, 18–23.
Yadav, M., Dahiya, N., Sehrawat, N., 2023. Mosquito gene targeted RNAi studies for vector control. Functional & integrative genomics 23 (2), 180.
Yamano, S., Dai, J., Moursi, A.M., 2010. Comparison of transfection efficiency of nonviral gene transfer reagents. Molecular biotechnology 46 (3), 287–300.

Yen, P.-S., Failloux, A.-B., 2020. A Review: Wolbachia-Based Population Replacement for Mosquito Control Shares Common Points with Genetically Modified Control Approaches. Pathogens 9 (5).
Yu, N., Christiaens, O., Liu, J., Niu, J., Cappelle, K., Caccia, S., Huvenne, H., Smagghe, G., 2013. Delivery of dsRNA for RNAi in insects: an overview and future directions. Insect science 20 (1), 4–14.

5 Published work

Chapter I

Gene silencing in the aedine cell lines C6/36 and U4.4 using long double-stranded RNA

Parasite & Vectors. 2024 June 11;17(1):255. doi: 10.1186/s13071-024-06340-3. PMID: 38863029 PMCID: PMC11167938

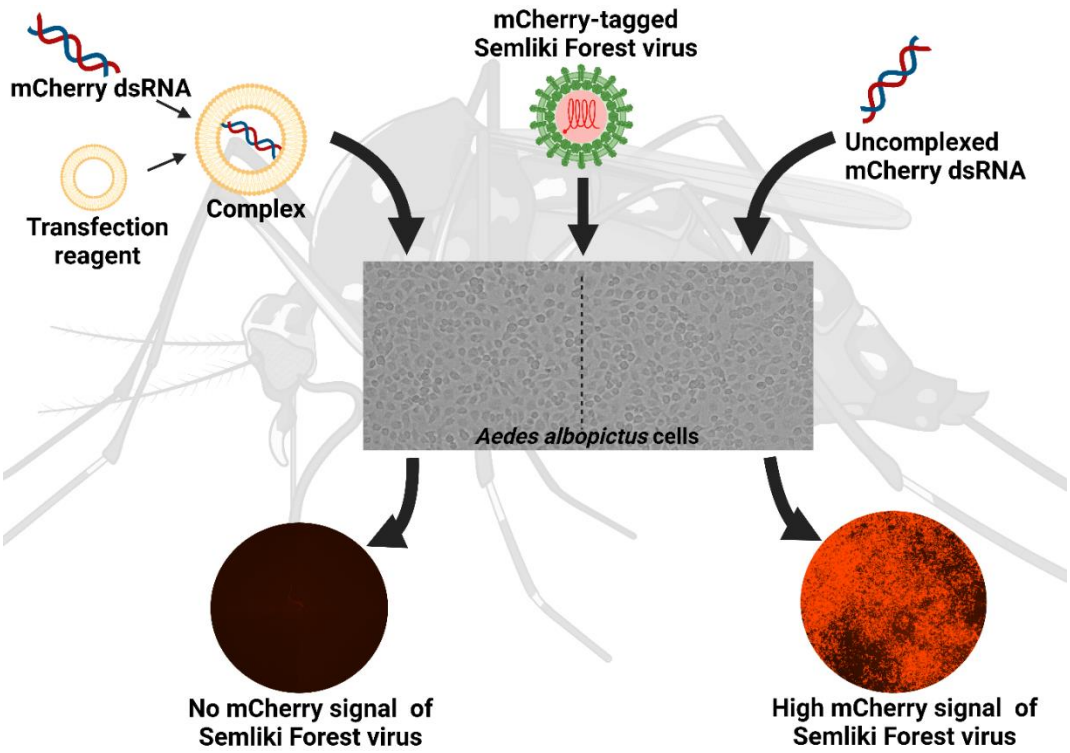

Omokungbe *et al. Parasites & Vectors* (2024) 17:255
https://doi.org/10.1186/s13071-024-06340-3

Parasites & Vectors

RESEARCH Open Access

Gene silencing in the aedine cell lines C6/36 and U4.4 using long double-stranded RNA

Bodunrin Omokungbe[1,2], Alejandra Centurión[1,3], Sabrina Stiehler[2], Antonia Morr[3], Andreas Vilcinskas[1,2,3], Antje Steinbrink[1,2] and Kornelia Hardes[1,3,4*]

Abstract

Background RNA interference (RNAi) is a target-specific gene silencing method that can be used to determine gene functions and investigate host–pathogen interactions, as well as facilitating the development of ecofriendly pesticides. Commercially available transfection reagents (TRs) can improve the efficacy of RNAi. However, we currently lack a product and protocol for the transfection of insect cell lines with long double-stranded RNA (dsRNA).

Methods We used agarose gel electrophoresis to determine the capacity of eight TRs to form complexes with long dsRNA. A CellTiter-Glo assay was then used to assess the cytotoxicity of the resulting lipoplexes. We also measured the cellular uptake of dsRNA by fluorescence microscopy using the fluorophore Cy3 as a label. Finally, we analyzed the TRs based on their transfection efficacy and compared the RNAi responses of *Aedes albopictus* C6/36 and U4.4 cells by knocking down an mCherry reporter Semliki Forest virus in both cell lines.

Results The TRs from Biontex (K4, Metafectene Pro, and Metafectene SI+) showed the best complexing capacity and the lowest dsRNA:TR ratio needed for complete complex formation. Only HiPerFect was unable to complex the dsRNA completely, even at a ratio of 1:9. Most of the complexes containing mCherry-dsRNA were nontoxic at 2 ng/µL, but Lipofectamine 2000 was toxic at 1 ng/µL in U4.4 cells and at 2 ng/µL in C6/36 cells. The transfection of U4.4 cells with mCherry-dsRNA/TR complexes achieved significant knockdown of the virus reporter. Comparison of the RNAi response in C6/36 and U4.4 cells suggested that C6/36 cells lack the antiviral RNAi response because there was no significant knockdown of the virus reporter in any of the treatments.

Conclusions C6/36 cells have an impaired RNAi response as previously reported. This investigation provides valuable information for future RNAi experiments by showing how to mitigate the adverse effects attributed to TRs. This will facilitate the judicious selection of TRs and transfection conditions conducive to RNAi research in mosquitoes.

Keywords RNAi, dsRNA, Transfection reagents, *Aedes albopictus*, Vector, Semliki Forest virus, Arbovirus, mCherry, Cell culture

*Correspondence:
Kornelia Hardes
kornelia.Hardes@ime.fraunhofer.de
Full list of author information is available at the end of the article

Background

Mosquitoes transmit many pathogens, including Zika virus (ZIKV), West Nile virus (WNV), dengue virus (DENV), chikungunya virus (CHIKV), *Mycobacterium ulcerans*, and malaria parasites [1, 2]. There are no vaccines or specific treatments available for the diseases caused by most of these pathogens [3–5]. Vector control is therefore needed to reduce the transmission risk of vector-borne diseases [6]. However, the efficacy of conventional vector-control methods is decreasing due to the emergence of resistant mosquito populations [7]. Furthermore, some chemical insecticides have been banned due to their adverse effects on nontarget insects, livestock animals, and humans [8]. In this regard, RNA interference (RNAi) is a powerful research tool for the analysis of gene functions and host–pathogen interactions that can also be exploited for the development of ecofriendly pesticides [9, 10].

RNAi is an evolutionarily conserved process in eukaryotes in which RNA molecules trigger posttranscriptional gene silencing [11, 12]. Efficient RNAi pathways are present in plants [13], nematodes [14], fungi [15], and insects [16]. In mosquitoes, the three RNAi pathways identified thus far are those based on microRNA (miRNA), Piwi-interacting RNA (piRNA), and small interfering RNA (siRNA) [17]. The siRNA machinery mainly provides defense against exogenous nucleic acids and transposable elements by targeted gene suppression [18, 19]. This pathway is triggered by the detection of cytoplasmic double-stranded RNA (dsRNA), which is cleaved into ~21-nucleotide (nt) siRNAs by Dicer-2 and R2D2 and then loaded onto an siRNA-induced silencing complex (siRISC) containing the protein Argonaute 2 (Ago2). Here, the siRNA is separated into single strands, one of which is retained to guide the siRISC to complementary target RNA sequences that are ultimately cleaved and degraded [16, 17, 20]. However, open questions in regards to the replication properties of some arboviruses, their interaction with innate immunity, and RNAi machinery remain [17].

The potential of RNAi as a control strategy against insect pests was first shown in beetles [21] and moths [22]. Prominent targets include nucampholin (NCM), Ras opposite (ROP), RNA polymerase II subunit-140 (RPII-140), and dre4, which were effective for the control of the red flour beetle *Tribolium castaneum* [23, 24]. In *Aedes albopictus*, potential target genes for RNAi-based control in mosquitoes include chitin synthase, β-tubulin, and the inhibitor of apoptosis (see [25] for a review). RNAi has been used to study 18 *Aedes aegypti* carboxypeptidase genes, where quantitative expression revealed that 11 of the genes were induced up to 40-fold in the midgut in response to blood feeding [26]. RNAi has also been used to study DENV and insect-specific flavivirus cell fusing agent virus (CFAV) in *Ae. albopictus* C6/36 cells and *Ae. aegypti* Aag2 cells. The production of siRNA was detected in Aag2 cells, whereas C6/36 cells demonstrated suboptimal Dcr2 cleavage efficiency when exposed to long dsRNA [27]. Target-specific dsRNA was also used to understand virus–host interactions and to inhibit the replication of Semliki Forest virus (SFV) in *Ae. albopictus* U4.4 cells [28].

The efficacy of RNAi is affected by factors such as dsRNA stability and internalization, the functionality of the RNAi machinery, systemic spreading of the RNAi signal, and the suitability of target genes [29]. The stability of dsRNA can be influenced by the presence of dsRNases that cause rapid degradation and also by the pH, because the optimal pH of dsRNA is 4.0–5.0 [29, 30]. The stability of dsRNA may therefore differ in the mosquito midgut, saliva, and hemolymph because the pH ranges from 7.5 to 11.0 [31, 32]. To overcome some of these barriers, dsRNA can be introduced using carrier systems such as cell-penetrating peptides [11], polymers [33], liposome-based transfection reagents (TRs) [34], and other nanoparticles [35]. These carriers can facilitate the transport of dsRNA into cells while protecting the cargo from degradation by dsRNases and pH changes [30].

TRs are designed to facilitate the introduction of nucleic acids into eukaryotic cells and usually feature a positively charged head group and one or two hydrocarbon chains that bind to negatively charged nucleic acids via electrostatic interactions to form cationic complexes (also known as lipoplexes). These complexes interact with the negatively charged phospholipid bilayer of the cell membrane, promoting uptake and intracellular release [36–39]. The formulation and composition of most commercially available TRs is not disclosed [40], making it difficult to rationally select TRs based on their components. Furthermore, certain TR components may be cytotoxic, thus affecting the reliability of transfection results [41, 42]. For example, six commercially available TRs (Arrest-In, ExpressFect, FuGENE HD, jetPEI, Lipofectamine 2000, and SuperFect) were examined based on their transfection efficiency and cytotoxicity using nine mammalian cell lines, revealing that FuGENE HD was most efficient for many of the cell lines, followed by Arrest-In and jetPEI, but jetPEI and ExpressFect were the least cytotoxic [41]. Currently, there are no commercially available TRs specifically designed for the introduction of long dsRNA (defined as dsRNA exceeding 300 bp [43]) and to our knowledge a comparative study assessing the efficiency of various TRs in aedine cells has not been published.

Cell culture can be used as a preliminary screening tool in RNAi studies to assess the feasibility, efficacy,

and specificity of RNAi constructs before transferring to in vivo experiments, optimizing the use of resources and minimizing ethical concerns [44]. We focused on the use of TRs (Table 1) from different manufacturers as dsRNA carrier systems for the introduction of long dsRNA into the aedine cell lines C6/36 and U4.4. We assessed the TRs according to their complexing capacity, cytotoxicity, impact on the uptake of dsRNA, and overall efficacy of the TRs. We also evaluated the suspected lack of an antiviral RNAi machinery in C6/36 cells [45]. Our results indicate the best conditions for testing dsRNA in aedine cells using various commercially available TRs and will facilitate RNAi research, e.g., the development of ecofriendly pesticides.

Methods

Cell culture

The *Ae. albopictus* cell lines C6/36 (kindly provided by Prof. Dr. Stefanie Becker) and U4.4 (Friedrich-Loeffler-Institute, Federal Research Institute for Animal Health, Greifswald, Riems, Germany) were cultured in insect cell growth medium (L15 medium GlutaMax) supplemented with 1% tryptose phosphate broth, 10% fetal calf serum, 1% MEM nonessential amino acids, and 1% penicillin/streptomycin at 28 °C. Baby hamster kidney (BHK-21) cells (CLS Cell Lines Service, Eppelheim, Germany) were maintained in mammalian cell growth medium (DMEM GlutaMax) supplemented with 10% fetal calf serum and 1% penicillin/streptomycin at 37 °C in a 5% CO_2 atmosphere. All media and supplements were from Thermo Fisher Scientific (Frankfurt, Germany).

Preparation of dsRNA

A glycerol stock of *Escherichia coli* NEB 5-α (New England BioLabs, Frankfurt, Germany) carrying vector pCMV-SFV6-2SG-mCherry was inoculated into 5 mL sterile lysogeny broth (LB) containing 125 µg kanamycin and incubated overnight at 37 °C, shaking at 200 rpm. Plasmid DNA was isolated using the NucleoSpin Plasmid DNA kit (Macherey–Nagel, Düren, Germany) according to the manufacturer's protocol. Gene-specific primers linked to a T7 promoter were used to amplify a part of the mCherry region from the SFV6-2SG-mCherry genome with OneTaq Hot Start Quick-Load 2× Master Mix (New England BioLabs) according to the manufacturer's protocol. The PCR products were used to synthesize the dsRNA in vitro using the MEGAscript T7 Transcription kit (Thermo Fisher Scientific). The dsRNA was purified by LiCl precipitation and resuspended in nuclease-free water. The concentration of the dsRNA was determined using a Nanodrop 2000 spectrophotometer (Thermo Fisher Scientific) with factor 46.0 and was stored at −80 °C. For dsRNA targeting green fluorescent protein (GFP), we followed the same procedure but used a glycerol stock of *E. coli* carrying vector pGEM-T-Easy-GFP-125 and gene-specific primers targeting GFP linked to the T7 promoter. See Table S1 in Additional file 1 for primer sequences and dsRNA sequences.

Complexation of dsRNA using commercially available transfection reagents

To determine the complexing capacity of TRs and the ratio needed to form complete complexes with mCherry-dsRNA, the TRs and dsRNA were diluted to 0.2 mg/mL (Table 1). The concentration of Lipofectamine RNAiMAX and HiPerFect were not provided by the manufacturers, so we equated these TRs to be 1.0 mg/mL. The components were mixed at dsRNA:TR ratios ranging from 1:0.3 to 1:9 (ratios adjusted according to the complexing capacity) and incubated at room temperature for the appropriate time (Table 1). Immediately after incubation, Mass Ruler loading dye (Thermo Fisher Scientific) was added to each complex and the complexes were resolved by 1.5% (w/v) agarose gel electrophoresis using pulse-field certified agarose (Bio-Rad Laboratories, Munich, Germany) for 80 min at 110 V and 150 mA in a

Table 1 List of commercially available transfection reagents used for the analysis of complexing capacity, including their concentration and parameters used for complex formation

Transfection reagent	Manufacturer	Concentration (mg/mL)	Dilution medium	Incubation time (min)
K4 Transfection System	Biontex	1.5	Grace's insect medium	20
Metafectene Pro	Biontex	1.5	Grace's insect medium	20
Metafectene SI+	Biontex	1.5	Grace's insect medium	20
Lipofectamine 2000	Invitrogen	1.0	OptiMEM reduced serum medium	5 + 20
Lipofectamine RNAiMAX	Invitrogen	–	OptiMEM reduced serum medium	5
CellFectin II	Invitrogen	1.0	Grace's insect medium	20
SiLentFect	BioRad	1.0	Grace's insect medium	20
HiPerFect	Qiagen	–	Grace's insect medium	10

Bio-Rad Sub-Cell GT (Bio-Rad Laboratories). The gel was visualized on Gel Doc XR+ using ImageLab v5.2.1 (both Bio-Rad Laboratories).

Cytotoxicity of the dsRNA/TR complexes in C6/36 and U4.4 cells

Cells were seeded in 96-well plates and treated at ~50% confluency with mCherry-dsRNA complexed with different TRs at concentrations ranging from 0.5 to 2 ng/µL, using the optimal dsRNA:TR ratios (Table 2). We used water, Grace's insect medium, and OptiMEM medium as negative controls. The ionophore ionomycin (Thermo Fisher Scientific) was used as a positive control (10 mM stock solution in water, 100 µM in the assay). The complexes were added to supplemented L-15 medium without penicillin/streptomycin to avoid antibiotic-related cytotoxicity and the plates were incubated at 28 °C. The medium was replenished after 6 h using supplemented medium with 1% penicillin/streptomycin. At 48 h post-treatment (hpt), cell viability was assessed by measuring ATP levels using the CellTiter-Glo Luminescent Cell Viability assay (Promega, Walldorf, Germany), according to the manufacturer's instructions. Luminescence was recorded using black 96-well plates in a Cytation 5 Cell Imaging Multimode Reader (Agilent Technologies, Waldbronn, Germany). The data were normalized to the untreated control and expressed as percentage (treatment/untreated × 100).

Stability of dsRNA in cell culture supernatant

Supernatant was collected from C6/36 and U4.4 cells at 80–100% confluency. The mCherry-dsRNA was diluted to 0.4 µg/µL and 1 µL of dsRNA was incubated for 20 or 240 min at 28 °C with 10 µL of supernatant. Water, unsupplemented L-15 medium, and fresh supplemented L-15 medium were used as negative controls. RNase III (New England BioLabs) was used as a positive control for dsRNA cleavage. Immediately after incubation, the samples were mixed with Mass Ruler loading dye and resolved by 2% agarose gel electrophoresis for 35 min at 110 V and 150 mA. The gel was visualized as described above.

Table 2 List of transfection reagents used and their determined optimal complexing ratio as well as the volume of reagent required to completely complex 400 ng mCherry-dsRNA. The ratio is expressed as dsRNA:TR (w/w)

Transfection reagent	Optimal ratio	Volume of TR required (µL)
Metafectene Pro	1:0.7	0.19
K4 transfection system	1:1	0.27
Metafectene SI +	1:1.5	0.40
Lipofectamine 2000	1:3	1.20
CellFectin II Reagent	1:5	2.00
Lipofectamine RNAiMAX	1:7	2.80
SiLentFect Lipid Reagent	1:7	2.80
HiPerFect Transfection Reagent	> 1:9	> 3.60

The * ratio is expressed as dsRNA:TR (w/w)

Uptake of dsRNA into C6/36 and U4.4 cells

The mCherry-dsRNA was labeled with Cy3 using the Silencer siRNA labeling kit (Thermo Fisher Scientific) according to the manufacturer's protocol. C6/36 and U4.4 cells were seeded in black F-bottom µclear 96-well plates (Greiner Bio-One, Frickenhausen, Germany) and transfected at a confluency of 80% with 50 or 200 ng of labeled dsRNA using K4, Metafectene Pro, Metafectene SI+, Lipofectamine 2000, or CellFectin II at the determined optimal complexation ratio (Table 2). Uncomplexed labeled dsRNA was added to the wells as control. At 6 hpt, cells were washed three times with unsupplemented L-15 medium and replenished with fresh supplemented medium. At 24 hpt, we added 8 µL of Hoechst 33,342 (NucBlue Live ReadyProbes Reagent, Thermo Fisher Scientific) per well and incubated the cells for 30 min at 28 °C. We monitored the Cy3 and Hoechst 33342 fluorescence signals using a Cytation 5 Cell Imaging Multimode reader. We captured bright-field images of each well at 20× magnification as well as fluorescence images using DAPI and Texas red filters. The images were processed using BioTek Gen5 Image Prime v3.12 (Agilent Technologies). The raw fluorescence signal of the untransfected control was subtracted from the treatments.

Virus production

BHK-21 cells at 90% confluency were transfected with the SFV6-2SG-mCherry plasmid (kindly provided by Prof. Dr. Andres Merits and Prof. Dr. Andreas Pichlmair) in infection medium [DMEM Glutamax supplemented with 1% penicillin/streptomycin and 0.2% bovine serum albumin (BSA; Serva Electrophoresis, Heidelberg, Germany)] using Lipofectamine 3000 (Thermo Fisher Scientific) according to the manufacturer's instructions. At 48 hpt, the virus-containing supernatant was collected, frozen in aliquots and stored at −80 °C prior to the infection of BHK-21 cells in T-75 flasks (Greiner Bio-One) to produce the virus stocks. Titers were determined in BHK-21 cells using a $TCID_{50}$ assay. Briefly, tenfold serial dilutions of each sample were inoculated with the cells, which were incubated for 1 h as described above. After infection, cells were incubated for 48 h at 37 °C in a 5% CO_2 atmosphere before virus replication was quantified by fluorescence analysis.

Efficacy of transfection reagents in C6/36 and U4.4 cells

Cells were seeded in a black F-bottom µclear 96-well plates and cultivated as described above until they reached ~50% confluency. The cells were transfected with dsRNAs (0.5 ng/µL) targeting GFP or mCherry using the TRs with the optimal complexing ratio (Table 2) in supplemented L-15 medium without penicillin/streptomycin. At 6 hpt, the medium was replaced with fresh supplemented L-15 medium including 1% penicillin/streptomycin. Cells at a confluency of 80% were infected 24 hpt with mCherry-SFV at a multiplicity of infection (MOI) of 0.01 using unsupplemented L-15 medium. The medium was replaced with supplemented L-15 medium after 1 h. At 30 h (for C6/36) and 56 h (for U4.4) post-infection (hpi), we added 8 µL of NucBlue Live ReadyProbes Reagent per well and incubated the cells for 30 min at 28 °C. We captured images of each well at 4× magnification using bright-field, DAPI, and Texas red filters as described above. The images were processed using BioTek Gen5 Image Prime v3.12 to determine the total intensity of red fluorescence per cell (total red intensity/cell count).

Statistical analysis

The statistical analysis and visualization of data was carried out using GraphPad Prism v9.5.1 (GraphPad Software, Boston, MA, USA). We used one-way analysis of variance (ANOVA) with Dunnett's or Šidák's multiple comparisons tests to determine the statistical significance of any differences in the efficacy between TRs ($P < 0.05$).

Results

Complexing capacity of the selected transfection reagents

To develop a protocol for the efficient transfection of aedine cells with long dsRNA, we compared the TRs K4, Metafectene Pro, Metafectene SI+, Lipofectamine 2000, Lipofectamine RNAiMAX, CellFectin II, SiLentFect, and HiPerFect. The complexing capacity of each TR was analyzed by agarose gel electrophoresis using the concentrations recommended by the manufacturers and 400 ng of dsRNA with a length of 409 bp to determine the optimal dsRNA:TR ratio. The TRs varied in their complex-formation capacity over a wide range. Metafectene Pro, K4, and Metafectene SI+ formed complexes most efficiently, with dsRNA:TR ratios of 1:0.7, 1:1, and 1:1.5, respectively (Table 2 and Additional file 1: Fig. S1). Lipofectamine 2000 complexed the same amount of dsRNA at a ratio of 1:3, whereas CellFectin II required a ratio of 1:5 and both Lipofectamine RNAiMAX and SiLentFect required a ratio of 1:7. Uniquely, HiPerFect was unable to complete the formation of complexes even at a ratio of 1:9. Based on these results, we excluded Lipofectamine RNAiMAX, SiLentFect, and HiPerFect from further experiments.

Toxicity of dsRNA/TR complexes in aedine cells

The toxicity of the five remaining TRs and their lipoplexes at the optimal dsRNA:TR ratios were determined in aedine cells by measuring the abundance of ATP using the CellTiter-Glo assay. The TRs were used to introduce 50–200 ng mCherry-dsRNA into C6/36 and U4.4 cells. None of the lipoplexes showed any significant toxicity against C6/36 cells (all values exceeded the toxicity threshold of 80% viability). Only the transfection with 200 ng mCherry-dsRNA using Lipofectamine 2000 was toxic, reducing cell viability to 78.5% (Fig. 1a). The same trend was observed in U4.4 cells. Here, Lipofectamine 2000 alone and in complexes with 100 or 200 ng of mCherry-dsRNA were toxic, reducing cell viability to 78.7%, 72.1%, and 62%, respectively (Fig. 1b).

Effect of the transfection reagents on the uptake of dsRNA into aedine cell lines

To ensure that the mCherry-dsRNA is not degraded before it is taken up by the cells, we tested its stability in the culture supernatant of C6/36 and U4.4 cells. We incubated the dsRNA in the supernatant for 20 and 240 min before analysis by agarose gel electrophoresis. RNase III was added to the mCherry-dsRNA as positive control for degradation. We observed no substantial degradation of the dsRNA in the cell culture supernatant at either of the time points (Fig. S2).

To study the uptake of dsRNA by aedine cells, mCherry-dsRNA was labeled with the fluorophore Cy3 and introduced into the cells using each of the five TRs. In most cases we transfected the cells with 200 ng of labeled dsRNA, but only 50 ng was used with Lipofectamine 2000 because cytotoxicity was observed at higher concentrations (Fig. 1). The fluorescence intensity following transfection varied among the five reagents, with CellFectin producing the strongest signal, followed by Metafectene SI+ in both C6/36 cells (Fig. 2) and U4.4 cells (Fig. 3). The signal from the cells treated with naked dsRNA was negligible. The Hoechst 33342 signal from the stained nuclei was comparable among the different treatments (Figs. 2b, 3b).

Knockdown of the virus reporter mCherry in aedine cell lines using long dsRNA

To study the knockdown of the reporter virus SFV-mCherry and the RNAi response of C6/36 and U4.4 cells, we transfected both cell lines with 0.5 ng/µL of dsRNA targeting the reporter gene mCherry using K4, Metafectene Pro, Metafectene SI+, Lipofectamine 2000, and CellFectin II. To ensure that the observed knockdown effects resulted from an RNAi response, we used GFP-dsRNA as a control. We infected both cell lines with the mCherry-tagged SFV 24 hpt and

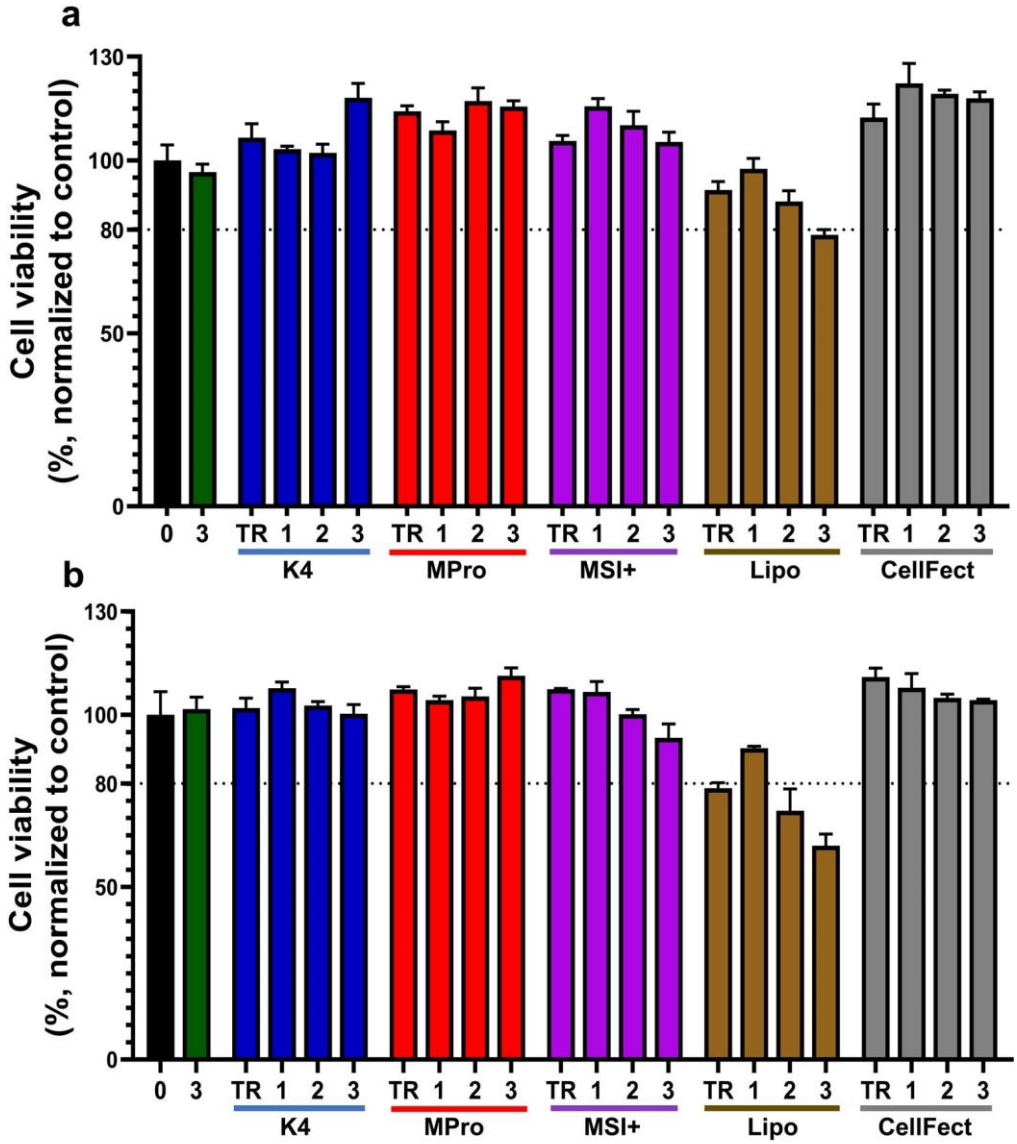

Fig. 1 Cytotoxicity of dsRNA complexed with five transfection reagents in *Ae. albopictus* (**a**) C6/36 and (**b**) U4.4 cells. The cells were treated at ~50% confluency with only the TR or with (1) 50, (2) 100, and (3) 200 ng of the complexes of TRs and mCherry-dsRNA per well ($n=6$). Cell viability was determined using a CellTiter-Glo assay. The data were normalized to the untreated control (treatment/control × 100) and the mean cell viability is displayed, with error bars representing coefficient of variation (both in %). The untreated control is represented as 0. The dotted line represents the toxicity cutoff set at 80%. Abbreviations: *K4* K4 transfection system, *MPro* Metafectene Pro, *MSI+* Metafectene SI+, *Lipo* Lipofectamine 2000, *CellFect* CellFectin II

acquired images showing the intensity of mCherry fluorescence and the total cell count at 30 (for C6/36) and 56 (for U4.4) hpi (Fig. 4). We observed no RNAi response in C6/36 cells, resulting in no significant differences between the treatments and control, except for the GFP-dsRNA transfection with Metafectene SI+ ($P=0.0156$). In contrast, U4.4 cells showed a potent RNAi response, resulting in the significant knockdown of reporter mCherry expression in the transfected cells. Cells treated with naked dsRNA showed no significant knockdown effects. The most efficient TR was K4, followed by Metafectene SI+, Lipofectamine 2000, Metafectene Pro, and CellFectin II. However, Šidák's multiple comparisons test revealed no significant differences in the ability of the TRs to knock down mCherry expression in U4.4 cells.

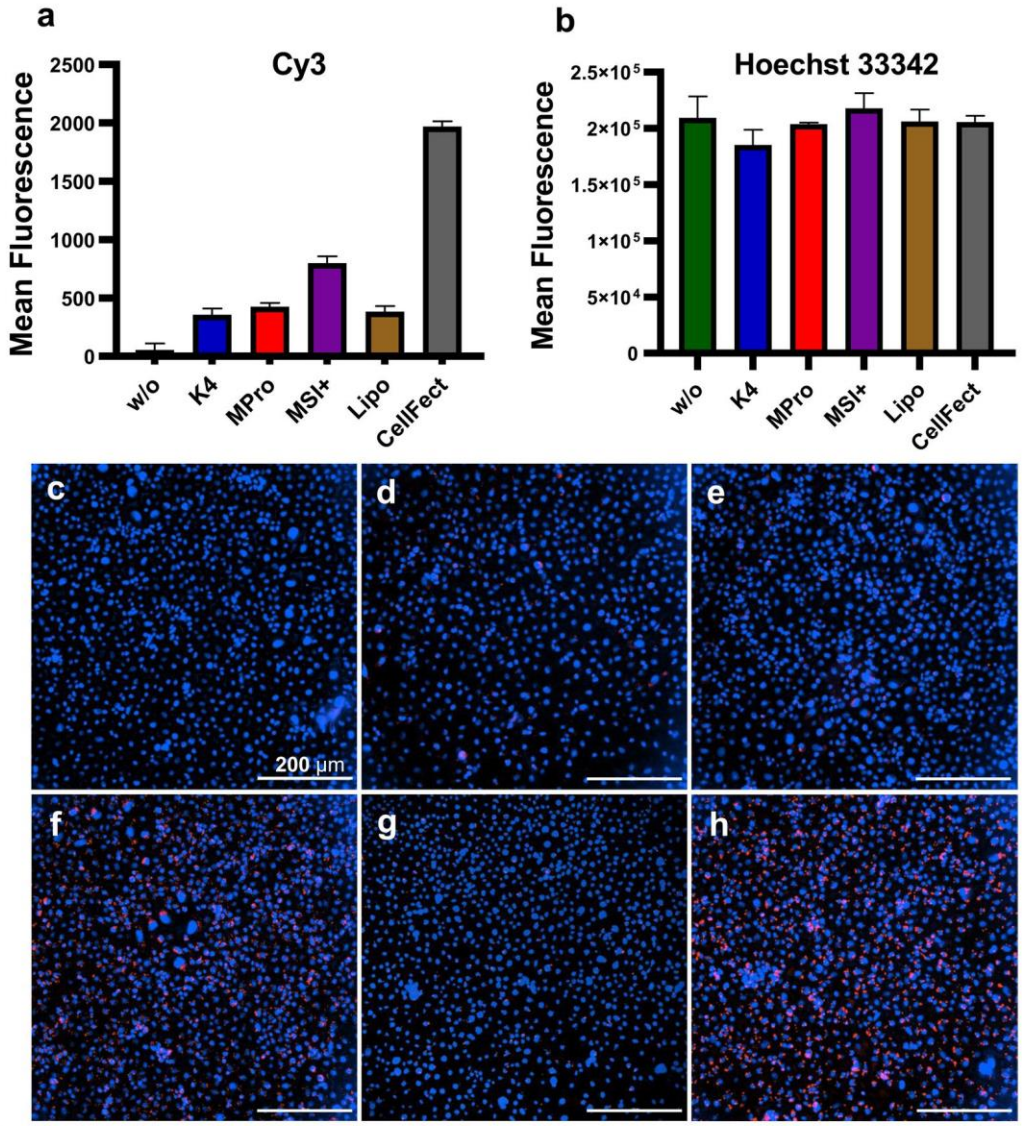

Fig. 2 Uptake of Cy3-labeled dsRNA into C6/36 cells 24 h post-transfection. **a** Mean fluorescence of Cy3 signal from the labeled dsRNA and (**b**) mean fluorescence of Hoechst 33342 (both $n = 3$, with error bars indicating standard deviations). **c**–**h** Fluorescence images taken at 20× magnification. **c** Labeled dsRNA was applied without transfection reagent (w/o). **d**–**h** Cells were transfected with the labeled dsRNA using (**d**) K4, (**e**) Metafectene Pro, (**f**) Metafectene SI+, (**g**) Lipofectamine 2000, and (**h**) CellFectin II. The TRs were used to transfect cells with 200 ng labeled dsRNA, except Lipofectamine 2000 with only 50 ng. The cell nuclei are stained in blue and the labeled dsRNA in red. The percentage of transfected cells per image for all conditions can be found in Table S2

Discussion

We compared eight TRs to determine their complexing capacity, cytotoxicity, impact on the uptake of dsRNA, and efficacy in two *Ae. albopictus* cell lines (C6/36 and U4.4), revealing the optimal dsRNA:TR ratios and concentrations that are compatible with these aedine cells. In addition to establishing these optimal transfection conditions, we also found evidence supporting previous claims that C6/36 cells lack a functional RNAi pathway.

Cell culture experiments can provide initial evidence to guide the application of RNAi in vivo [27, 44]. The use of TRs improves the cellular uptake of dsRNA by protecting it from enzymatic degradation as well as pH changes, which is necessary to ensure that an adequate amount of dsRNA reaches the cytoplasm to trigger RNAi [42, 46]. However, the composition and formulation of many TRs is unclear because the information is not publicly available [40]. Additionally, most protocols focus on the

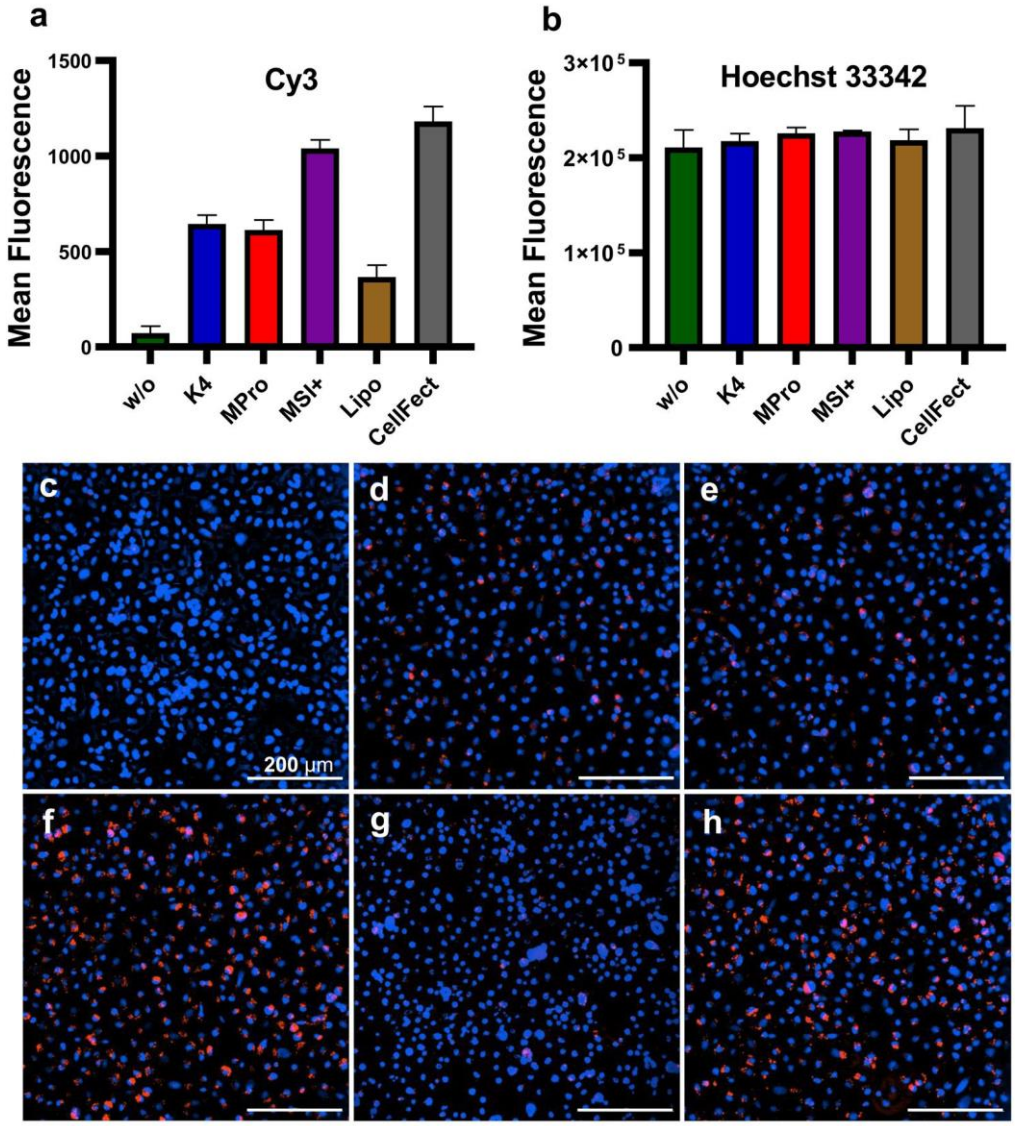

Fig. 3 Uptake of Cy3-labeled dsRNA into U4.4 cells 24 h post-transfection. **a** Mean fluorescence of Cy3 signal from the labeled dsRNA and (**b**) mean fluorescence of Hoechst 33342 (both $n = 3$, with error bars indicating standard deviations). **c**–**h** Fluorescence images taken at 20× magnification. **c** Labeled dsRNA was applied without transfection reagent (w/o). **d**–**h** Cells were transfected with the labeled dsRNA using (**d**) K4, (**e**) Metafectene Pro, (**f**) Metafectene SI+, (**g**) Lipofectamine 2000, and (**h**) CellFectin II. The TRs were used to transfect cells with 200 ng labeled dsRNA, except Lipofectamine 2000 with only 50 ng. The cell nuclei are stained in blue and the labeled dsRNA in red. The percentage of transfected cells per image for all conditions can be found in Table S2

transfection of cells with siRNA and plasmids [47, 48]. To our knowledge, there have been no comparative studies on the transfection of aedine cell lines with long dsRNA using TRs. Furthermore, there are no commercially available TRs specifically designed for long dsRNA. Therefore, it is necessary to establish protocols allowing the evaluation and optimization of commercially available TRs for the introduction of long dsRNA into aedine cell lines.

Accordingly, we used agarose gel electrophoresis to determine the complexing capacity of TRs and the optimal dsRNA:TR ratio (the lower the ratio, the better the complexing capacity and vice versa). The TRs from Biontex (K4, Metafectene Pro, and Metafectene SI+) showed the best complexing capacity with the lowest complexing ratios (Table 2 and Additional file 1: Fig. S1). Low ratios are advantageous because they reduce the potential for cytotoxicity by limiting the amount of TR needed for efficient transfection, also reducing costs, especially when large numbers of transfection experiments are required. Impressively, the complexing ratio

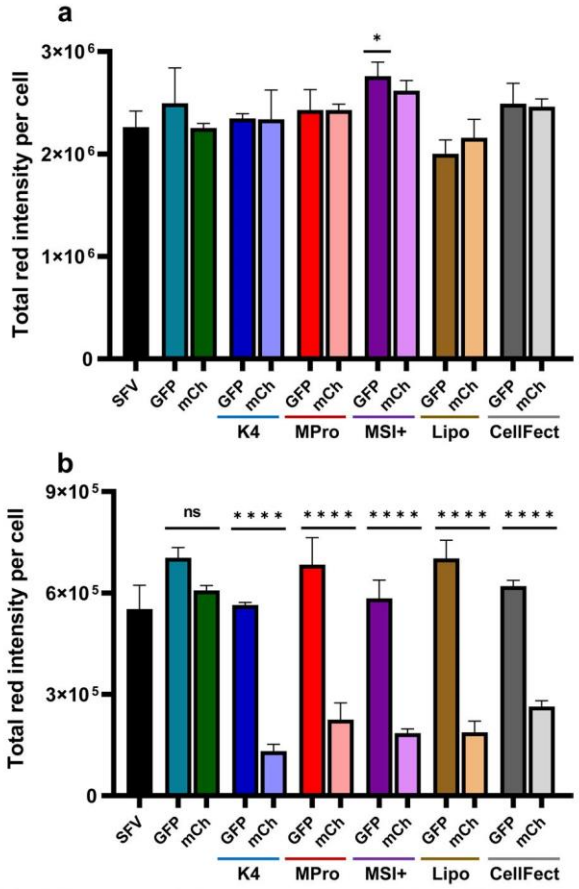

Fig. 4 Knockdown of virus reporter mCherry-SFV in (**a**) C6/36 and (**b**) U4.4 cells. Both cell lines were treated with 0.5 ng/µL dsRNA targeting GFP or mCherry (mCh). The dsRNAs were introduced into the cells using K4, Metafectene Pro (MPro), Metafectene SI+ (MSI), Lipofectamine 2000 (Lipo), or CellFectin II (CellFect). At 24 hpt, cells were infected with mCherry-SFV. The total intensity and cell count were analyzed at 30 (for C6/36) and 56 (for U4.4) hpi. The data are mean values ($n = 3$) of the total red intensity per cell (total red intensity/total cell count) and the error bars represent standard deviations. Statistical significance was determined by ANOVA and Šidák's multiple comparison test (****$P < 0.0001$, ns = $P > 0.05$)

of TRs from Biontex was lower than the ranges recommended by the manufacturer in their protocol (1:2–1:7) for transfection with DNA and RNA. In contrast, HiPerFect was the only TR that was unable to form complete complexes with the same amount of dsRNA even at a ratio of 1:9. This may reflect the specific design of HiPerFect for the transfection of cells with siRNA, miRNA mimics, and inhibitors (according to the manufacturer's information), potentially making it unsuitable for long dsRNA. Furthermore, for the Biontex TRs we relied on TR concentrations recommended by the manufacturer but not included in the instructions (Biontex, personal communication). For Lipofectamine RNAiMAX and HiPerFect, the manufacturers did not provide the concentrations of the TRs. The method we used to study the complexing capacity of the TRs has already been used to determine the optimum ratio of carrier systems, such as cationic polymers, nanoparticles, and TRs, for the complexation of nucleic acid molecules [46, 49, 50]. However, to the best of our knowledge, this method has only been used in one study to evaluate the encapsulation of long dsRNA, revealing that 1 µL of GenJet is required to completely complex 0.5 µg of the long dsRNA-targeting eGFP [46].

The commercially available TRs were specifically designed to deliver genetic material into cells but may have inherent cytotoxic effects [51, 52]. The viability of transfected cells is an important parameter for the accurate interpretation of RNAi results because it is necessary to distinguish between potential effects caused by RNAi and general cytotoxicity [51]. Most of the TRs we tested did not significantly affect cell viability at the concentrations we used, with the exception of Lipofectamine 2000 at high concentrations (Fig. 1). This is one of the most commonly used TRs in mammalian cells and consists of 1,2-dioleoyl-*sn*-glycero-3-phosphatidylethanolamine (DOPE) and 2′-(1′′,2′′-dioleoyloxypropyldimethylammonium bromide)-*N*-ethyl-6-amidospermine tetratrifluoroacetic acid salt (DOSPA) formulated with a helper/neutral co-lipid [53]. Lipofectamine 2000 has previously been shown to affect the viability of Huh-7 liver cancer cells, SHSY5Y neuroblastoma cells, JU77 lung mesothelioma cells, HL60 promyelocytic leukemia cells, HEK293 embryonic kidney cells, and U87MG brain cancer cells, when used to introduce single-stranded oligonucleotides (SSOs) at an SSO:TR ratio of 1:2 [51]. Similarly, a 31.9% reduction in cell viability was reported when Lipofectamine 2000 was used to transfect mouse protoblast MC3T3-E1 cells with plasmids encoding luciferase or β-galactosidase [41].

The uptake of dsRNA into cells is facilitated by TRs, thus enhancing RNAi efficacy [54]. For this reason, we also compared the TRs for their effects on the uptake of dsRNA into C6/36 and U4.4 cells. We found that CellFectin II facilitated the uptake of Cy3-labeled dsRNA most efficiently in both C6/36 and U4.4 cells after 24 h, followed by Metafectene SI+ (Figs. 2, 3). Only minimal amounts of the Cy3-labeled dsRNA were taken up in the absence of a TR, confirming the ability of TRs to significantly improve the uptake of nucleic acids [54, 55]. CellFectin II was the only TR we tested that is specifically designed for the transfection of insect cells, according to the manufacturer's information. It has been used for the transfection of *Drosophila* S2 cells with DNA [56] and for the in vivo transfection of adult-stage *Ae. aegypti* with plasmid DNA targeting *Ae. aegypti* thioester-containing

protein-1 (AeTEP-1), significantly inhibiting the infectivity of DENV [48].

Any TR that does not release a substantial amount of dsRNA in the cytoplasm is unlikely to initiate an effective RNAi response [57]. We therefore analyzed the TRs based on their ability to knock down the virus reporter mCherry by transfecting aedine cells with mCherry-dsRNA and then infecting them with the mCherry-SFV. We observed a substantial knockdown of the virus reporter in U4.4 cells transfected with mCherry-dsRNA using K4, Metafectene Pro, Metafectene SI+, Lipofectamine 2000, and CellFectin II (Fig. 4). We found no substantial differences among the TRs in terms of knockdown efficacy. In a previous study, Lipofectamine 2000 was compared with ExGen 500, TurboFectin 8.0, and PrimeFect I DNA, which were used to transfect mammalian cell lines NG108-15, SH-SY5Y, and CHO-K1 with DNA encoding GFP at a DNA:TR ratio of 1:2.5. Lipofectamine 2000 was 11-fold more efficient than TurboFectin 8.0 and was preferred in terms of transfection efficiency for NG108-15 and CHO-K1 cells [58]. On the other hand, in an experiment using *Ae. aegypti* adult females, CellFectin II was used to introduce long dsRNA targeting p400. CellFectin II only improved the knockdown efficiency when complexed with 2 µg of dsRNA, which was then injected into the mosquito. However, there was no significant knockdown of p400 when the complex contained either only 0.5 or 1 µg of the same dsRNA [59].

Most RNAi research on the control of mosquitos has focused on *Ae. aegypti* while neglecting *Ae. albopictus*, a competent vector of more than 22 arboviruses including ZIKV, DENV, and CHIKV [25, 60]. Candidate dsRNAs are usually screened in cell-based assays [61], but C6/36 cells, the most commonly used *Ae. albopictus* cell line, appear to have a dysfunctional RNAi pathway [45]. On the other hand, U4.4 cells are widely used for host–virus interaction studies [62] and show a normal RNAi response [28]. Because of this suspected dissimilarity, we compared C6/36 and U4.4 cell lines to determine their antiviral RNAi responses. We observed no significant knockdown of the virus reporter mCherry in transfected C6/36 cells (Fig. 4), whereas there was a significant difference between transfected and untransfected U4.4 cells in terms of viral replication. Furthermore, viral replication was faster and generated much higher titers in C6/36 compared to U4.4 cells (Fig. S3). These findings support the reported dysfunction of the antiviral RNAi response in C6/36 cells, preventing the suppression of viral replication [27, 45]. The infection of C6/36 cells and S2 cells (control cells from *Drosophila melanogaster*) with WNV, Sindbis virus (SINV), and La Crosse virus (LACV) resulted in the production of viral interfering RNA (viRNA) only 17 nt in length from WNV compared to 26–27 nt from SINV and LACV in C6/36 cells. In contrast, all three viruses induced the production of 21-nt viRNAs in S2 cells [45]. This suggests that C6/36 cells lack the capacity to process long dsRNAs into siRNAs that can be used by the RNAi machinery [27].

The testing of TRs in cell lines helps to establish conditions that are suitable for in vivo applications involving the introduction of siRNA, dsRNA, and plasmids [48]. The first TR used for the in vivo transfection of mosquitos was Effectene, allowing the delivery of dsRNA targeting MAPK p38 in *Ae. aegypti* larvae [34]. Cellfectin II was subsequently used to deliver plasmid DNA intrathoracically into adult stage *Ae. aegypti* and *Anopheles gambiae* [48]. Some toxic effects were also reported: for example, FuGene 6 was highly toxic to *Ae. aegypti*, with only one of 120 injected mosquitos surviving, whereas Cellfectin II was well tolerated under the same conditions, with 99% survival [48]. Similarly, RNA-free Effectene liposomes caused 5% mortality in *Ae. aegypti* larvae [34].

We analyzed the cytotoxicity, dsRNA uptake and overall efficacy of TRs according to their complexing capacity (Table 2), aiming to minimize the excess of TRs needed for the transfection of aedine cells. Consequently, our results may not be directly comparable because different dsRNA:TR ratios were used for each reagent. In summary, for the transfection of aedine cell lines, Lipofectamine 2000 improved dsRNA uptake and enhanced the knockdown against our target, but a low concentration is required to avoid cytotoxic effects. CellFectin II achieved the highest dsRNA uptake with no cytotoxicity and also led to the significant knockdown of our target, but the high dsRNA:TR ratio makes it less cost effective. K4, Metafectene Pro, and Metafectene SI+ are good candidates for further studies due to their high complexing capacity, absence of cytotoxicity, ability to promote the uptake of dsRNA, and efficient knockdown of the virus reporter mCherry.

Conclusions

In this study, we comprehensively compared eight TRs based on their complexing capacity, cytotoxicity, impact on the uptake of dsRNA, and efficacy in two *Ae. albopictus* cell lines (C6/36 and U4.4). Our data support previous studies reporting that C6/36 cells have a dysfunctional antiviral RNAi response, given the substantial differences we observed between the C6/36 and U4.4 cells. Our findings will facilitate RNAi research for the analysis of gene functions as well as vector control and will serve as a basis for the rational selection of TRs for future experiments in aedine cell lines.

Supplementary Information

The online version contains supplementary material available at https://doi.org/10.1186/s13071-024-06340-3.

Additional file 1.

Acknowledgements
The graphical abstract was designed using BioRender online software. We thank Prof. Dr. Stefanie Becker, University of Veterinary Medicine, Hannover, Germany, for the C6/36 cells. We also thank Prof. Dr. Andres Merits, University of Tartu, Estonia, and Prof. Dr. Andreas Pichlmair, Technical University of Munich, Germany, for providing pCMV-SFV6-2SG-mCherry. We also wish to thank Dr. Richard M Twyman for his editorial assistance.

Author contributions
Conceptualization: AS, KH. Data Curation: BO, AC, SS, KH. Formal analysis: BO, AC, SS, KH. Funding acquisition: AS, KH, AV. Investigation: BO, AC, SS, AM, KH. Methodology: BO, AC, SS, AM, KH. Project Administration: AS, KH. Resources: AS, KH, AV. Supervision: AS, KH, AV. Validation: BO, AC. Visualization: BO, AC. Writing–original draft preparation: BO, KH. Writing–review & editing: BO, AC, SS, AM, AS, AV, KH.

Funding
Open Access funding enabled and organized by Projekt DEAL. BO and AC are supported by the Landes-Offensive zur Entwicklung Wissenschaftlich-ökonomischer Exzellenz Program of the Hessian Ministry of Higher Education, Research and the Arts through the LOEWE Centre for Translational Biodiversity Genomics (LOEWE–TBG) with funding code: LOEWE/1/10/519/03/03.001(0014)/52. KH is supported by the BMBF (Project ASCRIBE—Grant Number 01KI2024).

Availability of data and materials
All data generated or analyzed during this study are included in this published article.

Declarations

Ethics approval and consent to participate
Not applicable.

Consent for publication
All authors read and approved the final manuscript.

Competing interests
The authors declare no competing of interests.

Author details
[1]LOEWE Centre for Translational Biodiversity Genomics (LOEWE TBG), Senckenberganlage 25, 60325 Frankfurt Am Main, Germany. [2]Institute for Insect Biotechnology, Justus-Liebig University, Heinrich-Buff-Ring 26-32, 35392 Giessen, Germany. [3]Fraunhofer Institute for Molecular Biology and Applied Ecology IME, Branch of Bioresources, Ohlebergsweg 12, 35392 Giessen, Germany. [4]BMBF Junior Research Group in Infection Research "ASCRIBE", Ohlebergsweg 12, 35392 Giessen, Germany.

Received: 13 March 2024 Accepted: 30 May 2024
Published online: 11 June 2024

References

1. Bamou R, Mayi MPA, Djiappi-Tchamen B, Nana-Ndjangwo SM, Nchoutpouen E, Cornel AJ, et al. An update on the mosquito fauna and mosquito-borne diseases distribution in Cameroon. Parasit Vectors. 2021. https://doi.org/10.1186/s13071-021-04950-9.
2. Mee PT, Buultjens AH, Oliver J, Brown K, Crowder JC, Porter JL, et al. Mosquitoes provide a transmission route between possums and humans for Buruli ulcer in southeastern Australia. Nat Microbiol. 2024;9:377–89. https://doi.org/10.1038/s41564-023-01553-1.
3. Lewis M, Amsden JR. Successful treatment of West Nile virus infection after approximately 3 weeks into the disease course. Pharmacotherapy. 2007;27:455–8. https://doi.org/10.1592/phco.27.3.455.
4. Galán-Huerta KA, Rivas-Estilla AM, Fernández-Salas I, Farfan-Ale JA, Ramos-Jiménez J. Chikungunya virus: a general overview. Medicina Universitaria. 2015;17:175–83. https://doi.org/10.1016/j.rmu.2015.06.001.
5. Da Silva S, Oliveira Silva Martins D, Jardim ACG. A Review of the Ongoing Research on Zika Virus Treatment. Viruses. 2018. https://doi.org/10.3390/v10050255.
6. Wilson AL, Courtenay O, Kelly-Hope LA, Scott TW, Takken W, Torr SJ, et al. The importance of vector control for the control and elimination of vector-borne diseases. PLoS Negl Trop Dis. 2020;14:e0007831.
7. Labbé P, Alout H, Djogbénou L, Pasteur N, Weill M. Evolution of resistance to insecticide in disease vectors. In: Genetics and evolution of infectious disease. Amsterdam: Elsevier; 2011. p. 363–409. https://doi.org/10.1016/B978-0-12-384890-1.00014-5.
8. Nicolopoulou-Stamati P, Maipas S, Kotampasi C, Stamatis P, Hens L. Chemical pesticides and human health: the urgent need for a new concept in agriculture. Front Public Health. 2016;4:178764.
9. Cherry S. Genomic RNAi screening in Drosophila S2 cells: what have we learned about host-pathogen interactions? Curr Opin Microbiol. 2008;11:262–70. https://doi.org/10.1016/j.mib.2008.05.007.
10. Lopez SBG, Guimarães-Ribeiro V, Rodriguez JVG, Dorand FAPS, Salles TS, Sá-Guimarães TE, et al. RNAi-based bioinsecticide for Aedes mosquito control. Sci Rep. 2019;9:4038. https://doi.org/10.1038/s41598-019-39666-5.
11. Airs PM, Bartholomay LC. RNA interference for mosquito and mosquito-borne disease control. Insects. 2017. https://doi.org/10.3390/insects8010004.
12. Wiltshire RM, Duman-Scheel M. Advances in oral RNAi for disease vector mosquito research and control. Curr Opin Insect Sci. 2020;40:18–23. https://doi.org/10.1016/j.cois.2020.05.002.
13. Fang X, Qi Y. RNAi in plants: an argonaute-centered view. Plant Cell. 2016;28:272–85. https://doi.org/10.1105/tpc.15.00920.
14. Almeida MV, Andrade-Navarro MA, Ketting RF. Function and evolution of nematode RNAi pathways. Noncoding RNA. 2019. https://doi.org/10.3390/ncrna5010008.
15. Lax C, Tahiri G, Patiño-Medina JA, Cánovas-Márquez JT, Pérez-Ruiz JA, Osorio-Concepción M, et al. The evolutionary significance of RNAi in the fungal kingdom. Int J Mol Sci. 2020. https://doi.org/10.3390/ijms21249348.
16. Olson KE, Blair CD. Arbovirus-mosquito interactions: RNAi pathway. Curr Opin Virol. 2015;15:119–26. https://doi.org/10.1016/j.coviro.2015.10.001.
17. Liu J, Swevers L, Kolliopoulou A, Smagghe G. Arboviruses and the challenge to establish systemic and persistent infections in competent mosquito vectors: the interaction with the RNAi mechanism. Front Physiol. 2019;10:890. https://doi.org/10.3389/fphys.2019.00890.
18. Blair CD. Mosquito RNAi is the major innate immune pathway controlling arbovirus infection and transmission. Future Microbiol. 2011;6:265–77. https://doi.org/10.2217/fmb.11.11.
19. Blair CD, Olson KE. Mosquito immune responses to arbovirus infections. Curr Opin Insect Sci. 2014;3:22–9. https://doi.org/10.1016/j.cois.2014.07.005.
20. Dong Y, Shengzhang D, Dizaji NB, Rutkowski N, Pohlenz T, Myles K, et al. The *Aedes aegypti* siRNA pathway mediates broad-spectrum defense against human pathogenic viruses and modulates antibacterial and antifungal defenses. PLoS Biol. 2022;20:e3001722. https://doi.org/10.1371/journal.pbio.3001722.
21. Baum JA, Bogaert T, Clinton W, Heck GR, Feldmann P, Ilagan O, et al. Control of coleopteran insect pests through RNA interference. Nat Biotechnol. 2007;25:1322–6. https://doi.org/10.1038/nbt1359.
22. Mao Y-B, Cai W-J, Wang J-W, Hong G-J, Tao X-Y, Wang L-J, et al. Silencing a cotton bollworm P450 monooxygenase gene by plant-mediated RNAi impairs larval tolerance of gossypol. Nat Biotechnol. 2007;25:1307–13. https://doi.org/10.1038/nbt1352.
23. Knorr E, Fishilevich E, Tenbusch L, Frey MLF, Rangasamy M, Billion A, et al. Gene silencing in *Tribolium castaneum* as a tool for the targeted identification of candidate RNAi targets in crop pests. Sci Rep. 2018;8:2061. https://doi.org/10.1038/s41598-018-20416-y.

24. Knorr E, Billion A, Fishilevich E, Tenbusch L, Frey MLF, Rangasamy M, et al. Knockdown of genes involved in transcription and splicing reveals novel RNAi targets for pest control. Front Agron. 2021. https://doi.org/10.3389/fagro.2021.715823.
25. Müller R, Bálint M, Hardes K, Hollert H, Klimpel S, Knorr E, et al. RNA interference to combat the Asian tiger mosquito in Europe: a pathway from design of an innovative vector control tool to its application. Biotechnol Adv. 2023;66:108167. https://doi.org/10.1016/j.biotechadv.2023.108167.
26. Isoe J, Zamora J, Miesfeld RL. Molecular analysis of the *Aedes aegypti* carboxypeptidase gene family. Insect Biochem Mol Biol. 2009;39:68–73. https://doi.org/10.1016/j.ibmb.2008.09.006.
27. Scott JC, Brackney DE, Campbell CL, Bondu-Hawkins V, Hjelle B, Ebel GD, et al. Comparison of dengue virus type 2-specific small RNAs from RNA interference-competent and -incompetent mosquito cells. PLoS Negl Trop Dis. 2010;4:e848. https://doi.org/10.1371/journal.pntd.0000848.
28. Attarzadeh-Yazdi G, Fragkoudis R, Chi Y, Siu RWC, Ulper L, Barry G, et al. Cell-to-cell spread of the RNA interference response suppresses Semliki Forest virus (SFV) infection of mosquito cell cultures and cannot be antagonized by SFV. J Virol. 2009;83:5735–48. https://doi.org/10.1128/JVI.02440-08.
29. Cooper AM, Silver K, Zhang J, Park Y, Zhu KY. Molecular mechanisms influencing efficiency of RNA interference in insects. Pest Manag Sci. 2019;75:18–28. https://doi.org/10.1002/ps.5126.
30. Romeis J, Widmer F. Assessing the risks of topically applied dsRNA-based products to non-target arthropods. Front Plant Sci. 2020;11:679. https://doi.org/10.3389/fpls.2020.00679.
31. Giblin RM, Platzer EG. Hemolymph pH of the larvae of three species of mosquitoes, and the effect of *Romanomermis culicivorax* parasitism on the blood pH of *Culex pipiens*. J Invertebr Pathol. 1984;44:63–6.
32. Linser PJ, Smith KE, Seron TJ, Neira OM. Carbonic anhydrases and anion transport in mosquito midgut pH regulation. J Exp Biol. 2009;212:1662–71. https://doi.org/10.1242/jeb.028084.
33. Das S, Debnath N, Cui Y, Unrine J, Palli SR. Chitosan, carbon quantum dot and silica nanoparticle mediated dsRNA delivery for gene silencing in *Aedes aegypti*: a comparative analysis. ACS Appl Mater Interfaces. 2015;7:19530–5. https://doi.org/10.1021/acsami.5b05232.
34. Cancino-Rodezno A, Alexander C, Villaseñor R, Pacheco S, Porta H, Pauchet Y, et al. The mitogen-activated protein kinase p38 is involved in insect defense against Cry toxins from *Bacillus thuringiensis*. Insect Biochem Mol Biol. 2010;40:58–63. https://doi.org/10.1016/j.ibmb.2009.12.010.
35. Zhang X, Zhang J, Zhu KY. Chitosan/double-stranded RNA nanoparticle-mediated RNA interference to silence chitin synthase genes through larval feeding in the African malaria mosquito (*Anopheles gambiae*). Insect Mol Biol. 2010;19:683–93.
36. Liu D, Ren T, Gao X. Cationic transfection lipids. Curr Med Chem. 2003;10:1307–15.
37. Carter M, Shieh J. Gene delivery strategies. In: Guide to research techniques in neuroscience. Amsterdam: Elsevier; 2015. p. 239–52. https://doi.org/10.1016/B978-0-12-800511-8.00011-3.
38. Balazs DA, Godbey WT. Balaz 2011_liposomes for use in gene delivery. J Drug Deliv. 2011;2011:12.
39. Do Minh A, Sharon D, Chahal P, Kamen AA. Cell transfection. In: Comprehensive biotechnology. Amsterdam: Elsevier; 2019. p. 383–90. https://doi.org/10.1016/B978-0-444-64046-8.00023-9.
40. Simberg D, Hirsch-Lerner D, Nissim R, Barenholz Y. Comparison of different commercially available cationic lipid-based transfection kits. J Liposome Res. 2000;10:1–13. https://doi.org/10.3109/08982100009031091.
41. Yamano S, Dai J, Moursi AM. Comparison of transfection efficiency of nonviral gene transfer reagents. Mol Biotechnol. 2010;46:287–300. https://doi.org/10.1007/s12033-010-9302-5.
42. Barry G, Alberdi P, Schnettler E, Weisheit S, Kohl A, Fazakerley JK, et al. Gene silencing in tick cell lines using small interfering or long double-stranded RNA. Exp Appl Acarol. 2013;59:319–38. https://doi.org/10.1007/s10493-012-9598-x.
43. Barak M, Porath HT, Finkelstein G, Knisbacher BA, Buchumenski I, Roth SH, et al. Purifying selection of long dsRNA is the first line of defense against false activation of innate immunity. Genome Biol. 2020;21:26. https://doi.org/10.1186/s13059-020-1937-3.
44. Ovcharenko D, Jarvis R, Hunicke-Smith S, Kelnar K, Brown D. High-throughput RNAi screening in vitro: from cell lines to primary cells. RNA. 2005;11:985–93. https://doi.org/10.1261/rna.7288405.
45. Brackney DE, Scott JC, Sagawa F, Woodward JE, Miller NA, Schilkey FD, et al. C6/36 Aedes albopictus cells have a dysfunctional antiviral RNA interference response. PLoS Negl Trop Dis. 2010;4:e856. https://doi.org/10.1371/journal.pntd.0000856.
46. Lin Y-H, Huang J-H, Liu Y, Belles X, Lee H-J. Oral delivery of dsRNA lipoplexes to German cockroach protects dsRNA from degradation and induces RNAi response. Pest Manag Sci. 2017;73:960–6. https://doi.org/10.1002/ps.4407.
47. Chang K, Marran K, Valentine A, Hannon GJ. RNAi in cultured mammalian cells using synthetic siRNAs. Cold Spring Harb Protoc. 2012;2012:957–61. https://doi.org/10.1101/pdb.prot071076.
48. Cheng G, Liu L, Wang P, Zhang Y, Zhao YO, Colpitts TM, et al. An in vivo transfection approach elucidates a role for *Aedes aegypti* thioester-containing proteins in flaviviral infection. PLoS ONE. 2011;6:e22786. https://doi.org/10.1371/journal.pone.0022786.
49. Taschauer A, Polzer W, Pöschl S, Metz S, Tepe N, Decker S, et al. Combined chemisorption and complexation generate siRNA Nanocarriers with biophysics optimized for efficient gene knockdown and air-blood barrier crossing. ACS Appl Mater Interfaces. 2020;12:30095–111. https://doi.org/10.1021/acsami.0c06608.
50. Aydin O, Kanarya D, Yilmaz U, Tunc CÜ. Determination of optimum ratio of cationic polymers and small interfering RNA with agarose gel retardation assay. Methods Mol Biol. 2022;2434:117–28.
51. Wang T, Larcher LM, Ma L, Veedu RN. Systematic screening of commonly used commercial transfection reagents towards efficient transfection of single-stranded oligonucleotides. Molecules. 2018. https://doi.org/10.3390/molecules23102564.
52. Chong ZX, Yeap SK, Ho WY. Transfection types, methods and strategies: a technical review. PeerJ. 2021;9:e11165. https://doi.org/10.7717/peerj.11165.
53. Fus-Kujawa A, Prus P, Bajdak-Rusinek K, Teper P, Gawron K, Kowalczuk A, et al. An overview of methods and tools for transfection of eukaryotic cells in vitro. Front Bioeng Biotechnol. 2021;9:701031. https://doi.org/10.3389/fbioe.2021.701031.
54. Nikcevic G, Kovacevic-Grujicic N, Stevanovic M. Improved transfection efficiency of cultured human cells. Cell Biol Int. 2003;27:735–7. https://doi.org/10.1016/s1065-6995(03)00143-4.
55. Shi B, Mengzhou X, Wang Y, Wang Y, Li D, Zhao X, et al. An improved method for increasing the efficiency of gene transfection and transduction. Int J Physiol Pathophysiol Pharmacol (IJPPP). 2018;10:95–104.
56. Cronshaw DG. Transfection of S2 cell with DNA using CellFectin reagent. Bio-Protocol. 2012;e-190.
57. Forsbach A, Müller C, Montino C, Kritzler A, Curdt R, Benahmed A, et al. Impact of delivery systems on siRNA immune activation and RNA interference. Immunol Lett. 2012;141:169–80. https://doi.org/10.1016/j.imlet.2011.10.001.
58. Martín-Montañez E, López-Téllez JF, Acevedo MJ, Pavía J, Khan ZU. Efficiency of gene transfection reagents in NG108-15, SH-SY5Y and CHO-K1 cell lines. Methods Find Exp Clin Pharmacol. 2010;32:291–7. https://doi.org/10.1358/mf.2010.32.5.1498327.
59. McFarlane M, Laureti M, Levée T, Terry S, Kohl A, Pondeville E. Improved transient silencing of gene expression in the mosquito female *Aedes aegypti*. Insect Mol Biol. 2021;30:355–65. https://doi.org/10.1111/imb.12700.
60. Lwande OW, Obanda V, Lindström A, Ahlm C, Evander M, Näslund J, et al. Globe-trotting *Aedes aegypti* and *Aedes albopictus*: risk factors for arbovirus pandemics. Vector Borne Zoonotic Dis. 2020;20:71–81. https://doi.org/10.1089/vbz.2019.2486.
61. Boutros M, Brás LP, Wolfgang H. Analysis of cell-based RNAi screens. Genome Biol. 2006;7:66.
62. Öhlund P, Delhomme N, Hayer J, Hesson JC, Blomström A-L. Transcriptome analysis of an *Aedes albopictus* cell line single- and dual-infected with Lammi virus and WNV. Int J Mol Sci. 2022. https://doi.org/10.3390/ijms23020875.

Additional file 1

Gene silencing in the aedine cell lines C6/36 and U4.4 using long double-stranded RNA

Bodunrin Omokungbe[1,2], Alejandra Centurión [1,3], Sabrina Stiehler[2], Antonia Morr[3], Andreas Vilcinskas[1,2,3], Antje Steinbrink[1,2], Kornelia Hardes[1,3,4]

[1] LOEWE Centre for Translational Biodiversity Genomics (LOEWE TBG), Senckenberganlage 25, 60325 Frankfurt am Main, Germany
[2] Institute for Insect Biotechnology, Justus-Liebig University, Heinrich-Buff-Ring 26-32, 35392 Giessen, Germany
[3] Fraunhofer Institute for Molecular Biology and Applied Ecology IME, Branch of Bioresources, Ohlebergsweg 12, 35392 Giessen, Germany
[4] BMBF Junior Research Group in Infection Research „ASCRIBE" Ohlebergsweg 12, 35392 Giessen, Germany

Table S1: List of primers for the synthesis of dsRNA and dsRNA template sequences.

Primer sequence	
Name	Sequence 5′→3′
mCherrydsR-T7-FW	TAATACGACTCACTATAGGGGCGTGATGAACTTCGAGGAC
mCherrydsR-T7-RV	TAATACGACTCACTATAGGGCTTGTACAGCTCGTCCATGC
GFP-T7-FW	CCCTTTAATACGACTCACTATAGGGAGAACCACATGAAGCAGCACGACTT
GFP-T7-RV	CCCTTTAATACGACTCACTATAGGGAGAGTCCATGCCGAGAGTGATCCCG
Template sequence	
mCherry-dsRNA	CGTGATGAACTTCGAGGACGGCGGCGTGGTGACCGTGACCCAGGACTCCTCC CTGCAGGACGGCGAGTTCATCTACAAGGTGAAGCTGCGCGGCACCAACTTCC CCTCCGACGGCCCCGTAATGCAGAAGAAGACCATGGGCTGGGAGGCCTCCTC CGAGCGGATGTACCCCGAGGACGGCGCCCTGAAGGGCGAGATCAAGCAGAG GCTGAAGCTGAAGGACGGCGGCCACTACGACGCTGAGGTCAAGACCACCTAC AAGGCCAAGAAGCCCGTGCAGCTGCCCGGCGCCTACAACGTCAACATCAAGT TGGACATCACCTCCCACAACGAGGACTACACCATCGTGGAACAGTACGAACG CGCCGAGGGCCGCCACTCCACCGGCGGCATGGACGAGCTGTACAAG
GFP-dsRNA (+T7)	CCCTTTAATACGACTCACTATAGGGAGAACCACATGAAGCAGCACGACTTCTT CAAGTCCGCCATGCCCGAAGGCTACGTCCAGGAGCGCACCATCTTCTTCAAG GACGACGGCAACTACAAGACCCGCGCCGAGGTGTAGTTCGAGGGCGACACCC TGGTGAACCGCATCGAGCTGAAGGGCATCGACTTCAAGGAGGACGGCAACAT CCTGGGGCACAAGCTGGAGTACAACTACAACAGCCACAACGTCTATATCATG GCCGACAAGCAGAAGAACGGCATCAAGGTGAACTTCAAGATCCGCCACAAC ATCGAGGACGGCAGCGTGCAGCTCGCCGACCACTACCAGCAGAACACCCCCA TCGGCGACGGCCCCGTGCTGCTGCCCGACAACCACTACCTGAGCACCCAGTC CGCCCTGAGCAAAGACCCCAACGAGAAGCGCGATCACATGGTCCTGCTGGAG TTCGTGACCGCCGCCGGGATCACTCTCGGCATGGACTCTCCCTATAGTGAGTC GTATTAAAGGG

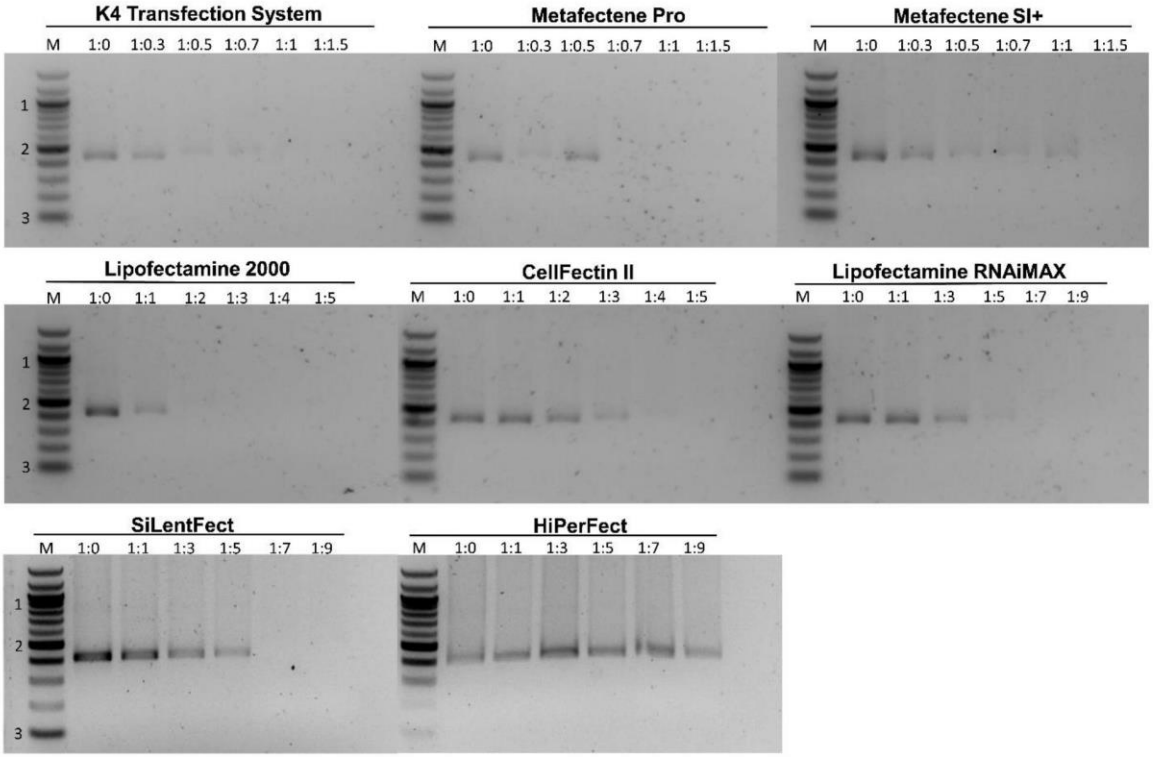

Fig. S1. Assessment of the complexing capacity of commercially available TRs using long dsRNA by incubating them at various ratios (dsRNA:TR) ranging from 1:0 to 1:9. Agarose gel electrophoresis was used to determine the point at which the TR completely complexed the dsRNA. M = 100 bp DNA Ladder (New England BioLabs); the numbers 1, 2 and 3 indicate the 1-kbp, 500-bp and 100-bp bands, respectively.

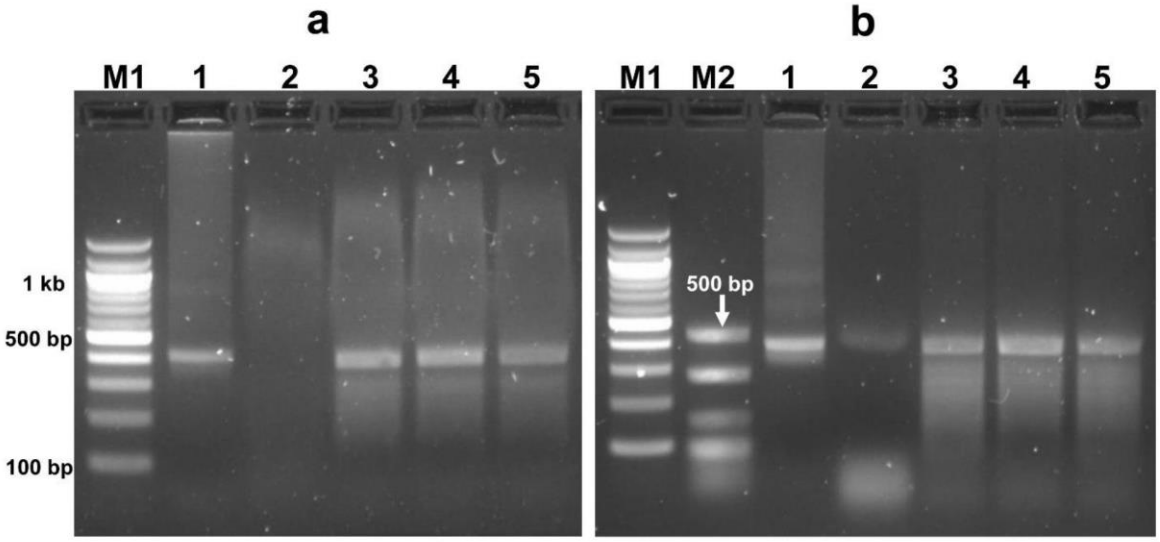

Fig. S2. Stability test of long dsRNA targeting mCherry in C6/36 and U4.4 cell supernatants. Agarose gel electrophoresis was used to determine the stability after incubation for 20 min (a) and 240 min (b). The dsRNA was incubated in 1: nuclease free water, 2: RNase III, 3: supplemented L-15 medium, 4: supernatant of C6/36 cell culture and 5: supernatant of U4.4 cell culture. The marker lanes are M1: 100 bp DNA Ladder and M2: dsRNA Ladder (both New England BioLabs).

Table S2. Uptake efficiency of dsRNA into C6/36 and U4.4 using TRs. Cells were transfected with labeled dsRNA using K4, Metafectene Pro, Metafectene SI+, Lipofectamine 2000, and CellFectin II. The TRs were used to transfect cells with 200 ng labeled dsRNA, except Lipofectamine 2000 with only 50 ng. Fluorescence pictures were taken at 24 hpt. The cells were counted using ImageJ v1.54d, the transfected cells were manually analyzed. The dsRNA uptake efficiency represents the ration of transfected cells to total cell count in percentage.

Transfection reagent	dsRNA uptake efficiency (%)
C6/36 cell	
No Transfection reagent (w/o)	3.09
K4 transfection system	95.52
Metafectene Pro	92.33
Metafectene SI+	99.71
Lipofectamine 2000	64.84
CellFectin II	97.24
U4.4 cell	
No Transfection reagent (w/o)	17.99
K4 transfection system	91.56
Metafectene Pro	90.22
Metafectene SI+	98.48
Lipofectamine 2000	59.83
CellFectin II	96.17

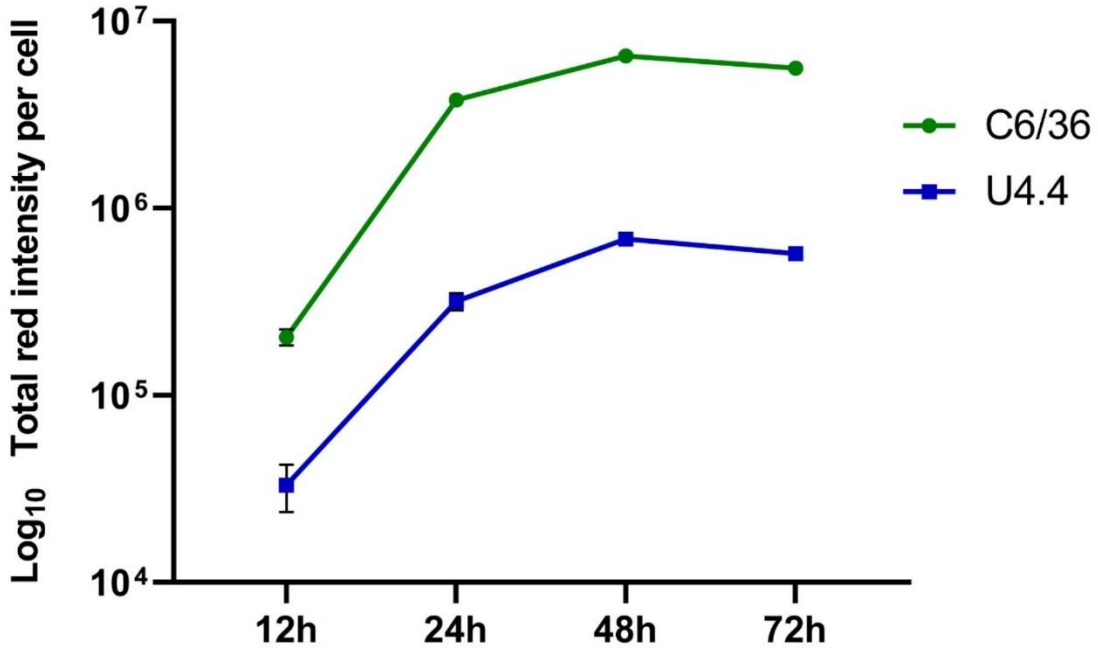

Fig. S3: Red fluorescence intensity in C6/36 and U4.4 cells after infection with mCherry-SFV. The cells were infected at full confluency with mCherry-SFV (MOI 0.01) and the total red intensity of the virus and cell count were analyzed at 12, 24, 48, and 72 hpi. The data are mean values (n = 3) of the total red intensity per cell (total red intensity/total cell count) and the error bars represent standard deviations.

Chapter II

RNA interference mediated mortality in *Aedes albopictus*: a challenging journey toward species-specific vector control

Parasite & Vectors. 2025 November 14;18(1):463. doi: 10.1186/s13071-025-07113-2. PMID: 41239436
PMCID: PMC12619383

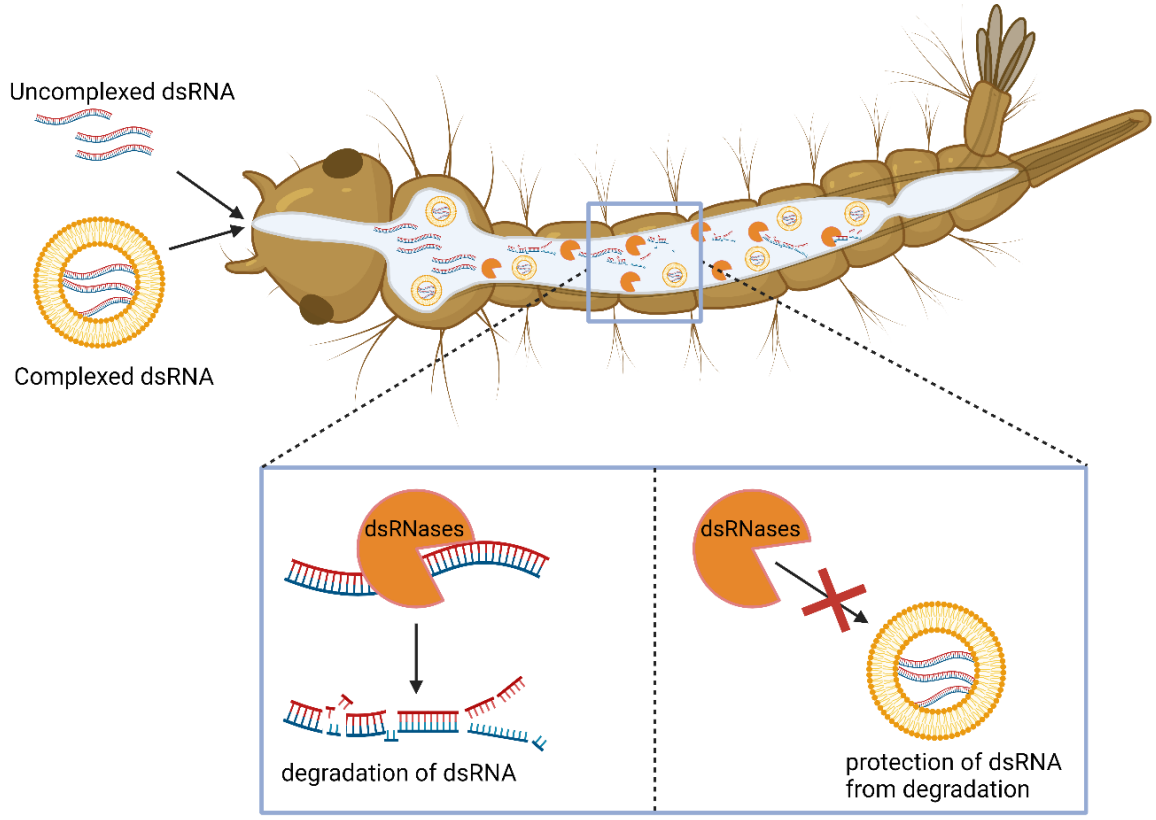

Omokungbe *et al. Parasites & Vectors* (2025) 18:463
https://doi.org/10.1186/s13071-025-07113-2

Parasites & Vectors

RESEARCH Open Access

RNA interference mediated mortality in *Aedes albopictus*: a challenging journey toward species-specific vector control

Bodunrin Omokungbe[1,2,3], Alejandra Centurión[1,3], Sabrina Stiehler[2], Magnus Wolf[4,5], Pascal Geisler[3], Andreas Vilcinskas[1,2,3], Antje Steinbrink[1,2] and Kornelia Hardes[1,3,6*]

Abstract

Background *Aedes albopictus* is a major vector of pathogens, including arboviruses, causing thousands of deaths annually. With no effective antiviral therapies and increasing concerns about the ecological impact of chemical insecticides, species-specific strategies, such as RNA interference (RNAi), are beneficial. Thus, identifying and validating target genes that induce mortality is essential. However, RNAi efficacy in *Ae. albopictus* is often inconsistent, owing to multiple factors including degradation by nucleases. Therefore, molecular identification and quantification of the underlying nucleases will provide a basis for improving RNAi efficacy.

Methods Target genes were selected from previous studies, identified in *Ae. albopictus*, and their corresponding long double-stranded RNAs (dsRNAs) were designed. Using U4.4. cells as a first model, cytotoxicity was assessed with the CellTiter-Glo assay and gene knockdown via RT-qPCR. Larval survival assays and RT-qPCR were then used to evaluate in vivo effects. Owing to the lack of significant larval mortality, dsRNA complex size was analyzed using dynamic light scattering and their oral uptake was visualized by fluorescence microscopy. Suspecting degradation, dsRNA stability was assessed by agarose gel electrophoresis following incubation with larval gut extracts. This prompted the identification, characterization, and validation of two putative dsRNases. Finally, transfection reagents (TRs) were tested for their ability to protect dsRNA from degradation.

Results Only one of the synthesized dsRNAs targeting the inhibitor of apoptosis (IAP) significantly reduced U4.4 cell viability to 65% (uncomplexed-dsRNA) and 13% (K4-complexed dsRNA). However, all tested dsRNAs achieved significant gene knockdown in the cell-based assay. None of the dsRNAs induced significant larval mortality, because dsRNA was rapidly degraded by larval gut extracts within 4 min. Although, gene knockdown was confirmed in the gut tissue. Each of the two identified dsRNases contained a signal peptide, catalytic residues, and substrate- and Mg^{2+}-binding sites, and were highly expressed in larval guts. Of the dsRNA, 65% remained intact at 15 min when complexed with K4, but declining to 13% by 24 h.

Conclusions All target genes were significantly silenced in cells, and IAP in larval gut tissue. Although TRs improved dsRNA stability in vitro, no significant larval mortality was observed, likely due to rapid gut degradation. Therefore, effective RNAi-based control of *Ae. albopictus* requires identifying gut-specific essential genes and improved delivery systems.

*Correspondence:
Kornelia Hardes
Kornelia.Hardes@ime.fraunhofer.de
Full list of author information is available at the end of the article

Keywords RNAi, dsRNA, dsRNases, Transfection reagents, Gene silencing, Nucleases, Arbovirus, dsRNA stability, RNAi formulation

Background

Mosquitoes are known to transmit important pathogens that cause viral, bacterial, and parasitic diseases [1]. Among them, *Aedes albopictus* is of particular concern owing to its continuing worldwide expansion and its capacity to transmit up to 26 arthropod-borne viruses (arboviruses), including Zika virus, dengue virus, and Chikungunya virus [2, 3]. There are currently no specific treatments available for most diseases caused by the pathogens transmitted by *Ae. albopictus* [4]. Hence, reduction of the mosquito population relies heavily on the use of chemical insecticides [5]. However, these vector control methods face numerous challenges, including insecticide resistances and off-target effects [6]. For these reasons, the use of RNA interference (RNAi) as a species-specific vector control method by inducing targeted gene knockdown is of great interest [7].

RNAi is an evolutionarily conserved mechanism present in almost all eukaryotes, in which RNA molecules trigger sequence-specific knockdown of genes after transcription. There are three known RNAi pathways in mosquitoes: small interfering RNA (siRNA), micro-RNA, and piwi interacting RNA [8]. The siRNA pathway primarily functions as a defense mechanism against foreign nucleic acids and transposable elements [9, 10]. This pathway can be triggered by either siRNA or double-stranded RNA (dsRNA), with the latter being cleaved into ~21 nucleotide (nt) siRNAs by the enzyme Dicer-2. The siRNA is separated into two strands, with one strand loaded into the RNA-induced silencing complex. Together with the protein Argonaute-2, the complex binds to complementary mRNA, leading to its degradation [8, 11].

The utilization of long dsRNA as a successful biocontrol method for gene silencing in insects has been previously demonstrated [12]. RNAi has been used in several insects to target diverse genes, leading to a weakened immune system, causing mortality, or the inability to develop or reproduce [7, 13]. For example, silencing the beta-tubulin (β-tub) and inhibitor of apoptosis (IAP) genes led to high larval mortality in *Aedes aegypti* [14, 15]. Similarly, knockdown of genes such as Dre4, Ras opposite (ROP), and Nucampholin (NCM) led to high mortality in the red flour beetle *Tribolium castaneum* [16]. Despite the success of RNAi in various insects, it faces several challenges.

A key limiting factor is the inefficient and inconsistent uptake of dsRNA, since RNAi is only initiated when the dsRNA enters the cells. Thus, the delivery method largely determines its efficiency [17]. The most common methods of delivering dsRNA are microinjection, oral feeding, and soaking. For RNAi-based mosquito control, targeting the larval stages is most practical. For this, dsRNA can be added to breeding water for direct ingestion, a method simulated in the laboratory via soaking assays [18]. Another limiting factor includes the rapid degradation of dsRNA by gut nucleases [19]. The degradation is mostly mediated by the activity of dsRNA-degrading nucleases (dsRNases), which belong to the DNA/RNA nonspecific endonuclease superfamily and are predominately expressed in the gut to digest exogenous nucleic acid [20–22]. Although, knowledge of these limitations on the use of RNAi for mosquito control is not new, specific molecular parameters such as dsRNA degradation time and identification of specific dsRNases need to be defined to help overcome them. Additionally, the use of carrier systems has been investigated to better understand cellular uptake [23], as well as to improve RNAi efficacy by protecting dsRNA from degradation, e.g., in *Ae. aegypti* [14]. We therefore hypothesized that encapsulating dsRNA in carriers, such as liposomes, can enhance its stability and uptake in *Ae. albopictus* larvae, improving gene knockdown and RNAi-induced mortality.

This study aimed to induce larval mortality in *Ae. albopictus* via RNAi. We selected and identified homologs of β-tub, Dre4, IAP, ROP, and NCM genes, previously shown to cause high mortality in other insects [14–16]. Initial evaluation of dsRNAs targeting these genes, both complexed with liposome-based transfection reagents (TRs) and uncomplexed, was conducted in U4.4 cells using cell viability and gene knockdown assays. We then tested the dsRNAs in larvae through survival assays and gene knockdown analyses. Owing to a lack of significant mortality in larvae, we examined the particle size of the dsRNA complexes and visualized their oral uptake, to identify potential limiting factors. We also assessed dsRNA degradation by larval gut extract and subsequently identified, characterized, and confirmed the presence of dsRNase genes in *Ae. albopictus*, with high activity in the gut. Finally, we tested whether TRs were able to protect the dsRNA from gut degradation in vitro. These findings advance the study of RNAi as a potential biocontrol strategy against *Ae. albopictus* and related species, by providing for the first time, precise quantification of nuclease activity, together with molecular

identification and characterization of the specific dsRNase genes underlying RNAi inefficacy in this mosquito.

Methods

Mosquito rearing

Ae. albopictus (Rimini strain) were obtained as dried eggs (provided by Dr. Hanano Yamada, Joint FAO/IAEA Centre, Vienna, Austria). Eggs were hatched using a vacuum pump system. Larvae were raised in plastic trays containing dechlorinated tap water and fed with pulverized Pleco tablets (Tetra, Melle, Germany). Emerged adults were supplied with 8% fructose solution ad libitum. Females received defibrinated sheep blood (Thermo Fisher Scientific, Frankfurt, Germany) via a Hemotek membrane feeder (Hemotek, Blackburn, UK). The colony was maintained at 28 ± 2 °C and 75 ± 5% humidity, and a 12:12 h light–dark cycle in a climate chamber (Regineering, Pollenfeld, Germany).

Cell culture

Ae. albopictus cell lines C6/36 (provided by Prof. Dr. Stefanie Becker, University of Veterinary Medicine, Hannover, Germany) and U4.4 (obtained from Friedrich-Loeffler-Institute, Greifswald, Germany) were maintained at 28 °C in Leibovitz's L-15 Medium GlutaMax, supplemented with 10% fetal bovine serum, 1% penicillin/streptomycin, 1% MEM nonessential amino acids, and 1% tryptose phosphate broth (all from Thermo Fisher Scientific).

Candidate gene target selection and double-stranded RNA design

To identify RNAi target genes in *Ae. albopictus*, we searched literature for previously validated genes in other insects. Sequences were retrieved from VectorBase or the National Center for Biotechnology Information (NCBI). The complete coding sequence collection of *Ae. albopictus* was used to construct a local BLAST database using the makeblastdb tool from NCBI BLAST + suite. Each gene was queried via BLASTN 2.9.0 +, and the top five hits were selected for high sequence similarity and reliable ortholog identification. Only full-length mRNA sequences were retained. Genes known to induce high mortality were chosen: β-tub and IAP from *Ae. aegypti* [14, 15]; NCM, ROP, and Dre4 from *Tribolium castaneum* [16]. Suitable target regions were identified using the siRNA-Finder v21 (siFi21) [24]. Two dsRNA constructs per gene were designed using NCBI Primer-BLAST (400 and 500 bp), for regions identified by si-Fi21 as the main target. T7 promoter sequence was incorporated to the 5' end of each primer for in vitro transcription. Primer details are provided in Table S1 (Supplementary Information).

Double-stranded RNA preparation

For the synthesis of dsRNA targeting β-tub, Dre4, ROP, IAP, and NCM, total RNA from L4 *Ae. albopictus* larvae was extracted using the Monarch Total RNA Miniprep Kit (New England Biolabs, Frankfurt, Germany). Gene-specific primers with T7 promoter sequences were used for RT-qPCR with OneTaq One-Step RT-PCR Kit (New England Biolabs) on Applied Biosystems SimpliAmp thermal cycler (Thermo Fisher Scientific). The PCR products were purified using the NucleoSpin Gel and PCR Clean-up Kit (Macherey–Nagel, Düren, Germany), and used for in vitro transcription with the MEGAscript T7 Transcription Kit (Thermo Fisher Scientific). The dsRNAs were purified using lithium chloride precipitation, resuspended in nuclease-free water (Thermo Fisher Scientific), quantified by NanoDrop 2000 spectrophotometer (Thermo Fisher Scientific) with a dilution factor of 46.0, and stored at −80 °C. For mCherry dsRNA, a glycerol stock of *Escherichia coli* NEB 5-α (New England Biolabs) carrying pCMV-SFV6-2SG-mCherry (provided by Prof. Dr. Andres Merits, University of Tartu, Estonia and Prof. Dr. Andreas Pichlmair, Technical University of Munich, Germany) was cultured in lysogeny broth with 125 µg/mL kanamycin at 37 °C, 200 rpm overnight. GFP dsRNA was prepared similarly using *E. coli* harboring pGEM-T-Easy-GFP-125. Plasmid DNA from both strains was extracted using the NucleoSpin Plasmid DNA Kit (Macherey–Nagel). OneTaq Hot Start Quick-Load 2 × Master Mix (New England Biolabs) was used for PCR amplification of mCherry and GFP templates, followed by in vitro transcription as described above.

Cytotoxic effects of RNAi in aedine cell lines

To assess RNAi-induced cytotoxic effects, two dsRNA constructs per gene were tested on U4.4 and C6/36 cells at ~50% confluency. C6/36 cells served as RNAi-deficient control [25–27]. Treatments were applied either uncomplexed or complexed with TRs, and then the plates were incubated at 28 °C. In a first analysis, uncomplexed dsRNA at 25 ng/µL per well was used. Concentrations were based on pilot experiments (data not shown). In the second analysis, dsRNA at 2 ng/µL either uncomplexed or complexed (dsRNA:TR) with K4 Transfection System (1:1, K4, Biontex, Munich, Germany), Metafectene Pro (1:07, Biontex), or CellFectin II (1:5, Thermo Fischer Scientific), were used based on our previous protocol [27]. All treatments were prepared in antibiotic-free supplemented L-15 medium. Controls included nuclease-free water, Grace's insect medium, TRs alone, untreated cells, and ionomycin (100 µM in the assay, Thermo Fisher Scientific). At 6 h post-treatment (hpt), medium was replaced with fully supplemented L-15 medium. Cell

viability was measured at 48 hpt using the CellTiter-Glo Luminescent Cell Viability Assay (Promega, Walldorf, Germany). Data were normalized to the untreated control.

Larval bioassay for evaluating dsRNA-mediated mortality

Two larval bioassays were designed to assess RNAi-induced mortality. In the first, L1-L2 larvae were exposed for 4 h to uncomplexed or K4-complexed dsRNA (1:1) at 100 ng/µL in 75 µL nuclease free water inside 1.5 mL tubes. Larvae and solution were then transferred into 24-well plates (10 larvae/well, 3 replicates), and the volume was adjusted to 500 µL with tap water. Grounded larval food solution (25 µL) was provided daily, and mortality was recorded every 24 h. In the second approach, larvae were directly incubated in 24-well plates with 500 µL K4-complexed dsRNA at 20 or 50 ng/µL, and kept in the solution throughout the experiment. Feeding and monitoring followed the same procedure.

Gene silencing analysis in U4.4 cells and larvae of *Aedes albopictus*

Prior to gene silencing analysis, primer efficiency was determined by standard curves (0.1–1000 ng, see Supplementary Information Sect. 3 for details). Gene knockdown was evaluated by RT-qPCR following dsRNA treatment. U4.4 cells were treated with 2 ng/µL K4-complexed dsRNAs, as described in the cytotoxicity assay. Total RNA was extracted at 48 hpt for the β-tub 1, Dre4 1, NCM 1, and ROP 1 dsRNAs, and at 24, 48, and 72 hpt for IAP 2 using the Monarch Total RNA Miniprep Kit. Larval RNA was extracted at 3 d post-treatment from whole bodies or dissected guts using the second larval bioassay approach described above. RNA quality was verified with a NanoDrop 2000. RT-qPCR was performed using the Luna Universal One-Step RT-qPCR Kit (New England Biolabs) on a QuantStudio 3 Real-Time PCR System (Applied Biosystems, Thermo Fisher Scientific). Details of reagents and cycling conditions are listed in Table S2. Actin was used as reference gene; mCherry dsRNA served as negative control. Relative expression was calculated via the $2^{-\Delta\Delta Ct}$ method.

Dynamic light scattering analysis of formulated dsRNA

To assess whether dsRNA:TR complex size limited larval mortality, we analyzed them by dynamic light scattering (DLS) at concentrations of 10, 20, or 50 ng/µL. See Supplementary Information Sect. 4 for detailed description.

Fluorescence uptake analysis of dsRNA in larval stage of *Aedes albopictus*

To assess dsRNA uptake, mCherry or IAP 2 dsRNA was labeled with Cy3 fluorophore using the Silencer siRNA Labeling Kit (Thermo Fisher Scientific). Labeled dsRNA, either uncomplexed or complexed with K4 (1:1) was incubated with larvae in breeding water for 1 h. Larvae were then rinsed and transferred to fresh wells containing clean tap water. Larvae incubated in tap water served as negative control. Fluorescence was examined at 1, 3, 6, 24, and 48 hpt using a M165 FC fluorescence microscope with EL6000 light source. Images were captured with a DFC450 C camera and processed using LAS-X v4.13 (All from Leica Microsystems, Wetzlar, Germany).

Ex vivo degradation of dsRNA with gut extract of *Aedes albopictus*

In total, 50-pooled L4 larval guts were dissected in 500 µL nuclease-free water on ice and homogenized with cold ceramic beads using a TissueLyser II (Qiagen, Hilden, Germany) for 2 min at 30 Hz. After two centrifugation steps at 4 °C, supernatants were collected. To assess degradation, 10 µL of gut extract (≈1 gut) was incubated with 1 µg of mCherry dsRNA for 1–8 min. Reactions were stopped with 5 µL of 50 mM EDTA [21]. For the EDTA-containing gut extract experiment, EDTA was added to the gut extract prior to dsRNA incubation for 10 min. Samples were run on 2% agarose gels (110 V, 150 mA, 40 min) with the Mass Ruler loading dye (Thermo Fisher Scientific). A Gel Doc™ XR+(BioRad Laboratories, Munich, Germany) was used to visualize the gel bands. The ImageLab v.5.2.1 (BioRad Laboratories) was used to capture images and analyze the relative band intensity. Data were normalized to the controls.

Identification and characterization of *Aedes albopictus* dsRNase proteins

Ae. albopictus dsRNases were identified by BLASTp search against its genome (NCBI RefSeq: GCF_035046485.1), using *Ae. aegypti* dsRNases as queries [28]. Protein features were predicted using the NCBI's conserved domain search (https://www.ncbi.nlm.nih.gov/Structure/cdd/wrpsb.cgi) and the InterProScan v99.0 [29]. The dsRNase proteins from 14 dipterans were retrieved and aligned by the ClusterW in MEGA v11. Phylogenetic analysis was performed using the Maximum Likelihood method with Poisson correction model and 1000 bootstrap replicates for the confidence value (%) of each branch.

Expression profile of *Aedes albopictus* dsRNase genes

For developmental gene expression analysis of dsRNases, total RNA was extracted from all larval stages (L1–L4), dissected L4 guts, and the remaining body tissue using the Monarch Total RNA Miniprep Kit. Sample sizes included 50 L1, 30 L2, 15 L3, and 10 L4 larvae, and 30 L4 larvae for gut dissections. RT-qPCR was performed using

primers for Aal-dsRNase1 and Aal-dsRNase2 with the Luna Universal One-Step RT-qPCR Kit. Reference genes included actin and protein phosphatase-2A. Data were analyzed using the extended-ΔCt method [30]. Primer sequences are in Table S1 (Supplementary Information).

To confirm specificity, Aal-dsRNase1 and Aal-dsRNase2 were amplified via RT-PCR using the OneTaq One-Step RT-PCR Kit. Amplicons were sequenced by LGC Genomics (Berlin, Germany), and aligned with the corresponding reference sequences (see Fig. S5).

Protection of dsRNA from degradation using commercially available transfection reagents

To assess dsRNA protection, mCherry dsRNA was complexed with K4 (1:1), Metafectene Pro (1:0.7), Metafectene SI + (Biontex; 1:1.5), or Lipofectamine 2000 (Invitrogen, Thermo Fisher Scientific; 1:3), then incubated with L4 gut extract for 10 min. For K4, additional time points were tested at 0.25–24 h. Uncomplexed dsRNA served as negative control and the addition of EDTA to gut extract prior to incubation served as controls for complexed-dsRNA samples. To decomplex samples for agarose gel analysis, gel loading dye purple (6X) containing SDS (New England Biolabs) was added before loading.

Statistical analysis and visualization

The graphical abstract was created with BioRender and data were analyzed using GraphPad Prism. One-way ANOVA with Dunnett's or Šidák's multiple comparison tests was used for gene knockdown analysis in cells and larvae, respectively. Larval survival was analyzed by Kaplan–Meier with Log-rank (Mantel–Cox) test. The expression of dsRNase and dsRNA protection assays were analyzed via one-way ANOVA.

Results

Selection of target genes for dsRNA synthesis

Target genes were selected based on previous studies in other insects reporting high RNAi-induced mortality. Homologous genes in *Ae. albopictus* with ≥ 70% sequence identity were identified using NCBI tools. Each sequence was screened with the si-Fi21 software [24] against a custom local database of the *Ae. albopictus* genome to ensure specificity. Two dsRNAs targeting high-efficiency regions of each gene were designed (Table 1). For synthesis, primers with T7-promoter sequences were used to amplify templates via RT-PCR, followed by in vitro transcription and purification.

RNAi-induced cytotoxicity in aedine cell lines

To assess the cytotoxic effects of the synthesized dsRNAs, U4.4 cells were treated with 25 ng/µL of uncomplexed dsRNA targeting β-tub, Dre4, IAP, ROP, and NCM genes. At 48 hpt, cell viability was assessed using the CellTiter-Glo assay and only IAP 2 dsRNA significantly reduced cell viability in U4.4 cells to 65%, while the other dsRNAs had no cytotoxic effect (Fig. 1a). To confirm RNAi specificity, we used RNAi-deficient C6/36 cells as a control, where the dsRNAs had no cytotoxic effect (Fig. 1b).

We proceeded to transfect U4.4 cells with 2 ng/µL dsRNAs complexed with K4, CellFectin II, or Metafectene Pro. Only IAP 2 dsRNA reduced cell viability to 13% with K4 (Fig. 1c), 34% with CellFectin II, and 40% with Metafectene Pro (Fig. S1, Supplementary Information). Other dsRNAs showed no effect. Similarly, transfection of complexed dsRNAs into C6/36 cells showed no significant cytotoxicity (Fig. 1d).

Gene knockdown analysis of complexed dsRNA in U4.4 cells

To further validate whether dsRNA-induced cytotoxicity was RNAi-specific, we selected one dsRNA variant

Table 1 List of target genes and dsRNA candidates along with their efficient siRNA hits and query accession numbers

Gene	Abbreviation of dsRNA candidate	Efficient siRNA hits (si-Fi21)	Insect	Accession number	Citation
β-tubulin (β-tub)	β-tub 1	237	*Aedes aegypti*	XM_001655975	[15]
	β-tub 2	240			
Inhibitor of apoptosis (IAP)	IAP 1	195	*Aedes aegypti*	DQ993355.1	[14]
	IAP 2	202			
Dre4	Dre4 1	197	*Tribolium castaneum*	XM_967384.1	[16]
	Dre4 2	214			
Nucampholin (NCM)	NCM 1	218	*Tribolium castaneum*	XM_001811253.1	[16]
	NCM 2	181			
Ras opposite (ROP)	ROP 1	239	*Tribolium castaneum*	NM_001170684.1	[16]
	ROP 2	226			

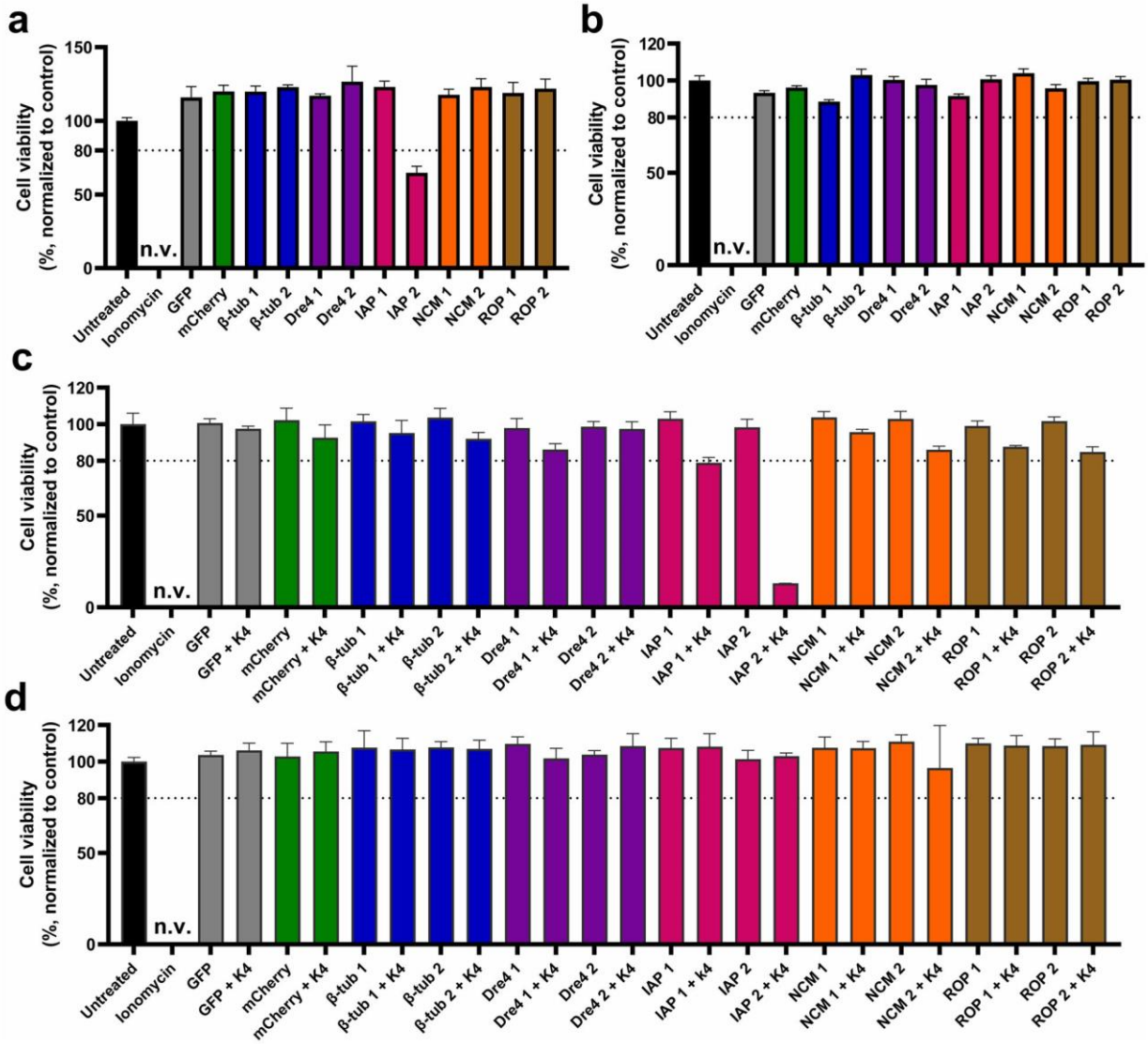

Fig. 1 Cytotoxic effects of dsRNAs on aedine cell lines. Cells at ~50% confluency were treated with dsRNAs. **a** U4.4 and **b** C6/36 cells treated with uncomplexed dsRNAs at 25 ng/µL. **c** U4.4 and **d** C6/36 cells treated with dsRNAs complexed with K4 Transfection System at 2 ng/µL (1:1). Cell viability was assessed at 48 h post-treatment using the CellTiter-Glo assay. Data ($n = 4$) were normalized to untreated controls (treatment/control × 100). Bars show mean viability; error bars represent coefficient of variation (%). The dotted line indicates the 80% toxicity threshold. *n.v.* near-zero viability

of each gene for knockdown analysis via RT-qPCR. The mCherry dsRNA was included as a nonspecific negative control and actin as a reference gene for normalization. The dsRNAs were transfected into the cells using K4 following the standard protocol. At 48 hpt, all target genes showed reduced mRNA levels, with ROP 1 dsRNA achieving the highest knockdown of 93%, while NCM 1 dsRNA had only 51% knockdown (Fig. 2a). A time-course with IAP 2 dsRNA showed increasing knockdown over time, with 44%, 63%, and 77% for 24, 48, and 72 hpt, respectively (Fig. 2b).

Larval mortality following dsRNA exposure in *Aedes albopictus*

To evaluate dsRNA-induced mortality in vivo, L1-L2 larvae were exposed to dsRNAs targeting β-tub, Dre4, IAP, ROP, or NCM genes, with or without complexation with K4. While TRs are not commonly used in vivo, we employed them in this study as a proof-of-concept to assess whether complexation enhances RNAi efficacy, given that uncomplexed dsRNA rarely achieves significant mortality in this species. Tap water and mCherry dsRNA served as negative controls. Two exposure

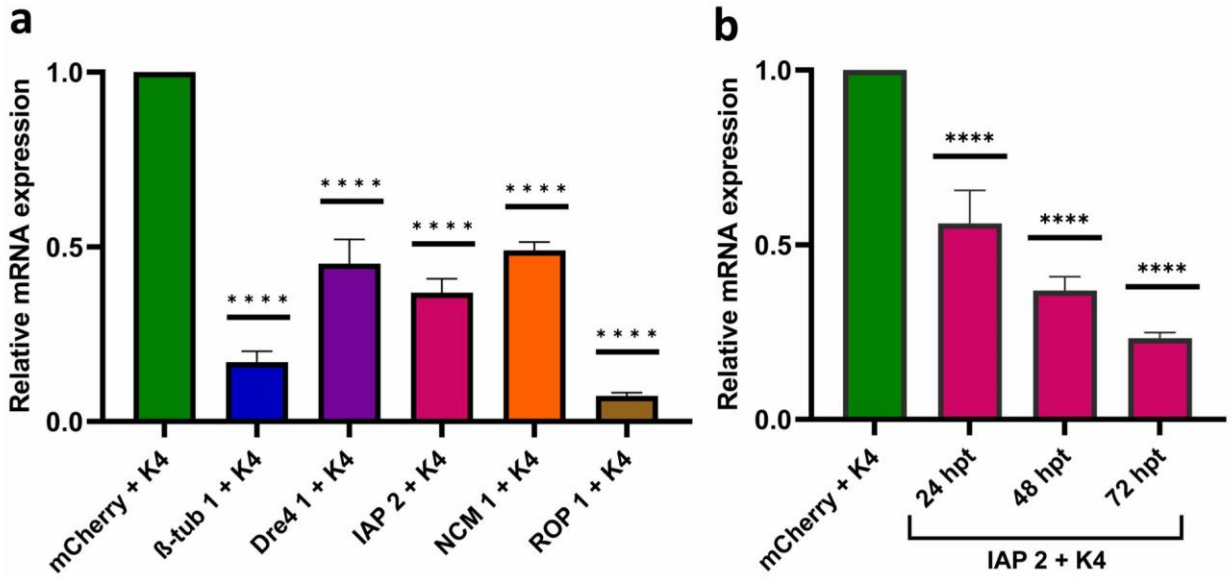

Fig. 2 Gene knockdown analysis in U4.4 cells following treatment with complexed dsRNAs using the K4 Transfection System (1:1). **a** Gene knockdown analysis of selected dsRNAs at 48 h post-treatment (hpt). **b** Time-course knockdown analysis of the IAP 2 dsRNA at 24, 48, and 72 hpt. Total RNA was extracted at each time point and used for RT-qPCR. Data were analyzed using the $2^{-\Delta\Delta Ct}$ method. Gene expression levels are shown relative to the nonspecific control mCherry dsRNA ($n=3$), with actin used as reference gene. Error bars represent standard deviations. The asterisk (****) represent a significant difference ($p<0.0001$) to the control via one way ANOVA and Dunnett's multiple comparison test

methods were used: In the first method, larvae were pre-incubated in 75 µL of dsRNA for 4 h ($n=30$), then transferred into 24-well plates with the final volume adjusted to 500 µL. In the second method, larvae were directly exposed to dsRNA in 24-well plates ($n=10$) for the entire duration of the experiment. Mortality was monitored daily in both cases. No significant mortality was observed with 100 ng/µL dsRNA in the first method (Fig. 3a and b), or 20 and 50 ng/µL in the second (Fig. 3c and d, respectively). However, in the second method, K4 alone showed toxicity at 50 ng/µL (Fig. 3d).

Gene knockdown analysis of complexed dsRNA in larvae of *Ae. albopictus*

To assess the gene silencing despite the lack of significant mortality, IAP 2 dsRNA was selected for RT-qPCR, with mCherry dsRNA as the control and actin as the reference gene for normalization. Larvae were treated with K4-complexed IAP 2 dsRNA (1:1) following the protocol of the second bioassay method. At 3 days post-treatment dissected gut or whole larvae were used for RNA extraction. RT-qPCR revealed a reduction in IAP mRNA levels in the gut, with knockdown of 34.7% and 51.5% at 20 and 50 ng/µL, respectively (Fig. 4). However, no significant knockdown was detected when whole larvae were analyzed (Fig S3, Supplementary Information).

Particle size determination and uptake dsRNA in larvae

Given the lack of RNAi-induce mortality, we investigated whether the dsRNA:TR complex size limited uptake. To determine the particle size of complexed mCherry dsRNA with K4, Metafectene Pro, or CellFectin II, we performed a DLS analysis using the side scattering method. The complex sizes formed at 10 ng/µL were similar, ranging between 150.6 and 165.8 nm (Supplementary Information, Table S3). The Polydispersity Index (PI) values were 0.10, 0.14, and 0.18 for K4, Metafectene Pro, and CellFectin II, respectively. In contrast, K4 complexes at 20 and 50 ng/µL were much larger (2461.7 and 5192.2 nm) with higher PI values (0.51 and 0.54).

To assess the oral uptake, larvae were incubated for 1 h in uncomplexed or K4-complexed Cy3-labeled mCherry or IAP 2 dsRNA at 200 ng/µL. Larvae were rinsed and placed in clean water. Both forms were taken up, with more pronounced fluorescence signal observed in those incubated with complexed dsRNA (Fig. 5). Uncomplexed dsRNA signal was not detectable at 24 and 48 h post-incubation, whereas complexed dsRNA remained noticeable.

Ex vivo degradation of dsRNA using *Aedes albopictus* gut extract

To investigate whether gut nucleases contributed to the lack of RNAi-induced mortality, we tested dsRNA stability by incubating 1 µg of mCherry dsRNA with L4 larval

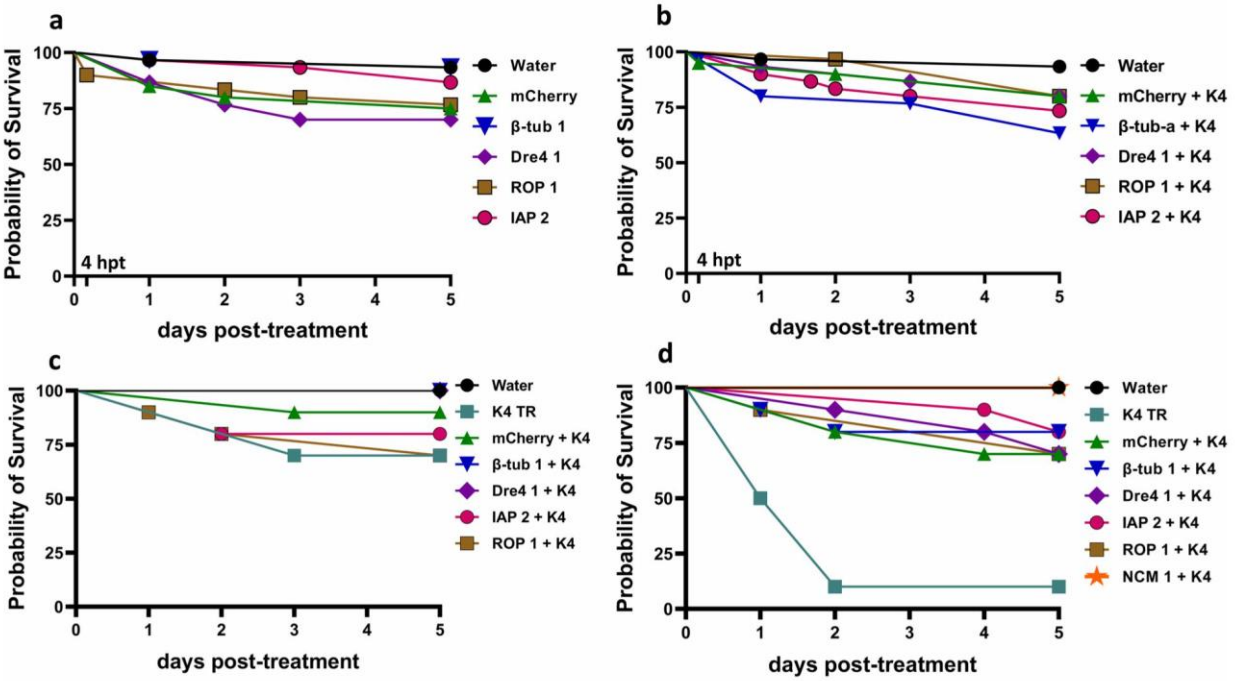

Fig. 3 RNAi-induced mortality in *Aedes albopictus* L1–L2 larvae following dsRNA treatment. In method one, larvae were incubated in **a** uncomplexed or **b** K4-complexed dsRNA (1:1), at 100 ng/µL for 4 h, then transferred to 24-well plates with a final volume of 500 µL. In method two, larvae remained in K4-complexed dsRNA solutions at **c** 20 or **d** 50 ng/µL for the entire experiment. Larval mortality was recorded daily. Survival probabilities were estimated using the Kaplan–Meier method and compared with the log-rank (Mantel-cox) test. Data are shown as percentages

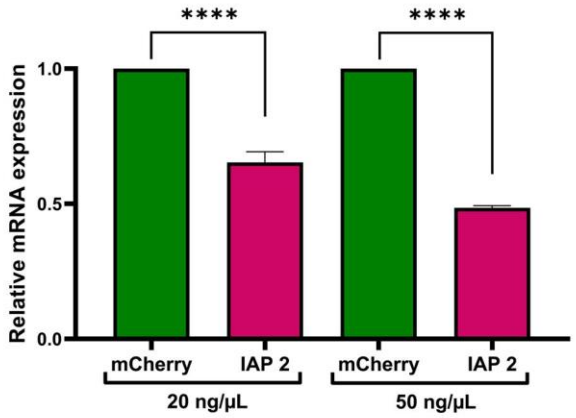

Fig. 4 Gene knockdown in larval guts following treatment with complexed IAP 2 dsRNA using the K4 Transfection System (1:1). Larvae were treated using the second approach, and guts were dissected at 3 days post-treatment for RNA extraction and RT-qPCR analysis. Actin was used as the reference gene, and relative expression was calculated using the $2^{-\Delta\Delta Ct}$ method, normalized to the nonspecific mCherry dsRNA control ($n = 3$). Error bars represent standard deviation. Asterisks (****) indicate a significant difference ($p < 0.0001$) by one-way ANOVA and Šidák's multiple comparison test

gut extract. Degradation was assessed by analyzing relative band intensity in agarose gel electrophoresis. The ex vivo analysis revealed rapid degradation of dsRNA, with complete degradation observed within 4 min (Fig. 6a). Meanwhile, degradation was completely inhibited when EDTA was added to the gut extract prior to incubation (Fig. 6b). The agarose gel images can be found in Fig. S4 (Supplementary Information).

Identification, characterization, and expression profile of *Aedes albopictus* dsRNases

The degradation of dsRNA observed in L4 larvae gut extract implies the activity of dsRNases. Therefore, we identified two dsRNases of *Ae. albopictus* via BLASTp search using dsRNase genes from *Ae. aegypti* [28] as queries. Highly related genes were identified, henceforth referred to in this study as Aal-dsRNase1 and Aal-dsRNase2. The protein sequences from both dsRNases cover 100% of the query, with 87.23% and 94.10% identity for Aal-dsRNase1 and Aal-dsRNase2, respectively, compared with *Ae. aegypti* (Table 2). Protein features analysis revealed the DNA/RNA nonspecific endonuclease domains (PF01223) of both dsRNases along with active-, substrate binding-, and Mg^{2+} binding sites (Fig. 7a). Given the ubiquity of dsRNases across the insect taxa [31], understanding their phylogenetic relationships in dipterans is of interest. Therefore, phylogenetic analysis

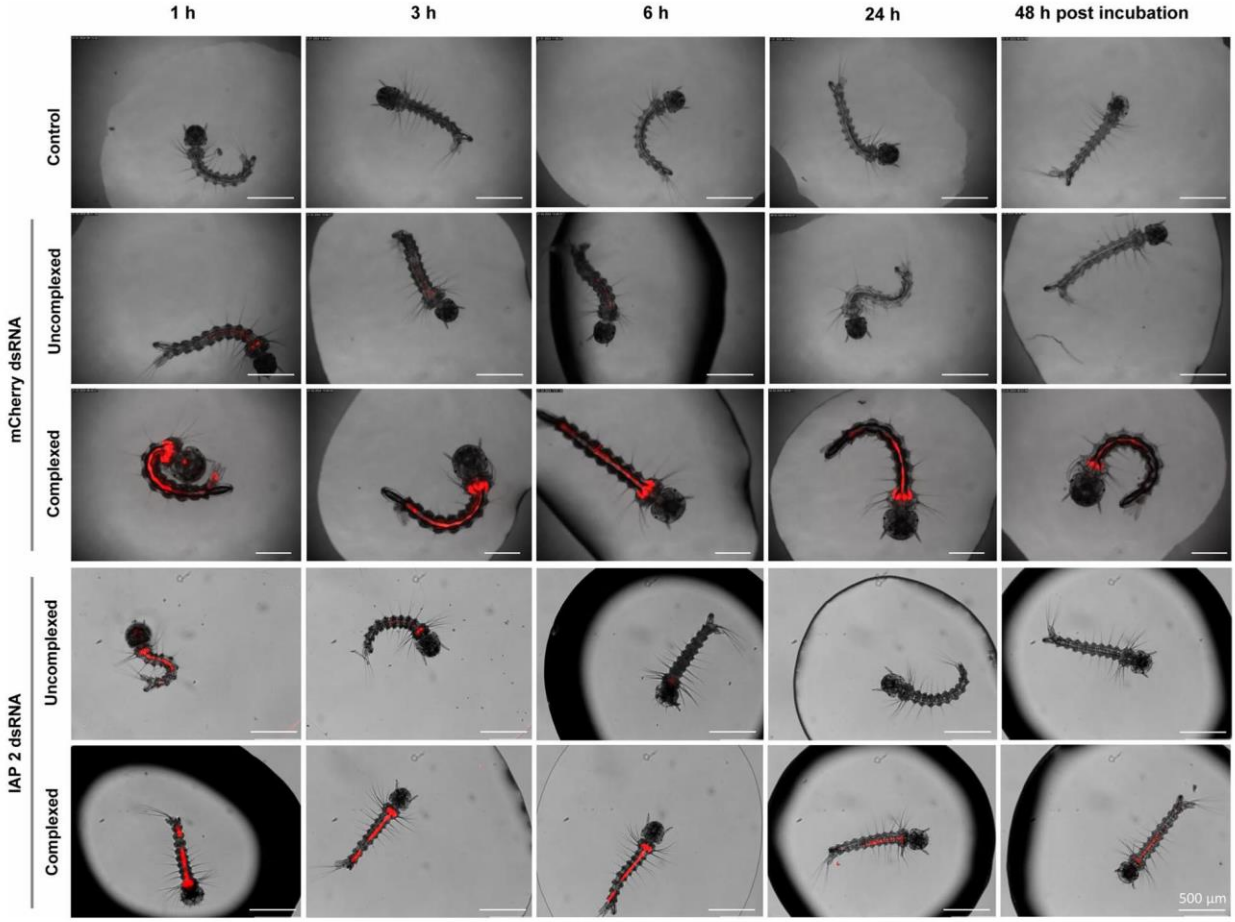

Fig. 5 Uptake analysis of dsRNA in the gut of *Aedes albopictus* larvae. Larvae were exposed to Cy3-labeled dsRNA, either uncomplexed or complexed with K4 Transfection System at 200 ng/µL for 1 h. Following incubation, the larvae were transferred to clean breeding water. Fluorescence signals from the dsRNA were monitored at multiple time points. Scalebar = 500 µm

of 26 dsRNase proteins from 14 dipteran species revealed that both dsRNases of *Ae. albopictus* are most closely related to those of *Ae. aegypti* (Fig. 8; Supplementary Information Table S4).

To better understand the developmental and tissue-specific expression of Aal-dsRNase1 and Aal-dsRNase2, we quantified their expression levels across all four larval stages (L1–L4) using RT-qPCR. The expression of Aal-dsRNase1 was most abundant in L1, followed by L3, L2, and L4 (Fig. 7b). While the expression of Aal-dsRNase2 was highest in L3 followed by L2, L1, and L4. Their expression was also quantified in the dissected gut and rest body of the L4 larvae, where the gut had higher expression of both dsRNases than the rest body (Fig. 7c). To ascertain the accuracy of the amplified targets, we used RT-PCR to amplify Aal-dsRNase1 and Aal-dsRNase2 genes and the products were sequenced and aligned to each respective dsRNase (Supplementary Information, Fig. S5).

Protection of dsRNA from degradation by *Aedes albopictus* gut extract using commercially available transfection reagents

To assess whether the TRs could protect dsRNA from degradation, mCherry dsRNA was complexed with four TRs and incubated with L4 larvae gut extract. All TRs provided protection, with Metafectene Pro offering the highest (90%), followed by Metafectene SI+, Lipofectamine 2000, and K4 (Fig. 9a). Since K4 was used in the larval bioassay, we further tested its protective effect over time. K4-complexed dsRNA retained 65% integrity at 0.25 h but decreased to 13% after 24 h (Fig. 9b, the agarose gel images can be found in Supplementary Information Fig. S6).

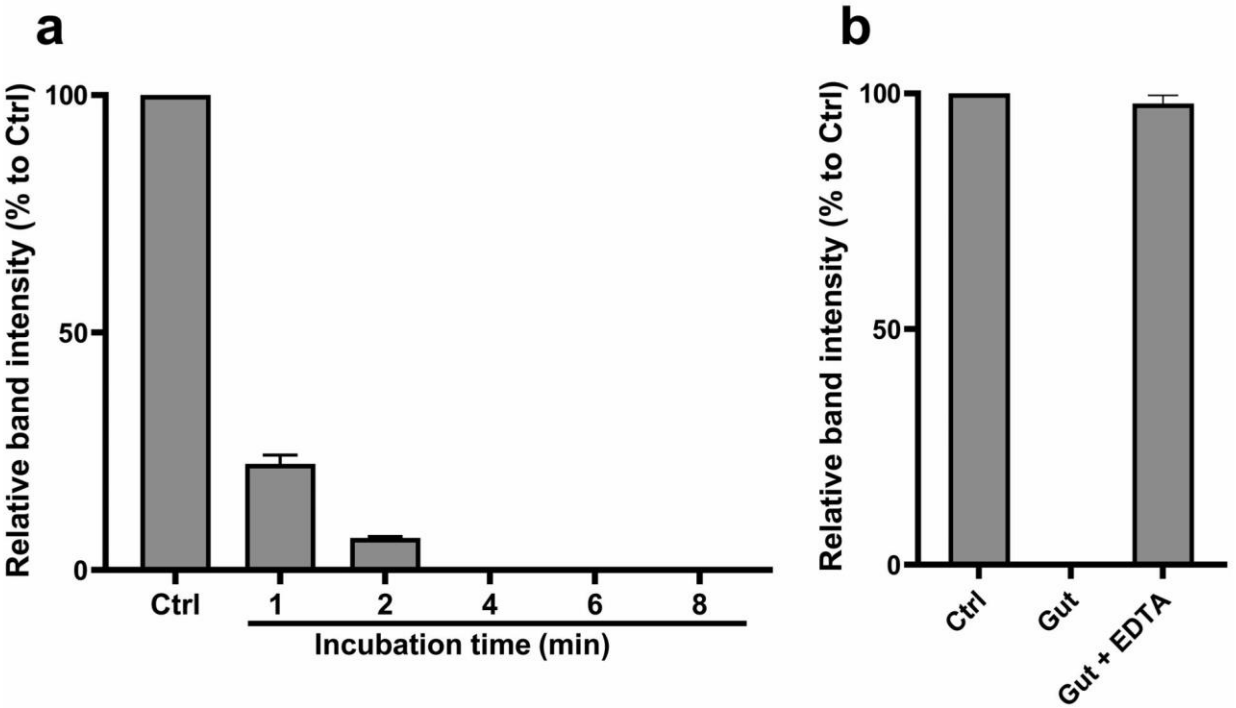

Fig. 6 Ex vivo degradation of dsRNA using gut extract of *Aedes albopictus* L4 larvae. Gut extract was used to incubate mCherry dsRNA. In **a**, the dsRNA was incubated with the gut extract for 1–8 min. In **b**, the dsRNA was incubated for 10 min with either gut extract alone or mixture of gut extract and EDTA. All samples were resolved on agarose gel electrophoresis immediately after incubation and the relative band intensity was determined and normalized to the control (Ctrl). The data shown are the normalized mean (%) of three independent experiments ($n = 3$) and the error bar represents the standard deviation

Table 2 Identification of *Aedes albopictus* dsRNases

Protein	Protein ID	EPL (aa)	BLASTp			
			Query (*Aedes aegyti*)	Query cover (%)	Identity (%)	E-value
Aal-dsRNase1	XP_019536384.3	415	XP_001648469.1	100	87.23	0.0
Aal-dsRNase2	XP_062714958.1	390	XP_001653479.2	100	94.10	0.0

The dsRNase were retrieved by BLASTp sequence similarity search using *Aedes aegypti* dsRNase 1 and 2 as queries

EPL Encoded Protein Length, *aa* amino acid

Discussion

RNAi is a promising tool for the control of insect vectors and agricultural pests, offering high specificity, minimal off-target effects, and strong environmental safety due to degradation of dsRNA outside the target organism [32, 33]. However, degradation within the larval gut can severely limit efficacy. In this study, we quantify key barriers to oral RNAi in *Ae. albopictus* larvae, showing that gut extracts rapidly degrade long dsRNA, leading to identifying two putative dsRNases potentially responsible for degradation. This study identified the key challenges associated with oral administration and established the design criteria required for more complex formulations to enable the efficient transport of target dsRNA across the epithelial barrier.

Target genes were selected on the basis of previous RNAi studies in other insect pests and vectors, including *Ae. aegypti* [14, 15] and *T. castaneum* [16]. Priority was given to genes associated with high mortality, such as β-tub, Dre4, IAP, ROP, and NCM. Gene-specific dsRNAs were designed using the si-Fi21 tool to ensure high silencing efficiency and minimal off-target effects [24]. Initial screening in *Ae. albopictus* U4.4 cells showed that only IAP 2 dsRNA significantly reduced cell viability, both when delivered alone or complexed with a TR (Fig. 1). Three TRs were tested, including K4, Metafectene Pro,

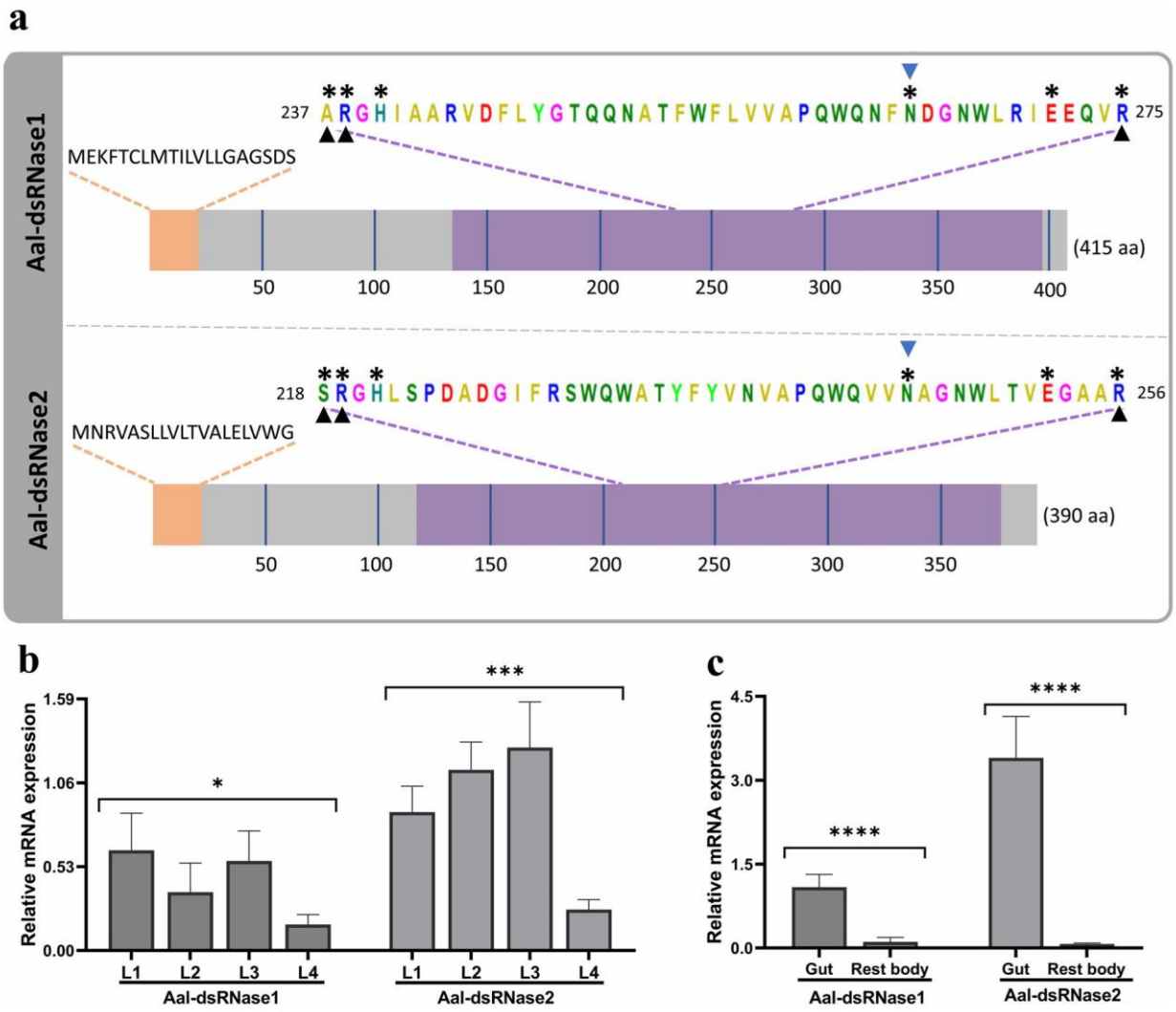

Fig. 7 Characterization of *Aedes albopictus* dsRNase proteins and their gene expression profile. **a** Schematic illustration of the two retrieved dsRNase proteins, with their conserved domains and total length (in brackets). The sequences of the signal peptides are specified. The active site (*), substrate binding site (▲), and Mg^{2+} binding site (▼) are also highlighted. The grey color indicates the noncytoplasmic domain, orange color shows the signal peptide region, while the purple color highlights the DNA/RNA nonspecific endonuclease domain. **b**, **c** Expression profiles of *Ae. albopictus* dsRNases. The expression of Aal-dsRNase1 and Aal-dsRNase2 was analyzed using RT-qPCR in **b** L1–L4 larval stages and in **c** dissected gut and rest body of L4 larvae. The relative mRNA level was calculated via the extended ΔCT method (e-ΔCT) using actin and protein phosphatase 2A as the reference genes for normalization, and the values are expressed as $2^{-\Delta CT}$. The data shown are mean of three biological replicates ($n = 3$) and the error bars representing standard deviation. Asterisks (*, ***, and ****) indicate a significant difference ($p < 0.05$, $p < 0.001$, and $p < 0.0001$) by one-way ANOVA

and CellFectin II, showing no substantial difference in their efficacy. To confirm specificity, we used RNAi-deficient C6/36 cells, which lack a functional RNAi pathway due to impaired Dicer-2 function [25, 26]. No cytotoxic effects were observed. RT-qPCR further validated these findings, confirming significant gene knockdown for all tested dsRNAs (Fig. 2). It remains unclear why only one IAP dsRNA variant reduced cell viability. This may be influenced by the biological role of the target gene, compensatory cellular mechanisms, or differences in mRNA structure affecting accessibility [34, 35].

The dsRNAs were further tested in larvae for mortality and gene knockdown. No significant mortality was observed, although gene knockdown occurred in the gut but not in whole larvae. This discrepancy may be due to mRNA dilution from unaffected tissues. Additionally, gut-specific knockdown may trigger compensatory upregulation in other tissues [35].

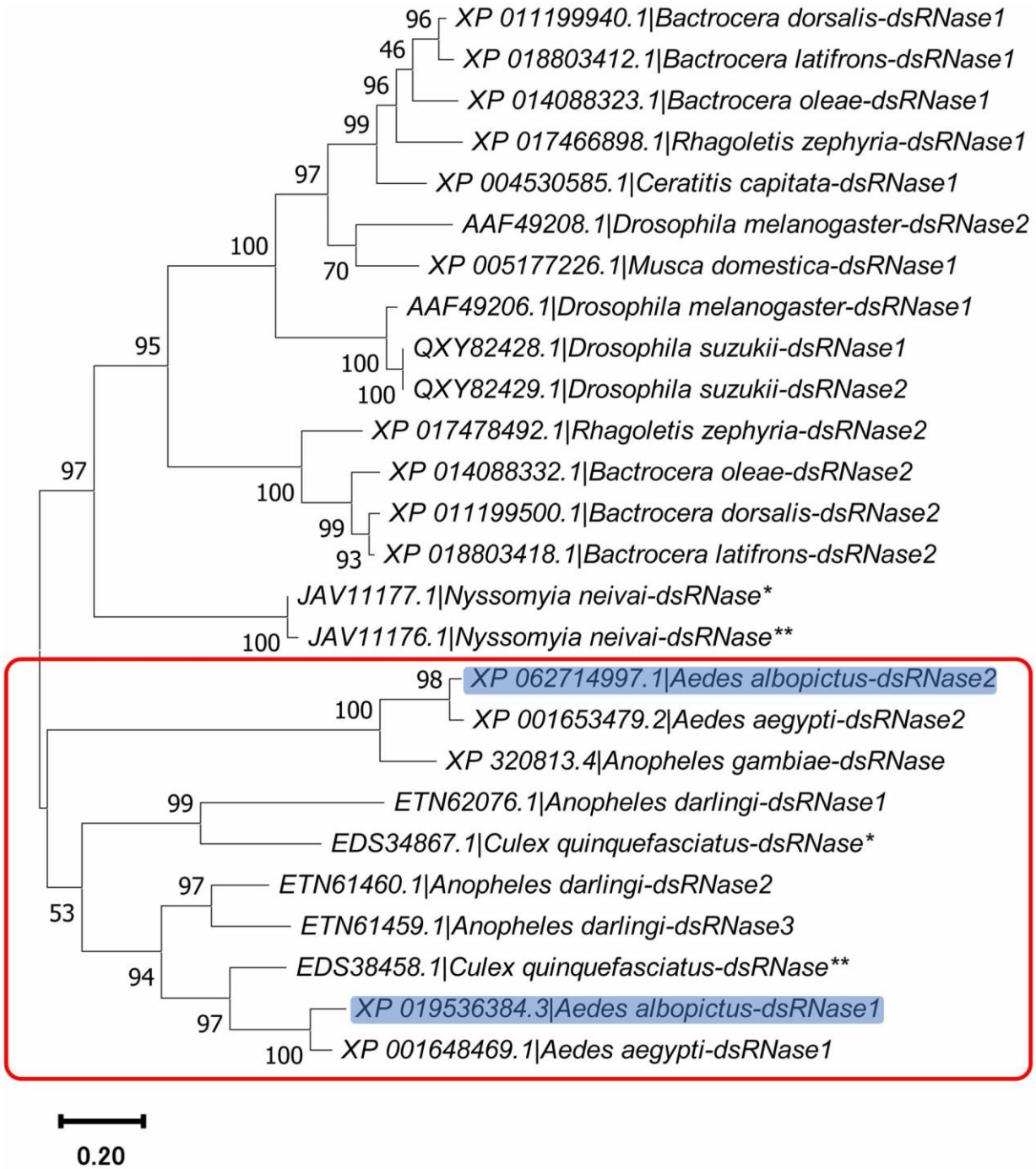

Fig. 8 Phylogenetic analysis of dsRNase proteins from dipterans. A phylogenetic tree of 26 dsRNase proteins from 14 species was constructed using the Maximum likelihood method based on the Poisson correction model, with bootstrap replicate (1000 replicates) for the confidence value of each branch (%). The accession numbers are displayed alongside the species names. Asterisks (*, **) distinguish unnumbered proteins within the same species. The complete table for the construction of this tree can be found in Table S2. The red box encompasses the dsRNases of mosquitoes and highlighted in blue are the dsRNases of *Aedes albopictus* reported in this study

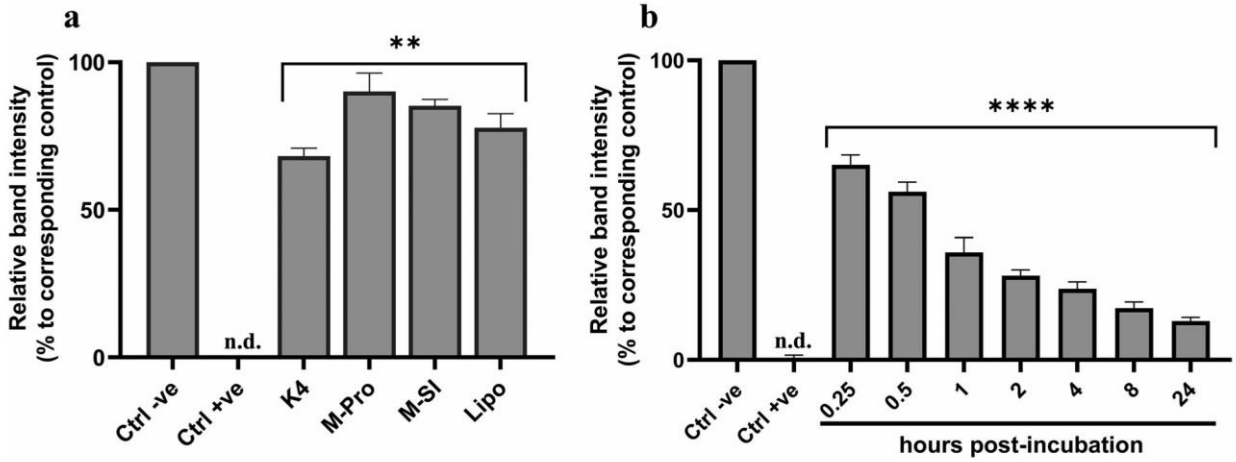

Fig. 9 Protection of dsRNA from degradation by *Aedes albopictus* L4 gut extract using transfection reagents. mCherry dsRNA was complexed in **a** with K4 Transfection System (K4), Metafectene Pro (M-Pro), Metafectene SI + (M-SI), or Lipofectamine 2000 (Lipo) and incubated with gut extract for 10 min. In **b**, dsRNA was complexed with K4 and incubated with gut extract for 0.25 to 24 h. EDTA was added post-incubation to stop degradation, and samples were analyzed by agarose gel electrophoresis. Negative control (Ctrl –ve) was incubated in nuclease-free water while positive control (Ctrl + ve) was incubated in gut extract. Gut extract containing EDTA served as independent control for each dsRNA:TR sample and time point. Band intensity was quantified and normalized to controls. Data represent the normalized mean (%) of three independent experiments ($n = 3$), with error bars showing standard deviation. *n.d.* not detectable

Meanwhile, K4 alone exhibited significant toxicity at 50 ng/µL, indicating a narrow safety window. Consequently, any potential mortality observed with this TR at that concentration may be difficult to interpret. This lack of mortality was unexpected, particularly for IAP 2 dsRNA, which reduced viability in U4.4 cells and achieved knockdown in both cells and larvae gut. To explore possible limitations related to delivery, we examined dsRNA:TR complex sizes and uptake. At lower concentrations, particle sizes were within the optimal range for endocytic internalization in insect cells, which typically occurs with particle size 100–200 nm [36]. However, a higher concentration resulted in much larger particles (up to 5192.2 nm) with high PIs values, indicating aggregation and broad size distribution [37]. Fluorescence microscopy confirmed dsRNA uptake into the gut, with stronger and more sustained signals for the complexed form (Fig. 5). However, the signal did not spread to the rest of the body. These findings suggest that the large particle size and nonsystemic spread are major contributors to the lack of significant mortality. Although *Ae. albopictus* U4.4 cells can transfer RNAi signal to neighboring cells in vitro [38], systemic RNAi in vivo appears limited. Following oral delivery, knockdown was restricted to the midgut, indicating the need for delivery approaches that enhance dsRNA stability in the gut and enable transcytosis across the midgut epithelium.

To determine whether dsRNA stability limits RNAi efficacy in *Ae. albopictus* larvae, we investigated its degradation in the gut environment. Complete degradation was observed within 4 min (Fig. 3a), much faster than in other insects. For example, only 77% of GFP dsRNA was degraded after 2 h in gut of the workers of tawny crazy ant, *Nylanderia fulva* [21]. The inhibition of degradation by EDTA (Fig. 6b) indicates that the responsible nucleases are metal ion-dependent. This led to the identification of two dsRNases (Aal-dsRNase1 and Aal-dsRNase-2), containing a signal peptide and a nonspecific endonuclease domain suggesting a role in extracellular degradation [21, 28, 39]. Their predicted Mg^{2+} binding sites (Fig. 7a) also supports their observed metal ion dependency. Phylogenetic analysis revealed close clustering with other mosquito dsRNases (Fig. 8). Developmental expression of both dsRNases declined in L4, likely owing to reduced feeding and metabolic shifts before pupation [40], but remained significantly higher in the gut than in the rest of the body (Fig. 7c). This expression pattern is consistent with observations from other insects [12, 21, 28, 41]. These findings suggest that rapid dsRNA degradation and high gut expression of dsRNases are major barriers to RNAi in larvae. Nevertheless, IAP 2 dsRNA achieved significant gut-specific knockdown, indicating that nuclease activity alone does not explain the limited efficacy. Additional factors such as endosomal degradation, suboptimal target selection, insufficient dose or exposure, and microbiota interactions are likely involved [42]. Therefore, achieving lethal effects in larvae requires addressing multiple biological hurdles beyond nuclease protection.

We assessed whether complexation could protect dsRNA from gut degradation. While it offered temporary protection, its effectiveness declined over time (Fig. 9), suggesting that dsRNA degradation in the gut may contribute to the lack of RNAi-induced mortality. Although, silencing dsRNase genes has improved RNAi efficacy in *Ae. aegypti* and other insects [40, 43, 44], this strategy may be ineffective here due to rapid degradation of the dsRNA itself. For instance, previous attempts to co-deliver short hairpin RNA (shRNA) against gut nucleases in *Ae. aegypti* and *Ae. albopictus* also did not enhance RNAi [19].

RNAi effects observed in U4.4 cells may not accurately reflect in vivo conditions, as the cell line originates from whole neonate *Ae. albopictus* larvae rather than specifically from gut tissue [45]. Consequently, dsRNA is not subjected to digestive or nuclease activity, microbiota interactions, and immune factors. While U4.4 cell model remains valuable for mechanistic screening, primary midgut cultures or ex vivo gut sacs would provide more physiologically relevant epithelial models, making them more suitable for target genes with pronounced tissue-dependent expression [46]. To the best of our knowledge, no study has reported significant mortality in *Ae. albopictus* larvae using uncomplexed dsRNA alone. However, in *Ae. aegypti*, uncomplexed dsRNA has successfully induced gene knockdown and mortality when targeting genes such as HSP83, β-tubulin, voltage-gated sodium channel, or chitin synthases A/B [15, 47, 48], highlighting a clear interspecies disparity in RNAi sensitivity. The enhanced RNAi efficacy observed in *Ae. aegypti* following dsRNase gene silencing may result from reduced dsRNase expression and activity, differences in the functionality of the core RNAi machinery, or variations in immune gene complexity, as *Ae. albopictus* possesses a larger genome with extensive gene duplications [43, 49–51]. While these factors could lead to interspecies difference in RNAi responsiveness, the molecular basis and direct evidence linking them are still lacking. Nevertheless, significant RNAi-induce mortality has been achieved in *Ae. albopictus* when using engineered *Saccharomyces cerevisiae* expressing shRNAs targeting synaptotagmin, ataxin-2-binding protein, or semaphoring-1a [52–54]. Therefore, their findings indicate that the gut barrier can be overcome, but effective RNAi will require an efficient delivery system.

Meanwhile, classical RNAi approaches without genetic modification are more compatible with current biosafety regulations [7, 55]. Nonetheless, the inconsistent RNAi response in *Ae. albopictus* remains a major challenge that must be overcome [19]. Given that the gut is the primary site of oral dsRNA uptake and IAP gene knockdown was achieved in the larval gut, future studies should focus on identifying gut-specific essential genes in *Ae. albopictus*. Our data identify key quantitative barriers to oral RNAi in *Ae. albopictus* larvae, driven by rapid degradation of dsRNA by gut nucleases, suboptimal complex size, and limited systemic spread. Consequently, delivery is the key determinant of efficacy, exceeding the influence of dsRNA design or dose. Promising delivery platforms include yeast-based delivery platforms, lipid vesicles, polymeric nanoparticles, biodegradable polyplexes, virus-like particles specific to mosquitoes, and inorganic hybrids [14, 54, 56–59]. Such formulations must protect dsRNA from early degradation in the gut by nucleases, maintain optimal particle sizes for efficient oral uptake, promote effective epithelial translocation, and provide controlled intracellular release. Additional strategies for improving stability may include chemical modification like a phosphorothioate backbone or co-delivery of species-specific nuclease inhibitors to reduce gut nuclease activity [60].

For field-ready larvicides, the product should pair effective formulations with deployment practicality. Target selection should prioritize gut-specific essential genes, ideally in multi-gene combinations to mitigate potential resistances, and efficacy should be validated under realistic environmental conditions. Development pipelines should incorporate laboratory, mesocosm, and pilot-scale trials to confirm persistence, safety, and scalability. Ultimately, a functional RNAi-based larvicide will rely on optimized formulations that ensure dsRNA stability, uptake, and reproducible efficacy, together with full regulatory compliance [7, 61].

Conclusions

This study highlights the potential and limitations of RNAi for controlling *Ae. albopictus*. Only one dsRNA construct induced cytotoxic effects in cell-based assays, despite all selected dsRNAs achieving significant gene knockdown. In larval assays, none of the dsRNAs induced mortality, despite a significant gene knockdown in the gut. Limited RNAi efficacy in the larvae may be as a result of insufficient systemic spread of dsRNA, poor cellular internalization, and its rapid degradation by gut nucleases. These findings emphasize the complexity of translating gene silencing into functional lethality in whole organisms, by specifically providing a quantitative degradation of the dsRNA, as well as molecular identification and characterization of *Ae. albopictus* dsRNases. Further research is needed to clarify the molecular basis of reduced RNAi sensitivity in *Ae. albopictus* compared with *Ae. aegypti*. Most importantly, identifying gut-specific essential genes, exploring suitable formulations, and understanding species-specific barriers, is crucial

for realizing RNAi's full potential as a control method against *Ae. albopictus*.

Supplementary Information

The online version contains supplementary material available at https://doi.org/10.1186/s13071-025-07113-2.

Additional file 1.

Acknowledgements
The graphical abstract was designed using BioRender online software. We wish to thank Dr. Hanano Yamada, Joint FAO/IAEA Centre of Nuclear Techniques in Food and Agriculture, Insect Pest Control Sub-Program (Vienna, Austria) for providing *Aedes albopictus* eggs. We thank Prof. Dr. Stefanie Becker, University of Veterinary Medicine, Hannover, Germany, for the C6/36 cells. We also thank Prof. Dr. Andres Merits, University of Tartu, Estonia, and Prof. Dr. Andreas Pichlmair, Technical University of Munich, Germany, for providing pCMV-SFV6-2SG-mCherry.

Author contributions
Conceptualization: AS and KH. Data Curation: BO, AC, SS, MW, and KH. Formal analysis: BO, AC, SS, and KH. Funding acquisition: AS, KH, and AV. Investigation: BO, AC, SS, PG, AS, and KH. Methodology: BO, AC, PG, SS, and KH. Project Administration: AS and KH. Resources: AS, KH, and AV. Supervision: AS, KH, and AV. Validation: BO and AC. Visualization: BO, AC, and KH. Writing—original draft preparation: BO, AS, and KH. Writing—review and editing: BO, AC, SS, MW, PG, AS, AV, and KH.

Funding
Open Access funding enabled and organized by Projekt DEAL. BO and AC were supported by the Landes-Offensive zur Entwicklung Wissenschaftlich-ökonomischer Exzellenz Program of the Hessian Ministry of Higher Education, Research and the Arts through the LOEWE Centre for Translational Biodiversity Genomics (LOEWE–TBG) with funding code: LOEWE/1/10/519/03/03.001(0014)/52. KH is supported by the BMBF (project ASCRIBE—grant number 01KI2024).

Availability of data and materials
All data generated or analyzed during this study are included in this published article.

Declarations

Ethics approval and consent to participate
Not applicable.

Consent for publication
All authors read and approved the final manuscript.

Competing interests
The authors declare no competing interests.

Author details
[1]LOEWE Centre for Translational Biodiversity Genomics (LOEWE TBG), Senckenberganlage 25, 60325 Frankfurt am Main, Germany. [2]Institute for Insect Biotechnology, Justus-Liebig University, Heinrich-Buff-Ring 26–32, 35392 Giessen, Germany. [3]Fraunhofer Institute for Molecular Biology and Applied Ecology IME, Branch of Bioresources, Ohlebergsweg 12, 35392 Giessen, Germany. [4]Institute for Evolution and Biodiversity (IEB), University of Muenster, Hufferstrasse 1, 48149 Muenster, Germany. [5]Senckenberg Biodiversity and Climate Research Centre (BiK-F), Georg-Voigt-Strasse 14-16, 60325 Frankfurt am Main, Germany. [6]BMBF Junior Research Group in Infection Research "ASCRIBE", Ohlebergsweg 12, 35392 Giessen, Germany.

Received: 3 July 2025 Accepted: 14 October 2025
Published online: 14 November 2025

References

1. Calzolari M. Mosquito-borne diseases in Europe: an emerging public health threat. RIP. 2016. https://doi.org/10.2147/RIP.S56780.
2. Paupy C, Delatte H, Bagny L, Corbel V, Fontenille D. *Aedes albopictus*, an arbovirus vector: from the darkness to the light. Microbes Infect. 2009;11:1177–85. https://doi.org/10.1016/j.micinf.2009.05.005.
3. Becker N, Petrić D, Zgomba M, Boase C, Madon MB, Dahl C, et al. Mosquitoes. Cham: Springer International Publishing; 2020.
4. Sukhralia S, Verma M, Gopirajan S, Dhanaraj PS, Lal R, Mehla N, et al. From dengue to Zika: the wide spread of mosquito-borne arboviruses. Eur J Clin Microbiol Infect Dis. 2019;38:3–14. https://doi.org/10.1007/s10096-018-3375-7.
5. Onen H, Luzala MM, Kigozi S, Sikumbili RM, Muanga C-JK, Zola EN, et al. Mosquito-borne diseases and their control strategies: an overview focused on green synthesized plant-based metallic nanoparticles. Insects. 2023;14:3–221. https://doi.org/10.3390/insects14030221.
6. Kaura T, Sylvia Walter N, Kaur U, Sehgal R. Different strategies for mosquito control: challenges and alternatives. In: Puerta-Guardo H, Manrique-Saide P, editors. Mosquito research—recent advances in pathogen interactions, immunity, and vector control strategies. IntechOpen; 2023. https://doi.org/10.5772/intechopen.104594.
7. Müller R, Bálint M, Hardes K, Hollert H, Klimpel S, Knorr E, et al. RNA interference to combat the Asian tiger mosquito in Europe: a pathway from design of an innovative vector control tool to its application. Biotechnol Adv. 2023;66:108167. https://doi.org/10.1016/j.biotechadv.2023.108167.
8. Liu J, Swevers L, Kolliopoulou A, Smagghe G. Arboviruses and the challenge to establish systemic and persistent infections in competent mosquito vectors: the interaction with the RNAi mechanism. Front Physiol. 2019;10:890. https://doi.org/10.3389/fphys.2019.00890.
9. Li Z, Rana TM. Molecular mechanisms of RNA-triggered gene silencing machineries. Acc Chem Res. 2012;45:1122–31. https://doi.org/10.1021/ar200253u.
10. Ortolá B, Daròs J-A. RNA interference in insects: from a natural mechanism of gene expression regulation to a biotechnological crop protection promise. Biology (Basel). 2024;13:3–137. https://doi.org/10.3390/biology13030137.
11. Dong Y, Dong S, Dizaji NB, Rutkowski N, Pohlenz T, Myles K, et al. The *Aedes aegypti* siRNA pathway mediates broad-spectrum defense against human pathogenic viruses and modulates antibacterial and antifungal defenses. PLoS Biol. 2022;20:e3001668. https://doi.org/10.1371/journal.pbio.3001668.
12. Tayler A, Heschuk D, Giesbrecht D, Park JY, Whyard S. Efficiency of RNA interference is improved by knockdown of dsRNA nucleases in tephritid fruit flies. Open Biol. 2019;9:190198. https://doi.org/10.1098/rsob.190198.
13. Vogel E, Santos D, Mingels L, Verdonckt T-W, Broeck JV. RNA interference in insects: protecting beneficials and controlling pests. Front Physiol. 2018;9:1912. https://doi.org/10.3389/fphys.2018.01912.
14. Dhandapani RK, Gurusamy D, Howell JL, Palli SR. Development of CS-TPP-dsRNA nanoparticles to enhance RNAi efficiency in the yellow fever mosquito, *Aedes aegypti*. Sci Rep. 2019;9:8775. https://doi.org/10.1038/s41598-019-45019-z.
15. Singh AD, Wong S, Ryan CP, Whyard S. Oral delivery of double-stranded RNA in larvae of the yellow fever mosquito, *Aedes aegypti*: implications for pest mosquito control. J Insect Sci. 2013;13:1–18.
16. Knorr E, Fishilevich E, Tenbusch L, Frey MLF, Rangasamy M, Billion A, et al. Gene silencing in *Tribolium castaneum* as a tool for the targeted identification of candidate RNAi targets in crop pests. Sci Rep. 2018;8:2061. https://doi.org/10.1038/s41598-018-20416-y.
17. Yu N, Christiaens O, Liu J, Niu J, Cappelle K, Caccia S, et al. Delivery of dsRNA for RNAi in insects: an overview and future directions. Insect Sci. 2013;20:4–14. https://doi.org/10.1111/j.1744-7917.2012.01534.x.
18. Munawar K, Alahmed AM, Khalil SMS. Delivery methods for RNAi in mosquito larvae. J Insect Sci. 2020;20:4. https://doi.org/10.1093/jisesa/ieaa074.
19. Figueiredo Prates LH, Fiebig J, Schlosser H, Liapi E, Rehling T, Lutrat C, et al. Challenges of robust RNAi-mediated gene silencing in Aedes mosquitoes. Int J Mol Sci. 2024;25:10–5218. https://doi.org/10.3390/ijms25105218.
20. Dalaisón-Fuentes LI, Pascual A, Crespo M, Andrada NL, Welchen E, Catalano MI. Knockdown of double-stranded RNases (dsRNases) enhances oral RNA interference (RNAi) in the corn leafhopper, *Dalbulus maidis*.

Pestic Biochem Physiol. 2023;196:105618. https://doi.org/10.1016/j.pestbp.2023.105618.
21. Lei J, Tan Y, List F, Puckett R, Tarone AM, Vargo EL, et al. Cloning and functional characterization of a double-stranded RNA-degrading nuclease in the tawny crazy ant (*Nylanderia fulva*). Front Physiol. 2022;13:833652. https://doi.org/10.3389/fphys.2022.833652.
22. Peng Y, Wang K, Zhu G, Han Q, Chen J, Elzaki MEA, et al. Identification and characterization of multiple dsrnases from a lepidopteran insect, the tobacco cutworm, *Spodoptera litura* (Lepidoptera: Noctuidae). Pestic Biochem Physiol. 2020;162:86–95. https://doi.org/10.1016/j.pestbp.2019.09.011.
23. Gurusamy D, Mogilicherla K, Shukla JN, Palli SR. Lipids help double-stranded RNA in endosomal escape and improve RNA interference in the fall armyworm, *Spodoptera frugiperda*. Arch Insect Biochem Physiol. 2020;104:e21678. https://doi.org/10.1002/arch.21678.
24. Lück S, Kreszies T, Strickert M, Schweizer P, Kuhlmann M, Douchkov D. SiRNA-finder (si-Fi) software for RNAi-target design and off-target prediction. Front Plant Sci. 2019;10:1023. https://doi.org/10.3389/fpls.2019.01023.
25. Brackney DE, Scott JC, Sagawa F, Woodward JE, Miller NA, Schilkey FD, et al. C6/36 *Aedes albopictus* cells have a dysfunctional antiviral RNA interference response. PLoS Negl Trop Dis. 2010;4:e856. https://doi.org/10.1371/journal.pntd.0000856.
26. Scott JC, Brackney DE, Campbell CL, Bondu-Hawkins V, Hjelle B, Ebel GD, et al. Comparison of dengue virus type 2-specific small RNAs from RNA interference-competent and -incompetent mosquito cells. PLoS Negl Trop Dis. 2010;4:e848. https://doi.org/10.1371/journal.pntd.0000848.
27. Omokungbe B, Centurión A, Stiehler S, Morr A, Vilcinskas A, Steinbrink A, et al. Gene silencing in the aedine cell lines C6/36 and U4.4 using long double-stranded RNA. Parasit Vectors. 2024;17:255. https://doi.org/10.1186/s13071-024-06340-3.
28. Yoon J-S, Ahn S-J, Flinn CM, Choi M-Y. Identification and functional analysis of dsRNases in spotted-wing drosophila, *Drosophila suzukii*. Arch Insect Biochem Physiol. 2021;107:e21822. https://doi.org/10.1002/arch.21822.
29. Paysan-Lafosse T, Blum M, Chuguransky S, Grego T, Pinto BL, Salazar GA, et al. Interpro in 2022. Nucleic Acids Res. 2023;51:D418–27. https://doi.org/10.1093/nar/gkac993.
30. Riedel G, Rüdrich U, Fekete-Drimusz N, Manns MP, Vondran FWR, Bock M. An extended ΔCT-method facilitating normalisation with multiple reference genes suited for quantitative RT-PCR analyses of human hepatocyte-like cells. PLoS ONE. 2014;9:e93031. https://doi.org/10.1371/journal.pone.0093031.
31. Singh IK, Singh S, Mogilicherla K, Shukla JN, Palli SR. Comparative analysis of double-stranded RNA degradation and processing in insects. Sci Rep. 2017;7:17059. https://doi.org/10.1038/s41598-017-17134-2.
32. Airs PM, Bartholomay LC. RNA interference for mosquito and mosquito-borne disease control. Insects. 2017;8:1–4. https://doi.org/10.3390/insects8010004.
33. He L, Huang Y, Tang X. RNAi-based pest control: production, application and the fate of dsRNA. Front Bioeng Biotechnol. 2022;10:1080576. https://doi.org/10.3389/fbioe.2022.1080576.
34. Tafer H, Ameres SL, Obernosterer G, Gebeshuber CA, Schroeder R, Martinez J, et al. The impact of target site accessibility on the design of effective siRNAs. Nat Biotechnol. 2008;26:578–83. https://doi.org/10.1038/nbt1404.
35. El-Brolosy MA, Stainier DYR. Genetic compensation: a phenomenon in search of mechanisms. PLoS Genet. 2017;13:e1006780. https://doi.org/10.1371/journal.pgen.1006780.
36. McGraw E, Roberts JD, Kunte N, Westerfield M, Streety X, Held D, et al. Insight into cellular uptake and transcytosis of peptide nanoparticles in *Spodoptera frugiperda* cells and isolated midgut. ACS Omega. 2022;7:10933–43. https://doi.org/10.1021/acsomega.1c06638.
37. Lundqvist M, Stigler J, Elia G, Lynch I, Cedervall T, Dawson KA. Nanoparticle size and surface properties determine the protein corona with possible implications for biological impacts. Proc Natl Acad Sci U S A. 2008;105:14265–70. https://doi.org/10.1073/pnas.0805135105.
38. Attarzadeh-Yazdi G, Fragkoudis R, Chi Y, Siu RWC, Ulper L, Barry G, et al. Cell-to-cell spread of the RNA interference response suppresses Semliki Forest virus (SFV) infection of mosquito cell cultures and cannot be antagonized by SFV. J Virol. 2009;83:5735–48. https://doi.org/10.1128/jvi.02440-08.
39. Cooper AMW, Song H, Shi X, Yu Z, Lorenzen M, Silver K, et al. Molecular characterizations of double-stranded RNA degrading nuclease genes from *Ostrinia nubilalis*. Insects. 2020;11:10. https://doi.org/10.3390/insects11100652.
40. Sharma R, Taning CNT, Smagghe G, Christiaens O. Silencing of double-stranded ribonuclease improves oral RNAi efficacy in Southern Green Stinkbug *Nezaraviridula*. Insects. 2020;11:10. https://doi.org/10.3390/insects12020115.
41. Spit J, Philips A, Wynant N, Santos D, Plaetinck G, Vanden BJ. Knockdown of nuclease activity in the gut enhances RNAi efficiency in the Colorado potato beetle, *Leptinotarsa decemlineata*, but not in the desert locust, Schistocerca gregaria. Insect Biochem Mol Biol. 2017;81:103–16. https://doi.org/10.1016/j.ibmb.2017.01.004.
42. Christiaens O, Whyard S, Vélez AM, Smagghe G. Double-stranded RNA technology to control insect pests: current status and challenges. Front Plant Sci. 2020;11:451. https://doi.org/10.3389/fpls.2020.00451.
43. Giesbrecht D, Heschuk D, Wiens I, Boguski D, LaChance P, Whyard S. RNA interference is enhanced by knockdown of double-stranded RNases in the yellow fever mosquito *Aedes aegypti*. Insects. 2020;11:10. https://doi.org/10.3390/insects11060327.
44. Prentice K, Smagghe G, Gheysen G, Christiaens O. Nuclease activity decreases the RNAi response in the sweetpotato weevil *Cylas puncticollis*. Insect Biochem Mol Biol. 2019;110:80–9. https://doi.org/10.1016/j.ibmb.2019.04.001.
45. Walker T, Jeffries CL, Mansfield KL, Johnson N. Mosquito cell lines: history, isolation, availability and application to assess the threat of arboviral transmission in the United Kingdom. Parasit Vectors. 2014;7:382. https://doi.org/10.1186/1756-3305-7-382.
46. Rosales Rosas AL, Wang L, Goossens S, Cuvry A, Li L-H, Santos-Ferreira N, et al. Ex vivo gut cultures of Aedes aegypti are efficiently infected by mosquito-borne alpha- and flaviviruses. Microbiol Spectr. 2023;11:e0519522. https://doi.org/10.1128/spectrum.05195-22.
47. Bona ACD, Chitolina RF, Fermino ML, Castro Poncio L, Weiss A, Lima JBP, et al. Larval application of sodium channel homologous dsRNA restores pyrethroid insecticide susceptibility in a resistant adult mosquito population. Parasit Vectors. 2016;9:397. https://doi.org/10.1186/s13071-016-1634-y.
48. Lopez SBG, Guimarães-Ribeiro V, Rodriguez JVG, Dorand FAPS, Salles TS, Sá-Guimarães TE, et al. RNAi-based bioinsecticide for Aedes mosquito control. Sci Rep. 2019;9:4038. https://doi.org/10.1038/s41598-019-39666-5.
49. Chen X-G, Jiang X, Gu J, Xu M, Wu Y, Deng Y, et al. Genome sequence of the Asian tiger mosquito, *Aedes albopictus*, reveals insights into its biology, genetics, and evolution. Proc Natl Acad Sci U S A. 2015;112:E5907–15. https://doi.org/10.1073/pnas.1516410112.
50. Palatini U, Masri RA, Cosme LV, Koren S, Thibaud-Nissen F, Biedler JK, et al. Improved reference genome of the arboviral vector *Aedes albopictus*. Genome Biol. 2020;21:215. https://doi.org/10.1186/s13059-020-02141-w.
51. Airs PM, Kudrna KE, Lubinski B, Phanse Y, Bartholomay LC. A comparative analysis of RNAi trigger uptake and distribution in mosquito vectors of disease. Insects. 2020;11:10. https://doi.org/10.3390/insects14060556.
52. Mysore K, Li P, Wang C-W, Hapairai LK, Scheel ND, Realey JS, et al. Characterization of a yeast interfering RNA larvicide with a target site conserved in the synaptotagmin gene of multiple disease vector mosquitoes. PLoS Negl Trop Dis. 2019;13:e0007422. https://doi.org/10.1371/journal.pntd.0007422.
53. Mysore K, Li P, Wang C-W, Hapairai LK, Scheel ND, Realey JS, et al. Characterization of a broad-based mosquito yeast interfering RNA larvicide with a conserved target site in mosquito semaphorin-1a genes. Parasit Vectors. 2019;12:256. https://doi.org/10.1186/s13071-019-3504-x.
54. Mysore K, Sun L, Hapairai LK, Wang C-W, Roethele JB, Igiede J, et al. A broad-based mosquito yeast interfering RNA pesticide targeting Rbfox1 represses Notch signaling and kills both larvae and adult mosquitoes. Pathogens. 2021;10:10–1251. https://doi.org/10.3390/pathogens10101251.
55. Chen Y, Schutter K. Biosafety aspects of RNAi-based pests control. Pest Manag Sci. 2024;80:3697–706. https://doi.org/10.1002/ps.8098.
56. Qiao L, Niño-Sánchez J, Hamby R, Capriotti L, Chen A, Mezzetti B, et al. Artificial nanovesicles for dsRNA delivery in spray-induced gene silencing for crop protection. Plant Biotechnol J. 2023;21:854–65. https://doi.org/10.1111/pbi.14001.

57. Zhou H, Wan F, Jian Y, Guo F, Zhang M, Shi S, et al. Chitosan/dsRNA polyplex nanoparticles advance environmental RNA interference efficiency through activating clathrin-dependent endocytosis. Int J Biol Macromol. 2023;253:127021. https://doi.org/10.1016/j.ijbiomac.2023.127021.
58. Scholle F, Girard YA, Zhao Q, Higgs S, Mason PW. Trans-packaged West Nile virus-like particles: infectious properties *in vitro* and in infected mosquito vectors. J Virol. 2004;78:11605–14. https://doi.org/10.1128/JVI.78.21.11605-11614.2004.
59. Kim JS, Park J, Choi JH, Kang S, Park N. RNA-DNA hybrid nano-materials for highly efficient and long lasting RNA interference effect. RSC Adv. 2023;13:3139–46. https://doi.org/10.1039/D2RA06249F.
60. Howard JD, Beghyn M, Dewulf N, de Vos Y, Philips A, Portwood D, et al. Chemically modified dsRNA induces RNAi effects in insects in vitro and in vivo: a potential new tool for improving RNA-based plant protection. J Biol Chem. 2022;298:102311. https://doi.org/10.1016/j.jbc.2022.102311.
61. Yadav M, Dahiya N, Sehrawat N. Mosquito gene targeted RNAi studies for vector control. Funct Integr Genomics. 2023;23:180. https://doi.org/10.1007/s10142-023-01072-6.

Publisher's Note

Supplementary Information

RNA interference mediated mortality in *Aedes albopictus*: a challenging journey toward species-specific vector control

Bodunrin Omokungbe[1,2,3], Alejandra Centurión[1,3], Sabrina Stiehler[2], Magnus Wolf[4,5], Pascal Geisler[3], Andreas Vilcinskas[1,2,3], Antje Steinbrink[1,2], Kornelia Hardes[1,3,4,*]

[1] LOEWE Centre for Translational Biodiversity Genomics (LOEWE TBG), Senckenberganlage 25, 60325 Frankfurt am Main, Germany
[2] Institute for Insect Biotechnology, Justus-Liebig University, Heinrich-Buff-Ring 26–32, 35392 Giessen, Germany
[3] Fraunhofer Institute for Molecular Biology and Applied Ecology IME, Branch of Bioresources, Ohlebergsweg 12, 35392 Giessen, Germany
[4] Institute for Evolution and Biodiversity (IEB), University of Muenster, Huefferstrasse 1, 48149, Muenster, Germany
[5] Senckenberg Biodiversity and Climate Research Centre (BiK-F), Georg-Voigt-Strasse 14-16, 60325, Frankfurt am Main, Germany
[6]BMBF Junior Research Group in Infection Research "ASCRIBE" Ohlebergsweg 12, 35392 Giessen, Germany

* Correspondence: Kornelia.Hardes@ime.fraunhofer.de

1 Candidate gene target selection, double-stranded RNA design and synthesis

To identify suitable RNAi target genes in *Aedes albopictus*, we conducted a literature search to compile genes previously associated with high mortality in other insect species. For each selected gene, two dsRNA constructs were designed and synthesized. The sequences of the primers used for dsRNA synthesis, gene knockdown validation, and analysis of dsRNase expression profiles are listed in Table S1.

Table S1: Primer sequences used for dsRNA synthesis, validation of gene knockdown, and expression profiles of dsRNases by RT-qPCR. The T7 promoter sequence (in lower case) was added to the 5′ end of each primer used for dsRNA synthesis. RT-qPCR primers for confirming gene knockdown were designed to bind near the 5′ region of the target gene, outside the dsRNA target sequence.

Gene	purpose	Name of fragment	Primer sequence 5' → 3'	size (bp)
Green fluorescent protein (GFP)	RNAi	gfp484_T7_fw	ccctttaatacgactcactatagggagaACCACATGAAGCAGCACGACTT	484
		gfp484_T7_rv	ccctttaatacgactcactatagggagaGTCCATGCCGAGAGTGATCCCG	
mCherry	RNAi	mCh_T7-fw	taatacgactcactatagggGCGTGATGAACTTCGAGGAC	409
		mCh_T7-rv	taatacgactcactatagggCTTGTACAGCTCGTCCATGC	
β-Tubulin (*β-tub*)	RNAi	β-tub-1_T7-fw	taatacgactcactatagggGTCGACGAACAGATGCTGAA	494
		β-tub-1_T7-rv	taatacgactcactatagggAAGTGGCGCAGATAGAGGAA	
		β-tub-2_T7-fw	taatacgactcactatagggCACGACATGGACGTTACCTG	496
		β-tub-2_T7-rv	taatacgactcactatagggGGGGGAGAAGGGTACAGAAG	
	RT-qPCR	β-tub-1_fw	GGTTTTCTCGTGTTCCGTCG	221
		β-tub-1_rv	GCGTCGATTCCATGCTCATC	
Dre4 (D*re4*)	RNAi	Dre4_T7-1_fw	taatacgactcactatagggTTTCGGTGAAGTTTTCGGGC	417
		Dre4_T7-1_rv	taatacgactcactatagggCCTCCTCGGCATCCTTCTCTA	
		Dre4_T7-2_fw	taatacgactcactatagggATCCGGCCATTATCCAGTCG	446
		Dre4_T7-2_rv	taatacgactcactatagggTGCCTCCTTGTTCTCCAAGC	
	RT-qPCR	Dre4_PCR_fw	CGGTCCCATCATAGTTCGTCC	
		Dre4_PCR_rev	ATGCGTCACTTCCTCCAGTT	
Ras Opposite (*ROP*)	RNAi	ROP-1_T7-fw	taatacgactcactatagggTGAGGTGTGCCCTGAAGAAC	495
		ROP-1_T7-rv	taatacgactcactatagggGCGTTCGGAGATGGGATGAA	
		ROP-2_T7-fw	taatacgactcactatagggGATTGCGTTTCTCCGTTGCT	447
		ROP-2_T7-rv	taatacgactcactatagggGCGCATGTGGTCCTTGATTT	
	RT-qPCR	ROP _fw	CTGGGTATCAACGTCATCGCT	243
		ROP_rv	TGACTTGTCCTTGTGCCAGT	
Inhibitor of apoptosis (*IAP*)	RNAi	IAP-1_T7-fw	taatacgactcactatagggCGTTGTGTGGTCGGTCTAGT	403
		IAP-1_T7-rv	taatacgactcactatagggATCTTGAGTTCGCGGCTGTT	
		IAP-2_T7-fw	taatacgactcactatagggACACCGGCAAAAGTGATCGT	425
		IAP-2_T7-rv	taatacgactcactatagggACAGGGCGAAAATGCCGTAT	
	RT-qPCR	IAP_ fw	GGCTCAAACGATGATGGCAC	173
		IAP_rv	TCTTGCTGATGAAGGGCACC	
Nucampholin (*NCM*)	RNAi	NCM-1_T7-fw	taatacgactcactatagggGATTCCCGTTTCGACTCCGA	449
		NCM-1_T7-rv	taatacgactcactatagggTTGTCCGTAATCTCCGCCTG	
		NCM-2_T7-fw	taatacgactcactatagggTCGTCGGAAAAAGAAAGGCA	408
		NCM-2_T7-rv	taatacgactcactatagggTCTACGGTCACAATACAGGGAA	
	RT-qPCR	NCM_ fw	GCGGGGCTATGAAAGAGAGG	222
		NCM_rv	CTCCGGCGACTAGAGGAAGA	
Actin	RT-qPCR	Actin_fw	AGATCCTGACTGAACGTGGC	162
		Actin_rv	CGTCGGGAAGTTCGTAGGAC	
Aal-dsRNase1	RT-qPCR	Aal-dsRNase1-fw	ATTCGATTTGGGAACCCGCT	237
		Aal-dsRNase1-rv	GCGAGTTCTTGCGATTGGAG	
Aal-dsRNase2	RT-qPCR	Aal-dsRNase2-fw	ACCCGAAAAATTGCGCTACG	204
		Aal-dsRNase2-rv	AGATGGTGGTAGTCTCGCCA	

2 Cytotoxicity effects of RNAi in aedine cell lines

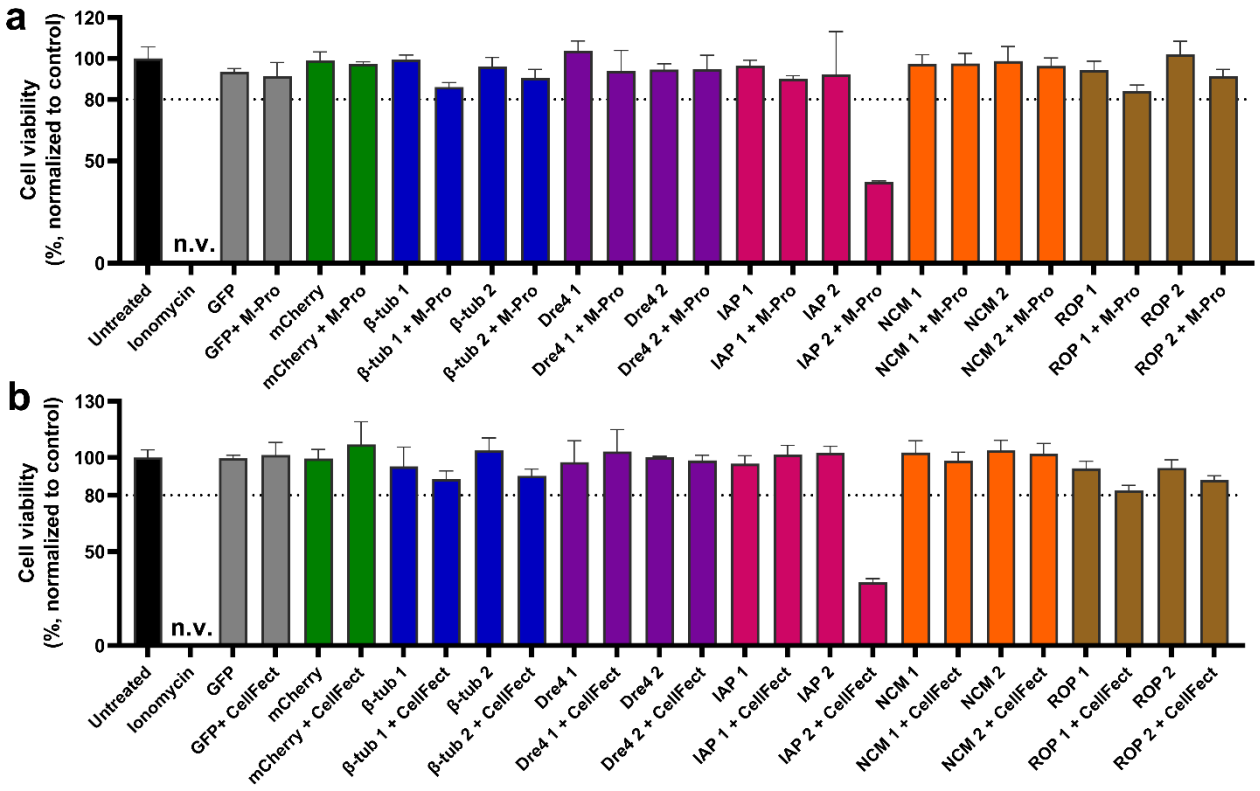

Fig. S1. Cytotoxic effects of complexed dsRNAs in *Aedes albopictus* U4.4 cells. Cells were treated at ~50% confluency with dsRNA at a concentration of 2 ng/µL per well (n = 4). The dsRNAs were complexed in (**a**) with Metafectene Pro (M-Pro) and in (**b**) CellFectin II (CellFect) before treatment. At 48 h post-treatment cell viability was assessed using the CellTiter-Glo assay. Data were normalized to the untreated control (treatment/control × 100), and mean cell viability is shown. Error bars represent the coefficient of variation (%). The dotted line indicates the toxicity threshold set at 80%. n.v. = near-zero viability.

3 Gene silencing analysis in U4.4 cells and larvae of *Aedes albopictus*

Prior to gene silencing analysis, a standard curve analysis (0.1–1000 ng) was performed for each primer pair to determine efficiency, using total RNA extracted from L4 larvae with the Monarch Total RNA Miniprep Kit (New England Biolabs, Frankfurt, Germany). RNA concentration and purity were assessed using a NanoDrop 2000 spectrophotometer (Thermo Fisher Scientific, Frankfurt, Germany). RT-qPCR was performed with the Luna Universal One-Step RT-qPCR Kit (New England Biolabs) on a QuantStudio 3 Real-Time PCR System (Applied Biosystems, Thermo Fisher Scientific). Detailed reaction components and thermal cycling conditions are provided in Table S2. Primer's efficiencies are shown in Fig. S2, and the gene knockdown results in whole larvae are presented in Fig. S3.

Table S2: Reaction mix and thermal program for RT-qPCR for gene knockdown and expression profile analysis.

Reaction mix			
Reaction component			**Volume (µL)**
Luna Universal One-Step Reaction Mix (2x)			10.0
Luna WarmStart RT Enzyme Mix (20x)			1.0
Gene-specific Forward Primer (10 µM)			0.8
Gene-specific Reverse Primer (10 µM)			0.8
Nuclease-free Water			2.4
Template RNA (20ng/µL)			5.0
Total Volume			**20.0**
Thermal parameter			
Cycle step	**Temperature**	**Time**	**Cycles**
Reverse Transcription	55°C	10 min	1
Initial Denaturation	95°C	1 min	1
Denaturation	95°C	10 sec	45
Extension	60°C	60 sec	
Melt Curve	60-95°C	various	1

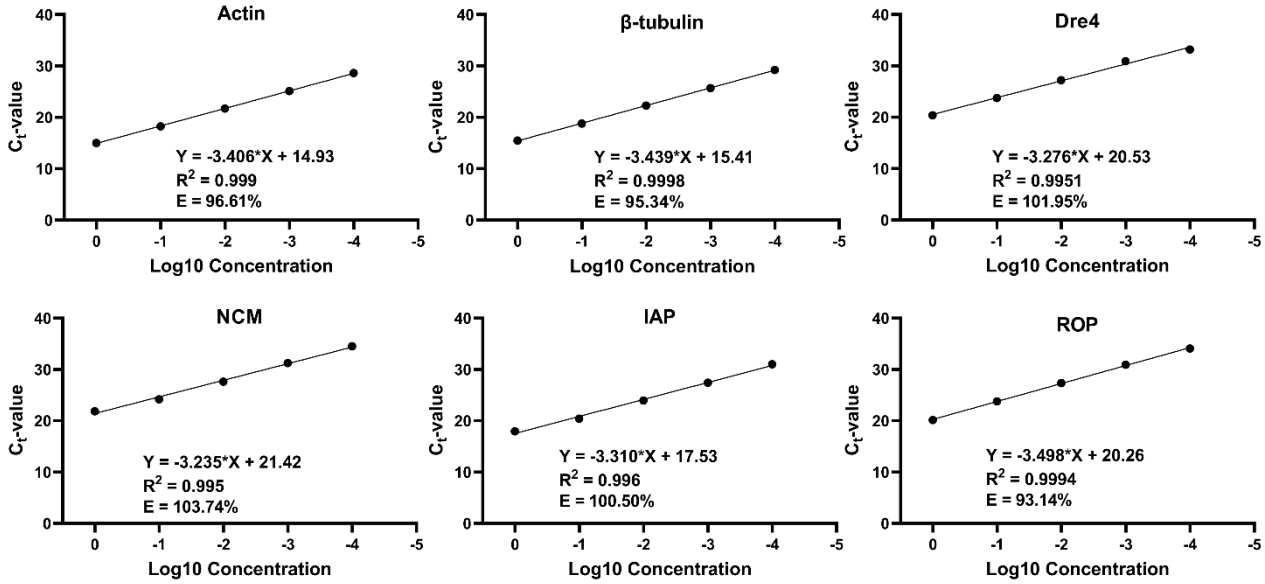

Fig. S2. Primer efficiency of RT-qPCR primers. The efficiency was assessed *via* the standard curve analysis using total RNA extracted from L4 larvae (0.1–1000 ng). C_t values were plotted against the logarithm of RNA concentrations to generate standard curves. The slope, Y-intercept, coefficient of determination (R^2), and primer efficiency (E) are indicated for each primer set.

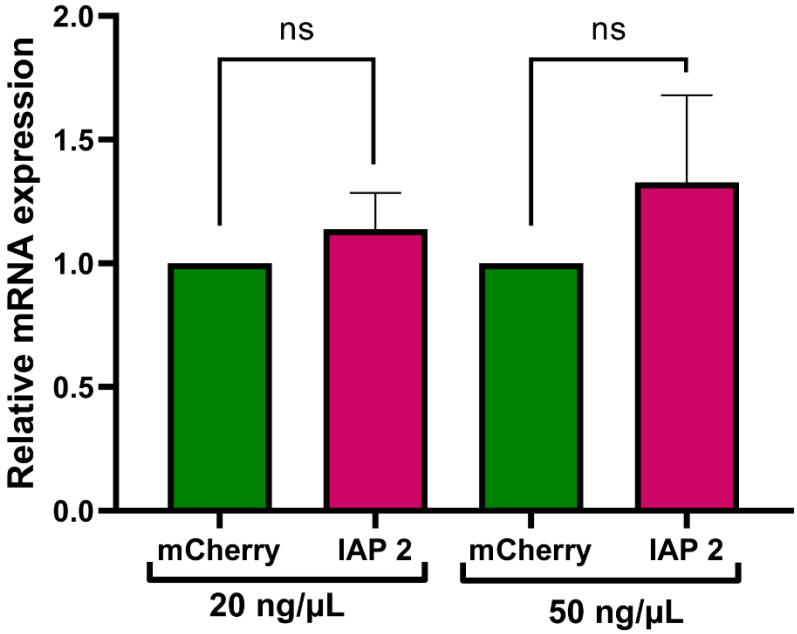

Fig. S3. Gene knockdown in whole larvae following treatment with complexed IAP 2 dsRNA using the K4 Transfection System (1:1). Larvae were treated using the second bioassay approach described in the main manuscript, and at 3 days post-treatment RNA were extracted for RT-qPCR analysis. Actin was used as the reference gene, and relative expression was calculated using the $2^{-\Delta\Delta Ct}$ method, normalized to the non-specific mCherry dsRNA control (n = 3). Error bars represent standard deviation. ns = no significant difference ($p > 0.05$), determined by one-way ANOVA and Šidák's multiple comparison test.

4 Dynamic light scattering analysis of formulated dsRNA

Since the dsRNAs did not caused mortality in larvae, we tested whether the size of the complexes was a limiting factor. Therefore, we performed dynamic light scattering (DLS) to determine the particle size of dsRNA:TR complexes. First, the mCherry dsRNA was complexed with either K4 (1:1), Metafectene Pro (1:0.7), or CellFectin II (1:5) to a final concentration of 10, 20, or 50 ng/µL. The complexes were incubated at room temperature for 20 min. Nuclease-free water was used as the base medium for all dilutions, instead of the recommended Grace's insect medium, to match the conditions used in the larval experiments. For particle size measurements, 5 µL of each complex was transferred into the capillary tube of a Zetasizer Low Volume Disposable Sizing Cell Kit (ZSU1002, Malvern Panalytical, Malvern, United Kingdom) and analyzed using a Malvern Ultra Red Zetasizer (Malvern Panalytical). Particle size was analyzed using the side scattering method. The results are shown in Table S3.

Table S3. Particle size distribution of dsRNA:TR complexes. mCherry dsRNA was complexed with K4 Transfection System, Metafectene Pro, or CellFectin II, and particle size was analyzed using dynamic light scattering with side scattering method. The sample size was n=3 and each sample replicate were measured three times.

Sample	Concentrations (ng/µL)	Particle size (Z-Average nm)	Polydispersity Index (PI)
K4 Transfection System	10	155.3	0.1018
	20	2461.7	0.5107
	50	5192.2	0.5426
Metafectene Pro	10	150.6	0.1348
CellFectin II	10	165.8	0.1776

5 Ex vivo degradation of dsRNA using *Aedes albopictus* gut extract

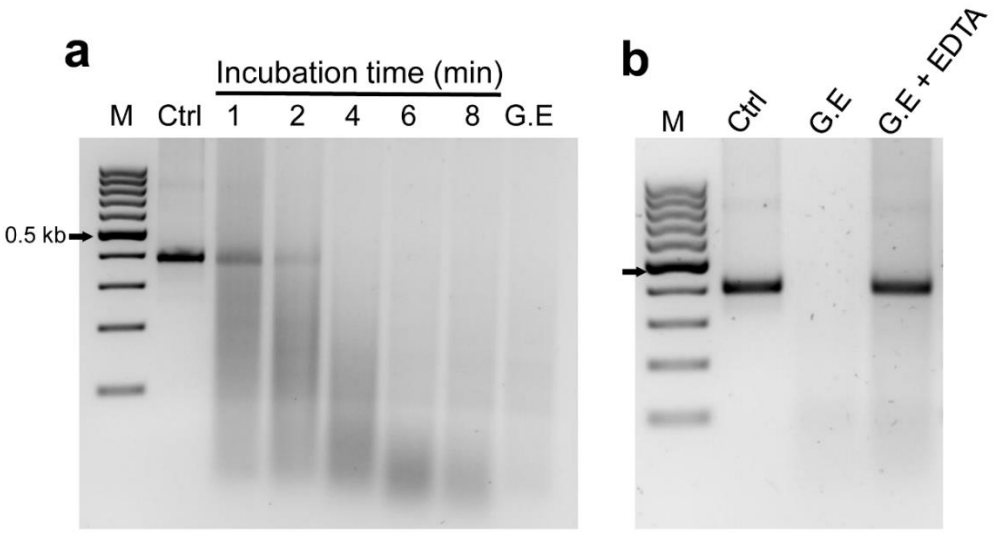

Fig. S4. Ex vivo degradation of dsRNA with gut extract of *Aedes albopictus* larvae. The gut extract from L4 larvae was used for the incubation of mCherry dsRNA. In (**a**), the dsRNA was incubated with gut extract for 1 – 8 min. In (**b**), the dsRNA was incubated for 10 min with either gut extract or gut extract containing EDTA. All samples were resolved on agarose gel electrophoresis immediately after each incubation and a GeneRuler 100 bp DNA ladder (M, Thermo Fisher scientific) was used as marker. The gel images displayed a representative of three independent experiments (n=3). Ctrl= mCherry dsRNA incubated in nuclease free water, G.E = gut extract alone, while G.E + EDTA = mixture of gut extract and ethylenediaminetetraacetic acid.

6 Identification, characterization, and expression profile of *Aedes albopictus* dsRNases

Table S4: List of dsRNase proteins used for the construction of the phylogenetic tree. The accession number for the nucleotide sequence were recovered from literature, quality-checked and the translated protein sequence were retrieved from NCBI (see Table S5 below). The asterisk (*,**) denotes multiple dsRNases within the same species

Species	dsRNase	Accession number	References
Aedes aegypti	Aae-dsRNase1	XP_001648469.1	Yoon et al 2021
	Aae-dsRNase2	XP_001653479.2	Yoon et al 2021
Aedes albopictus	Aal-dsRNase1	XP_019536384.3	This study
	Aal-dsRNase2	XP_062714997.1	This study
Anopheles darlingi	Ad-dsRNase1	ETN62076.1	Cooper et al 2020
	Ad-dsRNase2	ETN61460.1	Cooper et al 2020
	Ad-dsRNase3	ETN61459.1	Cooper et al 2020
Anopheles gambiae	Ag-dsRNase	XP_320813.4	Cooper et al 2020
Bactrocera dorsalis	Bd-dsRNase1	XP_011199940.1	Sharma et al 2021
	Bd-dsRNase2	XP_011199500.1	Sharma et al 2021
Bactrocera latifrons	Bl-dsRNase1	XP_018803412.1	Tayler et al 2019
	Bl-dsRNase2	XP_018803418.1	Tayler et al 2019
Bactrocera oleae	Bo-dsRNase1	XP_014088323.1	Tayler et al 2019
Ceratitis capitata	Cc-dsRNase1	XP_004530585.1	Tayler et al 2019
	Bo-dsRNase2	XP_014088332.1	Tayler et al 2019
Culex quinquefasciatus	Cq-dsRNase*	EDS34867.1	Cooper et al 2020
	Cq-dsRNase**	EDS38458.1	Cooper et al 2020
Drosophila melanogaster	Dm-dsRNase1	AAF49206.1	Cooper et al 2020
	Dm-dsRNase2	AAF49208.1	Cooper et al 2020
Drosophila suzukii	Ds-dsRNase1	QXY82428.1	Yoon et al 2021
	Ds-dsRNase2	QXY82429.1	Yoon et al 2021
Musca domestica	Mm-dsRNase1	XP_005177226.1	Tayler et al 2019
Nyssomyia neivai	Nn-dsRNase*	JAV11177.1	Cooper et al 2020
	Nn-dsRNase**	JAV11176.1	Cooper et al 2020
Rhagoletis zephyria	Rz-dsRNase1	XP_017466898.1	Tayler et al 2019
	Rz-dsRNase2	XP_017478492.1	Tayler et al 2019

Table S5: List of protein sequence used for the construction of the phylogenetic tree.

1	>XP_019536384.3|*Aedes albopictus*-dsRNase1 MEKFTCLMTILVLLGAGSDSKEIPSITSDNQRFAPSCSMNINNQLPRPQPLLLIPGTEEFRYPATSNRQL RLNPGETIELVCSSGFDLAPNKNSIIVSCVIDTIFNYDSTMHQFTDFSCRQIWYSNARRTYEPCERNASI IQIGFDLGTRFPKIMDICHNEETFENHWIKHEMFPFNAGYQSSNPRPNWYQGNFYPGIDTNYLYTNNKQR QTVAQILQSQELADDIIRDVGSGVYMARGHIAARVDFLYGTQQNATFWFLVVAPQWQNFNDGNWLRIEEQ VREFVAARNINVTVYGGTYGAHTQTDVNGDQQPIFLDYDPNGVQRLPAPKIYYKILHDERHNSGIALIGV NDIHITSMEQINGQYLLCDDIGDKVSWINWDRRNFKKGFAYACEVNPFLKRIGHLAHLDIPNLLI
2	>XP_062714997.1|*Aedes albopictus*-dsRNase2 MNRVASLLVLTVALELVWGQCTVNIRTNLVSPEPVFFRTATQLWSPDGPSLFWNSGETTTISCQSGTLTG FGVSTASLTCQSGTSFTIGGTAVSSSALTCTQRITGEIQTTTTSCGGGAGQLRNIGFLNPSGQMVTYIQS CYNVNTASVIYTRHIIPGRAINHAIQESYRPSFKVAGTASHVSPATSYTTASQATRLAVLLGSQAQADRF ITTSSYMSRGHLSPDADGIFRSWQWATYFYVNVAPQWQVVNAGNWLTVEGAARNIAGRLQEDVLIFNGC H DVMTLPHVNGQQIPITLEAGGIQAPKWYWKIIKSPSTNSGIALITNNDPFRTSMPAAEMLCSDVCSTYGW ANANYGNFGRGFTYCCTVAALMSAIPAIPAEAAASNVLRY
3	>QXY82428.1|*Drosophila suzukii*-dsRNase1 MKGLVLIALSGLFLASGQARILPKEDLPWELPAIPEVVNEIEPREAGCSIKIRSSELKDPQPLLIKSGTS EIVGFSDSGNVDVDKDKTIEFHCTSSLASPLSGKSVTAKCVGGTTFKIDDKEHDLSAIKCTSWPAFVGKK SGSSCNGGTTLIKVGFELSGSRFATQYEVCFNEDEEVTRYVYHRLEPGNNYYATGVDRITFGAGGYFAGK NVDKLYTQAVQKETIDKELDMDSAHYFNSAKNIFLARGHMGAKADFVFAPEQRATFLFINAAPQWQTFNA

	GNWARVEDGVRAWVAKEKKHVECWTGVWGVTTLANKNGEQRQLYLSHDKNGNGLIPVPKLYFRVVIEP SS KKGIVLIGVNNPHLSLEEIKRDYILCTDVSDKIDWISWKKTDLTAGYSYACEVAEFRKKVDHLPEFSVL
4	>QXY82429.1|*Drosophila suzukii*-dsRNase2 MKGLVLIALSGLFLASGQARILPKEDLPWELPAIPEVVNEIEPREAGCSIKIRSSELKDPQPLLIKSGTS EIVGFSDSGNVDVDKDKTIEFHCTSSLASPLSGKSVTAKCVGGTTFKIDDKEHDLSAIKCTSWPAFVGKK SGSSCNGGTTLIKVGFELSGSRFATQYEVCFNEDEEVTRYVYHRLEPGNNYYATGVDRITFGAGGYFAGK NVDKLYTQAVQKETIDKELDMDSAHYFNSAKNIFLARGHMGAKADFVFAPEQRATFLFINAAPQWQTFNA GNWARVEDGVRAWVAKEKKHVECWTGVWGVTTLANKNGEQRQLYLSHDKNGNGLIPVPKLYFRVVIEP SS KKGIVLIGVNNPHLSLEEIKRDYILCTDVSDKIDWISWKKTDLTAGYSYACEVAEFRKKVDHLPEFSVL
5	>XP_001648469.1|*Aedes aegypti*-dsRNase1 MAQFTILVTFLILLGARSESKELPSKVSDNQRFAPSCSININTQLPRPQPLLLIPGTEEFRYPATSNRLL RLNPGETVELVCSNGFNLAPSKNSIIVSCVIDTVFNYDSTMRQFSDFSCRQIWYSSARRTYEPCENSSSI IQIGFDLGARFPKIMDICHNEETFENHWIKHEMYAANAGYQSSNPRPNWYQGDFYPGIDTNYLYTVNKQR QTIAQILQSQDLADDIVRDVNSGIYMARGHIAARVDFIYGTQQNATFWFLVVAPQWQNFNDGNWLRVEEQ VRVFIAARNLNVTVYGGTYGAHTQTDANGDQQPIFLDYDPNGVQRLPAPKIYYKILHDERNQAGIALVGV NDIHITSMEQIEEQYMFCEDIGDKVSWINWERRNFKKGFAYACEVNPFLKRIGHLAHLDVPNLLI
6	>XP_001653479.2|*Aedes aegypti*-dsRNase2 MIRIGSLFVLAVALELVWGQCTVNLRTNLVSPEPVFFRTATQLWSPDGPSLFWNSGETTTISCQSGTLTG FGVSTASLTCQSGTSFTIGGIPVSSAALTCSQRITGEIQITSTSCGGGAGQLRNIGFLNPSSQLVTYIQS CYNVNTASVIYTRHIIPGRAINHAIQESYRPSFKVAGTASHVSPASSYTTASQATRLAVLLGSQAQADRF ITTSSYMSRGHLSPDADGIFRSWQWATYFYVNVAPQWQVVNAGNWLTVEGAARNIAGRLQEDVLIFNGC H DVMTLPHVNGQQIPITLEAGGIQAPKWYWKIIKSPNTNSGIALITNNDPFRTSMPAGEMLCQDVCSTYGW GNANYGNFARGFTYCCTVAALMSAIPAIPSEAAVANVLRY
7	>XP_011199940.1|*Bactrocera dorsalis*-dsRNase1 MKLTSTLLLLVAGSFCLFHGCTAGVVAVPEDVVDDWKADDHMSEQINILFERNLYVEPIKEDASQAIVPA EVEEDYVEPEPISEVQDELVQPDVDVNGKIEGRASECKVTIRGGLPTPQPLYLKSGSEEIYPYDTKGVMV VDAGSTLEMWCPGKFTTLDTTLVTATCVSGTNFRVDGTTYAFKELTCKAWPTFVAEKTGASCNGGIMVRV GFKISSTRFAKQYEVCFNEGDEVTRYVHHDLNPGANYYQTGVDRITFQTGGFFDGKNVDKLYTQATQLET INAHLGGDASKYFDSAKNVYLARGHMAAKADFDYGLEQRATFLFINAAPQWQVFNAGNWARIEDGVRAK V SSAGWYVDCYTGVYGVTTLANSDGVQTPLYLAYDSNNNGLIPVPKLYFRVVIEKTSKKGIVFIGVNNPHL TLDEIKKDYILCTDIADQVDYISWKRTDLTAGYSYACEVSDFRSKVTNLPSLSAPGGLLL
8	>XP_011199500.1|*Bactrocera dorsalis*-dsRNase2 MYSGGKAVKLALVLACLLAVVEAGILHSKETAVKSLLPNTDNDGPSTPYPTLSTADTYPTPPYINVTDET TDVTDEITDVTTDGPFSSTTPPPEISGGVVVRGDCAFDVNGDLNDPAPIFTPQNQLEWLVPSPSGVVELS NGAYIDMYCDKSFIAPFSNRTKVTAQCLQKQYFLVDGVIHPFSDFSCTSWPAYTARRTGRPCNGGTDLVE VGFVLTSGFLQIMDVCHDEVNEVTRYVHHKLNPSSAGYQHGVTRPSFITGDFYAGKNVDNLYTKVQQNNT ISKILGMDASPFFNDTIDVYLARGHMAAKVDFIFGAPQKATFFFVNAAPQWQMFNGRNWERVEDSVRRYA SDQALDLDCYTGIWGVSTLPDVNGVQRELYLAFDENNNGLIPVPKLYFRVVIDRKSRNGIVLIGVNNPHV TLEEIKKDYVICKDVGNRINWVSWDKENLMNGYSYACAVDDFISVVKDLPLDDLYTSGLLGVEALTIENI PS
9	>ETN62076.1|*Anopheles darlingi*-dsRNase1 MARQLVVLLICGAAVLQELFIRGVVSREYIEATTDALEWVLPVSEKKNDGTTDPACSISLHRDLTIMQPL LLKPGSSQFVWPRLNSTTVELDYGQPLELFCSHGFRDGSPVGKAKSAIVTCEGNDELGYAAGSYNISHFT CQRPVYHVAERTGGRCYGDSTLIRIGFELAPDRFVQLYEVCFNELQLHSHYVKYNLSPHNGHHQRAVKRP SFLQGGFYRDLKMNSIYTFVKQHATVQRILGTKARADAVLDSKRGLFLSRGHLAAKSDFIFGSHQRASFW LMNVAPQWQRFNALNWQRIETAVKEYITANDLWLTVYTGTYGVLELLDGNGDPQQIFLDYDAARDPPGRI PIPKLFYKVLIDEQTQSGIALIGVNNPHATPEEIAEQYVVCKDVSSAIDWIHWKRDSIPDGYSYACDVNE FNDVTGHLELVQPIGKLLL
10	>ETN61460.1|*Anopheles darlingi*-dsRNase2 MKFAVVSALLLLAAFVGARDIPPRAHQDVLFEEDIPEDVPLAGGYATGCSIRLNGDLPALQPLILVPGTA NFRYPMTSSGILTLNAGETLELACSNGFELYPEKNSIVAACVIDTQFNYDSKMYTFDQFSCTANWRSVAR RTERRCYNDATIVEVGFELGARFPKVMEVCHDEVTYHNHYIVHEFTPANAGFQTGVARPGWIQGNFYPGV NVNTLYTVNMQRETIATILNSQARADELVQTTANGIYMARGHIAARADFVYAPQQNATFWFLNAAPQWQ N FNAGNWERIENSAKSFVASRNINVRVYGGTYGVQTLADANGDHHEIFLDFDPNGRARLQAPKVYYKILHN EAQNSGIVLIGVNNVHISLEEIRRDYIFCTDVSSRIGWINWDRENLARGYSYACEVNEFNRVTGHLPNLN VASLLI
11	>ETN61459.1|*Anopheles darlingi*-dsRNase3 MKGTLCLLVALLSTSSLVSARDLRHEIPVEVPDVHLGVGFATACSVRMTGDLPRPQPLILRPGTDQFRYP ATDNGLLQLNAGETLELACQQGFALFPGKNTITISCVLNDQFNYDSQMFAFRDFACTENWLSTARRTAQR CFNGATIVQIGFELGSRFPRFLDVCHDEVTLDNHYVVHEFTPANAGFQQGVPRPGWYQGDFYPGININGL YTVNTQRSTLATILNSQARADQLVQGTDNGFFMARGHIAARSDFIYGTQQNGTFWFLNASPQWQTFNAGN WERIEASVKRFVASRNIHVRVYGGTYGIQTQADGNGDHRQIFLDFNANGRTRVRAPMVYYKILHNEAQNS GIVLIGVNNIHISLEEIRRDYIFCTDVSSRIGWINWERENLILGYSYACEVNEFNRVTGHLPNLNVASLL I

12	>EDS34867.1|*Culex quinquefasciatus*-dsRNase* MWNAFGLAALVLLAEIELNFSRIALETSTVDFGDSTGKDYEKDYGCKVSMNKDLNLKQPLFLVPGTKQFI TPITNTTDLLFHQGEQLELFCTRGFGHTGDKSIVTTCDDANEFVHNGKIYNISQLVCKAPVYHVASRTEE RCFNNARLVKVGFELDDRFLKLYEVCFDEETLGTHYVKHALYPWNVKHQSSKRPSFIQGDYFPDLKMSKL YSYDSQRDALARILGSPEHADTFLNKKKDIFLARGHLAARADFVYGSHQRATFWFLNVAPQWQKFNSFNW QRVETGVKDLIAQRGLEVTVYTGTYGILELPDANGDMQPIFLDFDPNNGGRVPVPKVFYKILHDEWHDAG IALIGVNNPHATPEQIQQDYVLCEDVSDQIKWLKWKPENILGGYSYACDVNEFNAVTKHLPLGKVEKLLV
13	>EDS38458.1|*Culex quinquefasciatus*-dsRNase** MKTLLCVVLGLAFTIEGRDLPLQEAGSVRFAPTCSLNINNQLPIPQPLILHTGTDQFRYPTSNNRILQLN AGETVELACDNGFNLAPTKTTIIVSCVFDQTFNYDSTMYQFQEFSCTRNWYSSARDTNEPCNQGATIIEI GFELGTRFPKIMDVCHNSETFENHWVKHEFRRAHAGYQQGVARPSWYQGEFYPGVNVNTLYTIVRQRQTI AEILNSQSLADDIVGDTSNGVYMSRGHIAARVDFIYATHQNATFWFLNAAPQWQNFNEGNWLKIEDSTRN FVAARNIRVTVYGGTYGAHTQTDVNGDQQPIFLDFDRNGVQRLPAPKIYYKILHDEQNKAGIVLIGVNDI HITSMEQIRNEYMFCEDIGDKVSWINWDRFNLKRGFSYACEVNEFLRKIGHLPELDVPNLLI
14	>JAV11177.1|*Nyssomyia neivai*-dsRNase* HLLPTACEIRISGGGLGEPQPLILNSGATEFIEPKDANGIIRLNPGDDISLFCTTGFQSPSTTNNIIRAT CTTGTIFIIDGNKGNEMTFSNINCKSYPYHTARKSGKTCGNGAGVDIEVGFIVKERFIELFHICHDDIME STMYVTHSMTPGNEGYQRSFPRPSWLSSGFFGGKNVDNIYTNVRQNARVAEILGSQELADKYIKPTTTST YLARGHMAAKVDFIFGSQQRATFWLMNVAPQWQSFNAGNWERVESSTRKMASQRNTHFDVYTGTYGVM TL PDINGQHQEIYLYFDENNNGQIPVPKIYYRVLYEKSTKRGIVLIGVNNIHITAEEAEEQNYIICEDVSDK INWINWERNDQILGYSYACEVEEFTKVVEHFPKLEISGLYV
15	>JAV11176.1|*Nyssomyia neivai*-dsRNase** IYYLYSQISFSDTSISDECQLCWHSIHSQVKNVIKTSSGTSASQSYYVREVWSIMRVVLFVSVLLHWQLS SARIPINDHHVISPLMEPCEIRISGGGLGEPQPLILNSGATEFIEPKDANGIIRLNPGDDISLFCTTGFQ SPSTTNDIIRATCTTGTIFIIDGNKGNEMTFSNIFCKSYPYHTARKSGKTCGNGAGVDIEVGFIVKERFI ELFHICHDDIMESTMYVTHSMSPGNEGYQRSFPRPSWLSSGFFGGKNVDNIYTNVRQNARVAEILGSQEL ADKYIKPTTTSTYLARGHMAAKVDFIFGSQQRATFWLMNVAPQWQSFNVGNWERVESSTRKMASQRNTH F DVYTGTYGVMTLPDINGQHQEIYLYFDENNNGQIPVPKIYYRVLYEKSTKRGIVLIGVNNIHITAEEAEE QNYIICEDVSDKINWINWERNDQILGYSYACEVEEFTKVVEHFPKLEISGLYV
16	>AAF49206.1|*Drosophila melanogaster*-dsRNase1 MKCLVLIAFSGLFLASAQARILPAEDLPWELPEVPVAVNEIEPRAAGCSIKIRSSELKDPQPLLIKSDTS EIVGFSDTGYVDVDKDKTIEFHCTSSLASPLSGKSVTAKCVGGTTFKIDDKEHDLSAIKCTSWPVFVGKK SGSSCNGGTTLIKVGFELSGSRFATQYEVCFNEDEEVTRYVYHRLEPGNNYYATGVDRITFGAGGYFAGK NVDKLYTQAVQKETIDKELDMDSSRFFDSAKNIFLARGHMGAKADFVFAPEQRATFLFINAAPQWQTFNA GNWARVEDGVRAWVAKENKHVECWTGVWGVTTLPNKNGEQRQLYLSHDNNGNGLIPVPKLYFRVVIEP ST KKGIVLIGVNNPHLSLEEIKRDYILCTDVSDRINWISWKKTDITAGYSYACEVPEFRKKVTHLPEFSVSG LLV
17	>AAF49208.1|*Drosophila melanogaster*-dsRNase2 MKCIRFSLLVVGLLAAPAAWARVPCPEVELPPVVEDDGIFERIAVAPPQPVGRAGACSVTIRGGLPSPEP VYLKTDSEDFYPFSDVGVMEFESGGSLQLWCPSGFNTHSENLLTASCVSGTTFSVGGSNFEFKDLYCKSW PGFKAVKSGATCNGGIVIRVGFEITSSRFAEQMQICFNEEEEVTRYTRHKLEPGSNYYETGVARITFQTA GFFDGKNVDKLYTQATQLETINNELGGDAEKYFDSSSNVYLARGHLGAKADFDYAPEQRATFLFINAAPQ WQTFNAGNWARVEDGLRAWVSKNKLNVNCYTGVYGVTTLPNKDGVETPLYLAKDDNNNGLIPVPKLYF RV VIDPSSHRGIVFVGVNNPHLTEEQIKRDYVICDDVSDQVTYINWKTTDIKAGWSYACEVADFLKTVKHLP ALTAKGGLLV
18	>XP_320813.4|*Anopheles gambiae*-dsRNase SECTVNIRTQLNAREPLFLRNNQLWAPNGPSLQWNAGETTLIACPGNTIQNTGTVTANIQCVSGTTFNLA GSNVNIADVSCTARSTGSHQTTGQSCGSGGTLLNLGFDVPGVGFVTYIQSCYNMQTASVIYTRHIIPGAA ISHSISESYRPSFKTAGTAPHVQPATSYTTAQQAIRFAQLLGSQAQADRFITSSSYLSRGHLSPDADGIF RPWQWATYFYVNVAPQWQATNGGNWLVVENAARNIAGRLNEDVLIFNGAHDILTLPHVNGQQVPITLEA G GIQTPKWYWKIIKSPRTNAAIALVNNNDPFRTSMPAGEMLCQDVCGQYGWGNANYGNFARGFTYCCTVA D LRRAIPSIPAEADAANVLRF
19	>XP_018803412.1|*Bactrocera latifrons*-dsRNase1 MKLTSTLLLLVAGSFFLFHGCTAGVVAVPEDVVDDWKAEDHTSELINILFERNLYVKRIKEDASQAIVPV EAEEAEEDYVEPEPISEVEDELVQPEVDVNGKIEGRASECKVTIRGGLPTPQPLYLKSGSEEIYPYDTKG VMVVNAGRTLEMWCPGKFTKLDTTLVTATCVSGTNFRVDGTTYAFKELTCKAWPTFVAEKTGASCNGGV M VRVGFKISSTRFAQQYEVCFNEGEEVTRYVHHDLNPGANYYQTGVDRITFQTGGFFDGKNVDKLYTQATQ LETINAHLGGDARKYFDSAKNVYLARGHMAAKADFDYGLEQRATFLFINAAPQWQVFNAGNWARIEDGV R AKVSSARWYVDCYTGVYGVTTLPNSDGVQTPLYLAYDSNNNGLIPVPKLYFRVVIEKTSKKGIVFIGVNN PHLTLDEIKKDYIICTDIADRVKYINWKRTDVTAGYSYACEVSDFRSKVTNLPNLSAPGGLLL
20	>XP_018803418.1|*Bactrocera latifrons*-dsRNase2 MYSGGKAVKLALLLACLLADVEAGILHSKETAVKSLLPNTENDGPRTPYPTLSTADTHPTPPYINVTDET

	TDVTTDGPFSSTTPPPEISGGVVVRGDCAFDVNGDLNDPAPIFTPPNQLEWLVPNPAGVVELSNGAYIDM YCDTSFIAPFSNLTKVTAQCLQKQYFLVDGVIHPFSDFSCTSWPAYTARRTGRPCNGGTDLVEVGFVLAS GFLQIMDVCHDEVNEVTRYVHHKLNPSSAGYQHGVTRPSFITGDFYAGKNVNNLYTKVQQNNTISKILGM DASPFFNDTIDVYLARGHMAAKVDFIFGAPQKATFLFVNAAPQWQMFNGRNWERVEDSVRRYASDQALD L DCYTGIWGVSTLPDVNGVQRELYLAFDENNNGLIPVPKIYFRVVIDRKSRNGIVLIGVNNPHVTLEEIKK DYVICKDVGKRIKWVSWDKENLMNGYSYACAVDDFISVVKDLPLEDLYTSGLLGVEELTIENIPS
2 1	>XP_014088323.1|*Bactrocera oleae*-dsRNase1 MKLASTLLLLVAGSFCLFHGCIASVIATPQHVNDESKADDQLSEPIAPISAINEEDKLEGLETLFERNLY VEPIKGADYQYIKSAAVSVDEKPAEVEEDYVEPEPNSEVEDELVQPEADVNGKPEGRANECKVTIRGGLP TPQPIYLKSGSEEFYPYDTRGVMVVDSGKTLEMWCPGKFTTIDKTLLTASCVSGTNFRVDGTTYSVKELT CKSWPGFVAEKTGASCNGGIMVRVGFKVSSRRFVEQYQVCFNEDEEVTRYVHHDLNPGSNYYQTGVDRIT FQTGGFFDSKNVDKLYTQVTQQATINAHLGGDASKYFTSNKNIYLARGHMAAKADFDYGSEQRATFLFIN VAPQWQVFNAGNWARIEDGVRAKVSSAKWYVDCYTGVYGVTTLPNSDGVQTPLYLSYDSNNNGQIPIPK L YFRVIIERSSQKGIVFIGVNNPHLTLNEIKKDYIICNDISDRVNYVNWKRTDITAGYSYACEVSDFRRKV THLPTLSAPGGLLL
2 2	>XP_014088332.1|*Bactrocera oleae*-dsRNase2 MYSGGKAVQLTLSLVCLLAAVEAGILYSKEPAVKSLILNTKDDGPRTPYRTSSTAATYSTPSFINVTDGP TDVTTDGPFSSTTPPPEISAGVVVRGDCAFDLNGDLNDPAPIFTPHNQLEWLVPNPAGIVELSNGAYIDM YCNKSFIAPFSNSTKVTAQCLQNQYFLVDGLIYPFSNFSCTNWPAYTARRTGRPCNGGTDLLEVGFELPT GFLQIMDICHDEVNEVTRYVHHNLNPSSAGYQHGVSRPSFITGDFYAGKNVNNLYTKVQQNRTISRILGM DASRFFNDTLDVYLARGHMAAKVDFIFGASQKATFYFVNAAPQWQMFNGRNWERVEDSVRRYASDKAL DL DCYTGIWGVSTLPDVNGIQRELYLAFDENNNGLIPVPKIYFRVVIDRKTRNGIVLIGVNNPHVTLEEIKK DYVICKDVGNRIKWVSWDKENLMNGYSYACAVDDFISVVKDLPLDELYTSGLLGVEELIIENIPL
2 3	>XP_017466898.1|*Rhagoletis zephyria*-dsRNase1 MVVDTGSSLQMWCPGQFSSIADTLITATCVSGSNFRVSGTTYAFKELACKAWPAFVAEKTGASCSGGIMV RVGYKISSSRFAQKYEVCFNEEEEVTRYVHHDLDPGSNYYETGVARITFQTAGFFDGKQVDNLYKQVTQQ ATIEAQLGNDASQYFDSNKNVYLARGHMAAKADFDYASGQRASFLFINAAPQWQVFNAGNWERIEDGVR S KVAASKWYVDCYTGVYGVTTLPNADGVQTPLYLAYDSNNNGLIPVPKLYFRIVIERTSQKGIVFIGVNNP HLSLEEIQKDYILCADVADQVDYINWKRTDLTAGYSYACTVDDFKQNVTYLPEVSASGGLLL
2 4	>XP_017478492.1|*Rhagoletis zephyria*-dsRNase2 MANTKRTLELFFALLCFSVAVQAGLLQSKQRQRYTELSTVVPAVEGTDPTPPSNITTDSP NNSTTDSPFNTTLTAPPSTATSPPDSGSGVVVRGDCAFDINGELNDPAPIFTPRNHFDWL VPNAAGVVELSNGAYIDMYCSTSFMAPFTNRTKVTAQCLQKKYFLVDGLIYPFANFSCTA WPAYTARRTGRPCNGGTDLLEVGFELEAGFLPTMDICHDEVNEVTRYVHHVLNPSSNGYQ HGVSRPSFITGDFYNGKNVNNLYTKVEQNKTISQILGMDASPYFNDTIDVYMARGHMAAK VDFIFGAPQKATFYFVNAAPQWQMFNGGNWERIEDGVRRFASDQALTLDCYTGIWGVSTL PDVNGVQQELYLAFDENNNGLIPVPMLYFRVVIDRESRKGIVLLGVNNPHISLEEIKRDY VICKDVGRRIDWIGWNKENLMKGYSYACAVDDFLKVVKHLPLEDLYTTGLLGVEELKIEN APIWEEH
2 5	>XP_004530585.1|*Ceratitis capitata*-dsRNase1 MKLTTTLLLLVTGSCCLLQGCTAGVIAVPEVVIDGLKIDEEKPEESVFERNLYVEPISGAEDDYVEPEDE LLPPAPVVDDKPKGRATACKVTIRGGLPTPQPVYLKSDSAEFYPYDSTGVMVVESGEKLDLWCPGKFTSL DKTLVSASCVSGTNFKVDGTTYTLKELTCKSWPSFVAEKTGSSCNGGVEVRVGFKVSSSRFVEQYKVCFD EDEEVTRYVHHDLNPGSNYYQTGVDRLTFQTGGFFDGKNVDKLYTQATQLTTINEQLGGDASKYFDSSKN VYLARGHLAAKADFDYGTEQRATFLFINAAPQWQVFNAGNWARIEDGVRAKVSKAQWYVDCWTGVYG VTT LANANGVQTPLYLAYDSNNNGLIPVPKLYFRVVIERTTKKGIVFIGVNNPHLTLAEIKKDYILCTDVADK VDYVNWKPTDITAGYSYACEVDDFKKKVSHLPDLPSVTGLLV
2 6	>XP_005177226.1|*Musca domestica*-dsRNase1 MKLATSLLLLVAGFACLIHVSVGGVVGVPTDLLENLKIADDLPEAPPVVEEEIFERNVVVDVLPEGRANE CQITIRTGLSEPQPVFLKTNAAEFYPYSNTGVMQVHAGGTLQMFCPGEFKVKATKLITATCVSGTTFKVD GTSYAFSELVCKSWPGFVAKKKGTTCNGGILVGVGFEVSSTRFVEQMEICYNEQEEVTRYVRHTLGPASN YYQTGVDRITFQTAGFFNGKNVDKLYTQATQLETINAELGGNAGKYFDSSKNIYLARGHMGAKADFMYG T QQRATFLFINAAPQWQVFNAGNWARVEDGVRAWVSKNSKTVNCYTGVYGVTTLPNKNGVQTPLYLAHD SN NNGLIPVPKLYFRVVIEPATKKGIVFVGVNNPHLTLEQIKKDYIICTDVSSKVNYISWKKDDITAGYSYA CEVADFLKTVKHLPALTATGGLLV

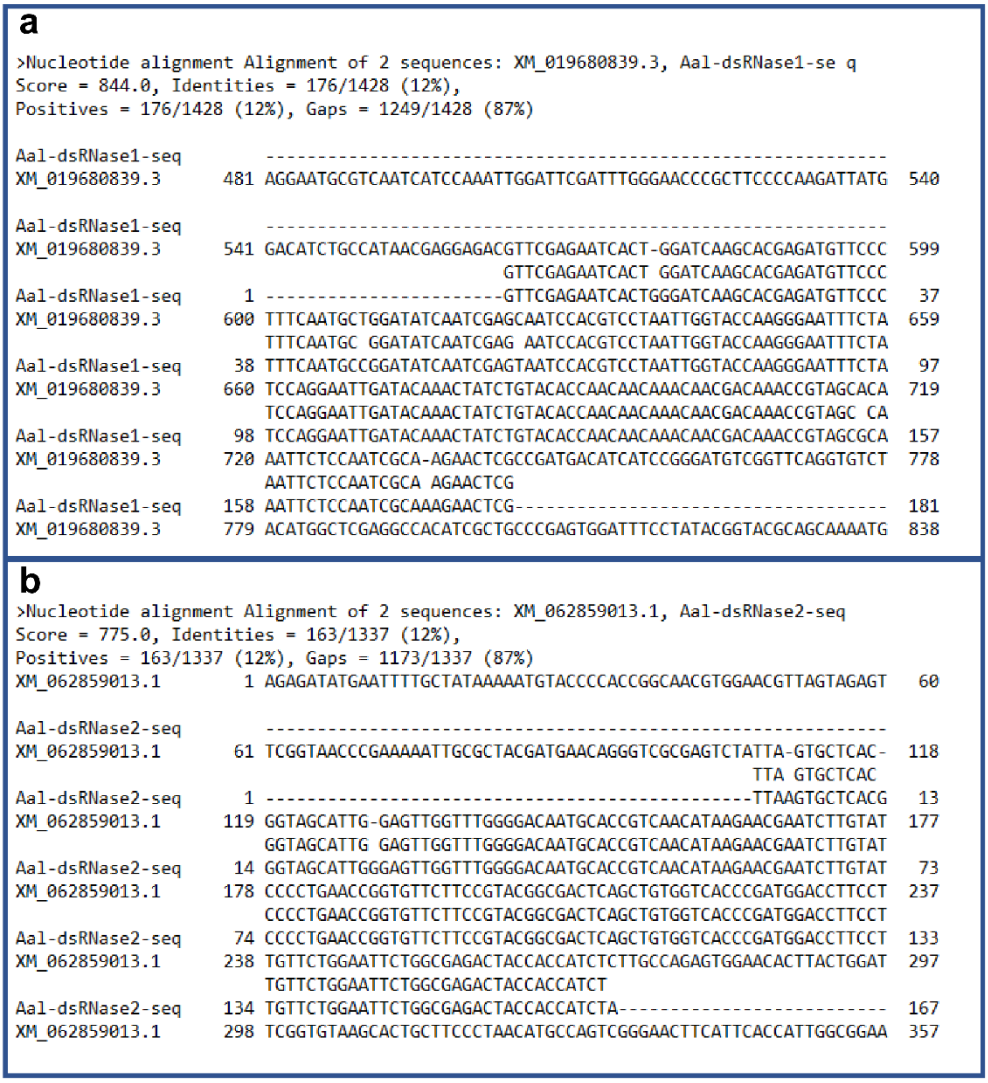

Fig. S5. Sequencing data of dsRNase genes of *Aedes albopictus*. The RT-PCR products of the (**a**) Aal-dsRNase1 and (**b**) Aal-dsRNase2 were sequenced and aligned with the corresponding reference sequences using Geneious Prime v2025.1.

7 Protection of dsRNA from degradation by *Aedes albopictus* gut extract using commercially available transfection reagents

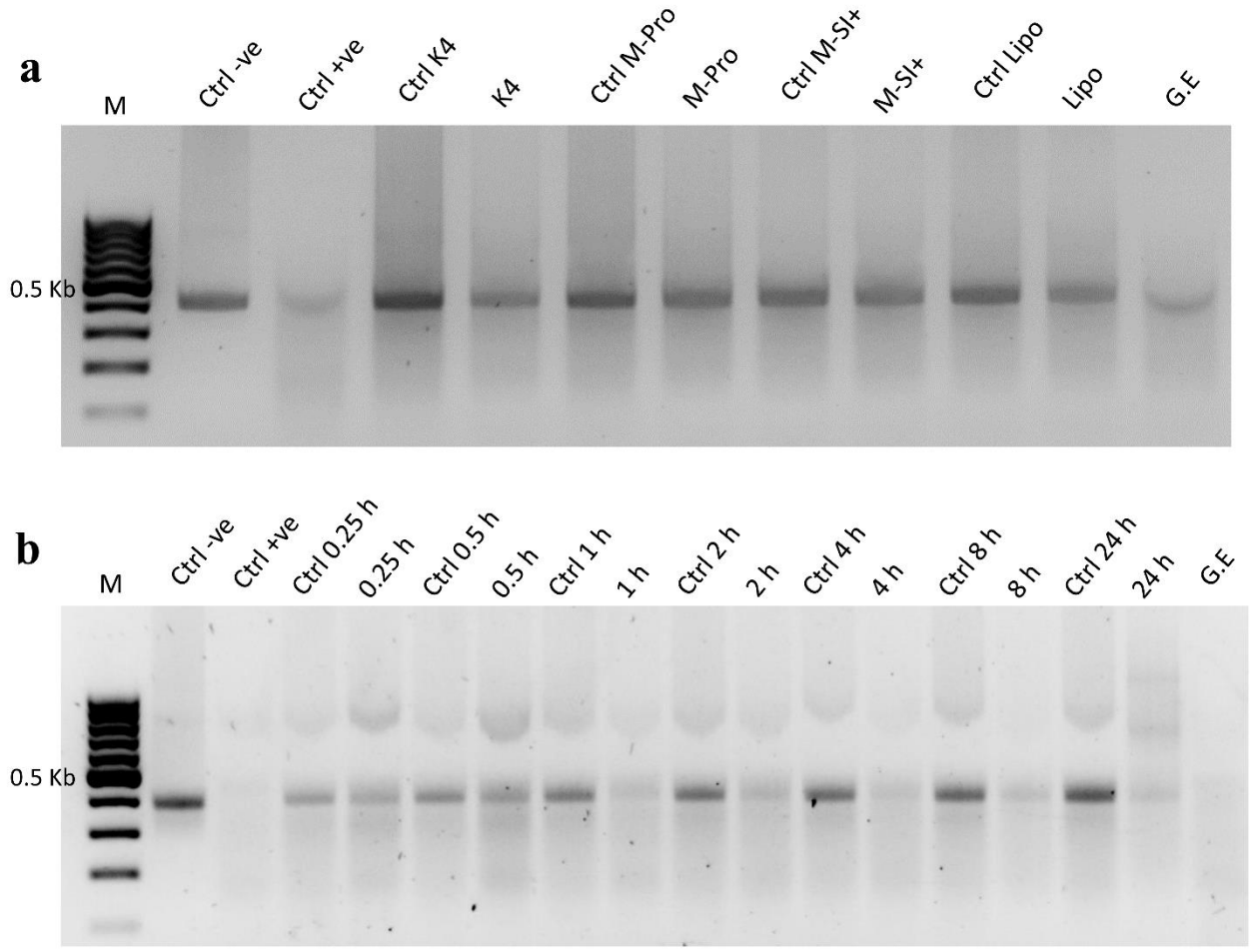

Fig. S6. Protection of dsRNA from degradation by *Aedes albopictus* gut extract. The dsRNA was complexed prior to the degradation assay in (**a**) with K4, Metafectene-Pro (M-Pro), Metafectene-SI+ (M-SI+), or Lipofectamine-2000 (Lipo). In (**b**), dsRNA was complexed with K4 and incubated with gut extract for 0.25 to 24 h. EDTA was added post-incubation to stop degradation, and samples were analyzed by agarose gel electrophoresis. Negative control (Ctrl -ve) was incubated in nuclease-free water while positive control (Ctrl +ve) was incubated in gut extract. Gut extract containing EDTA served as the independent control for each dsRNA:TR sample and time point. A GeneRuler 100 bp DNA ladder (M, Thermo Fisher scientific) was used as marker. The image shown are representative of three independent experiments (n=3). G.E = gut extract alone.

Chapter III

Quantitative fluorescence imaging of alphavirus infection for antiviral screenings

Journal of Visualized Experiments. 2026 March (). doi:10.3791/69384.

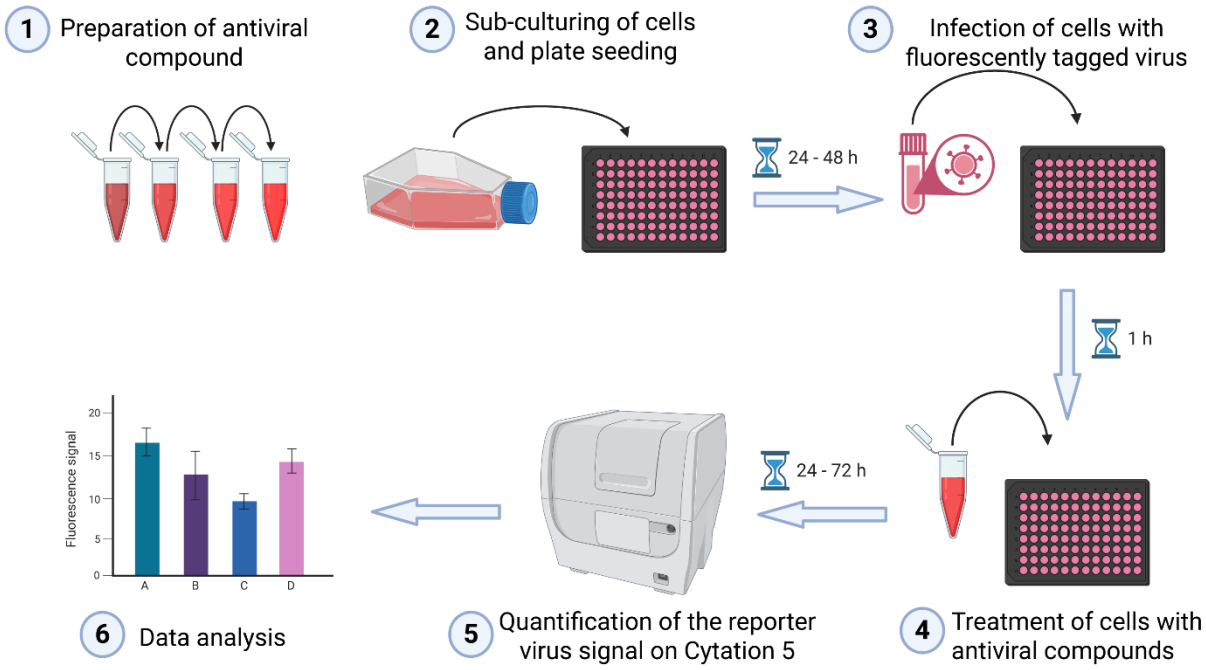

jove | All

DATE PUBLISHED February 27, 2026
DOI 10.3791/69384
URL jove.com/t/69384

Quantitative Fluorescence Imaging of Alphavirus Infection for Antiviral Screenings

Alejandra Centurión[*1,2], **Bodunrin Omokungbe**[*1,2], **Cross Chambers**[2], **Sabrina Stiehler**[3], **Andreas Vilcinskas**[1,2,3], **Kornelia Hardes**[1,2,4]

[1]LOEWE Centre for Translational Biodiversity Genomics (LOEWE-TBG) [2]Department of Pest and Vector Insect Control, Fraunhofer Institute for Molecular Biology and Applied Ecology IME, Branch of Bioresources [3]Institute for Insect Biotechnology, Justus-Liebig University [4]BMBF Junior Research Group in Infection Research "ASCRIBE", Fraunhofer Institute for Molecular Biology and Applied Ecology IME, Branch of Bioresources

Corresponding Author: Kornelia Hardes <kornelia.hardes@ime.fraunhofer.de>

*These authors contributed equally

Citation

Centurión, A., Omokungbe, B., Chambers, C., Stiehler, S., Vilcinskas, A., Hardes, K. Quantitative Fluorescence Imaging of Alphavirus Infection for Antiviral Screenings. *J. Vis. Exp.* (), e69384, doi:10.3791/69384. (2026).

Abstract

Fluorescence microscopy offers a highly sensitive and versatile approach for investigating alphavirus infection at the cellular level. By combining fluorescently labeled viruses with quantitative image analysis, this method enables detailed spatial and temporal characterization of infection dynamics, including the detection of subtle differences in replication kinetics and cell-to-cell spread. A central aim of this protocol is its application in antiviral screening assays. Image-based quantification of fluorescence intensity provides a robust and reproducible means to assess the efficacy of antiviral compounds, allowing early and sensitive detection of inhibitory effects in infected cells. This facilitates the identification of promising antiviral hits and supports the evaluation of dose-dependent responses. The approach is also well-suited for comparative studies of different alphavirus strains or mutants, as variations in replication behavior and dissemination patterns become readily apparent. Its flexibility, compatibility with multiple cell lines, and straightforward integration into automated imaging platforms makes the method scalable and suitable for high-throughput screening campaigns. Overall, this protocol advances the discovery and evaluation of antiviral strategies. Given that several alphaviruses cause significant human and veterinary diseases, lack approved antiviral therapies, and continue to expand geographically with emerging outbreaks, the identification of novel antivirals remains an urgent priority. Therefore, this fluorescence-based workflow represents a valuable and timely contribution to modern alphavirus research.

Introduction

Alphaviruses are enveloped, positive-sense, single-stranded ribonucleic acid (RNA) viruses belonging to the family *Togaviridae*[1,2,3]. They are primarily transmitted by mosquitoes and are responsible for a range of diseases in humans and animals. The alphavirus genus includes several medically significant viruses, such as Chikungunya virus (CHIKV), Sindbis virus, Eastern equine encephalitis virus, and Venezuelan equine encephalitis virus[4,5]. These pathogens cause symptoms ranging from febrile illness and rash to severe neurological complications[6]. Concerningly, CHIKV has re-emerged as a major public health concern. Since the beginning of 2025 alone, over 220,000 cases have been reported across 14 countries, resulting in at least 80 deaths[7]. Although the mortality rate is low, a significant proportion of infected individuals develop chronic joint pain, which can lead to long-term disability and reduced mobility[8]. To develop targeted antiviral strategies, a more comprehensive understanding of alphavirus replication and host-pathogen interactions is essential. Meanwhile, some alphaviruses, like Semliki Forest virus (SFV), show low pathogenicity in humans, despite sharing high genetic and structural similarity with more virulent alphaviruses. This

DOI 10.3791/69384

makes SFV an ideal model for studying alphaviruses without posing a high risk to human health[9,10,11].

Traditional assays such as plaque assays, 50% tissue culture infectious dose ($TCID_{50}$) assay, and quantitative polymerase chain reaction (qPCR) analysis are valuable for quantifying viral titers and gene expression but are limited to endpoint measurements and require cell lysis or fixation. As a result, they cannot capture the dynamics of infection within the same cells over time[12,13]. To address these limitations, real-time fluorescence imaging provides a powerful, non-destructive approach for monitoring infection kinetics across multiple time points. Using fluorescently tagged viruses, such as mCherry-labeled SFV, enables direct visualization and quantification of reporter virus signal and spread in living cells[14,15]. For the experiments described here, commonly used cell lines in arbovirus research were employed. U4.4 cells, derived from *Aedes albopictus* larvae, are mosquito cells that support efficient replication of many arboviruses and facilitate studies on vector-virus interactions[16,17]. In parallel, BHK-21 cells, a fibroblast-like mammalian cell line originating from baby hamster kidney tissue, provide a permissive vertebrate host system frequently used for viral propagation and molecular virology assays[18].

This protocol describes the monitoring of virus replication and the characterization of antiviral compounds in detail, using furin inhibitors as an example. Furin is a proprotein convertase found in many eukaryotes and plays a key role in activating precursors of growth factors, hormones, matrix metalloproteinases, plasma proteins, and receptors[19,20]. Many alphaviruses exploit furin to cleave and activate their surface proteins, a crucial step for successful replication[20]. Furin inhibitors are synthetically designed compounds that block furin activity, thereby preventing its use by viruses and reducing viral replication[21,22,23]. Given the limited availability of standardized protocols for automated fluorescencemicroscopy-based analysis of alphavirus infections using a cellimaging multimode reader, a detailed workflow for characterizing antiviral compounds in aedine cells is provided. The protocol outlines steps for cell culture, virus production, infection, antiviral compound (furin inhibitor) treatment, fluorescence imaging, and image analysis. However, the methods described here can be readily adapted to other viruses and alternative fluorescent labels.

Protocol

1. Biosafety

NOTE: The recombinant mCherry-tagged Semliki Forest virus (SFV-mCherry) used in this protocol is genetically modified[24,25,26]. Incorporation of a fluorescent reporter gene classifies it as a genetically modified organism, which makes it subject to additional containment and regulatory requirements. Work involving other alphaviruses, particularly more pathogenic viruses such as CHIKV, may require additional containment and permits.

1. Clean the biosafety cabinet with an appropriate disinfectant and apply UV for at least 30 min before and after viral assays.
2. Discard all contaminated material according to local biosafety regulations. Collect solid and liquid waste separately in autoclavable containers and autoclave before disposal.

2. Preparation of antiviral compounds

NOTE: Furin inhibitors MI-1130[27], MI-1131[27], and MI-1148[22,23] used in this study are examples of antiviral compounds selected for testing. Furin inhibitor MI-1148 was used as a negative control in the cytotoxicity assay and as a positive control in the antiviral assay.

1. Dissolve antiviral compounds in an appropriate solvent. When possible, use sterile water to avoid cytotoxic effects. Dimethyl sulfoxide or methanol can be used to a maximum of 2% (v/v). Using stock solutions of 10 mM in sterile water is recommended.
2. Store stock solutions at -20 °C, depending on stability and solubility, unless specified otherwise by the manufacturer.

3. Cell culture

1. Culture U4.4 cells in Leibovitz's L-15 Medium supplemented with 10% fetal bovine serum (FBS), 1% MEM non-essential amino acids, 1% tryptose phosphate broth, 1% glutamine, and 1% penicillin/streptomycin (Pen/Strep) (seeding density: 1 × 10^6 cells/T25 flask, culture volume: 5 mL). Maintain cells at 28 °C. Passage U4.4 cells at a 1:6 ratio once per week, but adjust seeding densities according to experimental needs.

   NOTE: Additional cell lines, such as C6/36 cells, are also compatible with this protocol. Alternative media and supplements may be used as appropriate. The inclusion of antibiotics is optional and may be omitted.

2. Culture Baby hamster kidney (BHK-21) cells in cell culture flasks using Dulbecco's Modified Eagle's Medium supplemented with 10% FBS, 1% glutamine, and 1% Pen/Strep (seeding density:

   ≈

   2 × 10^6 cells/T75 flask, culture volume: 10 mL). Maintain cells at 37 °C in a humidified incubator containing 5% CO_2. Passage cells at a 1:12 ratio every 4-5 days, with flexibility to modify seeding densities as required.
3. Ensure cells remain healthy and actively proliferating.

4. Virus production

1. Preparation of SFV-mCherry (SFV6-2SG-mCherry) stocks in BHK-21 cells.
    1. Culture BHK-21 cells (seeding density: ≈ 1×10^5 cells/well, culture volume: 500 µL) in a clear cell culture 24-well plate under the conditions described above.
    2. At approximately 90% confluency (target confluency: ≈ 2×10^5 cells), transfect BHK-21 cells with the SFV6-2SG-mCherry plasmid using a transfection reagent in infection medium (DMEM supplemented with 1% Pen/Strep and 0.2% bovine serum albumin). Therefore, dilute 1 µL of transfection reagent in 2 µL of reduced serum medium.
    3. In a separate tube, dilute 0. µg plasmid DNA and µL of a proprietary additive in 2 µL of reduced serum medium. Add the diluted DNA solution to the proprietary additive solution and incubate for 1 min at room temperature. Subsequently, add 5 µL of the resulting complex to the cells.

       NOTE: Other transfection reagents may be used, provided they are compatible with the specific cell line, and the instructions may vary depending on the reagent used.
    4. At 48 h post-transfection, collect the virus-containing supernatant using a pipette, aliquot 250 µL per DNA/RNA free tube, and store at -80 °C.
2. Titration by $TCID_{50}$ assay.
    1. Culture BHK-21 cells (seeding density: ≈ 3×10^4 cells/well, culture volume: 100 µL) in a black imaging grade 96-well plate under the conditions described above.
    2. Thaw virus aliquot, prepare tenfold serial dilutions of the virus sample in infection media (15 µL virus sample + 135 µL infection media), and add 100 µL of the dilutions to cells.
    3. Incubate cells for 1 h at 37 °C in a humidified incubator containing 5% CO_2 and replace with 100 µL fresh infection medium afterward.
    4. At 48 h post-infection (hpi), assess viral replication by fluorescence measurement using a multimode imaging well-plate reader (detailed description in section 7) and determine the cytopathic effect caused by the virus infection. Calculate the $TCID_{50}$ value based on the method of Reed-Muench[28] and convert to estimated viral titers (PFU/mL) using the standard Poisson-based approximation that 1 $TCID_{50}$ corresponds to 0.7 PFU.

5. Cytotoxicity determination

1. Culture U4.4 cells (seeding density: ≈ 3×10^4 cells/well, culture volume: 100 µL) in a clear cell culture 96-well plate under the conditions described above.

   NOTE: Outer wells (row A and H; columns 1 and 12) were seeded with cells but excluded from experimental analysis to avoid edge effects, including increased evaporation.
2. At 90% confluency (target confluency: ≈ 6×10^4 cells), treat cells with 100 µM of furin inhibitors MI-1130 and MI-1131 in a total volume of 100 µL. Add MI-1148, untreated cells, and cells treated with water as negative controls and ionomycin (100 µM in the assay) as a positive control for cytotoxicity.
3. At 48 h post-treatment (hpt), assess cell viability using a luminescent assay based on ATP quantification. Add an equal volume of the luminescent assay reagent to each well (1:1 relative to the culture medium), shake the plate for min to ensure cell lysis, and incubate for 10 min in the dark before measuring luminescence.
4. Record luminescence in a black or white 96-well plate using the multimode reader.

6. Viral infection and treatment with an antiviral compound

1. Culture U4.4 cells (seeding density: ≈ 3×10^4 cells/well, culture volume: 100 µL) in a black imaging-grade 96-well plate under the conditions described above.

   NOTE: Outer wells (row A and H; columns 1 and 12) were seeded with cells but excluded from experimental analysis to avoid edge effects, including increased evaporation.
2. Infect cells (target confluency: ≈ 6×10^4 cells) with SFV-mCherry at an MOI of 0.01 in non-supplemented L-15 medium using an inoculation volume of 10 µL, and incubate for h at 28 °C.

   NOTE: Only lowpassage reporter virus stocks should be used, particularly when working with very low MOIs and multi-day infections.
3. Dilute the furin inhibitors to 100, 50, 25, and 12.5 µM concentrations in a separate 96-well V-bottom plate using supplemented L-15 medium. Prepare 110 µL per well to allow for a 10% overage, and transfer 100 µL (final volume) onto the

DOI 10.3791/69384

cells. For controls, use infected cells with the solvent of the antiviral compounds and cells containing the virus only as a negative control. Uninfected, untreated cells also need to be added to measure the background fluorescence.

4. After the 1 h infection period, remove the infection medium and transfer 100 µL of the diluted furin inhibitors from the V-bottom plates to the black imaging-grade plates.
5. Incubate cells at 28 °C.

7. Live-cell fluorescence imaging, quantitative image analysis, and data presentation

1. Measurement of viral replication via fluorescence microscopy (see **Supplementary Figure 1, Supplementary Figure 2, Supplementary Figure 3, Supplementary Figure 4, Supplementary Figure 5, Supplementary Figure 6, and Supplementary Figure 7** for program setup).
    1. At 24 and 48 hpi, stain cell nuclei by adding 8 µL of a cell-permeant nuclear counterstain solution per well. Incubate for 30 min at 28 °C.

        NOTE: Infection can be monitored at multiple timepoints. However, measurements at 4 h post-infection provide the strongest signal (see **Supplementary Figure 8**) and allow antiviral effects to be assessed most reliably. Readouts at 2 h or intermediate timepoints are feasible, but extending incubation beyond 48 h increases the risk of cell overgrowth.

        NOTE: Select an appropriate cell confluency at the start of the experiment to ensure that cells do not become overgrown by the chosen time point for the readout. This will avoid the obstruction of an accurate cell count.
    2. After incubation (and in addition to the clear cover lid), add a clear view seal foil covering the top of the plate for safety.

        NOTE: When using an imaging device, it is essential to select the correct plate type. Illumination, integration time, and gain settings will vary depending on the reporter gene. It is highly recommended to perform preliminary measurements to determine the optimal parameters. Initial illumination, integration, and gain settings used to establish the protocol under the given conditions are provided in the **Supplementary Figure 2**, where the program setup is described in detail.
    3. Acquire whole-well images using image stitching (four fields per well at 4x magnification) using the multimode reader.
    4. Measure red fluorescence intensity using a Texas Red filter cube (Excitation: 586/15 nm; Emission: 647/57 nm).
    5. Determine the total cell count using the DAPI channel with the following settings (Excitation: 377/50 nm; Emission: 447/60 nm).
2. Quantitative image analysis.

    NOTE: For the fluorescence measurements, a microplate imaging reader was used. Detailed parameters used for this assay can be found in **Supplementary Figure 2**.
    1. Process the images using appropriate imaging software.
    2. Using the data reduction panel, select Image Stitching to DAPI and Texas Red channels to create a single image from the wells.
    3. Add Image Statistics and select Total intensity on the Texas Red Stitched channel. Apply Image Preprocessing to remove background noise from the DAPI Stitched channel.
    4. Run Cellular Analysis on the Preprocessed DAPI Stitched channel.
    5. Calculate the mean red fluorescence intensity per cell by subtracting the mean fluorescence of the uninfected, untreated control wells from each treated well, then dividing the result by the total cell count in the corresponding well.
3. Troubleshooting
    1. Monitor focus stability during the measurement, particularly for long imaging measurements or when using temperature-sensitive plates.
    2. Enable autofocus and increase autofocus frequency if focus drift is observed. Reduce acquisition speed or allow plates to equilibrate to the instrument's temperature before imaging if drift persists.
    3. Use imaging-grade plates to ensure consistent signal quality during acquisition. Prevent bleed-through and overexposure by avoiding excessive illumination and long integration times.
    4. Lower excitation intensity, shorten integration time, or reduce gain until signal saturation is avoided. Verify that fluorophore channels are well separated and adjust filter settings as needed.

        NOTE: Bleed-through between DAPI and mCherry is generally low but depends on the reporter construct used (e.g. GFP).
    5. Avoid over-confluency of cells to maintain proper infection kinetics and assay sensitivity. If over-confluency occurs, reduce incubation time before the measurement.

DOI 10.3791/69384

6. Monitor dye-related effects on cell viability and signal quality, particularly at high concentrations. Decrease dye concentration or shorten incubation times if dye-related toxicity or oversaturated background is observed.
7. Prepare and store dyes according to manufacturer recommendations to maintain signal stability.

Results

In this work, a detailed protocol for monitoring alphavirus replication and the evaluation of antiviral compounds (e.g., furin inhibitors) using fluorescence microscopy in a multi-well plate format is presented. To demonstrate the visualization of the inhibitory effects on viral replication, three previously synthesized furin inhibitors were selected for testing in aedine cell line U4.4: MI-1148, MI-1130, and MI-1131. An overview of the experimental workflow is illustrated in **Figure 1**.

Prior to assessing antiviral efficacy, it is essential to evaluate cytotoxicity to ensure that any reduction in viral replication is not due to cell death by the compound. Therefore, U4.4 cells were treated at 90% confluency with the inhibitors at 100, 50, 25, or 12.5 µM. Untreated cells and cells treated with water served as negative controls, while ionomycin was used as a positive control. The cell viability was assessed at 48 h post-treatment using a luminescent assay based on ATP quantification. For the furin inhibitors tested, no significant reduction in cell viability was observed (**Figure 2**).

Given the lack of cytotoxicity, the compounds were subsequently evaluated for antiviral activity. For this reason, U4.4 cells were infected with SFV-mCherry for 1 h, followed by treatment with the same furin inhibitors at the same concentrations. Infected, untreated cells and water-treated cells served as negative controls for antiviral activity, while uninfected, untreated cells were used to assess background fluorescence. At 48 h post-treatment, viral replication was quantified by fluorescence microscopy. Prior to imaging, 8 µL of a cell-permeant nuclear counterstain solution was added to each well and incubated for 30 min to stain cell nuclei. The red fluorescence signal corresponding to the expression of the viral reporter and the total number of nuclei were quantified from processed fluorescence images. Among the tested inhibitors, MI-1148 demonstrated potent antiviral activity, significantly reducing viral replication in a dose-dependent manner (**Figure 3**). In contrast, MI-1130 and MI-1131 showed no observable inhibition of viral replication at any of the tested concentrations. The raw data and analysis of the antiviral assay are provided in **Supplementary Table 1**.

The representative results demonstrate that the protocol reliably identifies compounds with antiviral activity, as shown by the strong reduction in reporter signal observed with MI1148. In contrast, the inhibitors MI1130 and MI1131 did not decrease reporter expression, confirming their lack of antiviral effect under these conditions (**Figure 4**). These findings highlight the assay's ability to distinguish active compounds from inactive ones and to support the identification of potent and relevant lead structures.

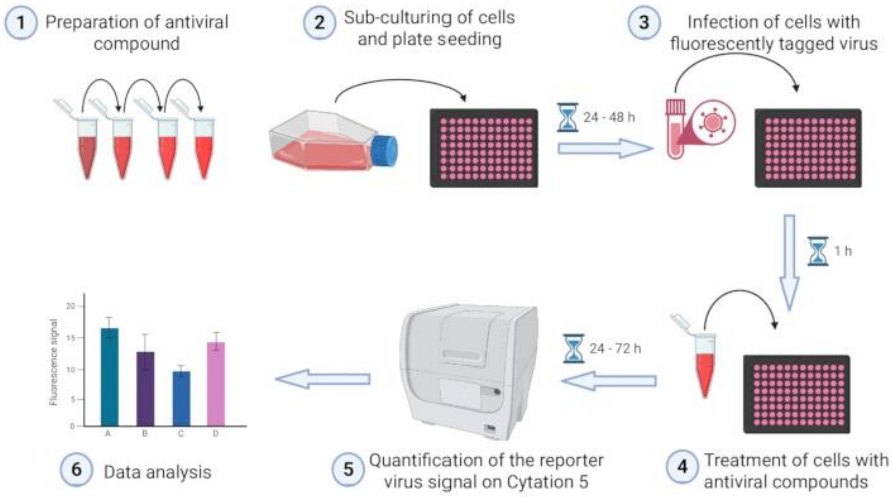

Figure 1: Experimental workflow. A schematic overview of the experimental procedure used to evaluate the antiviral activity of furin inhibitors in the aedine cell line U4.4. The workflow includes compound preparation, cell seeding, infection with mCherry-tagged Semliki Forest virus, compound treatment, fluorescence microscopy for real-time visualization, and quantification of viral replication. This illustration was created with BioRender.
Please click here to view a larger version of this figure.

DOI 10.3791/69384

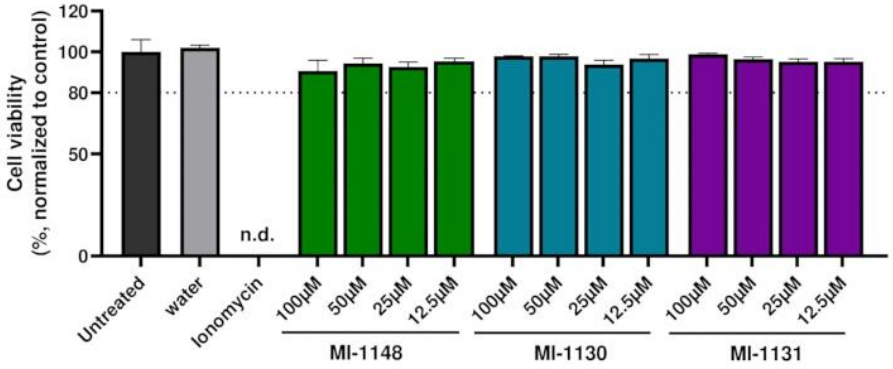

Figure 2: Cytotoxic effects of furin inhibitors in U4.4 cells. At approximately 90% confluency, U4.4 cells were treated with MI-1148, MI-1130, and MI-1131 at 100, 50, 25, and 12.5 µM. Untreated cells and cells treated with water served as negative controls, while ionomycin (100 µM) was used as a positive control. At 48 h post-treatment, the cell viability was assessed via ATP quantification. The data was normalized to the untreated control and expressed as percentage (%). The mean cell viability (n=3) is shown, and the error bars represent the coefficient of variation. The dotted line represents the cytotoxicity cut-off set at 80%. n.d. = not detectable. Please click here to view a larger version of this figure.

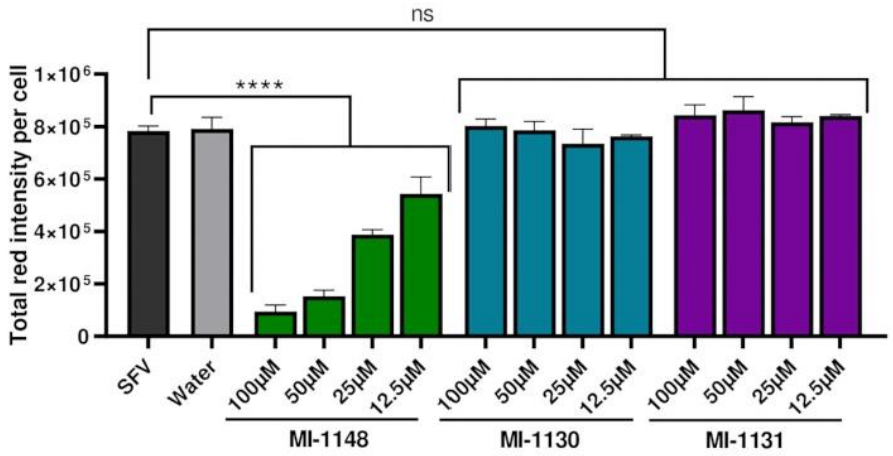

Figure 3: Antiviral activity of furin inhibitors against mCherry-tagged Semliki Forest virus (SFV) in the aedine cell line U4.4. At approximately 90% confluency, cells were infected with SFV-mCherry for 1 h, followed by treatment with MI-1148, MI-1130, and MI-1131 at 100, 50, 25, and 12.5 µM. At 48 h post-treatment, viral replication was quantified via fluorescence microscopy. Prior to imaging, 8 µL of a cell-permeant nuclear counterstain solution was added to each well and incubated for 30 min to stain cell nuclei. Fluorescence images were acquired using a Texas Red filter for viral signal and a DAPI filter for nuclei. Image analysis was performed to quantify total red fluorescence intensity (indicating viral replication) and the total number of cells per well. Data (n = 4) are presented as total red intensity per cell (total virus signal / total cell count). Error bars represent standard deviation. Statistical significance compared to SFV-infected control, using one-way ANOVA and Dunnett's multiple comparisons test: **** = P<0.0001; ns = P>0.05. Data representation and statistical analysis were performed with GraphPad Prism v9.5.1. Please click here to view a larger version of this figure.

DOI 10.3791/69384

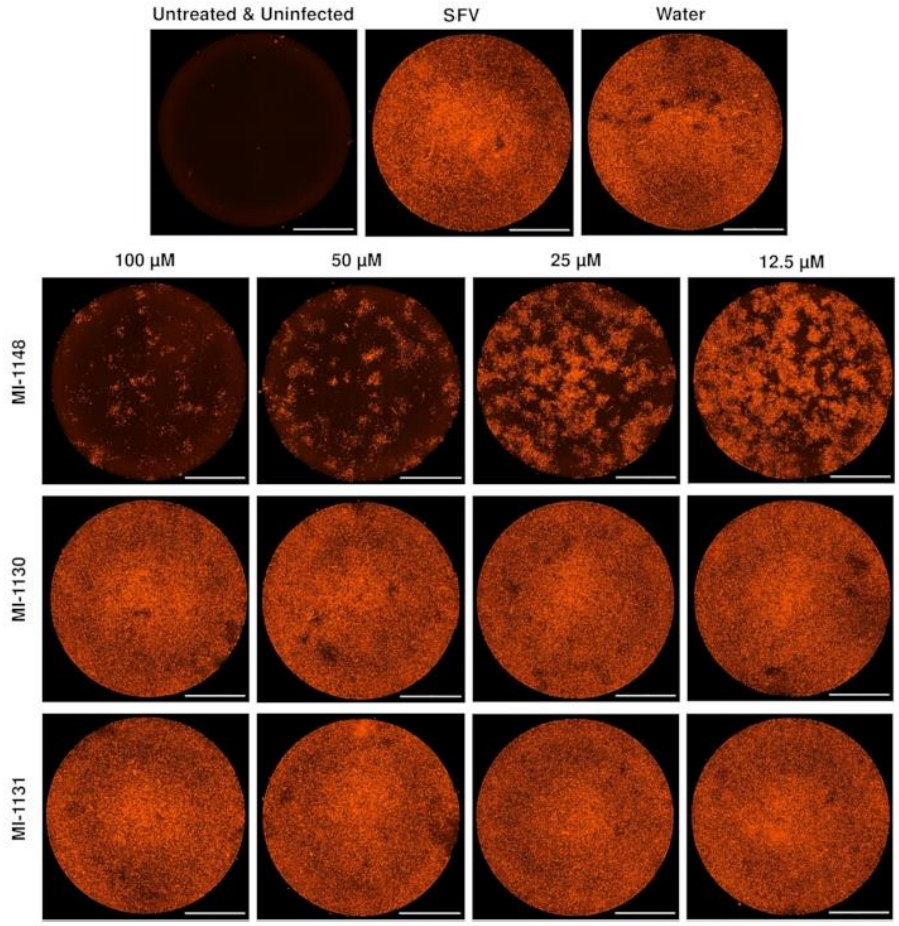

Figure 4: Representative fluorescence images showing the antiviral activity of furin inhibitors against mCherry-tagged Semliki Forest virus (SFV) in the aedine cell line U4.4. The cells at approximately 80% confluency were infected with SFV-mCherry for 1 h, followed by treatment with MI-1148, MI-1130, and MI-1131 at concentrations of 100, 50, 25, and 12. µM. Infected, untreated cells and water-treated cells served as negative controls, while uninfected, untreated cells were included as background controls. The reporter signal was assessed 48 h post-treatment by fluorescence microscopy using a Texas Red filter to capture the mCherry signal. Scale bar = 200 µm. Please click here to view a larger version of this figure.

Supplementary Table 1: Raw data of the total intensity of virus signal and the cell count. Please click here to download this File.

Supplementary Figure 1: Procedure steps used on the imaging reader for the representative results. First, a set on temperature (red) matching the rearing conditions of U4.4 cells. Then, there are three independent image action steps (orange) for measurements of DAPI, Texas Red, and Brightfield. Please click here to download this File.

Supplementary Figure 2: Image settings in the procedure steps used on the imaging reader for the representative results. The first settings to modify are: magnification (4x) and image size (Full WFOV). The fluorophore to be measured must be selected, and the Illumination, Integration time, and Gain parameters must be modified accordingly. Finally, the image montage (2x2) and overlap (30 µm x 30 µm) must be selected. Please click here to download this File.

Supplementary Figure 3: Data reduction steps used on the imaging reader for the representative results. The first step is Image stitching (blue) for DAPI and Texas Red channels. Second, Image Statistics (purple) gives the measurement for total intensity. Then, the image preprocessing step (green) is required to remove background noise from the DAPI channel. Finally, the Cellular Analysis (yellow) is performed on the preprocessed stitched image of DAPI. Please click here to download this File.

Supplementary Figure 4: Image stitching in the data reduction steps used on the imaging reader for the representative results. The most relevant setting is the downsizing of the final image (80%), because if it is lower, it affects the resolution of the image and therefore, the final measurement of the parameters. Please click here to download this File.

Supplementary Figure 5: Image statistics in the data reduction steps used on the imaging reader for the representative results. It is important to select the correct channel (Stitched: Fluorophore),

choose a minimum threshold (2500), and finally, the parameter to be measured (Total Intensity). For a more accurate measurement, an Image Plug can be made. Please click here to download this File.

Supplementary Figure 6: Image preprocessing in the data reduction steps used on the imaging reader for the representative results. The most relevant setting is the rolling ball parameter (30 µm), giving priority to fine results. Please click here to download this File.

Supplementary Figure 7: Cellular Analysis in the data reduction steps used on the imaging reader for the representative results. It is important to choose the channel that has the Image Preprocessed. Choose to divide the touching objects and fill holes with masks. It is critical to choose the correct range of object selection (5-50 µm). Finally, for refined results, an Image Plug can be made. Please click here to download this File.

Supplementary Figure 8: Antiviral activity of furin inhibitors against mCherry-tagged Semliki Forest virus (SFV) in the aedine cell line U4.4. At approximately 90% confluency, cells were infected with SFV-mCherry for 1 h, followed by treatment with MI-1148, MI-1130, and MI-1131 at 100, 50, 25, and 12.5 µM. At 24 h (red bars) and 48 h (green bars) post-treatment, viral replication was quantified via fluorescence microscopy. Error bars represent standard deviation (n = 4). Please click here to download this File.

Discussion

The capacity to observe alphavirus replication in real time offers a sequential and cumulative perspective on conventional endpoint tests. This multi-time live cell imaging protocol is a useful model for studying alphaviruses, as it provides a dynamic platform for observing viral spread.

The success of this protocol relies on several parameters. First, it is important to assess the cytotoxicity of the compounds before an antiviral assay to rule out false-positive results due to cell death. Once the evaluation for cytotoxic effects has been carried out, the antiviral activity of the compounds can be subsequently evaluated. For the test compounds, no cytotoxicity was observed. MI-1130 and MI-1131 showed no significant impact on viral replication, whereas MI-1148, used as a positive control, effectively suppressed it. Additionally, the timing of infection in relation to cell seeding is crucial. Cells must reach adequate confluency to ensure a reproducible infection without overgrowth. It is also important to optimize the multiplicity of infection depending on the cell line to observe a gradual infection without compromising the cell viability. Finally, the frequency of image acquisition must be carefully determined to allow visualization of gradual replication without large jumps. For most applications, acquiring images every eight hours, for example, provides an effective balance between temporal detail and sample integrity.

The main strength of this protocol is its adaptability. In this experiment, we used SFV-mCherry and U4.4 cells to demonstrate the real-time monitoring of viral replication and inhibition after treatment with furin inhibitors. However, the protocol can be optimized for the fluorescent analysis of alternative viruses with different reporter markers, such as GFP, as well as other host cell types, including primary cells and differentiated cell lines. Although the protocol focuses on compound treatment after infection, the workflow can also be readily adapted for time-of-addition experiments, including pre-treatment, co-treatment, immediate post-infection treatment, or delayed treatment, to further explore the mechanism of antiviral action. The protocol was initially used to compare the functionality of the RNAi machinery of C6/36 and U4.4 cells[14]. It has been further extended to examine how dsRNA directly targeting the virus inhibits its replication[15].

There are potential challenges that can be encountered while using this protocol. Reporter viruses, although very useful for numerous applications *in vivo*[29] and *in vitro*[30], can also show lower virulence[31] and the genetic instability of the reporter genes[32]. Cell detachment caused by over-confluency can obstruct clear visualization and imaging, thus affecting the cell count. Prolonged exposure to live-cell dyes (e.g., Hoechst 33342 for nuclei) may alter cell behavior or viability[15]. Furthermore, experiments involving highly pathogenic alphaviruses, such as CHIKV, may require higher biosafety measures and corresponding protocol adaptations. Additionally, focus drift can be observed in some cases due to the variability of the plates as well as the use of different plates. For example, fluorescence signals in transparent cell culture plates can bleed from wells into their adjacent wells, and white plates can cause overexposure. In both cases, the accuracy of the measurement of the fluorescent signal will be affected.

This protocol offers several advantages over conventional virological assays. For example, plaque assays and $TCID_{50}$ assays provide endpoint data on virus titers[12]. More so, qPCR offers sensitive detection of viral RNA, but it cannot distinguish between replication-competent viruses and non-infectious viral particles or residual nucleic acids. In contrast, this kind of fluorescence live imaging enables continuous, non-invasive assessment of viral progression, spread, and treatment effects within the same population of cells over time.

Beyond the examination of furin inhibitors as antiviral compounds, our protocol can be adapted for other applications. It is particularly well-suited for antiviral drug screening, enabling the quantification of dose-dependent responses to small molecules. It provides a platform for studying host-pathogen interactions, including the timing and localization of viral entry, replication, and spread. It can be used for the comparison between reporter viruses, different strains, or different alphaviruses. Additionally, it can be coupled with approaches such as gene knockdown using siRNA or dsRNA. Thus, this system can help identify and validate critical

targets and antiviral compounds for viral replication. However, this fluorescence-based assay represents an initial screening approach rather than a standalone confirmatory method; further investigations, including assays with wild-type viruses, will be necessary to substantiate the screening results.

Disclosures

The authors have no conflict of interest.

Acknowledgments

We thank Prof. Dr. Andres Merits, University of Tartu, Estonia, and Prof. Dr. Andreas Pichlmair, Technical University of Munich, Germany, for providing pCMV-SFV6-2SG-mCherry. We thank Prof. Dr. Stefanie Becker, University of Veterinary Medicine, Hannover, Germany, for the C6/36 cells. We thank Prof. Dr. Torsten Steinmetzer, University of Marburg, Marburg, Germany, for providing the furin inhibitors. This work was supported by the Landes-Offensive zur Entwicklung Wissenschaftlich-ökonomischer Exzellenz Program of the Hessian Ministry of Higher Education, Research, and the Arts through the LOEWE Centre for Translational Biodiversity Genomics (LOEWE-TBG) with funding code: LOEWE/1/10/519/03/03.001(0014)/52, and by the BMBF (Project ASCRIBE-Grant Number 01KI2024).

References

1. Powers, A.M. *Togaviruses: Alphaviruses*. eLS, (2014).
2. Shaw, A.R., Feinberg, M.B. Vaccines. *Clinical Immunology*. Elsevier (2008).
3. Gould, E.A. et al. Understanding the alphaviruses: recent research on important emerging pathogens and progress towards their control. *Antiviral Research*. **87** (2), 111-124 (2010).
4. Lim, E.X.Y., Lee, W.S., Madzokere, E.T., Herrero, L.J. Mosquitoes as suitable vectors for alphaviruses. *Viruses*. **10** (2) (2018).
5. Caluwé, L. de, Ariën, K.K., Bartholomeeusen, K. Host factors and pathways involved in the entry of mosquito-borne alphaviruses. *Trends in Microbiology*. **29** (7), 634-647 (2021).
6. Adizie, T., Adebajo, A.O. Travel- and immigration-related problems in rheumatology. *Best practice & research. Clinical Rheumatology*. **28** (6), 973-985 (2014).
7. ECDC Chikungunya virus disease worldwide overview: Situation update, June 2025, accessed 9 July (2025).
8. Paixão, E.S. et al. Chikungunya chronic disease: a systematic review and meta-analysis. *Transactions of the Royal Society of Tropical Medicine and Hygiene*. **112** (7), 301-316 (2018).
9. Atkins, G.J., Sheahan, B.J., Liljeström, P. The molecular pathogenesis of Semliki Forest virus: a model virus made useful? *The Journal of General Virology*. **80** (Pt 9), 2287-2297 (1999).
10. Contu, L., Balistreri, G., Domanski, M., Uldry, A.-C., Mühlemann, O. Characterisation of the Semliki Forest Virus-host cell interactome reveals the viral capsid protein as an inhibitor of nonsense-mediated mRNA decay. *PLoS Pathogens*. **17** (5) (2021).
11. Teppor, M. et al. Semliki Forest virus chimeras with functional replicase modules from related alphaviruses survive by adaptive mutations in functionally Important Hot Spots. *Journal of Virology*. **95** (20) (2021).
12. Smither, S.J. et al. Comparison of the plaque assay and 50% tissue culture infectious dose assay as methods for measuring filovirus infectivity. *Journal of Virological Methods*. **193** (2), 565-571 (2013).
13. Shan, L., Yang, D., Wang, D., Tian, P. Comparison of cell-based and PCR-based assays as methods for measuring infectivity of Tulane virus. *Journal of Virological Methods*. **231**, 1-7 (2016).
14. Omokungbe, B. et al. Gene silencing in the aedine cell lines C6/36 and U4.4 using long double-stranded RNA. *Parasites & Vectors*. **17** (1), 255 (2024).
15. Centurión, A., Omokungbe, B., Stiehler, S., Vilcinskas, A., Hardes, K. Inhibition of Semliki Forest virus replication with long double-stranded RNA in Aedes albopictus cells. *Virus Research*. **357** 199584 (2025).
16. Weger-Lucarelli, J. et al. Adventitious viruses persistently infect three commonly used mosquito cell lines. *Virology*. **521**, 175-180 (2018).
17. Attarzadeh-Yazdi, G. et al. Cell-to-cell spread of the RNA interference response suppresses Semliki Forest virus (SFV) infection of mosquito cell cultures and cannot be antagonized by SFV. *Journal of Virology*. **83** (11), 5735-5748 (2009).
18. Gahmberg, C.G., Simons, K. Isolation of plasma membrane fragments from BHK21 cells. *Acta pathologica et microbiologica Scandinavica. Section B: Microbiology and immunology*. **78** (2), 176-182 (1970).
19. Thomas, G. Furin at the cutting edge: from protein traffic to embryogenesis and disease. *Nature reviews. Molecular Cell Biology*. **3** (10), 753-766 (2002).
20. Garten, W. Characterization of proprotein convertases and their involvement in virus propagation. *Activation of Viruses by Host Proteases.*, Springer, Cham 205-248 (2018).
21. Becker, G.L., Hardes, K., Steinmetzer, T. New substrate analogue furin inhibitors derived from 4-amidinobenzylamide. *Bioorganic & Medicinal Chemistry Letters*. **21** (16), 4695-4697 (2011).
22. Hardes, K. et al. Novel furin inhibitors with potent anti-infectious activity. *ChemMedChem*. **10** (7), 1218-1231 (2015).
23. Hardes, K. et al. Elongated and shortened peptidomimetic inhibitors of the proprotein convertase furin. *ChemMedChem*. **12** (8), 613-620 (2017).
24. Pennemann, F.L. et al. Cross-species analysis of viral nucleic acid interacting proteins identifies TAOKs as innate immune regulators. *Nature Communications*. **12** (1) 7009 (2021).
25. Andersen, L.L. et al. Systematic P2Y receptor survey identifies P2Y11 as modulator of immune responses and virus replication in macrophages. *The EMBO Journal*. **42** (23) (2023).
26. Huang, Y., Urban, C., Hubel, P., Stukalov, A., Pichlmair, A. Protein turnover regulation is critical for influenza A virus infection. *Cell Systems*. **15** (10), 911-929 (2024).
27. Hardes, K. Synthese, Charakterisierung und Anwendung neuer Inhibitoren der Proproteinkonvertase Furin. *Doctoral Dissertation.*, Philipps-Universität Marburg (2014).
28. Reed, L.J., Muench, H. A simple method of estimating fifty percent endpoints. *American Journal of Epidemiology*. **27** (3), 493-497 (1938).
29. Manicassamy, B. et al. Analysis of in vivo dynamics of influenza virus infection in mice using a GFP reporter virus. *Proceedings of the*

DOI 10.3791/69384

National Academy of Sciences of the United States of America. **107** (25), 11531-11536 (2010).
30. Yang, P. et al. Imaging of viral replication in live cells by using split fluorescent protein-tagged reporter flaviviruses. *Virology*. **603**, 110374 (2025).
31. Jose, J., Taylor, A.B., Kuhn, R.J. Spatial and temporal analysis of alphavirus replication and assembly in mammalian and mosquito cells. *mBio*. **8** (1) (2017).
32. Eckert, N. et al. Influenza A virus encoding secreted Gaussia luciferase as useful tool to analyze viral replication and its inhibition by antiviral compounds and cellular proteins. *PloS One*. **9** (5) (2014).

jove

Materials List for

Quantitative Fluorescence Imaging of Alphavirus Infection for Antiviral Screenings

Alejandra Centurión[*1,2], **Bodunrin Omokungbe**[*1,2], **Cross Chambers**[2], **Sabrina Stiehler**[3], **Andreas Vilcinskas**[1,2,3], **Kornelia Hardes**[1,2,4]

[1]LOEWE Centre for Translational Biodiversity Genomics (LOEWE-TBG) [2]Department of Pest and Vector Insect Control, Fraunhofer Institute for Molecular Biology and Applied Ecology IME, Branch of Bioresources [3]Institute for Insect Biotechnology, Justus-Liebig University [4]BMBF Junior Research Group in Infection Research "ASCRIBE", Fraunhofer Institute for Molecular Biology and Applied Ecology IME, Branch of Bioresources

[*]These authors contributed equally

Corresponding Author

Kornelia Hardes

kornelia.hardes@ime.fraunhofer.de

Citation

Centurión, A., Omokungbe, B., Chambers, C., Stiehler, S., Vilcinskas, A., Hardes, K. Quantitative Fluorescence Imaging of Alphavirus Infection for Antiviral Screenings. *J. Vis. Exp.* (), e69384, doi:10.3791/69384 (2026).

Date Published

February 18, 2026

DOI

10.3791/69384

URL

jove.com/video/69384

Materials

Name	Company	Catalog Number	Comments
Albumin Bovine Fraction V, pH 7.0	SERVA Electrophoresis	11930.03	
BenchStable DMEM	Thermo Fisher Scientific	A4192101	
BHK-21 cells	CLS Cell Lines Service GmbH, Eppelheim, Germany	603126	
CELL CULTURE FLASK, 50 ML, 25 cm^2, PS, Red filter screw cap, Clear, CELLSTAR, TC, sterile	Greiner Bio-One	690175	
Cell culture microplate, 24 wells, PS, F-bottom, (Chimney well),Clear, CELLSTAR, TC, Lid with condensation rings, sterile	Greiner Bio-One	662160	
Cell culture microplate, 96 wells, PS, F-bottom, (Chimney well), µCLEAR, Black, CELLSTAR, TC, Lid with condensation rings, sterile	Greiner Bio-One	655090	
Cell culture microplate, 96 wells, PS, F-bottom, (Chimney well),Clear, CELLSTAR, TC, Lid with condensation rings, sterile	Greiner Bio-One	655180	
Cell culture microplate, 96 wells, PS, V-bottom, Clear	Greiner Bio-One	651101	
Cell scraper	VWR	734-2602	
CellTiter-Glo Luminescent Cell Viability Assay	Promega	G7573	
Cytation 5 Cell Imaging Multimode Reader	Biotek		
DAPI filter cube 1225100	Biotek		ex: 377/50 nm; em 447/60 nm
Dulbecco's Modified Eagle's Medium (DMEM GlutaMAX)	Thermo Fisher Scientific	A4192102	
Fetal Bovine Serum	Fisher Scientific	11550356	

Furin inhibitor MI-1130			This study
Furin inhibitor MI-1131			This study
Furin inhibitor MI-1148			Hardes et al. 2015. https://doi.org/10.1002/cmdc.201500103
Gen5 Prime Software	Biotek		
Ionomycin Calcium Salt, 99%	Thermo Fisher Scientific	J60628	
Leibovitz's L-15 Medium, GlutaMAX Supplement	Thermo Fisher Scientific	31415029	
Lipofectamine 3000 Transfections reagent	Thermo Fisher Scientific	L3000001	
MEM non-essential amino acids (100x)	Thermo Fisher Scientific	11140050	
Microplate, PS, 96 well, F-bottom, (Chimney well), Black, Fluotrac, Med.biding	Greiner Bio-One	655076	
NucBlue Live ReadyProbes Reagent (Hoechst 33342)	Thermo Fisher Scientific	R37605	
Opti-MEM	Thermo Fisher Scientific	31985062	
Penicillin-Streptomycin (10, 000 U/mL)	Thermo Fisher Scientific	15140122	
SFV6–2SG-mCherry			Prof. Dr. Andres Merits (University of Tartu, Estonia) and Prof. Dr. Andreas Pichlmair (Technical University of Munich, Germany)
Texas Red filter cube 1225102	Biotek		ex: 586/15 nm; em: 647/57 nm
Tryptose Phosphate Broth	Thermo Fisher Scientific	18050039	
U4.4 cells			Friedrich-Loeffler-Institute, Federal Research Institute for Animal Health, Greifswald, Germany
Viewseal Sealer, Clear	Greiner Bio-One	676070	

Quantitative Fluorescence Imaging of Alphavirus Infection for Antiviral Screenings

AUTHORS AND AFFILIATIONS:

Alejandra Centurión[1,2*], Bodunrin Omokungbe[1,2*], Cross Chambers[2], Sabrina Stiehler[3], Andreas Vilcinskas[1,2,3], Kornelia Hardes[1,2,4]

[1]LOEWE Centre for Translational Biodiversity Genomics (LOEWE-TBG), Frankfurt am Main, Germany

[2]Department of Pest and Vector Insect Control, Fraunhofer Institute for Molecular Biology and Applied Ecology IME, Branch of Bioresources, Germany

[3]Institute for Insect Biotechnology, Justus-Liebig University, Germany

[4]BMBF Junior Research Group in Infection Research „ASCRIBE", Fraunhofer Institute for Molecular Biology and Applied Ecology IME, Branch of Bioresources, Germany

Corresponding author:

Kornelia Hardes (Kornelia.Hardes@ime.fraunhofer.de)

*These authors contributed equally

Alejandra Centurión (Alejandra.Centurion@ime.fraunhofer.de)

Bodunrin Omokungbe (Bodunrin.Omokungbe@ime.fraunhofer.de)

Cross Chambers (Cross.Chambers2@ime.fraunhofer.de)

Sabrina Stiehler (Sabrina.Stiehler@agrar.uni-giessen.de)

Andreas Vilcinskas (Andreas.Vilcinskas@ime.fraunhofer.de)

Supplementary Table 1: Raw data of the total red intensity of the viral reporter and the cell count.

	Total intensity (viral signal)					
Treatment	**Rep1**	**Rep2**	**Rep3**	**Rep4**	**Mean**	**Mean minus background**
Untreated & uninfected (background)	44817704530	49207837324	45403643909	45514016236	46235800500	0
water	101020668158	105232278967	106336395040	105122009739	104427837976	58192037476
SFV	100931732965	105589351655	103296327293	105422853437	103810066338	57574265838
MI-1148_100µM	54813553456	51347196523	51237167787	53436119262	52708509257	6472708757
MI-1148_50µM	58736197649	54632760084	57161904081	55256463671	56446831371	10211030872
MI-1148_25µM	74962016010	73198410029	73272275762	74213197468	73911474817	27675674318
MI-1148_12.5µM	90387400153	81945393151	81146407926	85981658949	84865215045	38629414545
MI-1130_100µM	103722904437	103428710648	105489401677	105801486878	104610625910	58374825410
MI-1130_50µM	107296154721	104533142828	103308938567	102164565775	104325700473	58089899973
MI-1130_25µM	104797795553	97914222293	93904668483	101463390798	99520019282	53284218782
MI-1130_12.5µM	101406487848	100536437313	101832163098	98711768195	100621714114	54385913614
MI-1131_100µM	106839772420	102438790994	106669796117	107218533952	105791723371	59555922871
MI-1131_50µM	105362759576	103591335468	104633023152	107191641402	105194689900	58958889400
MI-1131_25µM	103198043689	102235630886	100564228523	102561373872	102139819243	55904018743
MI-1131_12.5µM	105490320078	103844850546	104774046631	104128368490	104559396436	58323595937
	Cell count					
Treatment	**Rep1**	**Rep2**	**Rep3**	**Rep4**		
Untreated & uninfected (background)	66754	74900	64854	72528		
water	73852	75280	70875	74484		
SFV	72335	74767	71543	75572		
MI-1148_100µM	68031	67322	68586	69935		
MI-1148_50µM	71381	67641	65507	62629		
MI-1148_25µM	69456	70855	73218	71900		
MI-1148_12.5µM	72325	73777	70492	67819		
MI-1130_100µM	74869	71940	72742	71716		
MI-1130_50µM	74659	77571	74896	69033		
MI-1130_25µM	73231	70515	71670	74407		
MI-1130_12.5µM	72475	70904	72411	69271		
MI-1131_100µM	72108	70767	71423	68406		
MI-1131_50µM	71079	70085	67695	65165		
MI-1131_25µM	68680	66873	68803	69723		
MI-1131_12.5µM	71055	68863	69245	68531		

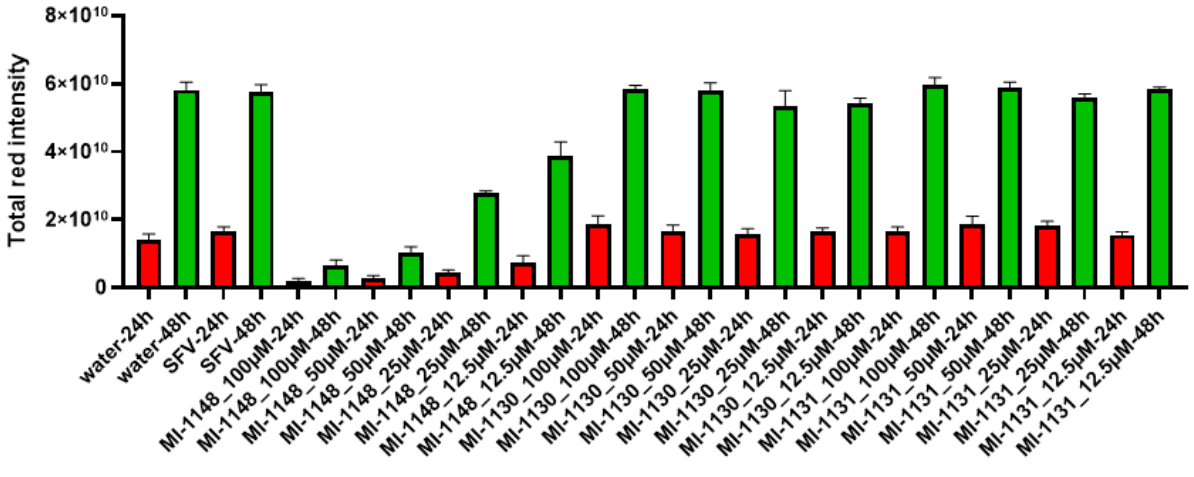

Supplementary Figure 1: Antiviral activity of furin inhibitors against mCherry-tagged Semliki Forest virus (SFV) in the aedine cell line U4.4. At approximately 90% confluency, cells were infected with SFV-mCherry for 1 h, followed by treatment with MI-1148, MI-1130, and MI-1131 at 100, 50, 25, and 12.5 µM. At 24 h (red bars) and 48 h (green bars) post-treatment, viral reporter gene expression was quantified via fluorescence microscopy. Error bars represent standard deviation.(n = 4).

Chapter IV

Inhibition of Semliki Forest virus replication with long double-stranded RNA in *Aedes albopictus* cells

Virus Research. 2025 May 357(2):199584. doi: 10.1016/j.virusres.2025.199584. PMCID: PMC12152901 PMID: 40389163

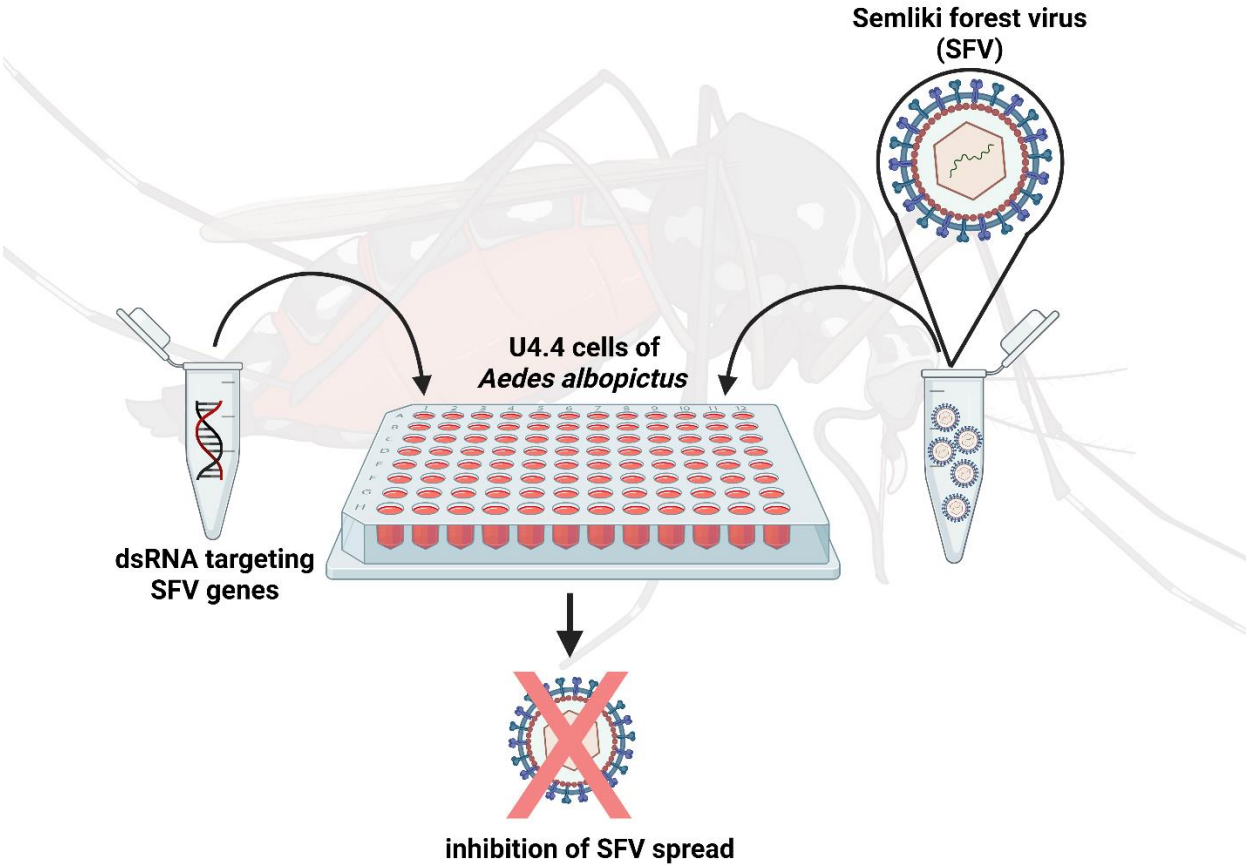

Virus Research 357 (2025) 199584

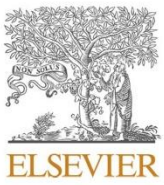

Contents lists available at ScienceDirect

Virus Research

journal homepage: www.elsevier.com/locate/virusres

Inhibition of Semliki Forest virus replication with long double-stranded RNA in *Aedes albopictus* cells

Alejandra Centurión [a,b], Bodunrin Omokungbe [a,c], Sabrina Stiehler [c], Andreas Vilcinskas [a,b,c], Kornelia Hardes [a,b,d,*]

[a] Centre for Translational Biodiversity Genomics (LOEWE TBG), Senckenberganlage 25, 60325 Frankfurt am Main, Germany
[b] Fraunhofer Institute for Molecular Biology and Applied Ecology IME, Branch of Bioresources, Ohlebergsweg 12, 35392 Giessen, Germany
[c] Institute for Insect Biotechnology, Justus-Liebig University, Heinrich-Buff-Ring 26-32, 35392 Giessen, Germany
[d] BMBF Junior Research Group in Infection Research "ASCRIBE", Ohlebergsweg 12, 35392, Giessen, Germany

ARTICLE INFO

Keywords:
RNA interference
Arbovirus
Alphavirus
U4.4
Cell culture
Mosquito
dsRNA

ABSTRACT

Arthropod-borne viruses represent an increasing threat to the global health system, requiring the development of novel and sustainable control strategies to reduce the risk of arboviral infections. RNA interference (RNAi) offers a potential approach to directly prevent viral replication within vectors due to its specificity in gene silencing. In this study, we evaluated the efficacy of long double-stranded RNAs (dsRNAs) targeting six regions of the Semliki Forest virus (SFV) genome in *Aedes albopictus* U4.4 cells. The antiviral efficiency of dsRNA alone is low, therefore we evaluated its use after complexing with the K4 Transfection System (K4). A cytotoxicity assay based on ATP quantification showed that both uncomplexed and complexed dsRNA had no cytotoxic effects on U4.4 cells at a concentration up to 2 ng/µL. Complexed dsRNA achieved higher antiviral efficacy, significantly reducing viral replication compared to uncomplexed dsRNA. We found that complexed dsRNA retained its antiviral activity when challenged with SFV up to 72 h post-transfection. Among our synthesized dsRNA constructs, nsP4-dsRNA in complex with K4 led to an 80 % reduction in viral replication at 72 h post-infection at 0.5 ng/µL. Using RT-qPCR, we confirmed a significant 32.2 % reduction of nsP4 mRNA after transfection of complexed nsP4-dsRNA. Dose response assays showed that complexed dsRNAs with a concentration of 0.5 ng/µL are effective for viral reduction. Our results highlight the importance of efficient dsRNA delivery and selection of critical viral targets, such as nsP4, for successful RNAi-mediated viral suppression. This work elucidates the potential of dsRNAs to target Semliki Forest virus replication, highlighting viral gene targeting as a viable strategy for RNAi-based suppression of arboviral replication.

1. Introduction

Arthropod-borne viruses (arboviruses) transmitted by mosquitoes are the cause of various mosquito borne diseases (MBDs) in humans, such as Dengue, Chikungunya, and Zika virus (Dahmana and Mediannikov, 2020; Kolimenakis et al., 2021). Dengue virus alone is estimated to infect almost 400 million people each year (Bhatt et al., 2013). Specific treatment and vaccines for these viral diseases are often limited or unavailable. One of the key vectors of these pathogens is the Asian tiger mosquito, *Aedes albopictus*, which is capable of transmitting at least 26 arboviruses (Paupy et al., 2009). Currently, efforts to control the spread of MBDs are mainly focused on vector control, however some methods have significant side effects on non-target organisms (Allgeier et al., 2019), or can lead to the development of resistances in mosquito populations (Moyes et al., 2017; Şengül Demirak and Canpolat, 2022).

A promising strategy for arbovirus control is the use of RNA interference (RNAi). RNAi is a gene regulatory mechanism in most eukaryotes (Agrawal et al., 2003; Kim and Rossi, 2008), and a naturally occurring immune response in insects against viral infections (Christiaens et al., 2020; Gammon and Mello, 2015). This mechanism leads to the silencing of gene transcription when foreign double-stranded RNA (dsRNA) is recognized in the cell cytoplasm. Since its discovery in *Caenorhabditis elegans* in 1998 (Fire et al., 1998), RNAi has been intensively researched due to its specificity and potential use to

* Corresponding author at: Fraunhofer Institute for Molecular Biology and Applied Ecology IME, Branch of Bioresources, Ohlebergsweg 12, 35392 Giessen, Germany.
E-mail address: kornelia.hardes@ime.fraunhofer.de (K. Hardes).

https://doi.org/10.1016/j.virusres.2025.199584
Received 1 April 2025; Received in revised form 7 May 2025; Accepted 9 May 2025
Available online 17 May 2025

study gene expression and therapeutic treatments (Kim and Rossi, 2008). Due to its ability to knock down essential genes, RNAi is used to study gene function and phenotypical changes in insects, as well as being used as a tool in pest control (Christiaens et al., 2020). There are three RNAi pathways leading to the silencing of genes in insects: the micro-RNAs (mi)RNA, the small interfering RNAs (exo-siRNA and endo-siRNA), and the Piwi-interacting RNAs (piRNA) pathway (Liu et al., 2019; Lucas et al., 2013; Vogel et al., 2018).

The exo-siRNA pathway is the main immune response triggered by the detection of exogenous dsRNA in the cytoplasm which is then processed by the enzyme Dicer2 (Dcr2) into siRNAs. These siRNAs are incorporated into the RNA-induced silencing complex (RISC). RISC, particularly the Argonaoute2 protein, then binds to complementary RNA sequences, leading to their degradation and thereby preventing the virus from replicating (Gammon and Mello, 2015; Schuster et al., 2019). Previously, the effectiveness of using exogenous siRNAs and dsRNAs to inhibit arbovirus replication in mosquito cells has been demonstrated (Caplen et al., 2002; Wu et al., 2019). Among the mosquito cell lines, the *Ae. albopictus* C6/36 larval cell line is one of the most commonly used, due to its capacity to generate high viral titers when infected (Igarashi, 1978). However, C6/36 cells exhibits a deficiency in their antiviral RNAi response, having a defective function of Dcr2 when cleaving long dsRNA, allowing a fast replication of the virus (Brackney et al., 2010; Scott et al., 2010). In contrast, cell lines such as *Ae. albopictus* U4.4 and the *Ae. aegypti* Aag2 cells, do not exhibit this deficiency (Omokungbe et al., 2024; Scott et al., 2010; Siu et al., 2011).

Semliki Forest virus (SFV) was first identified in Uganda in 1942 (Smithburn and Haddow, 1944). A first isolate (SFV L10) was designated as neurovirulent for mice (Atkins et al., 1999), causing lethal encephalitis and leading to the death of the animal (Tuittila et al., 2000). Since then, there have been multiple isolates and engineered vectors to study viral expression (Berglund et al., 1993; Fragkoudis et al., 2008; Qian et al., 2020), infection responses (Agboli et al., 2023; Deuber and Pavlovic, 2007; Glasgow et al., 1997), and gene therapy (Quetglas et al., 2012; Roche et al., 2010). For example, the isolate SFV6 generates high viremia and is neuroinvasive (Ferguson et al., 2015). In humans, SFV causes mild symptoms (Mathiot et al., 1990). However, a single fatal case of human encephalitis has been observed after a laboratory infection (Willems et al., 1979). SFV encodes for four non-structural proteins (nsP1, nsP2, nsP3, nsP4), which are responsible for the synthesis of viral RNA, and structural proteins like the capsid (C protein) and the envelope proteins (E1, E2, E3) (Atkins et al., 1999; Saul et al., 2015; Strauss and Strauss, 1994). Due to its wide host range and the high titer that can be produced (Atkins, 2013; Strauss and Strauss, 1994), combined with its similarity to other alphaviruses, SFV makes it the perfect model virus for arbovirus infection studies.

Our primary research goal is to synthesize and formulate dsRNA with the ability to inhibit arbovirus replication in adult mosquitoes, as well as to aid in the identification of suitable regions with high viral suppression. The potential use of RNAi as a preventive method for the spread of arboviruses within the host vector has been little explored. Mainly, due to RNAi been hampered by several challenges, most notably inefficient delivery, uptake, and degradation by dsRNases. We have previously found that uncomplexed dsRNA is inefficient at inhibiting SFV replication in U4.4 cells (Omokungbe et al., 2024). Therefore, using our already established protocols, we used RNAi to target different regions of the SFV genome in *Ae. albopictus* U4.4 cells as a proof-of-concept that formulated, exogenous dsRNA can be used to inhibit virus replication. The results of this proof-of-concept study are outlined in this paper and are the foundation for the transfer of the data to adult females in future research projects.

2. Material and methods

2.1. Cell culture

The *Ae. albopictus* cell line U4.4 (Friedrich-Loeffler-Institute, Federal Research Institute for Animal Health) was sub-cultured at 28 °C in insect growth medium (Leibovitz L-15 medium GlutaMAX) supplemented with 1 % tryptose phosphate broth, 10 % fetal calf serum (FCS), 1 % MEM non-essential amino acids, and 1 % penicillin/streptomycin.

Baby hamster kidney (BHK-21) cells (CLS Cell Lines Service) were maintained in Dulbecco's modified Eagle's medium (DMEM GlutaMAX) supplemented with 10 % FCS and 1 % penicillin/streptomycin at 37 °C in a 5 % CO_2 atmosphere. All media and supplements were purchased from Thermo Fisher Scientific.

2.2. Virus

For the infection assays the mCherry tagged SFV (SFV6–2SG-mCherry) was used (kindly provided by Prof. Dr. Andres Merits and Prof. Dr. Andreas Pichlmair). First, BHK-21 cells at 90 % confluency were transfected with the SFV6–2SG-mCherry plasmid in infection medium (DMEM GlutaMAX supplemented with 1 % penicillin/streptomycin and 0.2 % bovine serum albumin [Serva Electrophoresis]) using Lipofectamine 3000 (Thermo Fisher Scientific) according to the manufacturer's instructions. At 48 h post-transfection (hpt), the virus containing supernatant was collected, aliquoted, and stored at −80 °C prior to the infection of BHK-21 to produce the virus stocks used for the following experiments. Titers were determined using a $TCID_{50}$ assay in BHK-21 cells. Briefly, tenfold serial dilutions of each sample were inoculated with the cells in 96 well-format (Greiner Bio-One), which were incubated for 1 h. Then, media was removed and replenished with fresh infection media. Cells were incubated for 48 h at 37 °C in a 5 % CO_2 atmosphere before virus replication was quantified by fluorescence measurements and detection of cell viability using the Gen5 software in Cytation 5 (Biotek).

2.3. Sequence alignments, design, and synthesis of dsRNA

Complete genomes of Semliki Forest virus sourced from the National Center for Biotechnology Information (NCBI) (Table S1) were compared by aligning their full sequences. Semliki Forest virus 6 (KT009012.1) was used as reference for all comparisons (Table S2). Sequences from the non-annotated regions from Semliki Forest virus Viet Nam (EU350586.1), Semliki Forest Me Tri 5–71 (MH880789.1), and Semliki Forest Tanzania53 (MK280688.1) were manually annotated by comparison with the available annotated genomes (Supplementary information S1). The sequence alignments were carried out using Geneious v.10.2.6 with global alignment with free end gaps and a 65 % cost matrix.

The dsRNAs used in this study were designed by generating gene-specific primers from the SFV6–2SG-mCherry genome using NCBI Primer-BLAST. Primers were designed to cover 400 to 500 bp of the target regions (Table S3). A T7 promoter sequence was incorporated to the 5′ end of each primer to enable *in vitro* transcription. We have previously described the synthesis of dsRNA (Omokungbe et al., 2024). Briefly, a glycerol stock of the *Escherichia coli* carrying vector pCMV-SFV6–2SG-mCherry was inoculated in lysogeny broth (LB) containing kanamycin and incubated overnight. The plasmid DNA was isolated using the NucleoSpin Plasmid DNA kit (Macherey–Nagel) according to the manufacturer's protocol. Gene-specific primers were used to amplify the regions of interest from the SFV6–2SG-mCherry genome T7 promoter. The PCR products were used to synthesize the dsRNA sequence *in vitro* using the MEGAscript T7 Transcription kit (Thermo Fisher Scientific), before further purification by LiCl precipitation and resuspension in nuclease-free water. The concentration of the dsRNA was determined using a Nanodrop 2000 spectrophotometer (Thermo

Fisher Scientific). We followed the same procedure for dsRNA targeting green fluorescent protein (GFP), but used a glycerol stock of *E. coli* carrying vector pGEM-T-Easy-GFP-125 and gene-specific primers targeting GFP linked to the T7 promoter. Sequences of the dsRNAs and alignment information to SFV6 are shown in Table S4.

2.4. Cytotoxicity of dsRNA

To determine the cytotoxicity of dsRNA, we followed our previously established protocol (Omokungbe et al., 2024). In short, cells were grown to ~50 % confluence in 96-well plates and treated with either uncomplexed or complexed dsRNA with K4 Transfection System (K4, Biontex). Ionomycin (Sigma-Aldrich, now Merck, [10 mM stock in DMSO, 100 μM in the assay]), K4, or Grace insect medium (Thermo Fisher Scientific) were employed as controls. We used dsRNAs that target six regions of the SFV6–2SG-mCherry genome: the non-structural proteins (nsPs) 1–4 and the envelope proteins E1 and E2. We added mCH-dsRNA as a positive control for the later antiviral assays and GFP-dsRNA as a negative control. We have previously assessed the optimal complexing capacity of K4 (Omokungbe et al., 2024). Therefore, all dsRNAs and K4 were applied at 2 ng/μL. The dsRNA:K4 complexes were prepared at 1:1 ratio in Grace insect medium and incubated for 20 min. The treatments were added to the cells using supplemented L-15 GlutaMAX insect medium without penicillin/streptomycin, including the untreated control, to avoid increased toxicity due to a higher uptake of antibiotics. At 6 h post-treatment, the media was removed and fresh supplemented L-15 GlutaMAX insect medium (including penicillin/streptomycin) was added. Cell viability was assessed at 48 h post-treatment using the CellTiter-Glo Luminescent Cell Viability assay (Promega) according to the manufacturer's instructions. Luminescence was recorded using black 96-well plates in a Synergy H4 microplate reader (Biotek, now Agilent Technologies). Data were normalized to the untreated control and expressed as percentage (treatment/untreated × 100).

2.5. Efficiency of dsRNA complexes on SFV replication

To measure the antiviral efficiency of our dsRNAs, we first compared the dsRNA complexes prepared with K4 with uncomplexed ones. Therefore, U4.4 cells were seeded in 96-well black μClear plates (Greiner Bio-One). At ~50 % confluence, cells were treated either with 2 ng/μL of uncomplexed dsRNA, complexed dsRNA with K4 (1:1), or Grace insect media. We compared the dsRNAs targeting the SFV6 genome, GFP-dsRNA, and mCH-dsRNA. The complexing procedure was as described above. At 24 hpt, cells were infected with the mCherry tagged Semliki Forest virus (SFV-mCherry) at a multiplicity of infection (MOI) of 0.01 using unsupplemented L-15 GlutaMAX insect growth medium for 1 h based on previous studies (Attarzadeh-Yazdi et al., 2009; Barry et al., 2013; Omokungbe et al., 2024). After infection, media were replaced with supplemented L-15 GlutaMAX insect growth medium. Infected cells treated with Grace insect medium and untreated infected cells were used as positive controls, whereas untreated uninfected cells were used to measure the background fluorescence. Fluorescence measurements were carried out at 56 and 72 h post-infection (hpi) using 8 μL of NucBlue (NucBlue Live ReadyProbes Reagent, Thermo Fisher Scientific) to stain the nuclei of cells. These cells were then incubated for 20 min. Using the Cytation 5 Cell Imaging Multimode Reader (Agilent Technologies), 4× images were taken of each well and the total red intensity was measured along with the cell count using Biotek Gen5 Image Prime v3.12 (Agilent Technologies). To calculate the relative fluorescence per cell emitted, the mean value obtained from each untreated uninfected well was subtracted from each infected well and divided by the total cell count.

2.6. Time-dependent analysis of the dsRNA complex

We monitored the fluorescence signal of Cy3-labeled dsRNA via fluorescence microscopy as well as testing their antiviral efficiency at multiple time points. We have previously analyzed the uptake of mCH-dsRNA at 24 hpt using labeled mCH-dsRNA (Omokungbe et al., 2024). Briefly, we labeled nsP4-dsRNA with Cy3 using the Silencer siRNA labeling kit (Thermo Fisher Scientific) according to the manufacturer's protocol. Complexing of nsP4-dsRNA with K4 (1:1) was done as described above. At 6 hpt, cells were washed three times with unsupplemented L-15 medium and replenished with fresh supplemented medium. Using independent wells per time point, we added 8 μl of NucBlue per well at 24, 32, 48, 56, and 72 hpt, and incubated the cells for 20 min. We monitored the fluorescence signals of Cy3 and Hoechst 33342 with a Cytation 5. Brightfield images of each well were captured at 20× magnification, as well as fluorescence images using DAPI and Texas Red filters. Images were processed with Gen5 Software. The raw fluorescence signal of untransfected control was subtracted from the treatments.

Additionally, we followed the same procedure for complexing and infecting as described above in Section 2.5. However, cells were treated with 1 ng/μL of nsP1-dsRNA or GFP-dsRNA complexed with K4 (1:1) and infected with SFV-mCherry using independent virus aliquots at 8, 24, 32, 48, 56, and 72 hpt. Untreated and uninfected cells were used to measure the background fluorescence. Fluorescence measurements were carried out at 48 hpi for each time point and data analysis was performed as described above.

2.7. Quantification of viral gene expression level via RT-qPCR

As a confirmation of the dsRNA mediated reduction in viral gene expression, we quantified the expression of nsP4 in U4.4 cells via RT-qPCR after transfection with nsP4-dsRNA and GFP-dsRNA (as a control). We followed the same methodology for transfection of complexed dsRNAs and virus infection as described in Section 2.5 but using a 24 well-plate to seed the cells. At 72 hpi, we carried out RNA extractions from the cells using the Monarch Total RNA Miniprep Kit (New England BioLabs) according to manufacturer's protocol. RNA was quantified on a NanoDrop 2000 Spectrophotometer. The A_{260}/A_{280} value cutoff value was set between 1.8 and 2.2. Gene-specific primers were designed as described in Section 2.3 and the primer sequences and amplicon sizes are listed in Table S6. We determined the efficiency of the primer using the standard curve method (Fig. S2) with RNA template concentration ranging from 1000 ng to 0.1 ng, at 10-fold dilution series on a QuantStudio 3 qPCR system (Applied Biosystems). Each reaction was reverse transcribed and amplified using the Luna Universal One-Step RT-qPCR Kit (New England BioLabs), heated to 55 °C for 10 min and 95 °C for 1 min followed by 45 cycles of 95 °C for 10 s and 60 °C for 1 min, following the instrument recommendation for melt curves of 60 – 95 °C.

For the gene knockdown analysis, 100 ng of extracted RNA was used as a template for the RT-qPCR experiment following the same procedure. Actin was used as a reference gene for normalization and data were analyzed via the $2^{-\Delta\Delta Ct}$ method.

2.8. Dose response analysis of dsRNA on SFV replication

To analyze the inhibition of virus replication in a dose response manner, we followed the same methodology described in Section 2.5 but used different concentrations of the complexed dsRNA. Based on the results of the efficiency experiment, we selected nsP1-dsRNA, nsP2-dsRNA, nsP4-dsRNA, and E1-dsRNA for a dose response analysis. The mCH-dsRNA and GFP-dsRNA were used as controls. We used concentrations of 2, 1, 0.5, and 0.25 ng/μL in a 1:1 complexing ratio. Fluorescence measurements were carried out at 56 and 72 hpi and data analysis was performed as described above.

2.9. Statistical analysis

The statistical analysis and visualization of data was carried out using GraphPad Prism v9.5.1 (GraphPad Software). To determine statistically significant differences ($P < 0.05$), we used a one-way ANOVA with Dunnett's multiple comparison test to analyze the cytotoxicity of the dsRNAs and reagents and in the antiviral time-dependent assay, an unpaired *t*-test for the gene knockdown analysis and a two-way ANOVA with Dunnett's multiple comparisons in the efficacy analysis between uncomplexed and complexed dsRNAs and the dose response analysis.

3. Results

3.1. Design of gene-specific dsRNAs for SFV

We compared whole genome sequences of nine SFV strains. The alignments of the whole genome sequences showed that SFV strains have an average length of 11,822 bps and 97.1 % identical sites. Viral genes showed <2 % variation among them, making them potential targets for RNAi (Table 1). However, due to their short length E3 and 6 kDa genes of <200 nucleotides were not targeted by long dsRNA in this study.

Therefore, using SFV6–2SG-mCherry plasmid (Omokungbe et al., 2024; Pennemann et al., 2021) as template, we synthesized long dsRNAs with an approximate length ranging between 400 and 500 bps targeting the nsPs 1–4, E2, and E1 regions (Table S4). Overall, the nucleotide sequence identity between the nine SFV strains, and the designed dsRNAs was above 99 % (Table S5). Interestingly, the E1-dsRNA matched all nine SFV strains with 100 % identity.

Table 1
Comparison of nine Semliki Forest virus complete genome sequences and viral genes. The nucleotide (nt) coordinates for each gene of interest are derived from the SFV6 genome sequence (GenBank Accession KT009012.1).

Gene	Average nt size	nt begin	nt end	G/C content (%)	Identity (%)
nsP1	1611	86	1696	51.8	99.2
nsP2	2397	1697	4093	52.8	98.8
nsP3	1446	4094	5539	57.0	99.0
nsP4	1842	5540	7381	52.4	99.5
C	801	7423	8223	55.1	99.6
E3	198	8224	8421	58.1	100
E2	1266	8422	9687	53.9	99.7
6kDa	180	9688	9867	52.8	100
E1	1314	9868	11181	54.0	99.8

3.2. Cytotoxicity of dsRNA in U4.4 cells

First, the cytotoxicity of the dsRNA uncomplexed or in complexed form was tested in the *Ae. albopictus* cell line U4.4 using the CellTiter-Glo assay. Cells were grown at ~50 % confluency in 96 well-plates and treated with 2 ng/μL of dsRNA that was either uncomplexed or complexed with K4. Grace insect medium, K4, and ionomycin served as controls. At 48 h post-treatment we observed no cytotoxic effects from any of the treatments (Fig. 1), except of mCH-dsRNA which induced significant toxicity in treated cells with complexed dsRNA compared to those treated with uncomplexed dsRNA. However, the cell viability remained above the toxicity cut-off point set at 80 %. At this concentration, K4 was also not cytotoxic, but as expected, the ionophore ionomycin had a strong cytotoxic effect on the cells.

3.3. Effect of dsRNA on SFV replication in U4.4 cells

The efficacy of the dsRNA in reducing the viral replication by targeting the different regions of SFV genome was evaluated. U4.4 cells were treated at ~50 % confluency, this time with 1 ng/μL of dsRNA (either uncomplexed or complexed with K4). At 24 h post-treatment, cells were infected with the SFV-mCherry (MOI = 0.01) for 1 h. At 56 hpi (Fig. 2a), all complexed dsRNAs led to a significant reduction of the relative fluorescence per cell, indicator of virus spread, compared to SFV. We observed the most pronounced antiviral effect on the relative fluorescence per cell for nsP4-dsRNA. In contrast, the uncomplexed dsRNAs had limited antiviral effect, with only the dsRNA targeting nsP2 and nsP4 showing reduction in viral replication at 56 hpi, indicating some activity even without the presence of transfection reagent. However, this effect was only observed at 72 hpi for nsP2-dsRNA (Fig. 2b). The relative fluorescence per cell of the uncomplexed dsRNAs increased by up to 20 % between time points and remained comparable to SFV, as opposed to the complexed dsRNAs which showed little variation and

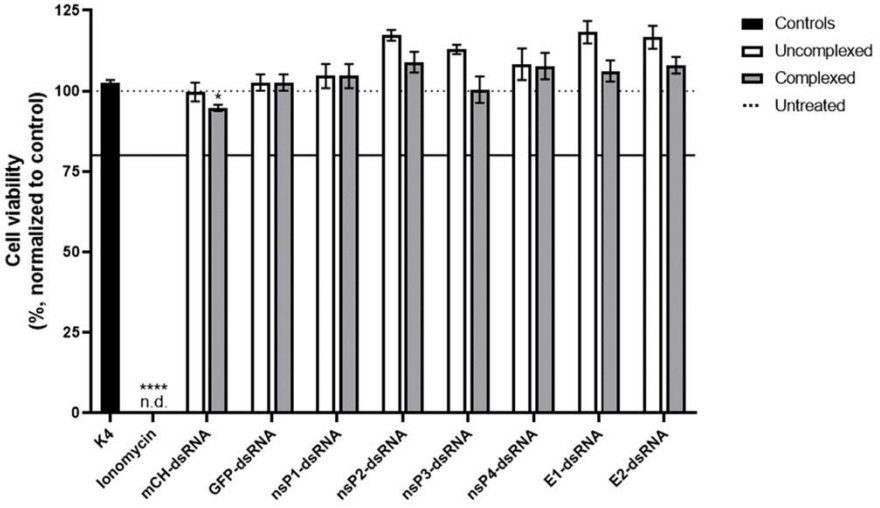

Fig. 1. Normalized cell viability of U4.4 cells after dsRNA treatment. Cells were treated with uncomplexed and complexed dsRNA (2 ng/μL) with the K4 Transfection System (K4). K4 and ionomycin (10 mM stock in DMSO, 100 μM in the assay) were used as controls. At 48 h post-treatment, the cell viability was assessed via ATP quantification by CellTiter-Glo Assay. The cell viability was normalized to the untreated control which was set to 100 %. The data are mean values (n = 5, biological replicates) of the cell viability and the error bars represent standard deviations. The dotted line represents the mean cell viability of the untreated control. The solid line represents the toxicity cut-off set to 80 %. Statistical significance was determined by one-way ANOVA and Dunnett's multiple comparison test between the treatments and untreated control (****$P < 0.0001$, *$P < 0.05$); n.d.= non-detectable.

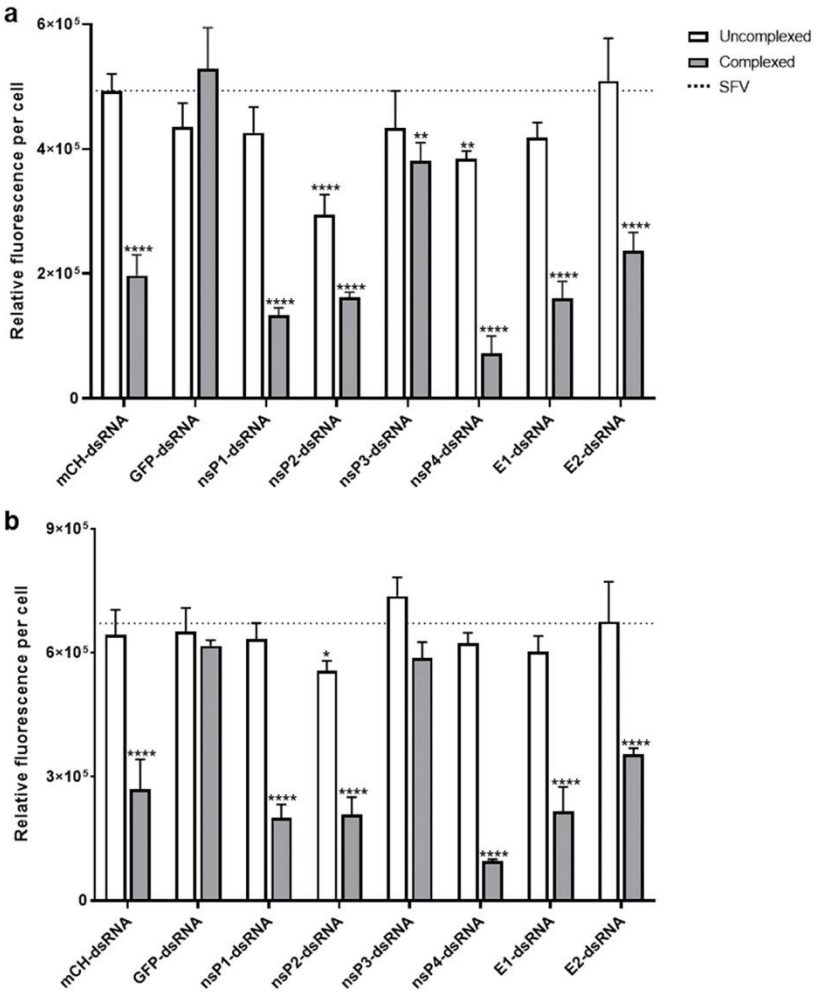

Fig. 2. Comparison of the antiviral efficacy between uncomplexed dsRNA and complexed dsRNA with the K4 Transfection System (K4) to inhibit Semliki Forest virus (SFV) replication. Cells were treated with 1 ng/μL of uncomplexed or K4-complexed dsRNA (1:1 ratio). At 24 h post-transfection, cells were infected with SFV-mCherry (MOI = 0.01) for 1 h. Total red intensity and cell count were measured at (a) 56 and (b) 72 h post-infection. The data are mean values (n = 3, biological replicates) of the relative fluorescence per cell (total red intensity/total cell count) and the error bars represent standard deviations. Background signal was removed using untreated control. The dotted line represents the mean relative fluorescence per cell of SFV. Statistical significance was determined by two-way ANOVA and Dunnett's multiple comparison test between the treatments and SFV (****$P < 0.0001$, **$P < 0.01$, *$P < 0.05$).

sustained effect between time points. At 72 hpi, complexed dsRNAs remained inhibiting SFV replication, except nsP3-dsRNA which no longer showed antiviral efficacy against SFV.

3.4. Time-dependent analysis of dsRNA complex in U4.4 cells

We performed two assays to monitor the fate of labeled dsRNA in U4.4 cells and antiviral efficiency after transfection at multiple time points. Cells were transfected with 1 ng/μL of Cy3 labeled nsP4-dsRNA complexed with K4 (1:1 ratio) and fluorescence measurements were carried out of Cy3 and Hoechst 33342. The Cy3 signal from the labeled dsRNA remained constant up to 72 hpt, while the Hoechst 33342 signal slightly increased over time due to continuing cell growth (Fig. 3a–h).

To evaluate the antiviral potential of the complexed dsRNAs over time, we infected cells with SFV-mCherry at multiple time points after transfection and assess its antiviral efficiency. We found that complexed nsP1-dsRNA significantly reduced SFV replication at all multiple transfection time points tested (Fig. 4). Furthermore, we observed no significant differences between SFV and GFP-dsRNA at any time point.

3.5. Gene silencing of SFV by dsRNA

To determine whether the inhibition of viral replication was mediated by RNAi-induced viral gene knockdown, we assessed the expression levels of nsP4 using RT-qPCR. Gene-specific primers targeting nsP4 were designed and validated for optimum efficiency using the standard curve method, resulting in an efficiency of 100 % (Fig. S2). For the gene knockdown experiment, U4.4 cells were treated with nsP4-dsRNA, while GFP-dsRNA served as a control. Gene expression analysis was performed at 72 hpi. Actin was used as a reference gene for normalization via the $2^{-\Delta\Delta Ct}$ method. The nsP4-dsRNA significantly reduced the expression level of nsP4 by 32.2 % compared to the control (Fig. 5). Although the biological reduction in mRNA expression was moderate, it suggests that partial knockdown of nsP4 is sufficient to affect viral replication.

3.6. Dose response analysis to block SFV replication

To further evaluate the inhibition of SFV replication by complexed dsRNAs, we performed a dose response analysis using mCH-dsRNA and GFP-dsRNA as controls. The four dsRNAs leading to the strongest reduction in virus replication (nsP1-dsRNA, nsP2-dsRNA, nsP4-dsRNA, and E1-dsRNA) were selected. This assay was carried out under the same

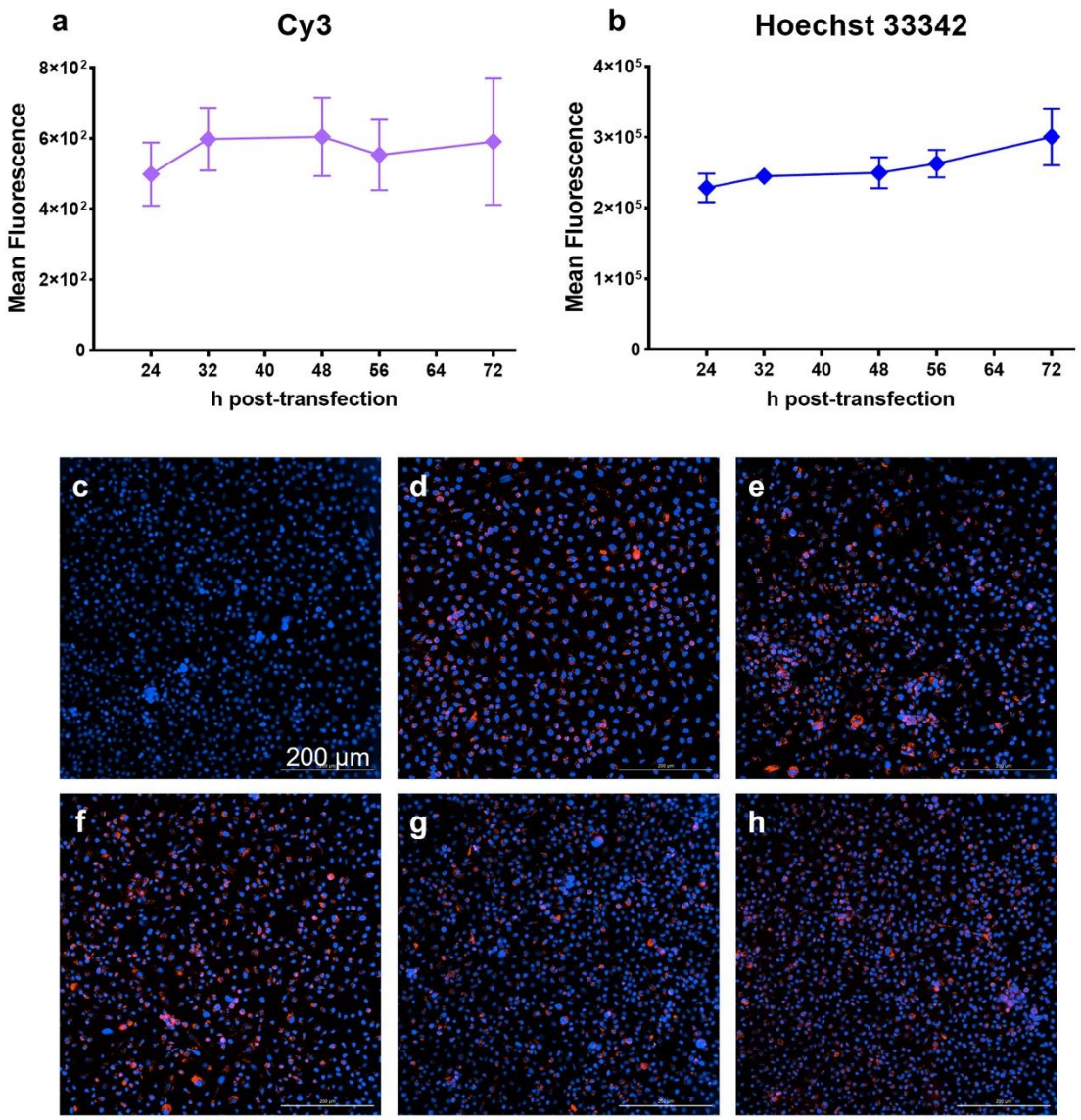

Fig. 3. Fluorescence signal of complexed dsRNA in U4.4 cells. Cells were transfected with 1 ng/µL of Cy3 labeled nsP4-dsRNA complexed with the K4 Transfection System (1:1) and independent measurements of the mean fluorescence of (a) Cy3 and (b) Hoechst 33342 ($n = 3$, biological replicates) were taken in the (c) untreated control, and at (d) 24, (e) 32, (f) 48, (g) 56, and (h) 72 h post-transfection.

conditions as when quantifying the efficiency of dsRNA complexes inhibition on SFV replication, but tested the dsRNAs at concentrations of 0.25, 0.5, 1, and 2 ng/µL. At 56 hpi, all dsRNAs, except GFP-dsRNA, were most effective already at 1 ng/µL, with a clear trend indicating that increasing dsRNA concentrations correspond to a reduction in viral replication (Fig. 6a). At both time points, the E1-dsRNA was the only target that showed no protection at 0.25 ng/µL and was less effective at 0.5 ng/µL. The GFP-dsRNA showed an opposite trend compared to the other complexes, whereby increasing dsRNA concentrations resulted in higher viral replication and showed no differences with SFV at both time points. Although at 72 hpi (Fig. 6b) viral inhibition by mCH-dsRNA, nsP1-dsRNA, and nsP2-dsRNA was significant at all concentrations, only nsP4-dsRNA showed a strong constant inhibition at all tested concentrations.

4. Discussion

Despite the burden they cause on society, mosquitoes, like any other organism, play an important role in the ecosystem. Mosquitoes are preyed upon by several generalist predators; however, the removal of mosquitoes from the environment is unlikely to significantly impact such predators' diets. A significant risk is that eliminating one mosquito species could, via competitive release, allow for a population increase of another species. This is of particular concern if the new species is also a disease vector, and, potentially, a more efficient one (Collins et al., 2019; Godfray, 2013). Therefore, the development of ecological alternatives to control the spread of MBDs is necessary. RNAi offers a promising alternative for the control of viral infections of vector populations, with the potential of targeting the virus specifically. In this study, we designed and evaluated dsRNA for six specific regions of the SFV6 genome in cell culture as a proof-of-concept. We focused on assessing their antiviral efficacy either complexed with K4 or uncomplexed in the U4.4 cell line of *Ae. albopictus*.

Cytotoxicity is a critical factor in cell culture experiments, as it is essential for differentiating between effects caused by RNAi, the formulation and those due to general cytotoxicity (Wang et al., 2018). Our cytotoxicity assays showed that none of the treatments with either uncomplexed or complexed dsRNA were under the toxicity cut-off at a

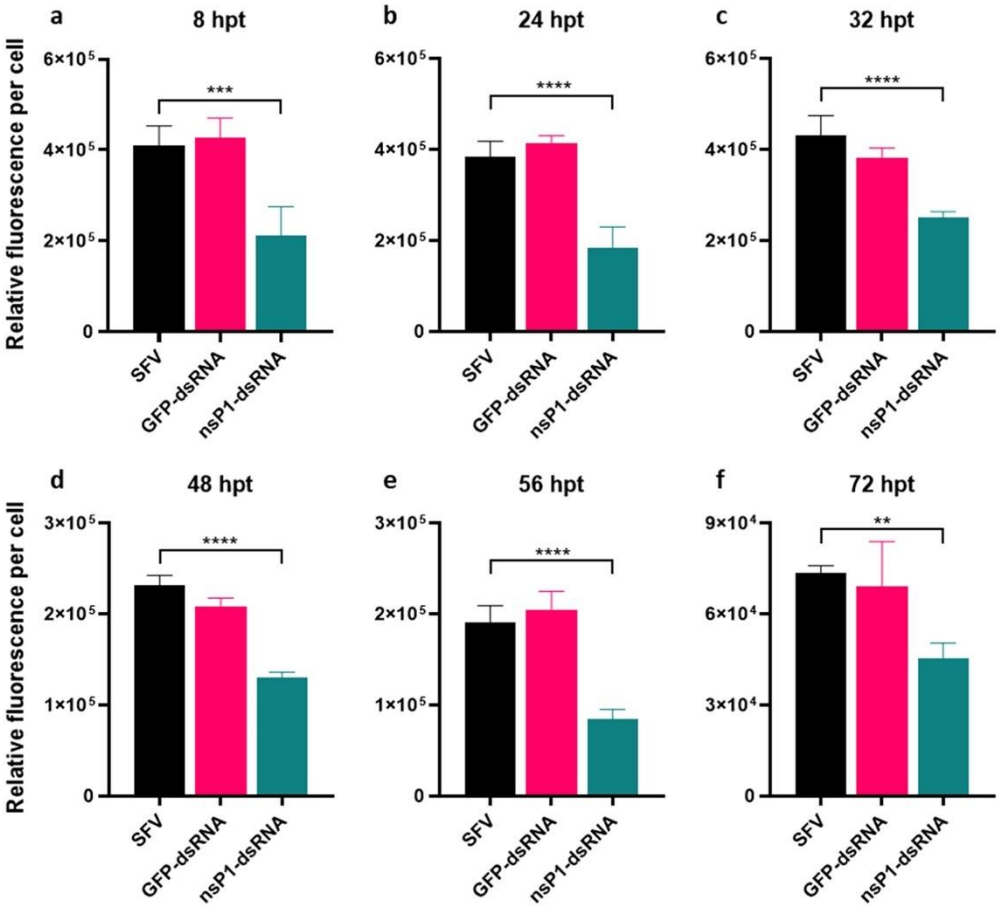

Fig. 4. Antiviral efficiency of complexed dsRNA in U4.4 cells at multiple transfection points. Cells were treated with 1 ng/μL of dsRNA complexed with K4 Transfection System (1:1) and infected with Semliki Forest virus-mCherry (MOI = 0.01) for 1 h at (a) 8, (b) 24, (c) 32, (d) 48, (e) 56, and (f) 72 h post-transfection (hpt). The total red intensity and cell count were measured at 48 h post-infection for each transfection time point (n = 4, biological replicates). The relative fluorescence per cell was calculated by the total red intensity/total cell count. Background signal was removed using untreated control. The data in graphs are mean values and the error bars represent standard deviations. Statistical significance was determined by one-way ANOVA and Dunnett's multiple comparison test between the treatments and SFV (****P < 0.0001, ***P < 0.001, **P < 0.01).

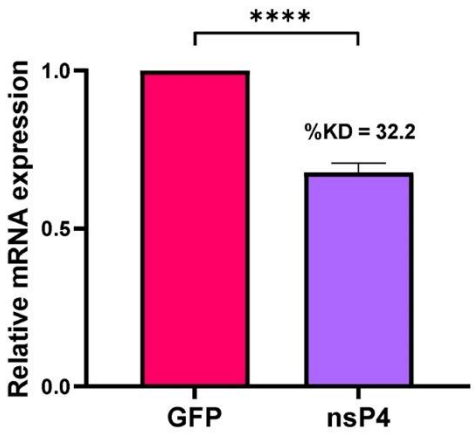

Fig. 5. Expression analysis of nsP4 mRNA in Semliki Forest virus (SFV) infected U4.4 cells. The cells were treated at 50 % confluency with nsP4-dsRNA or GFP-dsRNA (n = 3, biological replicates) and infected with SFV-mCherry (MOI = 0.01) for 1 h at 24 h post-transfection. At 72 h post-infection, gene expression was analyzed using RT-qPCR. Data were processed via the $2^{-\Delta\Delta Ct}$ method, with actin as the reference gene. The graph shows the mean relative expression level of nsP4, and the error bars indicate the standard deviation. Statistical significance was determined by unpaired t-test (****P < 0.0001).

concentration of 2 ng/μL (Fig. 1). These results align with previous findings where no cytotoxicity was observed in the *Ae. albopictus* C6/36 and U4.4 cells when transfected with dsRNA targeting mCherry using K4 Transfection System, Metafectene Pro, Metafectene SI+, and CellFectin II (Omokungbe et al., 2024). The absence of cytotoxic effects supports the use of dsRNA for gene silencing in cell culture.

A major limitation of RNAi in insects is its delivery into the cell, since RNAi is only initiated upon uptake of the dsRNA (Tan and Yin, 2004; Yu et al., 2013). One way to address this problem is through the use of transfection reagents that aid the efficient cellular uptake of the dsRNA (Cooper et al., 2019; Silver et al., 2021). We therefore compared the efficient delivery of the dsRNAs when complexed with K4, and when uncomplexed while targeting the six regions of the SFV genome. Our findings confirmed that virus gene silencing was more effective when the dsRNA was transfected into the cells using transfection reagent, as it was up to seven times more efficient, in the case of nsP4-dsRNA, than when it was uncomplexed (Fig. S3). These results highlight the role of delivery systems to improve RNAi outcomes, and goes in hand with previous reports in other insect cells using complexed dsRNA in *Drosophila* S2 cells (Caplen et al., 2000) and *Spodoptera frugiperda* Sf9 cells (Gurusamy et al., 2020). Similarly, a complexed siRNAs at 2 ng/μL at a 1:3 ratio (siRNA:HiPerFect) targeting Dengue virus showed inhibition of viral replication, and therefore reduction of cytopathic effects in C6/36 cells (Wu et al., 2010). Our results further underline the importance of cellular uptake for improved outcomes when using RNAi.

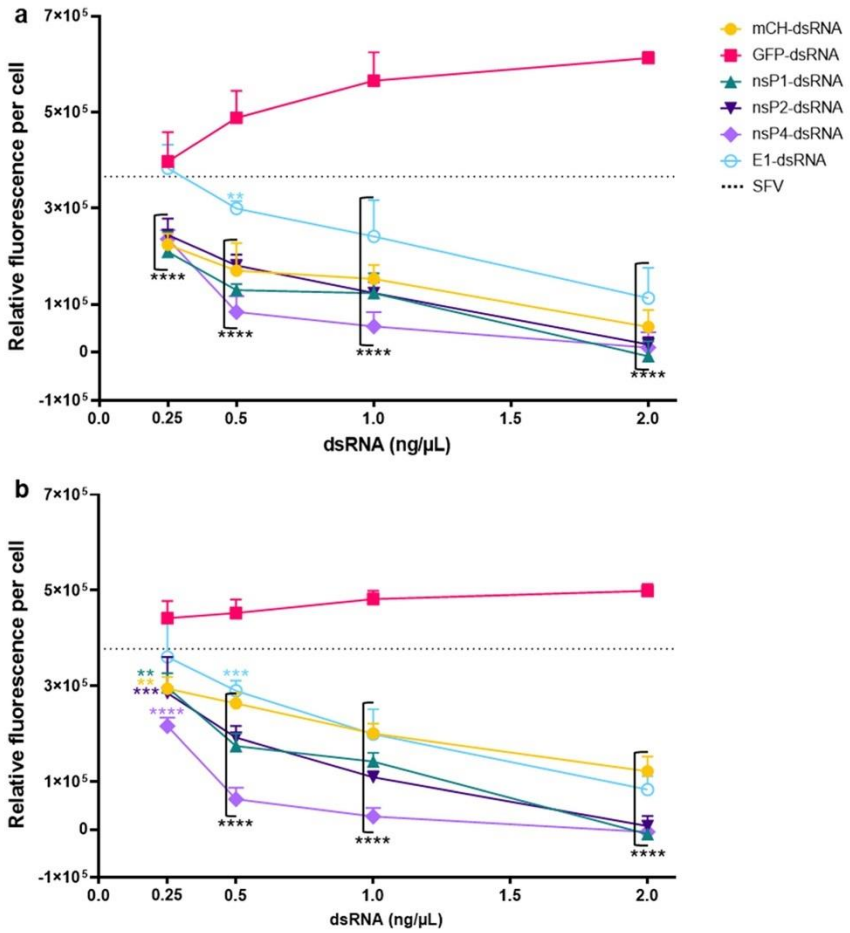

Fig. 6. Dose response analysis of complexed dsRNAs to inhibit Semliki Forest virus (SFV) replication in U4.4 cells. Cells were treated with 0.25, 0.5, 1, and 2 ng/µL complexed dsRNA using the K4 Transfection System (1:1 ratio). At 24 h post-transfection, cells were infected with SFV-mCherry (MOI = 0.01) for 1 h. Total red intensity and cell count were measured at (a) 56 and (b) 72 h post-infection. The data are mean values (n = 6, biological replicates) of the relative fluorescence per cell (total red intensity/total cell count) and the error bars represent standard deviations. Background signal was removed using untreated control. The dotted line represents the mean relative fluorescence per cell of SFV. Statistical significance was determined by two-way ANOVA and Dunnett's multiple comparison test between the treatments and SFV (****P < 0.0001, ***$P < 0.001$, **$P < 0.01$). Asterisks in matching color represent the statistical results of their treatment, while the asterisks in black represent the results of the remaining treatments.

Another key factor influencing the efficacy of dsRNA is its stability. Environmental factors such as nucleases, microorganisms and abiotic factors (Rank and Koch, 2021; Yang et al., 2022), as well as insect-derived dsRNases (Singh et al., 2017), can degrade dsRNA and prevent its ability to reach its target. In an antiviral set-up, dsRNA must be able to remain stable and effective for several hours post-treatment to combat an antiviral infection. As an initial approach, we used Cy3-labeled complexed dsRNA to monitor the fluorescence signal. The Cy3 signal emitted by the nsP4-dsRNA complexed with K4 remained constant up to 72 hpt (Fig. 3a–h), while the Hoechst 33342 signal increased due to cell proliferation. With the dsRNA presence confirmed up to 72 hpt, we proceeded to test its antiviral efficacy at multiple time points after transfection against SFV-mCherry. Previous studies have shown that dsRNAs targeting SFV remained active up to 24 hpt (Caplen et al., 2002; Omokungbe et al., 2024). Here, the nsP1-dsRNA effectively inhibited viral replication when challenged up to 72 h post-transfection (Fig. 4a–g). Both assays demonstrated not only the presence of complexed dsRNAs but also their sustained ability to inhibit virus replication up to 72 hpt. Although increasing cell confluency limited the length of the assessment, we observed a sustained antiviral effect of the complexes dsRNAs extending their active timeframe up to 48 h (Fig. S1).

Targeting specific viral genes can lead to the identification of key regions for viral replication (Caplen et al., 2002; Magalhaes et al., 2019). Of the six dsRNA target regions, we found that the nsPs dsRNA, except nsP3-dsRNA, were particularly effective in suppressing viral replication. Specifically, nsP4-dsRNA strongly reduced viral replication at 56 and 72 hpi at all tested concentrations (Fig. 3b). Similarly, targeting the nsP2 and nsP4 of SFV using dsRNAs expressing a GFP marker had shown significant reduction of the replication of SFV by 50 % in a 24 h period (Caplen et al., 2002). In this study, nsP4-dsRNA led to the highest reduction in virus replication. The effect of nsP4-dsRNA was confirmed via RT-qPCR, which showed a 32.2 % reduction on the nsP4 mRNA expression. Notably, the percentage reduction of nsP4 mRNA levels was lesser than the observed inhibition of SFV replication by fluorescence microscopy using nsP4-dsRNA, which showed a reduction of >50 %. This difference likely reflects the nature of the assays: RT-qPCR captures mRNA levels of a single gene, whereas fluorescence reflects overall viral replication and protein expression. Moderate knockdown of a key replication gene such as nsP4 may be sufficient to disrupt viral replication disproportionately (Lello et al., 2021; Strauss and Strauss, 1994). In addition, mRNA and protein levels are not directly correlated due to post-transcriptional regulation (Liu et al., 2016), which may further explain the enhanced antiviral effect observed. Thus, the mRNA expression levels of nsP4 may underestimate the impairment of replication efficiency of the complexed dsRNA. Finally, we cannot clearly state the underlying reason for nsP4's higher efficiency, as all nsPs of

alphaviruses are known to be essential for the RNA synthesis of the virus (Abu Bakar and Ng, 2018; Atkins et al., 1999). We found little variation (~2 %) between the genomes of the different strains of SFV and their coding regions (Table S2). Based on this, we suggest that the dsRNA constructs could also target other SFV strains examined in this study. Although we cannot rule out that our results could vary depending on the length of the dsRNA, self-aggregation of the dsRNA and the interaction of the specific target site within the virus regions, they do provide useful insights for the selection of effective targets among alphaviruses.

While effective targeting improves the results of viral suppression, it is vital for its success to find the appropriate concentration for RNAi application (Katoch et al., 2013; Zhu and Palli, 2020). The dose response analysis revealed that nsP4-dsRNA achieved significant suppression already at 0.25 ng/μL, providing effective viral gene silencing while requiring lower amount of dsRNA. Interestingly, we suggest that the addition of the non-target GFP-dsRNA is saturating the translational machinery components, and leading to higher replication of the virus (Christiaens and Smagghe, 2014; Kanasty et al., 2012). Identification of RNAi-susceptible regions in the viral genome and ensuring efficient delivery of dsRNA is essential. As a next step, we aim to perform our experiments *in vivo* to provide a more comprehensive assessment of efficacy. Various methods have been explored for RNAi in larvae and adult mosquitoes including microinjection (Mysore et al., 2020; Sánchez-Vargas et al., 2009), soaking/oral delivery (Coy et al., 2012; Singh et al., 2013; Taracena et al., 2019; Zhang et al., 2010), transgenic expression (in the mosquito or via associated organisms) (Bian et al., 2005; Lopez et al., 2019; Mysore et al., 2017) or topical application (Pridgeon et al., 2008). While microinjection is reliable for dsRNA transduction, it is invasive and time consuming as well as impractical for field application. Oral ingestion remains a promising method, however it faces challenges such as rapid degradation of ingested dsRNA in the insect gut and variability in uptake efficiency (Figueiredo Prates et al., 2024; Giesbrecht et al., 2020). The utilization of genetically modified organisms remains a subject of considerable debate (Bukhari et al., 2024; Müller et al., 2023; Woźniak et al., 2021). Additionally, optimization of the RNAi system is also critical when translating assay to *in vivo* testing, where environmental factors, developmental stage and tissue-specific activities influence the outcome (Peng et al., 2018; Romoli et al., 2024).

5. Conclusion

In summary, dsRNAs targeting specific regions of the viral genome demonstrated an effective antiviral effect when efficiently delivered. Here, we extended the current knowledge on the variation of the different strains of SFV. We developed effective dsRNA targeting various regions and found effective concentrations for their application, focusing on making the virus the target of RNAi rather than of the vector. Additionally, we showed that our dsRNAs remained effective against virus replication up to 72 hpt. Finally, we confirmed gene knockdown by our dsRNA by quantifying viral mRNA levels. We conclude that our proof-of-concept for antiviral effectivity of dsRNA was well stablished. Future research should focus on refining delivery systems, complementing their use with other control methods, and testing dsRNA efficacy against a broader range of arboviruses as well as developing proper protocols adaptations for *in vivo* research. Furthermore, future work should also aim to clarify the correlation between mRNA knockdown and viral replication inhibition by assessing corresponding protein levels and post-transcriptional effects. Ultimately, our research provides valuable insights into the use of RNAi-based methods for viral suppression and paves the way for the development of complementary sustainable tools to the current arboviral control methods.

Funding

Open Access funding enabled and organized by Projekt DEAL. This work was supported by the Landes-Offensive zur Entwicklung Wissenschaftlich-ökonomischer Exzellenz Program of the Hessian Ministry of Higher Education, Research and the Arts through the LOEWE Centre for Translational Biodiversity Genomics (LOEWE–TBG) with funding code: LOEWE/1/10/519/03/03.001(0014)/52, and by the BMBF (Project ASCRIBE—Grant Number 01KI2024).

Ethical approval

This article does not contain any studies with human participants or animals requiring ethical approval.

CRediT authorship contribution statement

Alejandra Centurión: Writing – review & editing, Writing – original draft, Visualization, Validation, Methodology, Formal analysis, Data curation. **Bodunrin Omokungbe:** Writing – review & editing, Writing – original draft, Validation, Methodology, Investigation, Formal analysis, Data curation. **Sabrina Stiehler:** Methodology, Investigation, Formal analysis, Data curation. **Andreas Vilcinskas:** Supervision, Resources, Funding acquisition. **Kornelia Hardes:** Writing – review & editing, Writing – original draft, Supervision, Resources, Project administration, Methodology, Investigation, Funding acquisition, Formal analysis, Data curation, Conceptualization.

Declaration of competing interest

The authors declare that they have no known competing financial interests or personal relationships that could have appeared to influence the work reported in this paper.

Acknowledgements

We thank Prof. Dr. Andres Merits, University of Tartu, Estonia, and Prof. Dr. Andreas Pichlmair, Technical University of Munich, Germany, for providing pCMV-SFV6–2SG-mCherry. We also wish to thank Sophie Chattington MSc for her editorial assistance.

Supplementary materials

Supplementary material associated with this article can be found, in the online version, at doi:10.1016/j.virusres.2025.199584.

Data availability

Data will be made available on request.

References

Abu Bakar, F., Ng, L.F.P., 2018. Nonstructural proteins of alphavirus-potential targets for drug development. Viruses. 10 (2), 71.

Agboli, E., Schulze, J., Jansen, S., Cadar, D., Sreenu, V.B., Leggewie, M., Altinli, M., Badusche, M., Jöst, H., Börstler, J., Schmidt-Chanasit, J., Schnettler, E., 2023. Interaction of mesonivirus and negevirus with arboviruses and the RNAi response in Culex tarsalis-derived cells. Parasites Vectors 16 (1), 361.

Agrawal, N., Dasaradhi, P.V.N., Mohmmed, A., Malhotra, P., Bhatnagar, R.K., Mukherjee, S.K., 2003. RNA interference: biology, mechanism, and applications. Microbiol. Mol. Biol. Rev.: MMBR 67 (4), 657–685.

Allgeier, S., Friedrich, A., Brühl, C.A., 2019. Mosquito control based on Bacillus thuringiensis israelensis (Bti) interrupts artificial wetland food chains. Sci. Total Environ. 686, 1173–1184.

Atkins, G.J., 2013. The Pathogenesis of Alphaviruses. ISRN Virol. 2013, 1–22.

Atkins, G.J., Sheahan, B.J., Liljeström, P., 1999. The molecular pathogenesis of Semliki Forest virus: a model virus made useful? J. Gen. Virol. 80 (Pt 9), 2287–2297.

Attarzadeh-Yazdi, G., Fragkoudis, R., Chi, Y., Siu, R.W.C., Ulper, L., Barry, G., Rodriguez-Andres, J., Nash, A.A., Bouloy, M., Merits, A., Fazakerley, J.K., Kohl, A., 2009. Cell-to-cell spread of the RNA interference response suppresses Semliki Forest virus (SFV) infection of mosquito cell cultures and cannot be antagonized by SFV. J. Virol. 83 (11), 5735–5748.

Barry, G., Alberdi, P., Schnettler, E., Weisheit, S., Kohl, A., Fazakerley, J.K., Bell-Sakyi, L., 2013. Gene silencing in tick cell lines using small interfering or long double-stranded RNA. Exp. Appl. Acarol. 59 (3), 319–338.
Berglund, P., Sjöberg, M., Garoff, H., Atkins, G.J., Sheahan, B.J., Liljeström, P., 1993. Semliki Forest virus expression system: production of conditionally infectious recombinant particles. Biotechnology (N.Y.) 11 (8), 916–920.
Bhatt, S., Gething, P.W., Brady, O.J., Messina, J.P., Farlow, A.W., Moyes, C.L., Drake, J. M., Brownstein, J.S., Hoen, A.G., Sankoh, O., Myers, M.F., George, D.B., Jaenisch, T., Wint, G.R.W., Simmons, C.P., Scott, T.W., Farrar, J.J., Hay, S.I., 2013. The global distribution and burden of dengue. Nature 496 (7446), 504–507.
Bian, G., Shin, S.W., Cheon, H.-M., Kokoza, V., Raikhel, A.S., 2005. Transgenic alteration of toll immune pathway in the female mosquito Aedes aegypti. Proc. Natl. Acad. Sci. U.S.A. 102 (38), 13568–13573.
Brackney, D.E., Scott, J.C., Sagawa, F., Woodward, J.E., Miller, N.A., Schilkey, F.D., Mudge, J., Wilusz, J., Olson, K.E., Blair, C.D., Ebel, G.D., 2010. C6/36 Aedes albopictus cells have a dysfunctional antiviral RNA interference response. PLoS Negl. Trop. Dis. 4 (10), e856.
Bukhari, T., Gichuhi, J., Mbare, O., Ochwal, V.A., Fillinger, U., Herren, J.K., 2024. Willingness to accept and participate in a Microsporidia MB-based mosquito release strategy: a community-based rapid assessment in western Kenya. Malar. J. 23 (1), 113.
Caplen, N.J., Fleenor, J., Fire, A., Morgan, R.A., 2000. dsRNA-mediated gene silencing in cultured Drosophila cells: a tissue culture model for the analysis of RNA interference. Gene 252 (1–2), 95–105.
Caplen, N.J., Zheng, Z., Falgout, B., Morgan, R.A., 2002. Inhibition of viral gene expression and replication in mosquito cells by dsRNA-triggered RNA interference. Mol. Ther.: J. Am. Soc. Gene Ther. 6 (2), 243–251.
Christiaens, O., Niu, J., Nji Tizi Taning, C., 2020. RNAi in insects: a revolution in fundamental research and pest control applications. Insects. 11 (7).
Christiaens, O., Smagghe, G., 2014. The challenge of RNAi-mediated control of hemipterans. Curr. Opin. Insect. Sci. 6, 15–21.
Collins, C.M., Bonds, J.A.S., Quinlan, M.M., Mumford, J.D., 2019. Effects of the removal or reduction in density of the malaria mosquito, Anopheles gambiae s.l., on interacting predators and competitors in local ecosystems. Med. Vet. Entomol. 33 (1), 1–15.
Cooper, A.M., Silver, K., Zhang, J., Park, Y., Zhu, K.Y., 2019. Molecular mechanisms influencing efficiency of RNA interference in insects. Pest Manag. Sci. 75 (1), 18–28.
Coy, M.R., Sanscrainte, N.D., Chalaire, K.C., Inberg, A., Maayan, I., Glick, E., Paldi, N., Becnel, J.J., 2012. Gene silencing in adult Aedes aegypti mosquitoes through oral delivery of double-stranded RNA. J. Appl. Entomol. 136 (10), 741–748.
Dahmana, H., Mediannikov, O., 2020. Mosquito-borne diseases emergence/resurgence and how to effectively control it biologically. Pathogens (Basel, Switzerland) 9 (4).
Deuber, S.A., Pavlovic, J., 2007. Virulence of a mouse-adapted Semliki Forest virus strain is associated with reduced susceptibility to interferon. J. Gen. Virol. 88 (Pt 7), 1952–1959.
Ferguson, M.C., Saul, S., Fragkoudis, R., Weisheit, S., Cox, J., Patabendige, A., Sherwood, K., Watson, M., Merits, A., Fazakerley, J.K., 2015. Ability of the encephalitic Arbovirus Semliki Forest virus to cross the blood-brain barrier is determined by the charge of the E2 glycoprotein. J. Virol. 89 (15), 7536–7549.
Figueiredo Prates, L.H., Fiebig, J., Schlosser, H., Liapi, E., Rehling, T., Lutrat, C., Bouyer, J., Sun, Q., Wen, H., Xi, Z., Schetelig, M.F., Häcker, I., 2024. Challenges of robust RNAi-mediated gene silencing in Aedes mosquitoes. Int. J. Mol. Sci. 25 (10), 5218.
Fire, A., Xu, S., Montgomery, M.K., Kostas, S.A., Driver, S.E., Mello, C.C., 1998. Potent and specific genetic interference by double-stranded RNA in Caenorhabditis elegans. Nature 391 (6669), 806–811.
Fragkoudis, R., Chi, Y., Siu, R.W.C., Barry, G., Attarzadeh-Yazdi, G., Merits, A., Nash, A. A., Fazakerley, J.K., Kohl, A., 2008. Semliki Forest virus strongly reduces mosquito host defence signaling. Insect Mol. Biol. 17 (6), 647–656.
Gammon, D.B., Mello, C.C., 2015. RNA interference-mediated antiviral defense in insects. Curr. Opin. Insect Sci. 8, 111–120.
Giesbrecht, D., Heschuk, D., Wiens, I., Boguski, D., LaChance, P., Whyard, S., 2020. RNA interference is enhanced by knockdown of double-stranded RNases in the yellow fever Mosquito Aedes Aegypti. Insects. 11 (6), 327.
Glasgow, G.M., McGee, M.M., Sheahan, B.J., Atkins, G.J., 1997. Death mechanisms in cultured cells infected by Semliki Forest virus. J. Gen. Virol. 78 (Pt 7), 1559–1563.
Godfray, H.C.J., 2013. Mosquito ecology and control of malaria. J. Anim. Ecol. 82 (1), 15–25.
Gurusamy, D., Mogilicherla, K., Shukla, J.N., Palli, S.R., 2020. Lipids help double-stranded RNA in endosomal escape and improve RNA interference in the fall armyworm, Spodoptera frugiperda. Arch. Insect Biochem. Physiol. 104 (4), e21678.
Igarashi, A., 1978. Isolation of a Singh's Aedes albopictus cell clone sensitive to Dengue and Chikungunya viruses. J. Gen. Virol. 40 (3), 531–544.
Kanasty, R.L., Whitehead, K.A., Vegas, A.J., Anderson, D.G., 2012. Action and reaction: the biological response to siRNA and its delivery vehicles. Mol. Ther. 20 (3), 513–524.
Katoch, R., Sethi, A., Thakur, N., Murdock, L.L., 2013. RNAi for insect control: current perspective and future challenges. Appl. Biochem. Biotechnol. 171 (4), 847–873.
Kim, D., Rossi, J., 2008. RNAi mechanisms and applications. Biotechniques 44 (5), 613–616.
Kolimenakis, A., Heinz, S., Wilson, M.L., Winkler, V., Yakob, L., Michaelakis, A., Papachristos, D., Richardson, C., Horstick, O., 2021. The role of urbanisation in the spread of Aedes mosquitoes and the diseases they transmit-A systematic review. PLoS Negl. Trop. Dis. 15 (9), e0009631.
Lello, L.S., Bartholomeeusen, K., Wang, S., Coppens, S., Fragkoudis, R., Alphey, L., Ariën, K.K., Merits, A., Utt, A., 2021. nsP4 Is a major determinant of alphavirus replicase activity and template selectivity. J. Virol. 95 (20), e0035521.
Liu, J., Swevers, L., Kolliopoulou, A., Smagghe, G., 2019. Arboviruses and the challenge to establish systemic and persistent infections in competent mosquito vectors: the interaction with the RNAi mechanism. Front. Physiol. 10, 890.
Liu, Y., Beyer, A., Aebersold, R., 2016. On the dependency of cellular protein levels on mRNA abundance. Cell 165 (3), 535–550.
Lopez, S.B.G., Guimarães-Ribeiro, V., Rodriguez, J.V.G., Dorand, F.A.P.S., Salles, T.S., Sá-Guimarães, T.E., Alvarenga, E.S.L., Melo, A.C.A., Almeida, R.V., Moreira, M.F., 2019. RNAi-based bioinsecticide for Aedes mosquito control. Sci. Rep. 9 (1), 4038.
Lucas, K.J., Myles, K.M., Raikhel, A.S., 2013. Small RNAs: a new frontier in mosquito biology. Trends Parasitol. 29 (6), 295–303.
Magalhaes, T., Bergren, N.A., Bennett, S.L., Borland, E.M., Hartman, D.A., Lymperopoulos, K., Sayre, R., Borlee, B.R., Campbell, C.L., Foy, B.D., Olson, K.E., Blair, C.D., Black, W., Kading, R.C., 2019. Induction of RNA interference to block Zika virus replication and transmission in the mosquito Aedes aegypti. Insect Biochem. Mol. Biol. 111, 103169.
Mathiot, C.C., Grimaud, G., Garry, P., Bouquety, J.C., Mada, A., Daguisy, A.M., Georges, A.J., 1990. An outbreak of human Semliki Forest virus infections in Central African Republic. Am. J. Trop. Med. Hyg. 42 (4), 386–393.
Moyes, C.L., Vontas, J., Martins, A.J., Ng, L.C., Koou, S.Y., Dusfour, I., Raghavendra, K., Pinto, J., Corbel, V., David, J.-P., Weetman, D., 2017. Contemporary status of insecticide resistance in the major Aedes vectors of arboviruses infecting humans. PLoS Negl. Trop. Dis. 11 (7), e0005625.
Müller, R., Bálint, M., Hardes, K., Hollert, H., Klimpel, S., Knorr, E., Kochmann, J., Lee, K.-Z., Mehring, M., Pauls, S.U., Smets, G., Steinbrink, A., Vilcinskas, A., 2023. RNA interference to combat the Asian tiger mosquito in Europe: a pathway from design of an innovative vector control tool to its application. Biotechnol. Adv. 66, 108167.
Mysore, K., Hapairai, L.K., Sun, L., Harper, E.I., Chen, Y., Eggleson, K.K., Realey, J.S., Scheel, N.D., Severson, D.W., Wei, N., Duman-Scheel, M., 2017. Yeast interfering RNA larvicides targeting neural genes induce high rates of Anopheles larval mortality. Malar. J. 16 (1), 461.
Mysore, K., Hapairai, L.K., Sun, L., Li, P., Wang, C.-W., Scheel, N.D., Lesnik, A., Igiede, J., Scheel, M.P., Wei, N., Severson, D.W., Duman-Scheel, M., 2020. Characterization of a dual-action adulticidal and larvicidal interfering RNA pesticide targeting the Shaker gene of multiple disease vector mosquitoes. PLoS Negl. Trop. Dis. 14 (7), e0008479.
Omokungbe, B., Centurión, A., Stiehler, S., Morr, A., Vilcinskas, A., Steinbrink, A., Hardes, K., 2024. Gene silencing in the aedine cell lines C6/36 and U4.4 using long double-stranded RNA. Parasit Vectors 17 (1), 255.
Paupy, C., Delatte, H., Bagny, L., Corbel, V., Fontenille, D., 2009. Aedes albopictus, an arbovirus vector: from the darkness to the light. Microbes infect 11 (14–15), 1177–1185.
Peng, Y., Wang, K., Fu, W., Sheng, C., Han, Z., 2018. Biochemical comparison of dsRNA degrading nucleases in four different insects. Front. Physiol. 9, 624.
Pennemann, F.L., Mussabekova, A., Urban, C., Stukalov, A., Andersen, L.L., Grass, V., Lavacca, T.M., Holze, C., Oubraham, L., Benamrouche, Y., Girardi, E., Boulos, R.E., Hartmann, R., Superti-Furga, G., Habjan, M., Imler, J.-L., Meignin, C., Pichlmair, A., 2021. Cross-species analysis of viral nucleic acid interacting proteins identifies TAOKs as innate immune regulators. Nat. Commun. 12 (1), 7009.
Pridgeon, J.W., Zhao, L., Becnel, J.J., Strickman, D.A., Clark, G.G., Linthicum, K.J., 2008. Topically applied AaeIAP1 double-stranded RNA kills female adults of Aedes aegypti. J. Med. Entomol. 45 (3), 414–420.
Qian, Q., Zhou, H., Shu, T., Mu, J., Fang, Y., Xu, J., Li, T., Kong, J., Qiu, Y., Zhou, X., 2020. The capsid protein of Semliki Forest Virus antagonizes RNA interference in mammalian cells. J. Virol. 94 (3).
Quetglas, J.I., Fioravanti, J., Ardaiz, N., Medina-Echeverz, J., Baraibar, I., Prieto, J., Smerdou, C., Berraondo, P., 2012. A Semliki forest virus vector engineered to express ifnα induces efficient elimination of established tumors. Gene Ther. 19 (3), 271–278.
Rank, A.P., Koch, A., 2021. Lab-to-field transition of RNA spray applications - how far are we? Front. Plant Sci. 12, 755203.
Roche, F.P., Sheahan, B.J., O'Mara, S.M., Atkins, G.J., 2010. Semliki Forest virus-mediated gene therapy of the RG2 rat glioma. Neuropathol. Appl. Neurobiol. 36 (7), 648–660.
Romoli, O., Henrion-Lacritick, A., Blanc, H., Frangeul, L., Saleh, M.-C., 2024. Limitations in harnessing oral RNA interference as an antiviral strategy in Aedes aegypti. iScience 27 (3), 109261.
Sánchez-Vargas, I., Scott, J.C., Poole-Smith, B.K., Franz, A.W.E., Barbosa-Solomieu, V., Wilusz, J., Olson, K.E., Blair, C.D., 2009. Dengue virus type 2 infections of Aedes aegypti are modulated by the mosquito's RNA interference pathway. PLoS Pathog. 5 (2), e1000299.
Saul, S., Ferguson, M., Cordonin, C., Fragkoudis, R., Ool, M., Tamberg, N., Sherwood, K., Fazakerley, J.K., Merits, A., 2015. Differences in processing determinants of nonstructural polyprotein and in the sequence of nonstructural protein 3 affect neurovirulence of Semliki Forest virus. J. Virol. 89 (21), 11030–11045.
Schuster, S., Miesen, P., van Rij, R.P., 2019. Antiviral RNAi in insects and mammals: parallels and differences. Viruses. 11 (5).
Scott, J.C., Brackney, D.E., Campbell, C.L., Bondu-Hawkins, V., Hjelle, B., Ebel, G.D., Olson, K.E., Blair, C.D., 2010. Comparison of dengue virus type 2-specific small RNAs from RNA interference-competent and -incompetent mosquito cells. PLoS Negl. Trop. Dis. 4 (10), e848.
Şengül Demirak, M.Ş., Canpolat, E., 2022. Plant-based bioinsecticides for Mosquito control: impact on insecticide resistance and disease transmission. Insects. 13 (2).

Silver, K., Cooper, A.M., Zhu, K.Y., 2021. Strategies for enhancing the efficiency of RNA interference in insects. Pest Manag. Sci. 77 (6), 2645–2658.
Singh, A.D., Wong, S., Ryan, C.P., Whyard, S., 2013. Oral delivery of double-stranded RNA in larvae of the yellow fever mosquito, Aedes aegypti: implications for pest mosquito control. J. Insect Sci. 13 (1), 69.
Singh, I.K., Singh, S., Mogilicherla, K., Shukla, J.N., Palli, S.R., 2017. Comparative analysis of double-stranded RNA degradation and processing in insects. Sci. Rep. 7 (1), 17059.
Siu, R.W.C., Fragkoudis, R., Simmonds, P., Donald, C.L., Chase-Topping, M.E., Barry, G., Attarzadeh-Yazdi, G., Rodriguez-Andres, J., Nash, A.A., Merits, A., Fazakerley, J.K., Kohl, A., 2011. Antiviral RNA interference responses induced by Semliki Forest virus infection of mosquito cells: characterization, origin, and frequency-dependent functions of virus-derived small interfering RNAs. J. Virol. 85 (6), 2907–2917.
Smithburn, K.C., Haddow, A.J., 1944. Semliki Forest Virus. J. Immunol. 49 (3), 141–157.
Strauss, J.H., Strauss, E.G., 1994. The alphaviruses: gene expression, replication, and evolution. Microbiol. Rev. 58 (3), 491–562.
Tan, F.L., Yin, J.Q., 2004. RNAi, a new therapeutic strategy against viral infection. Cell Res. 14 (6), 460–466.
Taracena, M.L., Hunt, C.M., Benedict, M.Q., Pennington, P.M., Dotson, E.M., 2019. Downregulation of female doublesex expression by oral-mediated RNA interference reduces number and fitness of Anopheles gambiae adult females. Parasites Vectors 12 (1), 170.
Tuittila, M.T., Santagati, M.G., Röyttä, M., Määttä, J.A., Hinkkanen, A.E., 2000. Replicase complex genes of Semliki Forest virus confer lethal neurovirulence. J. Virol. 74 (10), 4579–4589.
Vogel, E., Santos, D., Mingels, L., Verdonckt, T.-W., Broeck, J.V., 2018. RNA interference in insects: protecting beneficials and controlling pests. Front. Physiol. 9, 1912.
Wang, T., Larcher, L.M., Ma, L., Veedu, R.N., 2018. Systematic screening of commonly used commercial transfection reagents towards efficient transfection of single-stranded oligonucleotides. Molecules (Basel, Switzerland) 23 (10).
Willems, W.R., Kaluza, G., Boschek, C.B., Bauer, H., Hager, H., Schütz, H.J., Feistner, H., 1979. Semliki forest virus: cause of a fatal case of human encephalitis. Science (New York, N.Y.) 203 (4385), 1127–1129.
Woźniak, E., Tyczewska, A., Twardowski, T., 2021. A shift towards biotechnology: social opinion in the EU. Trends Biotechnol. 39 (3), 214–218.
Wu, P., Yu, X., Wang, P., Cheng, G., 2019. Arbovirus lifecycle in mosquito: acquisition, propagation and transmission. Expert Rev. Mol. Med. 21, e1.
Wu, X., Hong, H., Yue, J., Wu, Y., Li, X., Jiang, L., Li, L., Li, Q., Gao, G., Yang, X., 2010. Inhibitory effect of small interfering RNA on dengue virus replication in mosquito cells. Virol. J. 7, 270.
Yang, W., Wang, B., Lei, G., Chen, G., Liu, D., 2022. Advances in nanocarriers to improve the stability of dsRNA in the environment. Front. Bioeng. Biotechnol. 10, 974646.
Yu, N., Christiaens, O., Liu, J., Niu, J., Cappelle, K., Caccia, S., Huvenne, H., Smagghe, G., 2013. Delivery of dsRNA for RNAi in insects: an overview and future directions. Insect. Sci. 20 (1), 4–14.
Zhang, X., Zhang, J., Zhu, K.Y., 2010. Chitosan/double-stranded RNA nanoparticle-mediated RNA interference to silence chitin synthase genes through larval feeding in the African malaria mosquito (Anopheles gambiae). Insect Mol. Biol. 19 (5), 683–693.
Zhu, K.Y., Palli, S.R., 2020. Mechanisms, applications, and challenges of insect RNA interference. Annu. Rev. Entomol. 65, 293–311.

Inhibition of Semliki Forest virus replication with long double-stranded RNA in *Aedes albopictus* cells

Alejandra Centurión[a,b], Bodunrin Omokungbe[a,c], Sabrina Stiehler[c], Andreas Vilcinskas[a,b,c], Kornelia Hardes[a,b,d]

[a] Centre for Translational Biodiversity Genomics (LOEWE TBG), Senckenberganlage 25, 60325 Frankfurt am Main, Germany
[b] Fraunhofer Institute for Molecular Biology and Applied Ecology IME, Branch of Bioresources, Ohlebergsweg 12, 35392 Giessen, Germany
[c] Institute for Insect Biotechnology, Justus-Liebig University, Heinrich-Buff-Ring 26-32, 35392 Giessen, Germany
[d] BMBF Junior Research Group in Infection Research „ASCRIBE", Ohlebergsweg 12, 35392 Giessen, Germany

Correspondence:
Dr. Kornelia Hardes
kornelia.hardes@ime.fraunhofer.de
Fraunhofer Institute for Molecular Biology and Applied Ecology IME, Branch of Bioresources, Ohlebergsweg 12, 35392 Giessen, Germany

SUPPLEMENTARY MATERIAL

Table S1. Strains with complete genome sequences of SFV strains in NCBI.

Strains	NCBI accession number
SFV6	KT009012.1
SFV L10 isolate	KP271965.1
SFV4	KP699763.1
SFV NIV8913590	MH426977.1
SFV	NC_003215.1
SFV L10	AY112987.1
SFV Tanzania53	MK280688.1
SFV Me Tri 5-71	MH880789.1
SFV Vietnam	EU350586.1

Table S2. Homology between genome sequences of SFV strains.

	SFV	SFV4	SFV6	SFV L10	SFV L10 isolate	SFV Me tri 5-71	SFV NIV89 13590	SFV Tanzania53	SFV Viet Nam
SFV		99.729	99.712	99.667	99.694	97.282	99.546	97.333	97.278
SFV4	99.729		99.948	99.746	99.895	97.478	99.747	97.529	97.474
SFV6	99.712	99.948		99.798	99.948	97.512	99.782	97.581	97.508
SFV L10	99.667	99.746	99.798		99.833	97.368	99.649	97.445	97.364
SFV L10 isolate	99.694	99.895	99.948	99.833		97.529	99.799	97.598	97.525
SFV Me tri 5-71	97.282	97.478	97.512	97.368	97.529		97.700	99.829	99.953
SFV NIV89 13590	99.546	99.747	99.782	99.649	99.799	97.700		97.777	97.679
SFV Tanzania53	97.333	97.529	97.581	97.445	97.598	99.829	97.777		99.808
SFV Viet Nam	97.278	97.474	97.508	97.364	97.525	99.953	97.679	99.808	

Table S3. List of primers used for dsRNA synthesis. The T7 promoter sequence is highlighted in italics. SFV6 genome (Accession number: KT009012.1) was used as template for their design. FW: forward, RV: reverse.

Gene-specific primer	**Abbreviation**	**Primer sequence 5'→3'**
nsP1-T7	nsP1-dsRNA	FW: *TAATACGACTCACTATAGGG* TTCGCACCTGGCTACCAAAT RV: *TAATACGACTCACTATAGGG* AGCGCGTCAAACATAAACGG
nsP2-T7	nsP2-dsRNA	FW: *TAATACGACTCACTATAGGG* GTGTTATGCGGAGACCCCAA RV: *TAATACGACTCACTATAGGG* TCCACACCAGCCTATCCTCA
nsP3-T7	nsP3-dsRNA	FW: *TAATACGACTCACTATAGGG* AGACTGCAAGAGGCAAACGA RV: *TAATACGACTCACTATAGGG* GCCGTCACTACTATGGGAGC
nsP4-T7	nsP4-dsRNA	FW: *TAATACGACTCACTATAGGG* TGCTTGGACAGAGCGACATT RV: *TAATACGACTCACTATAGGG* TGGCTCCGCTGCTTGAATTA
E2-T7	E2-dsRNA	FW: *TAATACGACTCACTATAGGG* ATCAACAGACCACAGCGGAG RV: *TAATACGACTCACTATAGGG* ATCTGGGTGAAGGTGCAGTG
E1-T7	E1-dsRNA	FW: *TAATACGACTCACTATAGGG* TTGAAACCAGCCTCGAACCA RV: *TAATACGACTCACTATAGGG* ATCTTGTTGTCGAACGGGGT
mCherry-T7	mCH-dsRNA	FW: *TAATACGACTCACTATAGGG* GCGTGATGAACTTCGAGGAC RV: *TAATACGACTCACTATAGGG* CTTGTACAGCTCGTCCATGC
GFP-T7	GFP-dsRNA	FW: *CCCTTTAATACGACTCACTATAGGG* AGAACCACATGAAGCAGCACGACTT RV: *CCCTTTAATACGACTCACTATAGGG* AGAGTCCATGCCGAGAGTGATCCCG

Table S4. dsRNAs constructs. SFV6 genome (Accession number: KT009012.1) was used as template for their synthesis.

Name	dsRNA length	dsRNA begin	dsRNA end	dsRNA G-C content (%)
nsP1-dsRNA	435	217	651	53.8
Template sequence	TTCGCACCTGGCTACCAAATTGATCGAGCAGGAGACTGACAAAGACACACTCATCTTGGA TATCGGCAGTGCGCCTTCCAGGAGAATGATGTCTACGCACAAATACCACTGCGTATGCCC TATGCGCAGCGCAGAAGACCCCGAAAGGCTCGTATGCTACGCAAAGAAACTGGCAGCGGC CTCCGGGAAGGTGCTGGATAGAGAGATCGCAGGAAAAATCACCGACCTGCAGACCGTCAT GGCTACGCCAGACGCTGAATCTCCTACCTTTTGCCTGCATACAGACGTCACGTGTCGTAC GGCAGCCGAAGTGGCCGTATACCAGGACGTGTATGCTGTACATGCACCAACATCGCTGTA CCATCAGGCGATGAAAGGTGTCAGAACGGCGTATTGGATTGGGTTTGACACCACCCCGTT TATGTTTGACGCGCT			
nsP2-dsRNA	445	2,522	2,966	52.6
Template sequence	GTGTTATGCGGAGACCCCAAGCAATGCGGATTCTTCAATATGATGCAGCTTAAGGTGAAC TTCAACCACAACATCTGCACTGAAGTATGTCATAAAAGTATATCCAGACGTTGCACGCGT CCAGTCACGGCCATCGTGTCTACGTTGCACTACGGAGGCAAGATGCGCACGACCAACCCG TGCAACAAACCCATAATCATAGACACCACAGGACAGACCAAGCCCAAGCCAGGAGACATC GTGTTAACATGCTTCCGAGGCTGGGTAAAGCAGCTGCAGTTGGACTACCGTGGACACGAA GTCATGACAGCAGCAGCATCTCAGGGCCTCACCCGCAAAGGGGTATACGCCGTAAGGCAG AAGGTGAATGAAAATCCCTTGTATGCCCCTGCGTCGGAGCACGTGAATGTACTGCTGACG CGCACTGAGGATAGGCTGGTGTGGA			
nsP3-dsRNA	473	4,757	5,229	53.7
Template sequence	AGACTGCAAGAGGCAAACGAACAGATATGCCTATACGCGCTGGGCGAAACAATGGACAAC ATCAGATCCAAATGTCCGGTGAACGATTCCGATTCATCAACACCTCCCAGGACAGTGCCC TGCCTGTGCCGCTACGCAATGACAGCAGAACGGATCGCCCGCCTTAGGTCACACCAAGTT AAAAGCATGGTGGTTTGCTCATCTTTTCCCCTCCCGAAATACCATGTAGATGGGGTGCAG AAGGTAAAGTGCGAGAAGGTTCTCCTGTTCGACCCGACGGTACCTTCAGTGGTTAGTCCG CGGAAGTATGCCGCATCTACGACGGACCACTCAGATCGGTCGTTACGAGGGTTTGACTTG GACTGGACCACCGACTCGTCTTCCACTGCCAGCGATACCATGTCGCTACCCAGTTTGCAG TCGTGTGACATCGACTCGATCTACGAGCCAATGGCTCCCATAGTAGTGACGGC			
nsP4-dsRNA	480	6,011	6,490	53.1
Template sequence	TGCTTGGACAGAGCGACATTCTGCCCGGCGAAGCTCCGGTGCTACCCGAAACATCATGCG TACCACCAGCCGACTGTACGCAGTGCCGTCCCGTCACCCTTTCAGAACACACTACAGAAC GTGCTAGCGGCCGCCACCAAGAGAAACTGCAACGTCACGCAAATGCGAGAACTACCCACC ATGGACTCGGCAGTGTTCAACGTGGAGTGCTTCAAGCGCTATGCCTGCTCCGGAGAATAT TGGGAAGAATATGCTAAACAACCTATCCGGATAACCACTGAGAACATCACTACCTATGTG ACCAAATTGAAAGGCCCGAAAGCTGCTGCCTTGTTCGCTAAGACCCACAACTTGGTTCCG CTGCAGGAGGTTCCCATGGACAGATTCACGGTCGACATGAAACGAGATGTCAAAGTCACT CCAGGGACGAAACACACAGAGGAAAGACCCAAAGTCCAGGTAATTCAAGCAGCGGAGCCA			
E2-dsRNA	401	8,888	9,288	51.1
Template sequence	ATCAACAGACCACAGCGGAGACCGTGGAGGAAATCGACATGCATATGCCGCCAGATACGC CGGACAGGACGTTGCTATCACAGCAATCTGGCAATGTAAAGATCACAGTCGGAGGAAAGA AGGTGAAATACAACTGCACCTGTGGAACCGGAAACGTTGGCACTACTAATTCGGACATGA CGATCAACACGTGTCTAATAGAGCAGTGCCACGTCTCAGTGACGGACCATAAGAAATGGC AGTTCAACTCACCTTTCGTCCCGAGAGCCGACGAACCGGCTAGAAAAGGCAAAGTCCATA TCCCATTCCCGTTGGACAACATCACATGCAGAGTTCCAATGGCGCGCGAACCAACCGTCA TCCACGGCAAAAGAGAAGTGACACTGCACCTTCACCCAGAT			
E1-dsRNA	430	9,968	10,397	53
Template sequence	TTGAAACCAGCCTCGAACCAACCCTTAATTTGGAATACATAACCTGTGAGTACAAGACGG TCGTCCCGTCGCCGTACGTGAAGTGCTGCGGCGCCTCAGAGTGCTCCACTAAAGAGAAGC CTGACTACCAATGCAAGGTTTACACAGGCGTGTACCCGTTCATGTGGGGAGGGGCATATT GCTTCTGCGACTCAGAAAACACGCAACTCAGCGAGGCGTACGTCGATCGATCGGACGTAT GCAGGCATGATCACGCATCTGCTTACAAAGCCCATACAGCATCGCTGAAGGCCAAAGTGA GGGTTATGTACGGCAACGTAAACCAGACTGTGGATGTTTACGTGAACGGAGACCATGCCG TCACGATAGGGGGTACTCAGTTCATATTCGGGCCGCTGTCATCGGCCTGGACCCCGTTCG ACAACAAGAT			

Table S5. Homology of dsRNAs to viral target regions of the different SFV strains**.** dsRNAs were designed for SFV6.

	SFV Viet Nam	SFV Tanzania53	SFV NIV8913590	SFV Me Tri 5-71	SFV L10 isolate	SFV L10	**SFV6**	SFV4	SFV
nsP1	99.77	99.77	99.77	99.54	100	100	**100**	100	99.31
nsP2	100	100	100	100	100	99.10	**100**	100	99.78
nsP3	99.47	99.37	99.37	99.37	100	100	**100**	100	99.37
nsP4	99.58	100	100	99.58	100	99.79	**100**	100	100
E2	99.50	99.50	99.75	99.50	100	100	**100**	99.75	100
E1	100	100	100	100	100	100	**100**	100	100

Table S6. Primers used for gene knockdown assay. FW: forward, RV: reverse.

Gene-specific primer	**Primer sequence 5'→3'**	**Amplicon size**
nsP4	FW: ACTCCCCTACCGTGATCGAA RV: AATGTCGCTCTGTCCAAGCA	172
Actin	FW: AGATCCTGACTGAACGTGGC RV: CGTCGGGAAGTTCGTAGGAC	162

Supplementary information S1. Annotation of SFV strains: Viet Nam, Tanzania53 and Me Tri 5-71:

nsP1 nsP2 nsP3 nsP4 Capsid E3 E2 6kDa E1

SFV Viet Nam (EU350586.1)

ATGGCCGCCAAAGTGCATGTTGATATTGAGGCTGACAGCCCATTCATCAAGTCTTTGCAGAAGGCA
TTTCCGTCGTTCGAGGTGGAGTCATTGCAGGTCACACCAAATGACCATGCAAATGCCAGAGCATTT
TCGCACCTGGCTACCAAATTGATCGAGCAGGAGACTGACAAAGACACACTCATCTTGGATATCGGC
AGTGCGCCTTCCAGGAGAATGATGTCTACGCACAAATACCACTGCGTATGCCCTATGCGCAGCGCA
GAAGACCCCGAAAGGCTCGTATGCTACGCAAAGAAACTGGCAGCGGCCTCCGGGAAGGTGCTGGA
TAGAGAGATCGCAGGGAAAATCACCGACCTGCAGACCGTCATGGCTACGCCAGACGCTGAATCTC
CTACCTTTTGCCTGCATACAGACGTCACGTGTCGTACGGCAGCCGAAGTGGCCGTATACCAGGACG
TGTATGCTGTACATGCACCAACATCGCTGTACCATCAGGCGATGAAAGGTGTCAGAACGGCGTATT
GGATTGGGTTTGACACCACCCCGTTTATGTTTGACGCGCTAGCAGGCGCGTATCCAACCTACGCCA
CAAACTGGGCCGACGAGCAGGTGTTACAGGCCAGGAACATAGGACTGTGTGCAGCATCCTTGACT
GAGGGAAGACTCGGCAAACTGTCCATTCTCCGCAAGAAGCAATTGAAACCTTGCGACACAGTCAT
GTTCTCGGTAGGATCTACATTGTACACTGAGAGCAGAAAGCTACTGAGGAGCTGGCACTTACCCTC
CGTATTCCACCTGAAAGGTAAACAATCCTTTACCTGTAGGTGCGATACCATCGTATCATGTGAAGG
GTACGTAGTTAAGAAAATCACTATGTGCCCCGGCCTGTACGGTAAAACGGTAGGGTACGCCGTGAC
GTATCACGCGGAGGGATTCCTAGTGTGCAAGACCACAGACACTGTCAAAGGAGAAAGAGTCTCAT
TCCCTGTATGCACCTACGTCCCCTCAACCATCTGTGATCAAATGACTGGCATACTAGCGACCGACGT
CACACCGGAGGACGCACAGAAGTTGTTAGTGGGATTGAATCAGAGGATAGTTGTGAACGGAAGAA
CACAGCGAAACACTAACACGATGAAGAACTATCTGCTTCCGATTGTGGCCGTCGCATTTAGCAAGT
GGGCGAGGGAATACAAGGCAGACCTTGATGATGAAAAACCTCTGGGTGTCCGAGAGAGGTCACTT
ACTTGCTGCTGCTTGTGGGCATTTAAAACGAAGAAGATGCACACCATGTACAAGAAACCAGACACC
CAGACAATAGTGAAGGTGCCTTCAGAGTTTAACTCGTTCGTCATCCCGAGCCTATGGTCTACAGGC
CTCGCAATCCCAGTCAGATCACGCATTGAGATGCTTTTGGCCAAGAAGACCAAGCGAGAGTTAATG
CCTGTTCTCGACGCGTCGTCAGCCAGGGATGCTGAACAAGAGGAGAAGGAGAGGTTGGAGGCCGA
GCTGACTAGAGAAGCCTTACCACCCCTCGTCCCCATCGCGCCGGCGGAGACGGGAGTCGTCGACGT
CGACGTTGAAGAACTAGAGTATCACGCAGGTGCAGGGGTCGTGGAAACACCTCGCAGCGCGTTGA
AAGTCACCGCACAGCCGAACGACGTACTACTAGGAAATTACGTAGTTCTGTCCCCGCAGACCGTGC
TCAAGAGCTCCAAGTTGGCCCCCGTGCACCCTCTAGCAGAGCAGGTGAAAATAATAACACATAAC
GGGAGGGCCGGCCGTTACCAGGTCGACGGATATGACGGCAGGGTCCTACTACCATGTGGATCGGC
CATTCCGGTCCCTGAGTTTCAAGCTTTGAGCGAGAGCGCCACTATGGTGTACAACGAAAGGGAATT
CGTCAACAGGAAACTATACCATATTGCCGTTCACGGACCGTCGTTGAACACCGACGAGGAGAACTA
CGAGAAAGTCAGAGCTGAAAGAACTGACGCCGAGTACGTGTTCGACGTAGATAAAAAATGCTGCG
TCAAGAGAGAGGAAGCGTCGGGTTTGGTGTTGGTGGGAGAGCTAACCAACCCCCCGTTCCATGAAT
TCGCCTACGAAGGGCTGAAGATCAGGCCGTCGGCACCATATAAGACTACAGTAGTAGGAGTCTTTG
GGGTTCCGGGATCAGGCAAGTCTGCTATTATTAAGAGCCTCGTGACCAAACACGATCTGGTCACCA
GCGGCAAGAAGGAGAACTGCCAGGAAATAGTCAACGACGTGAAGAAGTACCGCGGACTGGACAT
CCAGGCAAAAACAGTGGACTCCATCCTGCTAAACGGGTGTCGTCGTGCCGTGGACATCCTATATGT
GGACGAGGCTTTCGCTTGCCATTCCGGTACTCTGCTGGCCCTAATTGCTCTTGTTAAACCTCGGAGC
AAAGTGGTGTTATGCGGAGACCCCAAGCAATGCGGATTCTTCAATATGATGCAGCTTAAGGTGAAC
TTCAACCACAACATCTGCACTGAAGTATGTCATAAAAGTATATCCAGACGTTGCACGCGTCCAGTC
ACGGCCATCGTGTCTACGTTGCACTACGGAGGCAAGATGCGCACGACCAACCCGTGCAACAAACC
CATAATCATAGACACCACAGGACAGACCAAGCCCAAGCCAGGAGACATCGTGTTAACATGCTTCC
GAGGCTGGGTAAAGCAGCTGCAGTTGGACTACCGTGGACACGAAGTCATGACAGCAGCAGCATCT
CAGGGCCTCACCCGCAAAGGGGTATACGCCGTAAGGCAGAAGGTGAATGAAAATCCCTTGTATGC
CCCTGCGTCGGAGCACGTGAATGTACTGCTGACGCGCACTGAGGATAGGCTGGTGTGGAAAACGCT
GGCCGGCGATCCCTGGATTAAGGTCCTATCAAACATTCCACAGGGTAACTTTATGGCCACATTGGA
AGAATGGCAAGAAGAACACGACAAAATAATGAAGGTGATTGAAGGACCGGCTGCGCCTGTGGACG
CGTTCCAGAACAAAGCGAACGTGTGTTGGGCGAAAAGCCTGGTGCCTGTCCTGGACACTGCCGGA
ATCAGATTGACAGCAGAGGAGTGGAGCACCATAATTACAGCATTTAAGGAGGACAGAGCTTACTC
TCCAGAGGTGGCCTTGAATGAAATTTGCACCAAGTACTATGGAGTTGACCTGGACAGTGGCCTGTT
TTCTGCCCCGAAGGTGTCCCTGTATTACGAGAACAACCACTGGGATAACAGACCTGGTGGAAGGAT
GTATGGATTCAATGCCGCAACAGCTGCCAGGCTGGAAGCTAGACATACCTTCCTGAAGGGGCAGTG
GCATACGGGCAAGCAGGCAGTTATCGCAGAAAGAAAAATCCAACCGCTTTCTGTGCTGGACAATG
TAATTCCTATCAACCGCAGGCTGCCGCACGCCCTGGTGGCTGAGTACAAGACGGTTAAAGGCAGTA
GGGTTGAGTGGCTGGTCAATAAAGTAAGAGGGTACCACGTTCTGCTGGTGAGTGAGTACAACCTGG
CTTTGCCTCGACGCAGGGTCACTTGGTTGTCACCGCTGAATGTCACAGGCGCCGATAGGTGCTACG
ACCTAAGTTTAGGACTGCCGGCTGACGCCGGCAGATTCGACTTGGTCTTTGTGAACATTCACACGG

AATTCAGAATCCACCACTACCAGCAGTGTGTCGACCACGCCATGAAGCTGCAGATGCTTGGGGGAG
ATGCGTTACGACTGCTAAAACCCGGCGGCAGCCTCTTGATGAGAGCTTACGGATACGCCGATAAAA
TCAGCGAAGCCGTTGTTTCCTCCTTAAGCAGAAAGTTCTCGTCTGCAAGAGTGTTGCGCCCGGATTG
TGTCACCAGCAATACAGAAGTGTTCTTGCTGTTCTCCAACTTTGACAACGGAAAGAGACCCTCTAC
GCTACACCAGATGAATACCAAGCTGAGTGCCGTGTATGCCGGAGAAGCCATGCACACGGCCGGGT
GTGCACCATCCTACAGAGTTAAGAGAGCAGACATAGCCACGTGCACAGAAGCGGCTGTGGTTAAC
GCAGCTAACGCCCGTGGAACTGTAGGGGATGGCGTATGCAGGGCCGTGGCGAAGAAATGGCCGTC
AGCCTTTAAGGGAGCAGCAACACCAGTGGGCACAATTAAAACAGTCATGTGCGGCTCGTACCCCGT
CATCCACGCTGTAGGGCCTAATTTCTCTGCCACGACTGAAGCGGAAGGGGACCGCGAATTGGCCGC
TGTCTACCGGGCAGTGGCCGCCGAAGTAAACAGACTGTCACTGAGCAGCGTAGCCATCCCGCTGCT
GTCCACAGGAGTGTTCAGCGGCGGAAGAGATAGGCTGCAGCAATCCCTCAACCATCTATTCACAGC
AATGGACGCCACGGACGCTGACGTGACCATCTACTGCAGAGACAAAAGTTGGGAGAAGAAAATCC
AGGAAGCCATAGACATGAGGACGGCTGTGGAGTTGCTCAATGATGACGTGGAGCTGACCACAGAC
TTGGTGAGAGTGCACCCGGACAGCAGCCTGGTGGGTCGTAAGGGCTACAGTACCACTGACGGGTC
GCTGTACTCGTACTTGGAAGGTACGAAATTCAACCAGGCTGCTATTGATATGGCAGAGATACTGAC
GTTGTGGCCCAGACTGCAAGAGGCAAACGAACAGATATGCCTATACGCGCTGGGCGAAACAATGG
ACAACATCAGATCCAAATGTCCGGTGAACGATTCCGATTCATCATCACCTCCCAGGACAGTGCCCT
GCCTGTGCCGCTACGCAATGACAGCAGAACGGATCGCCCGCCTTAGGTCACACCAAGTTAAAAGC
ATGGTGGTTTGCTCATCTTTTCCCCTCCCGAAATACCATGTAGATGGGGTGCAGAAGGTAAAGTGC
GAGAAGGTTCTCCTGTTCGACCCGACGGTACCTTCAGTGGTTAGTCCGCGGAAGTATGCCGCATCG
ACGACGGACCACTCAGATCGGTCGTTACGAGGGTTTGACTTGGACTGGACCACCGACTCGTCTTCC
ACTGCCAGCGATACCATGTCGCTACCCAGTTTGCAGTCGTGTGACATCGACTCGATCTACGAGCCA
ATRGCTCCCATAGTAGTGACGGCTGACGTACACCCTGAACCCGCAGGCATCGCGGACCTGGCGGCA
GATGTGCATCCTGAACCCGCAGACCATGTGGACCTCGAGAACCCGATTCCTCCACCGCGCCCGAAG
AGAGCTGCATACCTTGCCTCCCGCGCGGCGGAGCGACCGGTGCCGGCGCCGAGAAAGCCGACGCC
TGCCCCAAGGACTGCGTTTAGGAACAAGCTGCCTTTGACGTTCGGCGACTTTGACGAGCACGAGGT
CGATGCGTTGGCCTCCGGGATTACTTTCGGAGACTTCGACGACGTCCTGTGACTAGGCCGCGCGGG
TGCATATATTTTCTCCTCGGACACTGGCAGCGGACATTTACAACAAAAATCCGTTAGGCAGCACAA
TCTCCAGTGCGCACAACTGGATGCGGTCGAGGAGGAGAAAATGTACCCGCCAAAATTGGATACTG
AGAGGGAGAAGCTGTTGCTGCTGAAAATGCAGATGCACCCATCGGAGGCTAATAAGAGTCGATAC
CAGTCTCGCAAAGTGGAGAACATGAAAGCCACGGTGGTGGACAGGCTCACATCGGGGGCCAGATT
GTACACGGGAGCGGACGTAGGCCGCATACCAACATACGCGGTTCGGTACCCCCGCCCCGTGTACTC
CCCTACCGTGATCGAAAGATTCTCAAGCCCCGATGTAGCAATCGCAGCGTGCAACGAATACCTATC
CAGAAATTACCCAACAGTGGCGTCGTACCAGATAACAGATGAATACGACGCATACTTGGACATGG
TTGACGGGTCGGAGAGTTGCTTGGACAGAGCGACATTCTGCCCGGCGAAGCTCCGGTGCTACCCGA
AACATCATGCGTACCACCAGCCGACTGTACGCAGTGCCGTCCCGTCACCCTTTCAGAACACACTAC
AGAACGTGCTAGCGGCCGCCACCAAGAGAAACTGCAACATCACGCAAATGCGAGAACTACCCACC
ATGGACTCGGCAGTGTTCAACGTGGAGTGCTTCAAGCGCTATGCCTGCTCCGGAGAATATTGGGAA
GAATATGCTAAACAACCTATCCGGATAACCACTGAGAACATCACTACCTATGTGACCAAATTGAAA
GGCCCGAAAGCTGCTGCCTTGTTCGCTAAGACCCACAACTTGGTTCCGCTGCAGGAGGTTCCCATG
GACAGATTCACGGTCGACATGAAACGAGATGTCAAAGCCACTCCAGGGACGAAACACACAGAGGA
AAGACCCAAAGTCCAGGTAATTCAAGCAGCGGAGCCATTGGCGACCGCTTACCTGTGCGGCATCCA
CAGGGAATTAGTAAGGAGACTAAATGCTGTGTTACGCCCTAACGTGCACACATTGTTTGATATGTC
GGCCGAAGACTTTGACGCGATCATCGCCTCTCACTTCCACCCAGGAGACCCGGTTCTAGAGACGGA
CATTGCATCATTCGACAAAAGCCAGGACGACTCCTTGGCTCTTACAGGTTTAATGATCCTCGAAGA
TCTAGGGGTGGATCAGTACCTGCTGGACTTGATCGAGGCAGCCTTTGGGGAAATATCCAGCTGTCA
CCTACCAACTGGCACGCGCTTCAAGTTCGGAGCTATGATGAAATCGGGCATGTTTCTGACTTTGTTT
ATTAACACTGTTTTGAACATCACCATAGCAAGCAGGGTACTGGAGCAGAGACTCACTGACTCCGCC
TGTGCGGCCTTCATCGGCGACGACAACATCGTTCACGGAGTGATCTCCGACAAGCTGATGGCGGAG
AGGTGCGCGTCGTGGGTCAACATGGAGGTGAAGATCATTGACGCTGTCATGGGCGAAAAACCCCC
ATATTTTTGTGGGGGATTCATAGTTTTTGACAGCGTCACACAGACCGCCTGCCGTGTTTCAGACCCA
CTTAAGCGCCTGTTCAAGTTGGGTAAGCCGCTAACAGCTGAAGACAAGCAGGACGAAGACAGGCG
ACGAGCACTGAGTGACGAGGTTAGCAAGTGGTTCCGGACAGGCTTGGGGGCCGAACTTGAGGTGG
CACTAACATCTAGGTATGAGGTAGAGGGCTGCAAAAGTATCCTCATAGCCATGGCCACCTTGGCGA
GGGACATTAAGGCGTTTAAGAAATTGAGAGGACCTGTTATACACCTCTACGGCGGTCCTAAATTGG
TGCGTTAATACACAGAATTCTGATTATAGCGCACTATTATAGCACCATGAATTACATCCCTACGCA
AACGTTTTACGGCCGCCGGTGGCGCCCGCGCCCGGCGGCCCGTCCCTGGCCGTTGCAGGCCACTCC
GGTGGCTCCCGTCGTCCCCGACTTCCAGGCCCAGCAGATGCAGCAACTCATCAGCGCCGTAAATGC
GCTGACAATGAGACAGAACGCAATTGCTCCTGCTAGGCCTCCCAAACCAAAGAAGAAGAAGACAA
CCAAACCAAAGCCGAAAACGCAGCCCAAGAAGATCAAAGGAAAAACGCAGCAGCAAAAGAAGAA
AGACAAGCAAGCCGACAAGAAGAAGAAGAAACCCGGAAAAAGAGAAAGAATGTGCATGAAGATT
GAAAATGACTGTATCTTCGAAGTCAAACACGAAGGAAAGGTCACTGGGTACGCCTGCCTGGTGGG

CGACAAAGTCATGAAACCTGCCCACGTGAAAGGAGTCATCGACAACGCGGACCTGGCAAAGCTAG
CTTTCAAGAAATCGAGCAAGTATGACCTTGAGTGTGCCCAGATACCAGTTCACATGAGGTCGGATG
CCTCAAAGTACACGCATGAGAAGCCCGAGGGACACTATAACTGGCACCACGGGGCTGTTCAGTAC
AGCGGAGGTAGGTTCACTATACCGACAGGAGCGGGCAAACCGGGAGACAGTGGCCGGCCCATCTT
TGACAACAAGGGGAGGGTAGTCGCTATCGTCCTGGGCGGGGCCAACGAGGGCTCACGCACAGCAC
TGTCGGTGGTCACCTGGAACAAAGATATGGTGACTAGAGTGACCCCCGAGGGGTCCGAAGAGTGG
TCCGCCCCGCTGATTACTGCCATGTGTGTCCTTGCCAATGCTACCTTCCCGTGCTTCCAGCCCCCGT
GTGTACCTTGCTGCTATGAAAACAACGCAGAGGCCACACTACGGATGCTCGAGGATAACGTGGAT
AGGCCAGGGTACTACGACCTCCTTCAGGCAGCCTTGACGTGCCGAAACGGAACAAGACACCGGCG
CAGCGTGTCGCAACACTTCAACGTGTATAAGGCTACACGCCCTTACATCGCGTACTGCGCCGACTG
CGGAGCAGGGCACTCGTGTCATAGCCCCGTAGCAATTGAAGCGATCAGGTCCGAAGCTACCGACG
GGATGCTGAAGATTCAGTTCTCGGCACAAATTGGCATAGATAAGAGTGACAATCATGACTACACGA
AGATAAGGTACGCAGACGGGCACGCCATTGAGAATGCCGTCCGGTCATCTTTGAAGGTAGCCACCT
CCGGAGACTGTTTCGTCCATGGCACAATGGGACATTTCATACTGGCAACGTGCCCACCGGGTGAAT
TTCTGCAGGTCTCGATCCAGGACACCAGAAACGCGGTCCGTGCCTGCAGAATACAATATCATCATG
ACCCTCAACCGGTGGGTAGAGAAAAATTTACAATTAGACCACACTATGGAAAAGAGATCCCTTGC
ACCACTTATCAACAGACCACAGCGGAGACCGTGGAGGAAATCGACATGCATATGCCGCCAGATAC
GCCGGACAGGACGTTGCTATCACAGCAATCTGGCAATGTAAAGATCACAGTCGGAGGAAAGAAGG
TGAAATACAACTGCACCTGTGGAACCGGAAACGTTGGCACTACTAATTCGGACAAGACGATCAAC
ACGTGTCTAATAGAGCAGTGCCACGTCTCAGTGACGGACCATAAGAAATGGCAGTTCAACTCACCT
TTCGTCCCGAGAGCCGACGAACCGGCTAGAAAAGGCAAAGTCCATATCCCATTCCCGTTGGACAAC
ATCACATGCAGAGTTCCAATGGCGCGCGAACCAACCGTCATCCACGGCAAAAGAAAAGTGACACT
GCACCTTCACCCAGATCATCCCACGCTCTTTTCCTACCGCACACTGGGTGAGGACCCGCAGTATCAC
GAGGAATGGGTGACAGCGGCGGTGGAACGGACCATACCCGTACCAGTGGACGGGATGGAGTACCA
CTGGGGAAACAACGACCCAGTGAGGCTTTGGTCTCAACTCACCACTGAAGGGAAACCGCACGGCT
GGCCGCATCAGATCGTACAGTACTACTATGGGCTTTACCCGGCCGCTACAGTATCCGCGGTCGTCG
GGATGAGCTTACTGGCGTTGATATCGATCTTCGCGTCGTGCTACATGCTGGCTGCGGCCCGCAGTA
AGTGCTTGACCCCTTATGCTTTAACACCAGGAGCTGCAGTTCCGTGGACGCTGGGGATACTCTGCT
GCGCCCCGCGGGCGCACGCAGCTAGTGTGGCAGAGACTATGGCCTACTTGTGGGACCAAAACCAA
GCGTTGTTCTGGTTGGAGTTTGCGGCCCCTGTTGCCTGCATCCTCATCATCACGTATTGCCTCAGAA
ACGTGCTGTGTTGCTGTAAGAGCCTTTCTTTTTTAGTGCTACTGAGCCTCGGGGCAACCGCCAGAGC
TTACGAACATTCGACAGTAATGCCGAACGTGGTGGGGTTCCCGTATAAGGCTCACATTGAAAGGCC
AGGATATAGCCCCCTCACTTTGCAGATGCAGGTTGTTGAAACCAGCCTCGAACCAACCCTTAATTT
GGAATACATAACCTGTGAGTACAAGACGGTCGTCCCGTCGCCGTACGTGAAGTGCTGCGGCGCCTC
AGAGTGCTCCACTAAAGAGAAGCCTGACTACCAATGCAAGGTTTACACAGGCGTGTACCCGTTCAT
GTGGGGAGGGGCATATTGCTTCTGCGACTCAGAAAACACGCAACTCAGCGAGGCGTACGTCGATC
GATCGGACGTATGCAGGCATGATCACGCATCTGCTTACAAAGCCCATACAGCATCGCTGAAGGCCA
AAGTGAGGGTTATGTACGGCAACGTAAACCAGACTGTGGATGTTTACGTGAACGGAGACCATGCC
GTCACGATAGGGGGTACTCAGTTCATATTCGGGCCGCTGTCATCGGCCTGGACCCCGTTCGACAAC
AAGATAGTCGTGTACAAAGACGAAGTGTTCAATCAGGACTTCCCGCCGTACGGATCTGGGCAACCA
GGGCGCTTCGGCGACATCCAAAGCAGAACAGTGGAGAGTAACGACCTGTACGCGAACACGGCACT
GAAGCTGGCACGCCCTTCACCCGGCACGGTCCATGTACCGTACACACAGACACCTTCAGGGTTCAA
ATATTGGCTAAAGGAAAAAGGGACAGCCCTAAATACGAAGGCTCCTTTTGGCTGCCAAATCAAAA
CGAACCCTGTCAGGGCCATGAACTGCGCCGTGGGAAACATCCCTGTCTCCATGAATTTGCCTGACA
GCGCCTTTACCCGCATTGTCGAGGCGCCGACCATCACTGACCTGACTTGCACAGTGGCTACCTGTA
CGCACTCCTCGGATTTCGGCGGCGTCTTGACACTGACGTACAAGACCGACAAGAACGGGGACTGCT
CTGTACACTCGCACTCTAACGTAGCTACTCTACAGGAGGCCACAGCAAAAGTGAAGACAGCACGT
AAGGTGACCTTACACTTCTCCACGGCAAGCGCATCACCTTCTTTTGTGGTGTCGCTATGCAGTGCTA
AGGCCACCTGTTCAGCGTCGTGTGAGCCCCCGAAAGACCACATAGTCCCATATGCGGCTAGCCACA
GTAACGTAGTGTTTCCAGACATGTCGGGCACCGCACTATCATGGGTGCAGAAAATCTCGGGTGGTC
TGGGGGCCTTCGCAATCGGCGCTATCCTGGTGCTAGTTGTGGTCACTTGCATTGGGCTCCGCAGATA
A

SFV Me Tri 5-71 (MH880789.1)

ATGGCCGCCAAAGTGCATGTTGATATTGAGGCTGACAGCCCATTCATCAAGTCTTTGCAGAAGGCA
TTTCCGTCGTTCGAGGTGGAGTCATTGCAGGTCACACCAAATGACCATGCAAATGCCAGAGCATTT
TCGCACCTGGCTACCAAATTGATCGAGCAGGAGACTGACAAAGACACACTCATCTTGGATATCGGC
AGTGCGCCTTCCAGGAGAATGATGTCTACGCACAAATACCACTGCGTATGCCCTATGCGCAGCGCA
GTAGACCCCGAAAGGCTCGTATGCTACGCAAAGAAACTGGCAGCGGCCTCCGGGAAGGTGCTGGA
TAGAGAGATCGCAGGGAAAATCACCGACCTGCAGACCGTCATGGCTACGCCAGACGCTGAATCTC
CTACCTTTTGCCTGCATACAGACGTCACGTGTCGTACGGCAGCCGAAGTGGCCGTATACCAGGACG

TGTATGCTGTACATGCACCAACATCGCTGTACCATCAGGCGATGAAAGGTGTCAGAACGGCGTATT
GGATTGGGTTTGACACCACCCCGTTTATGTTTGACGCGCTAGCAGGCGCGTATCCAACCTACGCCA
CAAACTGGGCCGACGAGCAGGTGTTACAGGCCAGGAACATAGGACTGTGTGCAGCATCCTTGACT
GAGGGAAGACTCGGCAAACTGTCCATTCTCCGCAAGAAGCAATTGAAACCTTGCGACACAGTCAT
GTTCTCGGTAGGATCTACATTGTACACTGAGAGCAGAAAGCTACTGAGGAGCTGGCACTTACCCTC
CGTATTCCACCTGAAAGGTAAACAATCCTTTACCTGTAGGTGCGATACCATCGTATCATGTGAAGG
GTACGTAGTTAAGAAAATCACTATGTGCCCCGGCCTGTACGGTAAAACGGTAGGGTACGCCGTGAC
GTATCACGCGGAGGGATTCCTAGTGTGCAAGACCACAGACACTGTCAAAGGAGAAAGAGTCTCAT
TCCCTGTATGCACCTACGTCCCCTCAACCATCTGTGATCAAATGACTGGCATACTAGCGACCGACGT
CACACCGGAGGACGCACAGAAGTTGTTAGTGGGATTGAATCAGAGGATAGTTGTGAACGGAAGAA
CACAGCGAAACACTAACACGATGAAGAACTATCTGCTTCCGATTGTGGCCGTCGCATTTAGCAAGT
GGGCGAGGGAATACAAGGCAGACCTTGATGATGAAAAACCTCTGGGTGTCCGAGAGAGGTCACTT
ACTTGCTGCTGCTTGTGGGCATTTAAAACGAAGAAGATGCACACCATGTACAAGAAACCAGACACC
CAGACAATAGTGAAGGTGCCTTCAGAGTTTAACTCGTTCGTCATCCCGAGCCTATGGTCTACAGGC
CTCGCAATCCCAGTCAGATCACGCATTGAGATGCTTTTGGCCAAGAAGACCAAGCGAGAGTTAATG
CCTGTTCTCGACGCGTCGTCAGCCAGGGATGCTGAACAAGAGGAGAAGGAGAGGTTGGAGGCCGA
GCTGACTAGAGAAGCCTTACCACCCCTCGTCCCCATCGCGCCGGCGGAGACGGGAGTCGTCGACGT
CGACGTTGAAGAACTAGAGTATCACGCAGGTGCAGGGGTCGTGGAAACACCTCGCAGCGCGTTGA
AAGTCACCGCACAGCCGAACGACGTACTACTAGGAAATTACGTAGTTCTGTCCCCGCAGACCGTGC
TCAAGAGCTCCAAGTTGGCCCCCGTGCACCCTCTAGCAGAGCAGGTGAAAATAATAACACATAAC
GGGAGGGCCGGCCGTTACCAGGTCGACGGATATGACGGCAGGGTCCTACTACCATGTGGATCGGC
CATTCCGGTCCCTGAGTTTCAAGCTTTGAGCGAGAGCGCCACTATGGTGTACAACGAAAGGGAGTT
CGTCAACAGGAAACTATACCATATTGCCGTTCACGGACCGTCGTTGAACACCGACGAGGAGAACTA
CGAGAAAGTCAGAGCTGAAAGAACTGACGCCGAGTACGTGTTCGACGTAGATAAAAAATGCTGCG
TCAAGAGAGAGGAAGCGTCGGGTTTGGTGTTGGTGGGAGAGCTAACCAACCCCCCGTTCCATGAAT
TCGCCTACGAAGGGCTGAAGATCAGGCCGTCGGCACCATATAAGACTACAGTAGTAGGAGTCTTTG
GGGTTCCGGGATCAGGCAAGTCTGCTATTATTAAGAGCCTCGTGACCAAACACGATCTGGTCACCA
GCGGCAAGAAGGAGAACTGCCAGGAAATAGTCAACGACGTGAAGAAGTACCGCGGACTGGACAT
CCAGGCAAAAACAGTGGACTCCATCCTGCTAAACGGGTGTCGTCGTGCCGTGGACATCCTATATGT
GGACGAGGCTTTCGCTTGCCATTCCGGTACTCTGCTGGCCCTAATTGCTCTTGTTAAACCTCGGAGC
AAAGTGGTGTTATGCGGAGACCCCAAGCAATGCGGATTCTTCAATATGATGCAGCTTAAGGTGAAC
TTCAACCACAACATCTGCACTGAAGTATGTCATAAAAGTATATCCAGACGTTGCACGCGTCCAGTC
ACGGCCATCGTGTCTACGTTGCACTACGGAGGCAAGATGCGCACGACCAACCCGTGCAACAAACC
CATAATCATAGACACCACAGGACAGACCAAGCCCAAGCCAGGAGACATCGTGTTAACATGCTTCC
GAGGCTGGGTAAAGCAGCTGCAGTTGGACTACCGTGGACACGAAGTCATGACAGCAGCAGCATCT
CAGGGCCTCACCCGCAAAGGGGTATACGCCGTAAGGCAGAAGGTGAATGAAAATCCCTTGTATGC
CCCTGCGTCGGAGCACGTGAATGTACTGCTGACGCGCACTGAGGATAGGCTGGTGTGGAAAACGCT
GGCCGGCGATCCCTGGATTAAGGTCCTATCAAACATTCCACAGGGTAACTTTATGGCCACATTGGA
AGAATGGCAAGAAGAACACGACAAAATAATGAAGGTGATTGAAGGACCGGCTGCGCCTGTGGACG
CGTTCCAGAACAAAGCGAACGTGTGTTGGGCGAAAAGCCTGGTGCCTGTCCTGGACACTGCCGGA
ATCAGATTGACAGCAGAGGAGTGGAGCACCATAATTACAGCATTTAAGGAGGACAGAGCTTACTC
TCCAGAGGTGGCCTTGAATGAAATTTGCACCAAGTACTATGGAGTTGACCTGGACAGTGGCCTGTT
TTCTGCCCCGAAGGTGTCCCTGTATTACGAGAACAACCACTGGGATAACAGACCTGGTGGAAGGAT
GTATGGATTCAATGCCGCAACAGCTGCCAGGCTGGAAGCTAGACATACCTTCCTGAAGGGGCAGTG
GCATACGGGCAAGCAGGCAGTTATCGCAGAAAGAAAAATCCAACCGCTTTCTGTGCTGGACAATG
TAATTCCTATCAACCGCAGGCTGCCGCACGCCCTGGTGGCTGAGTACAAGACGGTTAAAGGCAGTA
GGGTTGAGTGGCTGGTCAATAAAGTAAGAGGGTACCACGTTCTGCTGGTGAGTGAGTACAACCTGG
CTTTGCCTCGACGCAGGGTCACTTGGTTGTCACCGCTGAATGTCACAGGCGCCGATAGGTGCTACG
ACCTAAGTTTAGGACTGCCGGCTGACGCCGGCAGATTCGACTTGGTCTTTGTGAACATTCACACGG
AATTCAGAATCCACCACTACCAGCAGTGTGTCGACCACGCCATGAAGCTGCAGATGCTTGGGGGAG
ATGCGTTACGACTGCTAAAACCCGGCGGCAGCCTCTTGATGAGAGCTTACGGATACGCCGATAAAA
TCAGCGAAGCCGTTGTTTCCTCCTTAAGCAGAAAGTTCTCGTCTGCAAGAGTGTTGCGCCCGGATTG
TGTCACCAGCAATACAGAAGTGTTCTTGCTGTTCTCCAACTTTGACAACGGAAAGAGACCCTCTAC
GCTACACCAGATGAATACCAAGCTGAGTGCCGTGTATGCCGGAGAAGCCATGCACACGGCCGGGT
GTGCACCATCCTACAGAGTTAAGAGAGCAGACATAGCCACGTGCACAGAAGCGGCTGTGGTTAAC
GCAGCTAACGCCCGTGGAACTGTAGGGGATGGCGTATGCAGGGCCGTGGCGAAGAAATGGCCGTC
AGCCTTTAAGGGAGCAGCAACACCAGTGGGCACAATTAAAACAGTCATGTGCGGCTCGTACCCCGT
CATCCACGCTGTAGGGCCTAATTTCTCTGCCACGACTGAAGCGGAAGGGGACCGCGAATTGGCCGC
TGTCTACCGGGCAGTGGCCGCCGAAGTAAACAGACTGTCACTGAGCAGCGTAGCCATCCCGCTGCT
GTCCACAGGAGTGTTCAGCGGCGGAAGAGATAGGCTGCAGCAATCCCTCAACCATCTATTCACAGC
AATGGACGCCACGGACGCTGACGTGACCATCTACTGCAGAGACAAAAGTTGGGAGAAGAAAATCC
AGGAAGCCATAGACATGAGGACGGCTGTGGAGTTGCTCAATGATGACGTGGAGCTGACCACAGAC

TTGGTGAGAGTGCACCCGGACAGCAGCCTGGTGGGTCGTAAGGGCTACAGTACCACTGACGGGTC
GCTGTACTCGTACTTGGAAGGTACGAAATTCAACCAGGCTGCTATTGATATGGCAGAGATACTGAC
GTTGTGGCCCAGACTGCAAGAGGCAAACGAACAGATATGCCTATACGCGCTGGGCGAAACAATGG
ACAACATCAGATCCAAATGTCCGGTGAACGATTCCGATTCATCATCACCTCCCAGGACAGTGCCCT
GCCTGTGCCGCTACGCAATGACAGCAGAACGGATCGCCCGCCTTAGGTCACACCAAGTTAAAAGC
ATGGTGGTTTGCTCATCTTTTCCCCTCCCGAAATACCATGTAGATGGGGTGCAGAAGGTAAAGTGC
GAGAAGGTTCTCCTGTTCGACCCGACGGTACCTTCAGTGGTTAGTCCGCGGAAGTATGCCGCATCG
ACGACGGACCACTCAGACCGGTCGTTACGAGGGTTTGACTTGGACTGGACCACCGACTCGTCTTCC
ACTGCCAGCGATACCATGTCGCTACCCAGTTTGCAGTCGTGTGACATCGACTCGATCTACGAGCCA
ATGGCTCCCATAGTAGTGACGGCTGACGTACACCCTGAACCCGCAGGCATCGCGGACCTGGCGGCA
GATGTGCATCCTGAACCCGCAGACCATGTGGACCTCGAGAACCCGATTCCTCCACCGCGCCCGAAG
AGAGCTGCATACCTTGCCTCCCGCGCGGCGGAGCGACCGGTGCCGGCGCCGAGAAAGCCGACGCC
TGCCCCAAGGACTGCGTTTAGGAACAAGCTGCCTTTGACGTTCGGCGACTTTGACGAGCACGAGGT
CGATGCGTTGGCCTCCGGGATTACTTTCGGAGACTTCGACGACGTCCTGTGACTAGGCCGCGCGGG
TGCATATATTTTCTCCTCGGACACTGGCAGCGGACATTTACAACAAAAATCCGTTAGGCAGCACAA
TCTCCAGTGCGCACAACTGGATGCGGTCGAGGAGGAGAAAATGTACCCGCCAAAATTGGATACTG
AGAGGGAGAAGCTGTTGCTGCTGAAAATGCAGATGCACCCATCGGAGGCTAATAAGAGTCGATAC
CAGTCTCGCAAAGTGGAGAACATGAAAGCCACGGTGGTGGACAGGCTCACATCGGGGGCCAGATT
GTACACGGGAGCGGACGTAGGCCGCATACCAACATACGCGGTTCGGTACCCCCGCCCCGTGTACTC
CCCTACCGTGATCGAAAGATTCTCAAGCCCCGATGTAGCAATCGCAGCGTGCAACGAATACCTATC
CAGAAATTACCCAACAGTGGCGTCGTACCAGATAACAGATGAATACGACGCATACTTGGACATGG
TTGACGGGTCGGAGAGTTGCTTGGACAGAGCGACATTCTGCCCGGCGAAGCTCCGGTGCTACCCGA
AACATCATGCGTACCACCAGCCGACTGTACGCAGTGCCGTCCCGTCACCCTTTCAGAACACACTAC
AGAACGTGCTAGCGGCCGCCACCAAGAGAAACTGCAACATCACGCAAATGCGAGAACTACCCACC
ATGGACTCGGCAGTGTTCAACGTGGAGTGCTTCAAGCGCTATGCCTGCTCCGGAGAATATTGGGAA
GAATATGCTAAACAACCTATCCGGATAACCACTGAGAACATCACTACCTATGTGACCAAATTGAAA
GGCCCGAAAGCTGCTGCCTTGTTCGCTAAGACCCACAACTTGGTTCCGCTGCAGGAGGTTCCCATG
GACAGATTCACGGTCGACATGAAACGAGATGTCAAAGCCACTCCAGGGACGAAACACACAGAGGA
AAGACCCAAAGTCCAGGTAATTCAAGCAGCGGAGCCATTGGCGACCGCTTACCTGTGCGGCATCCA
CAGGGAATTAGTAAGGAGACTAAATGCTGTGTTACGCCCTAACGTGCACACATTGTTTGATATGTC
GGCCGAAGACTTTGACGCGATCATCGCCTCTCACTTCCACCCAGGAGACCCGGTTCTAGAGACGGA
CATTGCATCATTCGACAAAAGCCAGGACGACTCCTTGGCTCTTACAGGTTTAATGATCCTCGAAGA
TCTAGGGGTGGATCAGTACCTGCTGGACTTGATCGAGGCAGCCTTTGGGGAAATATCCAGCTGTCA
CCTACCAACTGGCACGCGCTTCAAGTTCGGAGCTATGATGAAATCGGGCATGTTTCTGACTTTGTTT
ATTAACACTGTTTTGAACATCACCATAGCAAGCAGGGTACTGGAGCAGAGACTCACTGACTCCGCC
TGTGCGGCCTTCATCGGCGACGACAACATCGTTCACGGAGTGATCTCCGACAAGCTGATGGCGGAG
AGGTGCGCGTCGTGGGTCAACATGGAGGTGAAGATCATTGACGCTGTCATGGGCGAAAAACCCCC
ATATTTTTGTGGGGGATTCATAGTTTTTGACAGCGTCACACAGACCGCCTGCCGTGTTTCAGACCCA
CTTAAGCGCCTGTTCAAGTTGGGTAAGCCGCTAACAGCTGAAGACAAGCAGGACGAAGACAGGCG
ACGAGCACTGAGTGACGAGGTTAGCAAGTGGTTCCGGACAGGCTTGGGGGCCGAACTGGAGGTGG
CACTAACATCTAGGTATGAGGTAGAGGGCTGCAAAAGTATCCTCATAGCCATGGCCACCTTGGCGA
GGGACATTAAGGCGTTTAAGAAATTGAGAGGACCTGTTATACACCTCTACGGCGGTCCTAAATTGG
TGCGTTAATACACAGAATTCTGATTATAGCGCACTATTATAGCACCATGAATTACATCCCTACGCA
AACGTTTTACGGCCGCCGGTGGCGCCCGCGCCCGGCGGCCCGTCCCTGGCCGTTGCAGGCCACTCC
GGTGGCTCCCGTCGTCCCCGACTTCCAGGCCCAGCAGATGCAGCAACTCATCAGCGCCGTAAATGC
GCTGACAATGAGACAGAACGCAATTGCTCCTGCTAGGCCTCCCAAACCAAAGAAGAAGAAGACAA
CCAAACCAAAGCCGAAAACGCAGCCCAAGAAGATCAAAGGAAAAACGCAGCAGCAAAAGAAGAA
AGACAAGCAAGCCGACAAGAAGAAGAAGAAACCCGGAAAAAGAGAAAGAATGTGCATGAAGATT
GAAAATGACTGTATCTTCGAAGTCAAACACGAAGGAAAGGTCACTGGGTACGCCTGCCTGGTGGG
CGACAAAGTCATGAAACCTGCCCACGTGAAAGGAGTCATCGACAACGCGGACCTGGCAAAGCTAG
CTTTCAAGAAATCGAGCAAGTATGACCTTGAGTGTGCCCAGATACCAGTTCACATGAGGTCGGATG
CCTCAAAGTACACGCATGAGAAGCCCGAGGGACACTATAACTGGCACCACGGGGCTGTTCAGTAC
AGCGGAGGTAGGTTCACTATACCGACAGGAGCGGGCAAACCGGGAGACAGTGGCCGGCCCATCTT
TGACAACAAGGGGAGGGTAGTCGCTATCGTCCTGGGCGGGGCCAACGAGGGCTCACGCACAGCAC
TGTCGGTGGTCACCTGGAACAAAGATATGGTGACTAGAGTGACCCCCGAGGGGTCCGAAGAGTGG
TCCGCCCCGCTGATTACTGCCATGTGTGTCCTTGCCAATGCTACCTTCCCGTGCTTCCAGCCCCCGT
GTGTACCTTGCTGCTATGAAAACAACGCAGAGGCCACACTACGGATGCTCGAGGATAACGTGGAT
AGGCCAGGGTACTACGACCTCCTTCAGGCAGCCTTGACGTGCCGAAACGGAACAAGACACCGGCG
CAGCGTGTCGCAACACTTCAACGTGTATAAGGCTACACGCCCTTACATCGCGTACTGCGCCGACTG
CGGAGCAGGGCACTCGTGTCATAGCCCCGTAGCAATTGAAGCGATCAGGTCCGAAGCTACCGACG
GGATGCTGAAGATTCAGTTCTCGGCACAAATTGGCATAGATAAGAGTGACAATCATGACTACACGA
AGATAAGGTACGCAGACGGGCACGCCATTGAGAATGCCGTCCGGTCATCTTTGAAGGTAGCCACCT

CCGGAGACTGTTTCGTCCATGGCACAATGGGACATTTCATACTGGCAACGTGCCCACCGGGTGAAT
TTCTGCAGGTCTCGATCCAGGACACCAGAAACGCGGTCCGTGCCTGCAGAATACAATATCATCATG
ACCCTCAACCGGTGGGTAGAGAAAAATTTACAATTAGACCACACTATGGAAAAGAGATCCCTTGC
ACCACTTATCAACAGACCACAGCGGAGACCGTGGAGGAAATCGACATGCATATGCCGCCAGATAC
GCCGGACAGGACGTTGCTATCACAGCAATCTGGCAATGTAAAGATCACAGTCGGAGGAAAGAAGG
TGAAATACAACTGCACCTGTGGAACCGGAAACGTTGGCACTACTAATTCGGACAAGACGATCAAC
ACGTGTCTAATAGAGCAGTGCCACGTCTCAGTGACGGACCATAAGAAATGGCAGTTCAACTCACCT
TTCGTCCCGAGAGCCGACGAACCGGCTAGAAAAGGCAAAGTCCATATCCCATTCCCGTTGGACAAC
ATCACATGCAGAGTTCCAATGGCGCGCGAACCAACCGTCATCCACGGCAAAAGAAAAGTGACACT
GCACCTTCACCCAGATCATCCCACGCTCTTTTCCTACCGCACACTGGGTGAGGACCCGCAGTATCAC
GAGGAATGGGTGACAGCGGCGGTGGAACGGACCATACCCGTACCAGTGGACGGGATGGAGTACCA
CTGGGGAAACAACGACCCAGTGAGGCTTTGGTCTCAACTCACCACTGAAGGGAAACCGCACGGCT
GGCCGCATCAGATCGTACAGTACTACTATGGGCTTTACCCGGCCGCTACAGTATCCGCGGTCGTCG
GGATGAGCTTACTGGCGTTGATATCGATCTTCGCGTCGTGCTACATGCTGGCTGCGGCCCGCAGTA
AGTGCTTGACCCCTTATGCTTTAACACCAGGAGCTGCAGTTCCGTGGACGCTGGGGATACTCTGCT
GCGCCCCGCGGGCGCACGCAGCTAGTGTGGCAGAGACTATGGCCTACTTGTGGGACCAAAACCAA
GCGTTGTTCTGGTTGGAGTTTGCGGCCCCTGTTGCCTGCATCCTCATCATCACGTATTGCCTCAGAA
ACGTGCTGTGTTGCTGTAAGAGCCTTTCTTTTTTAGTGCTACTGAGCCTCGGGGCAACCGCCAGAGC
TTACGAACATTCGACAGTAATGCCGAACGTGGTGGGGTTCCCGTATAAGGCTCACATTGAAAGGCC
AGGATATAGCCCCCTCACTTTGCAGATGCAGGTTGTTGAAACCAGCCTCGAACCAACCCTTAATTT
GGAATACATAACCTGTGAGTACAAGACGGTCGTCCCGTCGCCGTACGTGAAGTGCTGCGGCGCCTC
AGAGTGCTCCACTAAAGAGAAGCCTGACTACCAATGCAAGGTTTACACAGGCGTGTACCCGTTCAT
GTGGGGAGGGGCATATTGCTTCTGCGACTCAGAAAACACGCAACTCAGCGAGGCGTACGTCGATC
GATCGGACGTATGCAGGCATGATCACGCATCTGCTTACAAAGCCCATACAGCATCGCTGAAGGCCA
AAGTGAGGGTTATGTACGGCAACGTAAACCAGACTGTGGATGTTTACGTGAACGGAGACCATGCC
GTCACGATAGGGGGTACTCAGTTCATATTCGGGCCGCTGTCATCGGCCTGGACCCCGTTCGACAAC
AAGATAGTCGTGTACAAAGACGAAGTGTTCAATCAGGACTTCCCGCCGTACGGATCTGGGCAACCA
GGGCGCTTCGGCGACATCCAAAGCAGAACAGTGGAGAGTAACGACCTGTACGCGAACACGGCACT
GAAGCTGGCACGCCCTTCACCCGGCACGGTCCATGTACCGTACACACAGACACCTTCAGGGTTCAA
ATATTGGCTAAAGGAAAAAGGGACAGCCCTAAATACGAAGGCTCCTTTTGGCTGCCAAATCAAAA
CGAACCCTGTCAGGGCCATGAACTGCGCCGTGGGAAACATCCCTGTCTCCATGAATTTGCCTGACA
GCGCCTTTACCCGCATTGTCGAGGCGCCGACCATCACTGACCTGACTTGCACAGTGGCTACCTGTA
CGCACTCCTCGGATTTCGGCGGCGTCTTGACACTGACGTACAAGACCGACAAGAACGGGGACTGCT
CTGTACACTCGCACTCTAACGTAGCTACTCTACAGGAGGCCACAGCAAAAGTGAAGACAGCACGT
AAGGTGACCTTACACTTCTCCACGGCAAGCGCATCACCTTCTTTTGTGGTGTCGCTATGCAGTGCTA
AGGCCACCTGTTCAGCGTCGTGTGAGCCCCCGAAAGACCACATAGTCCCATATGCGGCTAGCCACA
GTAACGTAGTGTTTCCAGACATGTCGGGCACCGCACTATCATGGGTGCAGAAAATCTCGGGTGGTC
TGGGGGCCTTCGCAATCGGCGCTATCCTGGTGCTAGTTGTGGTCACTTGCATTGGGCTCCGCAGATA
A

SFV Tanzania53 (MK280688.1)

ATGGCCGCCAAAGTGCATGTTGATATTGAGGCTGACAGCCCATTCATCAAGTCTTTGCAGAAGGCA
TTTCCGTCGTTCGAGGTGGAGTCATTGCAGGTCACACCAAATGACCATGCAAATGCCAGAGCATTT
TCGCACCTGGCTACCAAATTGATCGAGCAGGAGACTGACAAAGACACACTCATCTTGGATATCGGC
AGTGCGCCTTCCAGGAGAATGATGTCTACGCACAAATACCACTGCGTATGCCCTATGCGCAGCGCA
GAAGACCCCGAAAGGCTCGTATGCTACGCAAAGAAACTGGCAGCGGCCTCCGGGAAGGTGCTGGA
TAGAGAGATCGCAGGGAAAATCACCGACCTGCAGACCGTCATGGCTACGCCAGACGCTGAATCTC
CTACCTTTTGCCTGCATACAGACGTCACGTGTCGTACGGCAGCCGAAGTGGCCGTATACCAGGACG
TGTATGCTGTACATGCACCAACATCGCTGTACCATCAGGCGATGAAAGGTGTCAGAACGGCGTATT
GGATTGGGTTTGACACCACCCCGTTTATGTTTGACGCGCTAGCAGGCGCGTATCCAACCTACGCCA
CAAACTGGGCCGACGAGCAGGTGTTACAGGCCAGGAACATAGGACTGTGTGCAGCATCCTTGACT
GAGGGAAGACTCGGCAAACTGTCCATTCTCCGCAAGAAGCAATTGAAACCTTGCGACACAGTCAT
GTTCTCGGTAGGATCTACATTGTACACTGAGAGCAGAAAGCTACTGAGGAGCTGGCACTTACCCTC
CGTATTCCACCTGAAAGGTAAACAATCCTTTACCTGTAGGTGCGATACCATCGTATCATGTGAAGG
GTACGTAGTTAAGAAAATCACTATGTGCCCCGGCCTGTACGGTAAAACGGTAGGGTACGCCGTGAC
GTATCACGCGGAGGGATTCCTAGTGTGCAAGACCACAGACACTGTCAAAGGAGAAAGAGTCTCAT
TCCCTGTATGCACCTACGTCCCCTCAACCATCTGTGATCAAATGACTGGCATACTAGCGACCGACGT
CACACCGGAGGACGCACAGAAGTTGTTAGTGGGATTGAATCAGAGGATAGTTGTGAACGGAAGAA
CACAGCGAAACACTAACACGATGAAGAACTATCTGCTTCCGATTGTGGCCGTCGCATTTAGCAAGT
GGGCGAGGGAATACAAGGCAGACCTTGATGATGAAAAACCTCTGGGTGTCCGAGAGAGGTCACTT
ACTTGCTGCTGCTTGTGGGCATTTAAAACGAAGAAGATGCACACCATGTACAAGAAACCAGACACC

CAGACAATAGTGAAGGTGCCTTCAGAGTTTAACTCGTTCGTCATCCCGAGCCTATGGTCTACAGGC
CTCGCAATCCCAGTCAGATCACGCATTGAGATGCTTTTGGCCAAGAAGACCAAGCGAGAGTTAATA
CCTGTTCTCGACGCGTCGTCAGCCAGGGATGCTGAACAAGAGGAGAAGGAGAGGTTGGAGGCCGA
GCTGACTAGAGAAGCCTTACCACCCCTCGTCCCCATCGCGCCGGCGGAGACGGGAGTCGTCGACGT
CGACGTTGAAGAACTAGAGTATCACGCAGGTGCAGGGGTCGTGGAAACACCTCGCAGCGCGTTGA
AAGTCACCGCACAGCCGAACGACGTACTACTAGGAAATTACGTAGTTCTGTCCCCGCAGACCGTGC
TCAAGAGCTCCAAGTTGGCCCCCGTGCACCCTCTAGCAGAGCAGGTGAAAATAATAACACATAAC
GGGAGGGCCGGCCGTTACCAGGTCGACGGATATGACGGCAGGGTCCTACTACCATGTGGATCGGC
CATTCCGGTCCCTGAGTTTCAAGCTTTGAGCGAGAGCGCCACTATGGTGTACAACGAAAGGGAGTT
CGTCAACAGGAAACTATACCATATTGCCGTTCACGGACCGTCGCTGAACACCGACGAGGAGAACT
ACGAGAAAGTCAGAGCTGAAAGAACTGACGCCGAGTACGTGTTCGACGTAGATAAAAAATGCTGC
GTCAAGAGAGAGGAAGCGTCGGGTTTGGTGTTGGTGGGAGAGCTAACCAACCCCCCGTTCCATGA
ATTCGCCTACGAAGGGCTGAAGATCAGGCCGTCGGCACCATATAAGACTACAGTAGTAGGAGTCTT
TGGGGTTCCGGGATCAGGCAAGTCTGCTATTATTAAGAGCCTCGTGACCAAACACGATCTGGTCAC
CAGCGGCAAGAAGGAGAACTGCCAGGAAATAGTCAACGACGTGAAGAAGCACCGCGGACTGGAC
ATCCAGGCAAAAACAGTGGACTCCATCCTGCTAAACGGGTGTCGTCGTGCCGTGGACATCCTATAT
GTGGACGAGGCTTTCGCTTGCCATTCCGGTACTCTGCTGGCCCTAATTGCTCTTGTTAAACCTCGGA
GCAAAGTGGTGTTATGCGGAGACCCCAAGCAATGCGGATTCTTCAATATGATGCAGCTTAAGGTGA
ACTTCAACCACAACATCTGCACTGAAGTATGTCATAAAAGTATATCCAGACGTTGCACGCGTCCAG
TCACGGCCATCGTGTCTACGTTGCACTACGGAGGCAAGATGCGCACGACCAACCCGTGCAACAAAC
CCATAATCATAGACACCACAGGACAGACCAAGCCCAAGCCAGGAGACATCGTGTTAACATGCTTC
CGAGGCTGGGTAAAGCAGCTGCAGTTGGACTACCGTGGACACGAAGTCATGACAGCAGCAGCATC
TCAGGGCCTCACCCGCAAAGGGGTATACGCCGTAAGGCAGAAGGTGAATGAAAATCCCTTGTATG
CCCCTGCGTCGGAGCACGTGAATGTACTGCTGACGCGCACTGAGGATAGGCTGGTGTGGAAAACG
CTGGCCGGCGATCCCTGGATTAAGGTCCTATCAAACATTCCACAGGGTAACTTTACGGCCACATTG
GAAGAATGGCAAGAAGAACACGACAAAATAATGAAGGTGATTGAAGGACCGGCTGCGCCTGTGG
ACGCGTTCCAGAACAAAGCGAACGTGTGTTGGGCGAAAAGCCTGGTGCCTGTCCTGGACACTGCCG
GAATCAGATTGACAGCAGAGGAGTGGAGCACCATAATTACAGCATTTAAGGAGGACAGAGCTTAC
TCTCCAGAGGTGGCCTTGAATGAAATTTGCACCAAGTACTATGGAGTTGACCTGGACAGTGGCCTG
TTTTCTGCCCCGAAGGTGTCCCTGTATTACGAGAACAACCACTGGGATAACAGACCTGGTGGAAGG
ATGTATGGATTCAATGCCGCAACAGCTGCCAGGCTGGAAGCTAGACATACCTTCCTGAAGGGGCAG
TGGCATACGGGCAAGCAGGCAGTTATCGCAGAAAGAAAAATCCAACCGCTTTCTGTGCTGGACAA
TGTAATTCCTATCAACCGCAGGCTGCCGCACGCCCTGGTGGCTGAGTACAAGACGGTTAAAGGCAG
TAGGGTTGAGTGGCTGGTCAATAAAGTAAGAGGGTACCACGTCCTGCTGGTGAGTGAGTACAACCT
GGCTTTGCCTCGACGCAGGGTCACTTGGTTGTCACCGCTGAATGTCACAGGCGCCGATAGGTGCTA
CGACCTAAGTTTAGGACTGCCGGCTGACGCCGGCAGATTCGACTTGGTCTTTGTGAACATTCACAC
GGAATTCAGAATCCACCACTACCAGCAGTGTGTCGACCACGCCATGAAGCTGCAGATGCTTGGGGG
AGATGCGCTACGACTGCTAAAACCCGGCGGCAGCCTCTTGATGAGAGCTTACGGATACGCCGATAA
AATCAGCGAAGCCGTTGTTTCCTCCTTAAGCAGAAAGTTCTCGTCTGCAAGAGTGTTGCGCCCGGA
TTGTGTCACCAGCAATACAGAAGTGTTCTTGCTGTTCTCCAACTTTGACAACGGAAAGAGACCCTCT
ACGCTACACCAGATGAATACCAAGCTGAGTGCCGTGTATGCCGGAGAAGCCATGCACACGGCCGG
GTGTGCACCATCCTACAGAGTTAAGAGAGCAGACATAGCCACGTGCACAGAAGCGGCTGTGGTTA
ACGCAGCTAACGCCCGTGGAACTGTAGGGGATGGCGTATGCAGGGCCGTGGCGAAGAAATGGCCG
TCAGCCTTTAAGGGAGCAGCAACACCAGTGGGCACAATTAAAACAGTCATGTGCGGCTCGTACCCC
GTCATCCACGCTGTAGGGCCTAATTTCTCTGCCACGACTGAAGCGGAAGGGGACCGCGAATTGGCC
GCTGTCTACCGGGCAGTGGCCGCCGAAGTAAACAGACTGTCACTGAGCAGCGTAGCCATCCCGCTG
CTGTCCACAGGAGTGTTCAGCGGCGGAAGAGATAGGCTGCAGCAATCCCTCAACCATCTATTCACA
GCAATGGACGCCACGGACGCTGACGTGACCATCTACTGCAGAGACAAAAGTTGGGAGAAGAAAAT
CCAGGAAGCCATAGACATGAGGACGGCTGTGGAGTTGCTCAATGATGACGTGGAGCTGACCACAG
ACTTGGTGAGAGTGCACCCGGACAGCAGCCTGGTGGGTCGTAAGGGCTACAGTACCACTGACGGG
TCGCTGTACTCGTACTTGGAAGGTACGAAATTCAACCAGGCTGCTATTGATATGGCAGAGATACTG
ACGTTGTGGCCCAGACTGCAAGAGGCAAACGAACAGATATGCCTATACGCGCTGGGCGAAACAAT
GGACAACATCAGATCCAAATGTCCGGTGGACGATTCCGATTCATCAACACCTCCCAGGACAGTGCC
CTGCCTGTGCCGCTACGCAATGACAGCAGAACGGATCGCCCGCCTTAGGTCACACCAAGTTAAAAG
CATGGTGGTTTGCTCATCTTTTCCCCTCCCGAAATACCATGTAGATGGGGTGCAGAAGGTAAAGTG
CGAGAAGGTTCTCCTGTTCGACCCGACGGTACCTTCAGTGGTTAGTCCGCGGAAGTATGCCGCATC
GACGACGGACCACTCAGACCGGTCGTTACGAGGGTTTGACTTGGACTGGACCACCGACTCGTCTTC
CACTGCCAGCGATACCATGTCGCTACCCAGTTTGCAGTCGTGTGACATCGACTCGATCTACGAGCC
AATGGCTCCCATAGTAGTGACGGCTGACGTACACCCTGAACCCGCAGGCATCGCGGACCTGGCGGC
AGATGTGCATCCTGAACCCGCAGACCATGTGGACCTCGAGAACCCGATTCCTCCACCGCGCCCGAA
GAGAGCTGCATACCTTGCCTCCCGCGCGGCGGAGCGACCGGTGCCGGCGCCGAGAAAGCCGACGC
CTGCCCCAAGGACTGCGTTTAGGAACAAGCTGCCTTTGACGTTCGGCGACTTTGACGAGCACGAGG

TCGATGCGTCGGCCTCCGGGATTACTTTCGGAGACTTCGACGACGTCCTGAGACTAGGCCGCGCGG
GTGCATATATTTTCTCCTCGGACACTGGCAGCGGACATTTACAACAAAAATCCGTTAGGCAGCACA
ATCTCCAGTGCGCACAACTGGATGCGGTCGAGGAGGAGAAAATGTACCCGCCAAAATTGGATACT
GAGAGGGAGAAGCTGTTGCTGCTGAAAATGCAGATGCACCCATCGGAGGCTAATAAGAGTCGATA
CCAGTCTCGCAAAGTGGAGAACATGAAAGCCACGGTGGTGGACAGGCTCACATCGGGGGCCAGAT
TGTACACGGGAGCGGACGTAGGCCGCATACCAACATACGCGGTTCGGTACCCCCGCCCCGTGTACT
CCCCTACCGTGATCGAAAGATTCTCAAGCCCCGATGTAGCAATCGCAGCGTGCAACGAATACCTAT
CCAGAAATTACCCAACAGTGGCGTCGTACCAGATAACAGATGAATACGACGCATACTTGGACATG
GTTGACGGGTCGGAGAGTTGCTTGGACAGAGCGACATTCTGCCCGGCGAAGCTCCGGTGCTACCCG
AAACATCATGCGTACCACCAGCCGACTGTACGCAGTGCCGTCCCGTCACCCTTTCAGAACACACTA
CAGAACGTGCTAGCGGCCGCCACCAAGAGAAACTGCAACGTCACGCAAATGCGAGAACTACCCAC
CATGGACTCGGCAGTGTTCAACGTGGAGTGCTTCAAGCGCTATGCCTGCTCCGGAGAATATTGGGA
AGAATATGCTAAACAACCTATCCGGATAACCACTGAGAACATCACTACCTATGTGACCAAATTGAA
AGGCCCGAAAGCTGCTGCCTTGTTCGCTAAGACCCACAACTTGGTTCCGCTGCAGGAGGTTCCCAT
GGACAGATTCACGGTCGACATGAAACGAGATGTCAAAGTCACTCCAGGGACGAAACACACAGAGG
AAAGACCCAAAGTCCAGGTAATTCAAGCAGCGGAGCCATTGGCGACCGCTTACCTGTGCGGCATCC
ACAGGGAATTAGTAAGGAGACTAAATGCTGTGTTACGCCCTAACGTGCACACATTGTTTGATATGT
CGGCCGAAGACTTTGACGCGATCATCGCCTCTCACTTCCACCCAGGAGACCCGGTTCTAGAGACGG
ACATTGCATCATTCGACAAAAGCCAGGACGACTCCTTGGCTCTTACAGGTTTAATGATCCTCGAAG
ATCTAGGGGTGGATCAGTACCTGCTGGACTTGATCGAGGCAGCCTTTGGGGAAATATCCAGCTGTC
ACCTACCAACTGGCACGCGCTTCAAGTTCGGAGCTATGATGAAATCGGGCATGTTTCTGACTTTGTT
TATTAACACTGTTTTGAACATCACCATAGCAAGCAGGGTACTGGAGCAGAGACTCACTGACTCCGC
CTGTGCGGCCTTCATCGGCGACGACAACATCGTTCACGGAGTGATCTCCGACAAGCTGATGGCGGA
GAGGTGCGCGTCGTGGGTCAACATGGAGGTGAAGATCATTGACGCTGTCATGGGCGAAAAACCCC
CATATTTTTGTGGGGGATTCATAGTTTTTGACAGCGTCACACAGACCGCCTGCCGTGTTTCAGACCC
ACTTAAGCGCCTGTTCAAGTTGGGTAAGCCGCTAACAGCTGAAGACAAGCAGGACGAAGACAGGC
GACGAGCACTGAGTGACGAGGTTAGCAAGTGGTTCCGGACAGGCTTGGGGGCCGAACTGGAGGTG
GCACTAACATCTAGGTATGAGGTAGAGGGCTGCAAAAGTATCCTCATAGCCATGGCCACCTTGGCG
AGGGACATTAAGGCGTTTAAGAAATTGAGAGGACCTGTTATACACCTCTACGGCGGTCCTAAATTG
GTGCGTTAATACACAGAATTCTGATTATAGCGCACTATTATAGCACCATGAATTACATCCCTACGC
AAACGTTTTACGGCCGCCGGTGGCGCCCGCGCCCGGCGGCCCGTCCCTGGCCGTTGCAGGCCACTC
CGGTGGCTCCCGTCGTCCCCGACTTCCAGGCCCAGCAGATGCAGCAACTCATCAGCGCCGTAAATG
CGCTGACAATGAGACAGAACGCAATTGCTCCTGCTGGGCCTCCCAAACCAAAGAAGAAGAAGACA
ACCAAACCAAAGCCGAAAACGCAGCCCAAGAAGATCAAAGGAAAAACGCAGCAGCAAAAGAAGA
AAGACAAGCAAGCCGACAAGAAGAAGAAGAAACCCGGAAAAAGAGAAAGAATGTGCATGAAGAT
TGAAAATGACTGTATCTTCGAAGTCAAACACGAAGGAAAGGTCACTGGGTACGCCTGCCTGGTGG
GCGACAAAGTCATGAAACCTGCCCACGTGAAAGGAGTCATCGACAACGCGGACCTGGCAAAGCTA
GCTTTCAAGAAATCGAGCAAGTATGACCTTGAGTGTGCCCAGATACCAGTTCACATGAGGTCGGAT
GCCTCAAAGTACACGCATGAGAAGCCCGAGGGACACTATAACTGGCACCACGGGGCTGTTCAGTA
CAGCGGAGGTAGGTTCACTATACCGACAGGAGCGGGCAAACCGGGAGACAGTGGCCGGCCCATCT
TTGACAACAAGGGGAGGGTAGTCGCTATCGTCCTGGGCGGGGCCAACGAGGGCTCACGCACAGCA
CTGTCGGTGGTCACCTGGAACAAAGATATGGTGACTAGAGTGACCCCCGAGGGGTCCGAAGAGTG
GTCCGCCCCGCTGATTACTGCCATGTGTGTCCTTGCCAATGCTACCTTCCCGTGCTTCCAGCCCCCG
TGTGTACCTTGCTGCTATGAAAACAACGCAGAGGCCACACTACGGATGCTCGAGGATAACGTGGAT
AGGCCAGGGTACTACGACCTCCTTCAGGCAGCCTTGACGTGCCGAAACGGAACAAGACACCGGCG
CAGCGTGTCGCAACACTTCAACGTGTATAAGGCTACACGCCCTTACATCGCGTACTGCGCCGACTG
CGGAGCAGGGCACTCGTGTCATAGCCCCGTAGCAATTGAAGCGATCAGGTCCGAAGCTACCGACG
GGATGCTGAAGATTCAGTTCTCGGCACAAATTGGCATAGATAAGAGTGACAATCATGACTACACGA
AGATAAGGTACGCAGACGGGCACGCCATTGAGAATGCCGTCCGGTCATCTTTGAAGGTAGCCACCT
CCGGAGACTGTTTCGTCCATGGCACAATGGGACATTTCATACTGGCAACGTGCCCACCGGGTGAAT
TTCTGCAGGTCTCGATCCAGGACACCAGAAACGCGGTCCGTGCCTGCAGAATACAATATCATCATG
ACCCTCAACCGGTGGGTAGAGAAAAATTTACAATTAGACCACACTATGGAAAAGAGATCCCTTGC
ACCACTTATCAACAGACCACAGCGGAGACCGTGGAGGAAATCGACATGCATATGCCGCCAGATAC
GCCGGACAGGACGTTGCTATCACAGCAATCTGGCAATGTAAAGATCACAGTCGGAGGAAAGAAGG
TGAAATACAACTGCACCTGTGGAACCGGAAACGTTGGCACTACTAATTCGGACAAGACGATCAAC
ACGTGTCTAATAGAGCAGTGCCACGTCTCAGTGACGGACCATAAGAAATGGCAGTTCAACTCACCT
TTCGTCCCGAGAGCCGACGAACCGGCTAGAAAAGGCAAAGTCCATATCCCATTCCCGTTGGACAAC
ATCACATGCAGAGTTCCAATGGCGCGCGAACCAACCGTTATCCACGGCAAAAGAGAAGTGACACT
GCACCTTCACCCAGATCATCCCACGCTCTTTTCCTACCGCACACTGGGTGAGGACCCGCAGTATCAC
GAGGAATGGGTGACAGCGGCGGTGGAACGGACCATACCCGTACCAGTGGACGGGATGGAGTACCA
CTGGGGAAACAACGACCCAGTGAGGCTTTGGTCTCAACTCACCACTGAAGGGAAACCGCACGGCT
GGCCGCATCAGATCGTACAGTACTACTATGGGCTTTACCCGGCCGCTACAGTATCCGCGGTCGTCG

GGATGAGCTTACTGGCGTTGATATCGATCTTCGCGTCGTGCTACATGCTGGCTGCGGCCCGCAGTA
AGTGCTTGACCCCTTATGCTTTAACACCAGGAGCTGCAGTTCCGTGGACGCTGGGGATACTCTGCT
GCGCCCCGCGGGCGCACGCAGCTAGTGTGGCAGAGACTATGGCCTACTTGTGGGACCAAAACCAA
GCGTTGTTCTGGTTGGAGTTTGCGGCCCCTGTTGCCTGCATCCTCATCATCACGTATTGCCTCAGAA
ACGTGCTGTGTTGCTGTAAGAGCCTTTCTTTTTTAGTGCTACTGAGCCTCGGGGCAACCGCCAGAGC
TTACGAACATTCGACAGTAATGCCGAACGTGGTGGGGTTCCCGTATAAGGCTCACATTGAAAGGCC
AGGATATAGCCCCCTCACTTTGCAGATGCAGGTTGTTGAAACCAGCCTCGAACCAACCCTTAATTT
GGAATACATAACCTGTGAGTACAAGACGGTCGTCCCGTCGCCGTACGTGAAGTGCTGCGGCGCCTC
AGAGTGCTCCACTAAAGAGAAGCCTGACTACCAATGCAAGGTTTACACAGGCGTGTACCCGTTCAT
GTGGGGAGGGGCATATTGCTTCTGCGACTCAGAAAACACGCAACTCAGCGAGGCGTACGTCGATC
GATCGGACGTATGCAGGCATGATCACGCATCTGCTTACAAAGCCCATACAGCATCGCTGAAGGCCA
AAGTGAGGGTTATGTACGGCAACGTAAACCAGACTGTGGATGTTTACGTGAACGGAGACCATGCC
GTCACGATAGGGGGTACTCAGTTCATATTCGGGCCGCTGTCATCGGCCTGGACCCCGTTCGACAAC
AAGATAGTCGTGTACAAAGACGAAGTGTTCAATCAGGACTTCCCGCCGTACGGATCTGGGCAACCA
GGGCGCTTCGGCGACATCCAAAGCAGAACAGTGGAGAGTAACGACCTGTACGCGAACACGGCACT
GAAGCTGGCACGCCCTTCACCCGGCACGGTCCATGTACCGTACACACAGACACCTTCAGGGTTCAA
ATATTGGCTAAAGGAAAAAGGGACAGCCCTAAATACGAAGGCTCCTTTTGGCTGCCAAATCAAAA
CGAACCCTGTCAGGGCCATGAACTGCGCCGTGGGAAACATCCCTGTCTCCATGAATTTGCCTGACA
GCGCCTTTACCCGCATTGTCGAGGCGCCGACCATCACTGACCTGACTTGCACAGTGGCTACCTGTA
CGCACTCCTCGGATTTCGGCGGCGTCTTGACACTGACGTACAAGACCGACAAGAACGGGGACTGCT
CTGTACACTCGCACTCTAACGTAGCTACTCTACAGGAGGCCACAGCAAAAGTGAAGACAGCAGGT
AAGGTGACCTTACACTTCTCCACGGCAAGCGCATCACCTTCTTTTGTGGTGTCGCTATGCAGTGCTA
AGGCCACCTGTTCAGCGTCGTGTGAGCCCCCGAAAGACCACATAGTCCCATATGCGGCTAGCCACA
GTAACGTAGTGTTTCCAGACATGTCGGGCACCGCACTATCATGGGTGCAGAAAATCTCGGGTGGTC
TGGGGGCCTTCGCAATCGGCGCTATCCTGGTGCTAGTTGTGGTCACTTGCATTGGGCTCCGCAGATA
A

Fig. S1

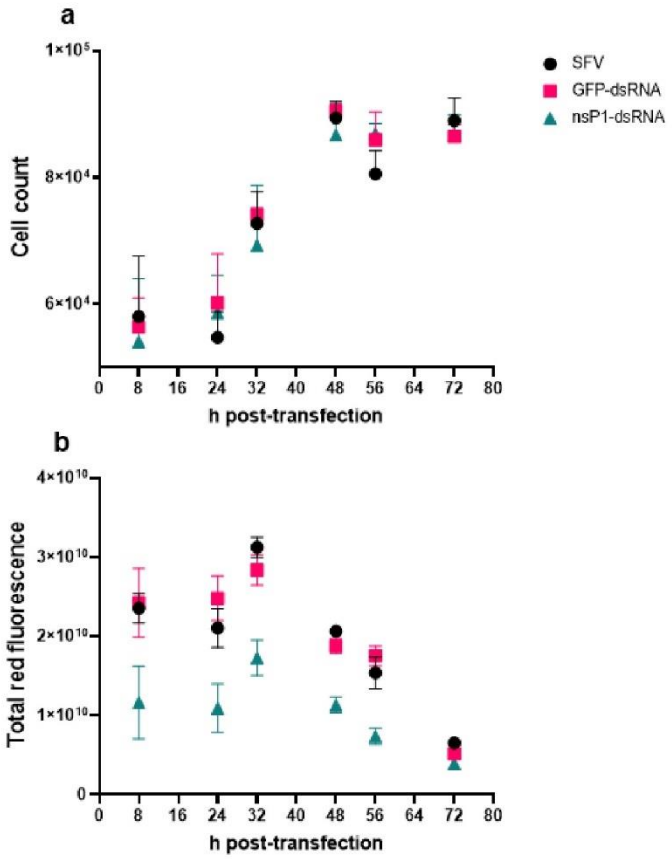

Fig. S1. Cell count and total red fluorescence of U4.4 cells at multiple time points. Cells were treated with 1 ng/µL of dsRNA complexed with K4 (1:1) and infected with Semliki Forest virus-mCherry (MOI=0.01) for 1 h at 8, 24, 32, 48, 56 and, 72 h post-transfection. The (a) cell count and (b) total red intensity were measured at 48 h post-infection for each transfection time point (n=4, biological replicates). Background signal was removed using untreated control. The data points are mean values of the cell count and the total red intensity and the error bars represent standard deviations.

Fig. S2

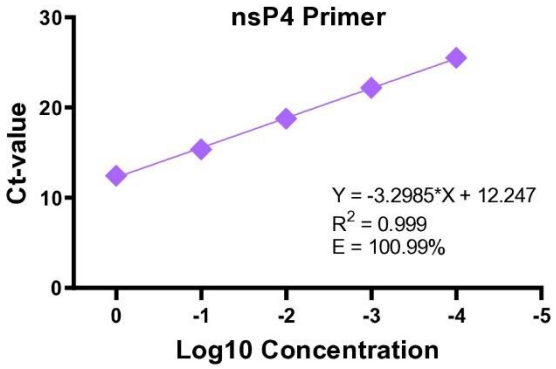

Fig. S2. Standard curve of nsP4 primer. Efficiency of the nsP4 primer with RNA template concentration ranging from 1000 ng to 0.1 ng, at 10-fold dilution series. Each reaction was reverse transcribed and amplified using rt-qPCR.

Fig. S3.

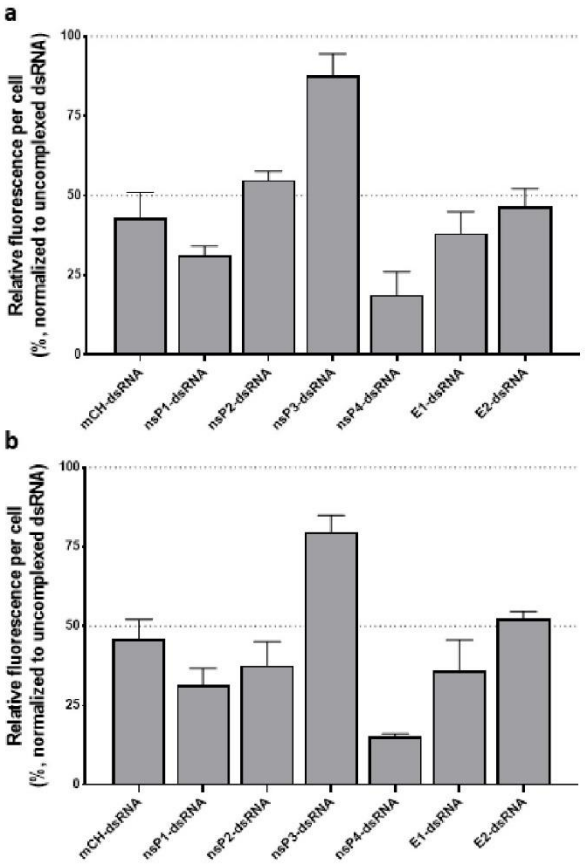

Fig. S3. Normalized inhibition of Semliki Forest virus (SFV) replication by complexed dsRNA using the K4 Transfection System (K4) to uncomplexed dsRNA. Cells were treated with 1 ng/μL of uncomplexed or K4-complexed dsRNA (1:1 ratio). At 24 h post-transfection, cells were infected with SFV-mCherry (MOI=0.01) for 1 h. Total red intensity and cell count were measured at (a) 56 and (b) 72 h post-infection. The data are normalized mean values (n = 3, biological replicates) of the relative fluorescence per cell (total red intensity/total cell count) of complexed dsRNAs to uncomplexed dsRNA and the error bars represent standard deviations. Background signal was removed using untreated control.

6 Appendix

Further publications

The following publications were produced during the period of this research but were not included in the writing of this thesis.

Dersh L, Krämer J, Hurka S, Damm M, Bohlken O, Centurión A, **Omokungbe B**, Schulte L, Marner M, Hardes K, Schäberle T, Vilcinskas A, Lüddecke T. Vector Venom: Venomics of Aedes albopictus reveals novel cecropin-peptides with activity against E. coli. *npj Drug Discovery* (2025; in review)

Centurión A, **Omokungbe B**, Oberpaul M, Dersch L, Stiehler S, Lechner M, Lüddecke T, Vilcinskas A, Steinmetzer T, Hardes K. Furin as a target for suppression of mosquito-borne viruses. *Virology journal* (2025; under revision)

Albuquerque W, Ghezellou P, Lee K-Z, Schneider Q, Gross P, Kessel T, **Omokungbe B**, Spengler B, Vilcinskas A, Zorn H, Gand M. Peptidomics as a Tool to Assess the Cleavage of Wine Haze Proteins by Peptidases from *Drosophila suzukii* Larvae. *Biomolecules*. 2023; 13(3):451. https://doi.org/10.3390/biom13030451

List of abbreviations

Bti	=	*Bacillus thuringiensis israelensis*
Cas9	=	CRISPR-associated protein 9
CHIKV	=	Chikungunya virus
CRISPR	=	Clustered regularly interspaced short palindromic
DDT	=	Dichlorodiphenyltrichloroethane
DENV	=	Dengue virus
dsRNA	=	double-stranded RNA
GMO	=	Genetically modified organisms
IAP	=	Inhibitor of apoptosis
IGRs	=	Insect growth regulators
miRNA	=	MicroRNA
NCM	=	Nucampholin
nsp	=	Non-structural protein
piRNA	=	PIWI-interacting RNA
RISC	=	RNA-induced silencing complex
RNAi	=	RNA interference
ROP	=	Ras opposite
RT-qPCR	=	Reverse Transcription-quantitative Polymerase Chain Reaction
SFV	=	Semliki Forest virus
shRNA	=	Short hairpin RNA
siRNA	=	Small interfering RNA
SIT	=	Sterile insect techniques
TE	=	Transposable elements
TR	=	Transfection reagent
ZIKV	=	Zika virus

Conference and seminar contributions

TBG-Retreat: LOEWE Centre for Translational Biodiversity Genomics (LOEWE-TBG), 2024, Glashütten, Germany
Poster presentation: RNAi as an alternative control strategy against mosquito population

Institute Seminar: Fraunhofer Institute for molecular Biology and Applied Ecology (IME), 2024, Giessen, Germany
Oral presentation: RNAi as an alternative control strategy against mosquitoes

PhD Seminar: Fraunhofer Institute for molecular Biology and Applied Ecology (IME), 2023, Aachen, Germany
Poster presentation: RNA interference as an alternative control strategy against mosquito population

XI International Conference of the European Mosquito Control Association (EMCA), 2023, Palma de Mallorca, Spain
Poster presentation: RNA interference as an alternative control strategy against mosquito population

TBG-Retreat: LOEWE Centre for Translational Biodiversity Genomics (LOEWE-TBG), 2023, Giessen, Germany
Poster presentation: RNAi mediated effects in cell lines of *Aedes albopictus*

TBG-Retreat: LOEWE Centre for Translational Biodiversity Genomics (LOEWE-TBG), 2022, Frankfurt, Germany
Poster presentation: RNAi as an alternative control strategy against mosquito population

Grant raised

German Academic Exchange Service (DAAD), 2023: Travel Grant for the XI International Conference of the European Mosquito Control Association (EMCA), 2023, Palma de Mallorca, Spain

Acknowledgement

First and foremost, I want to thank Prof. Dr. Andreas Vilcinskas, my *Doktorvater*, for giving me the opportunity to be a doctoral candidate under his guidance and for agreeing to be my first reviewer. Your immense support is wholeheartedly appreciated. I am also grateful to Prof. Dr. Miklós Bálint for agreeing to be my second supervisor. Although we did not have many in-person meetings, I thank you sincerely for believing in me.

My appreciation also goes to Dr. Antje Steinbrink as my initial group leader at the Justus-Liebig University Giessen. Though our academic time together was only about a year and a half. I thank you for your extraordinary patience in spite of the many challenges of setting up the experimental workflows. Thank you for continuing to support me even after leaving the institute by reading my manuscripts and staying involved in one way or another.

A very special thanks to Dr. Kornelia Hardes for your support from my master's studies through to the end of my PhD. I transitioned from your working group to start my PhD at the university, then came back halfway through and was welcomed with open arms to continue my research. Your support in my daily laboratory work was incredible. Despite your busy schedule as a group leader, you always took time to discuss the planning and the detailed steps of our projects. I am also thankful for your help with manuscript corrections and advice. Knowing you has been a blessing, and I am forever grateful.

I also want to thank Alejandra Centurión. Thank you for your support in conducting experiments together and for your special "moral support." Sharing an office with you and working on similar projects was extremely helpful for the success of this PhD, because we always discussed each experiment whenever possible. My thanks also go to Sabrina Stiehler for helping me from the beginning to the end of my PhD in both our previous and current working groups. Your support in setting up experiments and in carrying out some laboratory assays is forever appreciated. Without the support of you both, this PhD would have been more challenging.

Beyond that, I want to thank some past and current members of the Antiviral Strategies working group: Dr. Markus Oberpaul, Johanna Eichberg, Elena Maiworm, Stephanie Schlimbach, Antonia Morr, and Cross Chamber. Your contributions and help are deeply appreciated, especially during weekly meetings when we discussed results, planned experiments, and troubleshot together.

I want to especially thank Dr. Kwang-Zin Lee (Sunny) for your support and for introducing me to practical science as well as to Fraunhofer. My first job as a HiWi student was given to me by you, and I learned so much from that experience. Without you, I might not have crossed paths with the amazing people I met at the Fraunhofer Institute. Thank you for seeing the potential in me.

I also want to thank Dr. Tim Lüddecke and Dr. Till Röthig. Whenever I needed advice, your doors were always open, and your helpful comments are truly appreciated. To my fellow PhD colleagues, some of you are more than colleagues; you are true friends. Thank you so much: Ludwig, Josephine, Lennart, Frisca, and others including Hanna. In addition, special thanks to my postdoc colleagues Jonas and Ignazio for always being ready to lift the mood with your amazing jokes during lunch breaks.

Outside of academia, I was lucky to be surrounded by people who lifted my spirits and supported me from start to finish. A special thanks to Joshua, since the day I set foot in Germany, your support and advice have made this path far easier. Lennart Scheer, your and Joshua's efforts to keep my motivation high after lab work with gym sessions and other sports were extremely

helpful. Hugo, Solomon (Chucks), and Victor, thank you for your support. I am happy to have you all in my life.

I also want to thank Marc and John-Arved. We've nearly all attained our Dr. titles, even if our fields differ. Knowing you both, as well as Dennis and Armin have been a blessing in my life. Living together in the same apartment was a pleasant experience, despite my limited German at the time. Furthermore, I would like to thank Franzi. You were very supportive and extremely patient. I am forever grateful for your support.

Most importantly, I would like to thank my family for their immense support. Even when it was difficult to find time to visit, you met me with patience and understanding. Thank you for the constant check-ins, the encouraging messages, and for believing in me.